A Statistical Method for the Design of Rock Slopes

By
B. K. McMahon, D.Sc.
(Associate, Dames and Moore, Sydney)

SUMMARY.- Procedures are introduced for the design of rock slopes by determination of the probability that the slope will be undercut by joints, or combinations of joints, in unstable orientations. The procedures include graphic methods for the statistical analysis of joints, graphic tests for kinematic and kinetic stability, and procedures for the economic analysis of rock slopes.

I. INTRODUCTION

The principal sources of uncertainty in the design of a rock slope are usually the locations and orientations of the joints and other rock defects in the rock mass behind the slope. Steep rock slopes have a higher risk of failure than flatter ones mainly because of the greater probability of undercutting joints, or combinations of joints, in unstable orientations.

This paper introduces graphic procedures for determining the probability of failure of a rock slope by statistical analysis of joint orientations in conjunction with graphic kinematic and kinetic analyses of stability over a range of possible slope angles. The design slope is then selected on the basis of one of the following criteria:

1. Where safety is the overriding consideration; the design slope is the slope angle at which the probability of failure approaches zero.

2. Where partial failure of the slope can be allowed; the design slope is the slope with the minimum total cost consisting of the initial cost of excavation plus the costs resulting from partial slope failure.

3. Where the slope with minimum total cost has an unacceptably high probability of failure, the slope angle may be decreased to an acceptable compromise between the above two criteria.

In the following sections the design procedure is first demonstrated by reference to a simple example involving sliding along a single joint. Extension of the procedure towards the design of slopes where the failure occurs along combinations of joints is then discussed.

II NOTATION

A_u Area of Schmidt Projection covered by unsafe orientations of joints.

A_t Total area of a Schmidt Projection.

c Cohesion

C_a Portion of costs of slope failure that are independant of volume of slide material.

C_b Unit cost of slope failure where costs are related to volume of slide material.

Co Cost of initial excavation.

co Unit cost of bulk excavation.

C_f Cost of slope failure.

C_t Total cost of a rock slope.

i Angle of roughness.

M Multiple of the standard deviation being contoured.

N_a Average number of joint directions observed in a small element of the rock mass.

N_u Number of joint poles in unsafe orientations.

N_t Total number of joints in sample.

n Number of small elements in the rock mass behind the slope.

P_c Percentage of joints in a set that are judged to be sufficiently extensive and continuous to result in a slope failure.

P_f Probability of slope failure.

P_i Probability that the ith element will be undercut by joints in unstable orientations.

P_j Probability of a joint occurring in an unsafe orientation.

ϕ Angle of surface friction.

ϕa Apparent angle of friction.

S_x Sample standard deviation in x-direction.

S_y Sample standard deviation in y-direction.

σ Normal stress at failure.

τ Shearing stress at failure.

u Hydrostatic uplift

V_o Volume of initial excavation.

V_f Expected volume of material involved in slope failure.

V_i Volume of the ith element.

x X-co-ordinate.

y Y-co-ordinate.

III THE EXAMPLE

The following example will be used to illustrate the design procedure:-

A rock slope 100 feet high and facing due West is to be excavated for a highway running N-S. The natural ground surface slopes at 27° and the rock consists of a gneissic granite, with a well-developed foliation. Outcrops are scattered and the foliation is observed to change direction in complex fashion between outcrops. Joints parallel to the foliation extend several hundred feet and are termed joint set 1. Other joints extend less than 10 feet. The groundwater table is below the base of the slope.

Observations on several existing slope failures in the area indicate that failure invariably occurs whenever the true dip of foliation is undercut by a slope and exceeds 34 degrees. It is also observed that sliding on a serious scale only occurs along the foliation joints but that tensile failure can occur in almost any direction in the rock mass, due to separation along combinations of minor joints, whenever necessary to permit sliding on the major joints.

The slope will be allowed to stand for 18 months after excavation before the highway is opened for traffic. Initial bulk excavation is estimated to be $1.00 per cubic yard (in-situ). Clean-up of partial slope failure is estimated to be $5.00 per cubic yard including allowances for scaling down, repair of pavement, and general inconvenience.

IV DESIGN PROCEDURE

The following steps are necessary for the design of a rock slope by the proposed method:

(a) Geological Mapping

Regardless of whether the problem is to design a highway slope, or the slope of an open-pit mine, the first step must be geological mapping to divide the area into structural regions that are statistically homogeneous with respect to jointing and other rock defects (Ref. 1). This mapping also serves to locate major features such as wide fault zones which must be treated as individuals rather than as statistics for the purpose of rock slope design.

(b) Statistical Sampling

An adequately representative sample of joint orientation must be obtained from each structural region included in the slope. Since only joints exposed on rock outcrops, excavated surfaces or a limited number of bore holes are available for measurement, a perfectly random sample, which would imply that every individual in the population has an equal chance of being chosen for the sample, is clearly impossible. When extensive outcrops are available, formal sampling schemes, which are carefully designed to minimise observer bias, may be applied (Ref. 2). Where only scattered exposures are available, an adequate sample can often be obtained by measuring the three to five most prominent joint directions at each outcrop visited (Ref. 3).

(c) Statistical Analysis

The purpose of taking any sample is to reach conclusions regarding the properties of the population (i.e. the totality of all things that the sample is designed to represent).

Graphic statistical analysis of the joint orientation data in three dimensions is made possible by the Schmidt method of representing the orientation of each joint as a point (pole) on a Lambert Equal-Area Projection* of a sphere, as shown in Fig. 1. Detailed procedures for working with this projection are given in Refs. 1 and 4.

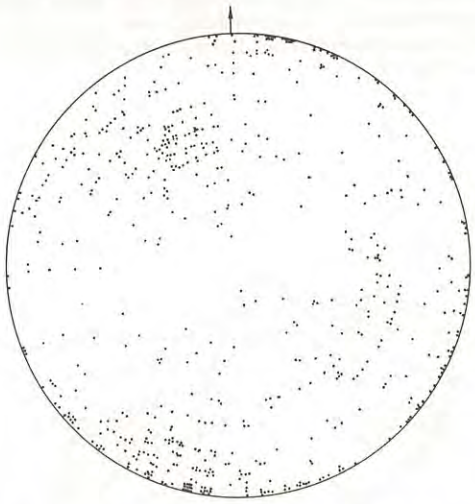

Fig. 1: Representation of joint orientations as poles on a Lambert Equal-Area Projection (631 poles to joints from Geehi Gorge, N.S.W.)

The traditional geologic method of contouring Schmidt Diagrams in terms of the density of poles as shown in Fig. 2 has statistical usefulness only when the underlying population is suspected of being uniform as demonstrated by Winchell (Ref. 5), and Flynn (Ref. 6). In most actual cases however, preferred orientations in geologic data are self-evident and the poles are seen to be clustered into groups which, in the case of joints, are called sets.

---

* Throughout this paper the lower hemisphere of the Lambert Equal-Area Projection is used.

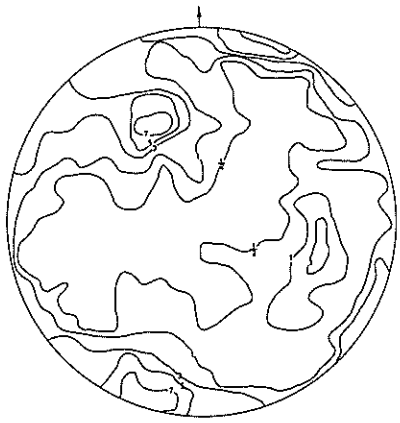

Fig. 2: Conventional contours of the density of poles shown in Fig. 1. Contours ½, 1, 3, 5, 7% per 1% area.

If it can be considered that the centre of the set represents the ideal orientation of the joints and that the scatter of joints around this ideal orientation is due to chance causes then, as shown by Vistelius (Ref. 7) and subject to some additional limitations discussed by him, the population distribution along any cross section through the joint set may be approximated by the Normal Distribution.

Extending this concept to three-dimensions, if the probability distributions along any two cross-sections at right angles through the population are normal and mutually independant, the population follows a two-dimensional normal distribution as shown in Fig. 3.

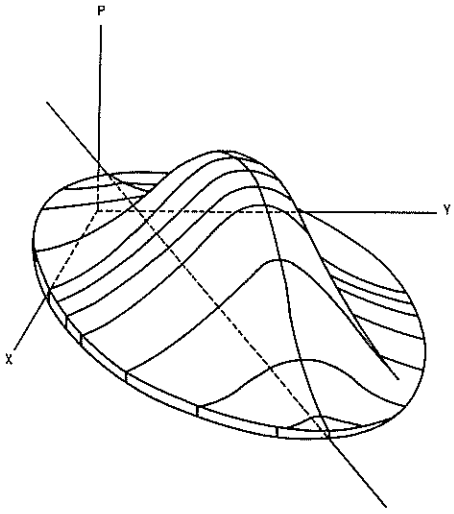

Fig. 3: Representation of a Two-dimensional Normal Distribution (From Crow, Davis and Maxfield Ref.8)

Fitting two-dimensional normal distributions to joint data is complicated by the presence of several joint sets, of which some may be overlapping. The following graphic procedure makes use of the powerful human ability for pattern recognition and, therefore in the writer's opinion, has considerable practical advantages over methods based on vector procedures which are purely mathematical and difficult to envisage.

The first step is to divide the joint system into joint sets using the density contours as a guide. Two great circles, mutually at right angles are then drawn along the directions of near-symmetry through the centre of each joint set. Fitting great circles in this manner is a standard procedure in structural geology (Ref. 1). Where the joint sets are elongated, the correct position of the great circles is obvious. Where the joint sets are near equant, the great circles may be placed arbitrarily.

The standard deviation of the angular distances of the joint poles is then determined along each great circle in turn. Where two joint sets overlap the standard deviations are computed from the non-overlapping portions.

Elliptical contours, distorted by the properties of the projection, are then drawn with the great circles as principal axes for various multiples of the standard deviation as shown in Fig. 4. These contours define the estimated probability distribution of the population represented by the joint set. They are smooth in contrast to the density contours whose minor irregularities are usually not reproducible for different samples, and are therefore meaningless in terms of the population.

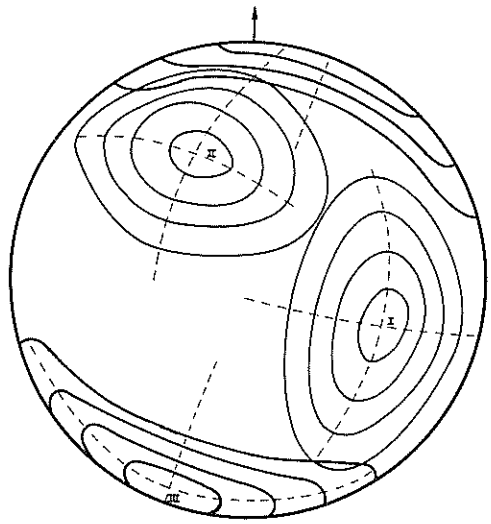

Fig. 4: Contours of 2-dimensional normal distributions fitted to three joint sets from the data shown in Figs. 1 and 2. Contours are ½, 1, 1½, 2 standard deviations from the mean.

The equation of the elliptical contours, may be derived from the standard formula for an ellipse. With respect to the two great circle axes labelled X and Y, the equation is:

$$y = \pm M^2 Sy^2 \left(1 - \frac{x^2}{M^2 Sx^2} \right)^{\frac{1}{2}} \quad \text{----- (1)}$$

Using the properties of the two-dimensional normal distribution given by Crow, Davis and Maxfield (Ref. 8), the theoretical probability of a joint falling within any part of the distribution can be computed. The goodness-of-fit of the distribution can therefore be checked by means of the Chi-Square Test (Ref. 8).

Although the normal distribution has the practical advantages that its properties are well known and easily accessible in tabulated form, its theoretical development assumes distribution on a plane and it is therefore an approximation when used to represent the distribution of points on a projection of a sphere. The approximation is best when the dispersion is small. If required, more precise representation such as Fisher's distribution on a sphere could be used (Ref. 15).

Although the writer believes that the two-dimensional normal distribution is probably the best estimation of the probability distribution of most natural joint sets it is emphasised that the proposed design procedure does not necessarily depend on this assumption. For example, in highly irregular joint systems it may be suspected that the underlying probability distribution is uniform. In this case the area enclosed by any density contour may be predicted from the Poisson Distribution (Refs. 3 & 5), and the goodness-of-fit determined by means of a chi-square test.

Where no theoretical distribution appears applicable, the sample frequency distribution may be taken as the best estimate of the population probability distribution. However, in this case, a much larger sample is normally required.

(d) Kinematic Testing

The purpose of kinematic testing is to determine the range of joint orientations for which movement is possible. If the action of the resultant force is to move the block into the slope then failure is clearly impossible and further consideration of the shear strength of the joint is unnecessary. Extensive discussions on kinematic tests for blocks bounded by two or three joints are given in Refs. 4,9,10 and 11. The simple tests given by Panet (Ref. 9) are particularly useful.

Panet's tests distinguish between wedge type failure, where the sliding occurs along the intersection of two joints, and block type failure where sliding occurs along a single joint. Wedge type failure is kinematically possible only if the line of joint intersection is undercut by the slope. Block type failure can occur only if the line of the direction of movement on the joint is undercut by the slope. Panet examines only the case where the direction of movement is along the true dip of the sliding joint which is the case where gravity and hydrostatic uplift are the only active forces. However the method can be generalised to include the effects of earthquakes and any external forces by using the methods described by John (Ref. 4) to determine the direction of the resultant force. The direction of movement is then given on the equal-area projection by the intersection of the great circle representing the joint plane and the vertical great circle containing the direction of the resultant force.

The problem of kinematic analysis is reduced to its simplest form in the situation where gravity and hydrostatic uplift are the only forces involved, sliding can occur only along one set of joints, and tensile separation can occur in many directions in the rock mass. Failure in this case is kinematically possible only when the true dip of a foliation joint is undercut by the slope.

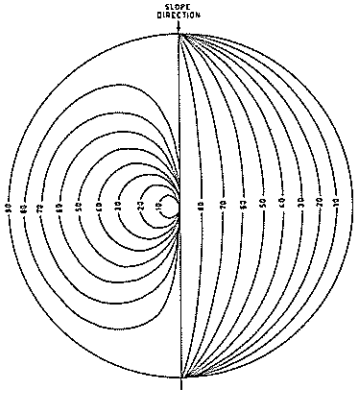

Fig. 5: Kinematic Test for sliding along a single joint. Use is explained in text.

On Fig. 5 the great circles on the right hand side of the diagram represent various possibilities for the design rock slope. The closed curves on the left hand side are the loci of the poles of the joints whose true dips lie on the corresponding rock slope (e.g. joint 3 in Fig. 4). These curves enclose the poles of all joints whose true dips are undercut by the indicated slope; that is, all joints that are kinematically unstable with respect to the slope.

(e) Limiting Equilibrium Analysis

A review of limiting equilibrium methods by Hoek (Ref. 12) shows that the relationship between shear stress τ and normal stress σ at failure can be adequately approximated by a straight line relationship:

$$\tau = c + (\sigma - u) \tan (\phi + i) \quad \text{---- (2)}$$

In rock slopes the cohesion c is primarily due to the presence of rock bridges between joints as discussed by Jennings (Ref. 13) and Robertson (Ref.2). The surface friction ϕ is determined by the nature of the rock material and probably by the effects of minor undulations on the joint surface.

The angle of roughness (i) is defined by Patton (Ref. 12) as the average angle between the major undulations on the joint surface and the direction of sliding along the joint.

In the writer's opinion, the best estimates of the shear strength parameters are those obtained by back-calculation of existing slope failures using the same analytical method that will be used to design the planned slopes. Assuming that the sliding blocks can be regarded as rigid and as long as the old failures are in slopes of approximately the same height as the planned slopes and have similarly continuous joints the cohesion and friction can be treated as a single angular quantity (ϕa), computed as follows:

$$\phi_a = \tan^{-1} \left(\frac{\tau}{\sigma} \right) \quad \text{---- (3)}$$

Usually the least satisfactory aspect of back-calculating old failures is that the groundwater conditions at failure are poorly known. However, a realistic approach is to use the same assumptions regarding the height of the water table in both the back calculation and the design analysis. A conservative approach is to assume a higher level for the water table than that used in the back calculation.

In areas where old landslides are not available, the shear strength parameters must be estimated from laboratory and field tests and by judgment based on first principles. In this case, particularly, careful observation of the slope behaviour in the early stages of construction, followed by re-design if necessary, should be considered an integral part of the design process.

The designer has the option of applying a safety factor during the limiting equilibrium analysis (Ref. 4). The value assigned will naturally depend on the purpose of the slope and the possible consequences of failure.

In most cases however, where partial failures are considered acceptable, the writer prefers an approach whereby the limiting equilibrium analysis is carried out for a safety factor of one and judgement applied to the consideration of an acceptable level for the probability of failure.

In the case of a simple block slide an area of kinetic stability is defined as a small circle of angular radius ϕa centred on the piercement point of the resultant force. For a dry rock slope affected only by gravity this small circle is centred on the centre of the projection as shown in Fig. 6 for the example where ϕa is 34°.

Superposition of the small circle defining the area of kinematic instability and the curves defining areas of kinematic instability for various design rock slope angles on the probability distribution of the joint set 1 (from Fig. 4) is shown in Fig. 6. Joints with poles lying inside the area of kinematic instability and outside the area of kinetic stability are in unsafe orientations with respect to the indicated slopes.

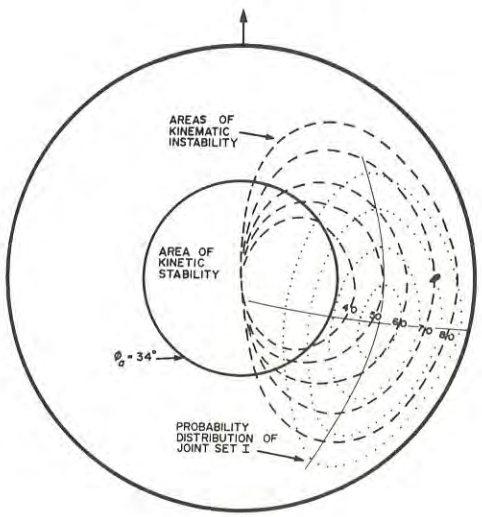

Fig. 6: Superposition of area of kinetic stability and areas of kinematic instability on the probability distribution of a joint set. Contours of the joint set are ½, 1, 1½, 2 standard deviations from the mean.

(f) Determination of the Probability of Joints Occurring in Unsafe Orientations

In any small portion of a rock mass joints are usually found to occur in between 3 and 6 directions. Where the joint system can be divided into sets it can be assumed for the purposes of slope design that one member of each set is present in any small element of the rock mass.

For any specific rock slope, it is usually found that sliding can occur only along joints belonging to one or two of the joint sets. These joint sets and the safe and unsafe orientations within them are determined by superimposing the results of the kinematic and limiting equilibrium analyses on the contours of the joint set. The probability that a joint will occur in an unsafe orientation behind the slope is obtained in one of the following three ways:

(1) If the joint set fits a two-dimensional normal distribution the probability that the joint will occur in an unstable orientation can be determined by the graphic transformation (for example Fig. 7 shows a graphic transformation of Fig. 6) which is superimposed one quadrant at a time over the Rectangular Normal Probability Chart published by Crow, Davis & Maxfield (Ref. 8) and reproduced in Fig. 8. The probability of an event occurring in any portion of this diagram can then be determined by counting rectangles.

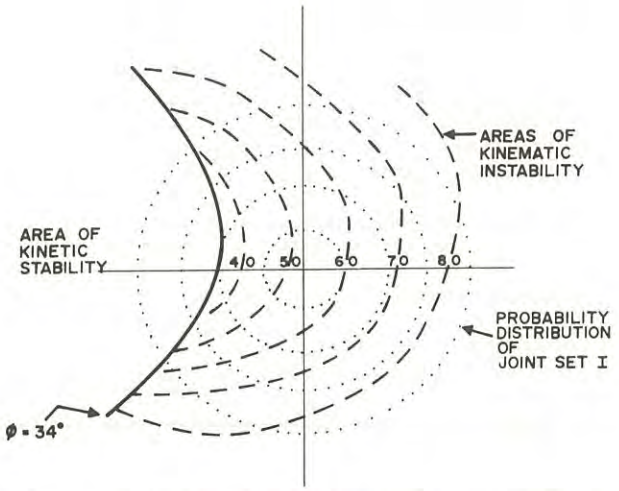

Fig. 7 : Graphic transformation of the data on Fig. 6. The elliptical contours defining the probability distribution of the joints in Fig. 6 are transformed to circles of radius suitable for superposition on Fig. 8.

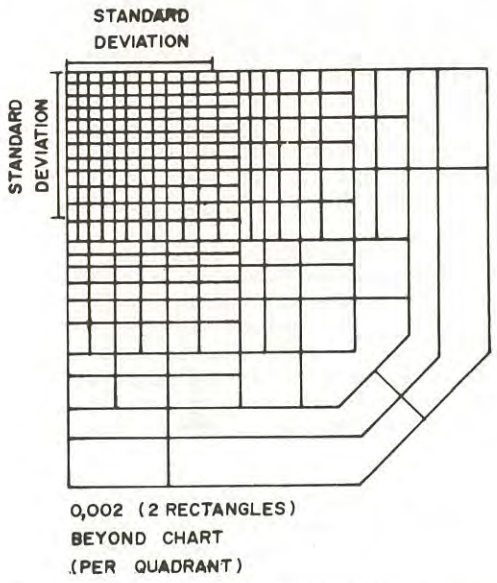

Fig. 8: Rectangular Normal Probability Chart Reproduced from Crow, Davis and Maxfield (Ref. 8) and attributed by them to A.D. Sprague. Each rectangular area represents a probability of 0.001.

(2) If the joint system has a uniform population distribution the probability Pj that a joint will occur in an unstable orientation is given by:

$$Pj = Na\,(Au/At) \quad \text{---- (4)}$$

(3) If the assumption is made that the sample distribution represents the best estimate of the population probability distribution the probability that a joint will occur in an unstable orientation is given by:

$$Pj = N_a\,(Nu/Nt) \quad \text{---- (5)}$$

(g) Determination of the Probability of Failure for a Range of Slope Angles.

In simple cases where the joints are uniformly continuous for distances that are large compared to the size of the slope, the probability that a joint occurs in an unstable orientation, Pj, can be taken as the probability of failure. Where only a proportion, Pc, of the joints of any set are sufficiently continuous to result in a slope failure the probability of failure, Pf, is given by:

$$Pf = Pj.Pc \quad \text{----(6)}$$

The probability of failure is then computed for a range of slope angles as shown in Fig. 9.

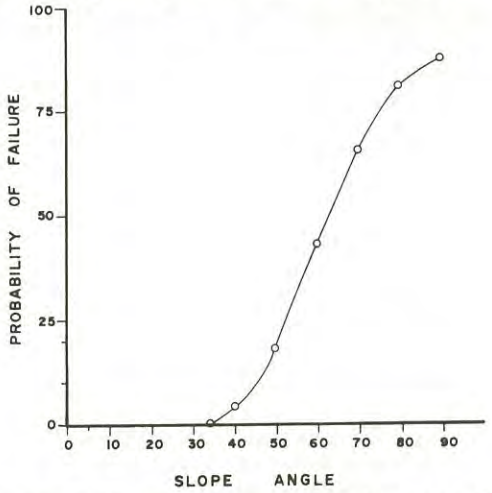

Fig. 9: Curve of Probability of Failure vs. Slope Angle for the example shown in Figs. 6 and 7. (In this case Pc = 1).

Where a slope is to be designed with safety as the over-riding consideration, the slope angle at which the curve becomes asymptotic to zero would be the appropriate design angle. Where partial slope failure can be contemplated the design slope angle is determined as described in the following section.

(h) Determination of the Most Economic Slope Angles

The total cost of a rock slope is given by:

$$C_t = C_o + C_f \quad \text{---- (7)}$$

where:

C_t = the total cost of the slope

C_o = the initial cost of excavation

C_f = the cost of failure

For any rock slope the initial cost of excavation can be considered to be the cost of excavation of the volume of rock in excess of that required for a vertical rock slope; therefore:

$$C_o = co\ Vo \quad \text{---- (8)}$$

where:

co = the unit cost of bulk rock excavation

V_o = the volume of rock excavated in excess of that required for a vertical slope

The cost of slope failure is given by:

$$C_f = P_f (C_a + C_b V_f) \text{ ---- (9)}$$

Where C_a represents those costs that are independant of the volume of material in the slide, such as part of the costs for loss of production, mobilization of equipment, and the costs of slope monitoring.

Determination of the portion of the cost of failure that is proportional to slide volume is complicated by the fact that the probability of failure and the expected volume of failure are related quantities and are both determined by the probability distribution of the joints behind the slope. A steep slope will fail back to the plane of the undercutting joint which can lie anywhere between the plane of zero probability of failure and the excavated slope surface. The product Vf Pf is therefore best determined by an incremental procedure as follows:

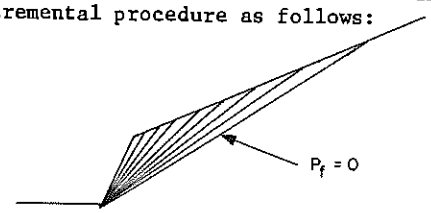

Fig. 10: Slope divided into a series of n elements.

If the slope is considered to be divided into a series of n elements as shown in Fig. 10 such that the base of the 1st element is along the plane with zero probability of failure, the top of the nth element is along the proposed slope surface, the volume of the ith element is Vi and the probability that a joint undercuts the base of the ith element is Pi then:

$$P_f V_f = \sum_{i=1,n} P_i V_i \text{ ----- (10)}$$

Fig. 11 shows the curve of total cost per foot of slope vs. slope angle for the example, assuming $C_a = 0$ and the slope direction and probability distribution of the joints are as shown in Fig. 6 and the probability of failure is as shown in Fig. 9.

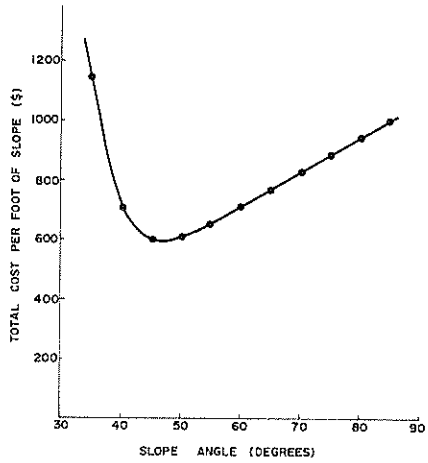

Fig. 11: Plot of Total Cost of Slope vs. Slope Angle.

The following conclusions may be drawn from Figs. 9 and 11:

(1) The slope with the least total cost ($600 per foot of slope length) is between 45 and 50°. The probability of failure for a slope of 45° is 10% compared to 19% for a slope of 50°.

(2) The slope with zero probability of failure is 34°. This slope has a total cost of $1,130 per foot.

It is interesting to note that a safety factor of 1.5, applied to the slope of zero probability of failure in this case would result in a cut slope of 24° which would be 3° flatter than the natural slope. This illustrates the absurdity of applying arbitrary safety factors to slope designs already based on the worst likely conditions.

V EXTENSION OF THE PROCEDURE TO SLIDING ON COMBINATIONS OF JOINTS

When more than one joint set is involved in the formation of the sliding surface the problem is complicated by the fact that the joint sets are rarely independant in their orientations. A conservative method is to assume that the joint sets are completely dependant so that any joint in the first set will be combined with a joint in the second set that is orientated to form the least stable combination. The methods of John (Ref 4) can then be used to define the areas of kinematically and kinetically unstable orientations for joint set 1. The slope design can then be completed as described in the previous section.

The least conservative approach is to consider that the joint sets are independant so that the probability of finding any combination of orientations is the product of the probabilities of finding each orientation alone. An intermediate approach, which the writer feels is probably the most realistic in many cases is to assume that any joint in one set is combined with the mean joint orientation in the other set.

In open pit mines large scale failures occur along complex failure surfaces which may consist partly of major weakness such as faults and partly of step-like surfaces composed of many joints. If as shown in Fig. 12, the failure is rotational it may be analysed by the methods of soil mechanics as suggested by Wilson (Ref. 14) using the failure criterion given in equation 2. In this case one of the principal variables is the roughness of the step-like series of joints. The probability distribution of the roughness can be determined for any small portion of the failure surface by the following method:

(1) Determine the probability distribution of the joint set forming the flatter portion of the step.

(2) Plot the direction of the average failure surface as a pole. The angle between this pole and a given joint orientation is the angle of roughness where this joint direction prevails.

(3) Determine the probability that a joint pole lies within any required radius of the pole to the failure surface by constructing inclined small circles around the pole and analysing by the graphic procedure described in the preceding section.

(4) The probability of failure is then given by the probability that the roughness is less than that required to provide the required safety factor.

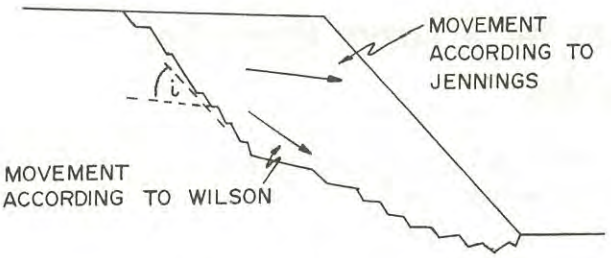

Fig. 12: Rotational Failure along step-like patterns of joints.

If as shown in Fig. 12, the failure takes place by sliding along the flatter joints and separation along the steeper joints as suggested by Jennings (Ref. 14) the problem is simply an extension of the problem of sliding along a single joint as described in the preceding example.

In actual slopes, the sliding mass is of course non rigid and the initial movement is probably partly rotational and partly transitional.

If the step-like failure surface is considered to be very large with respect to the joint spacing so that it contains a large number of joints then the mean direction of the joints, in the direction of sliding, can be used in the analysis as suggested by Jennings (Ref. 14). In this case the probability that the joint continuity is greater than the value required for stability may become the principal basis for design.

For very large slopes the probability that the slope will fail can be interpreted as the percentage of the slope that can be expected to fail. Estimation of this percentage is the principal problem in open-pit design.

CONCLUSIONS

The probability of failure provides a realistic basis for the design of rock slopes where the locations and orientations of the rock defects behind the slope are not known in detail.

ACKNOWLEDGEMENTS

The writer is particularly grateful for the encouragement by Dr. Ing. Klaus John of Karlsruhr whose pioneering work in the graphic analysis of rock slopes provided the inspiration for this study. He is also grateful to Mr. John Herington of the Sydney office of Dames and Moore for his assistance and constructive criticism during the preparation of this paper.

Permission of Dames and Moore, Consulting Engineers in the Applied Earth Sciences, for the publication of this paper is also acknowledged.

REFERENCES

1. Turner, F.J. and Wiess, L.E. - Structural analysis of the metamorphic tectorites, especially Chapter 3, Graphic Treatment of Fabric Data. New York, McGraw-Hill, 1963 pp 46-75.
2. Robertson, A. MacG. - The Interpretation of Geological Factors for Use in Slope Theory, Preprints South African Symposium on Slope Stability in Open-Pit Mines, Sept. 1970.
3. McMahon, B.K. - Indices related to the mechanical properties of jointed rock, in Grosvenor N.E. and Paulding B.W. Ed., Status of Practical Rock Mechanics, New York, American Institute of Mining, Metallurgical and Petroleum Engineers Inc., 1968 pp 117 - 133.
4. John, K.W. - Graphical stability analysis of slopes in jointed rock. J. Soil Mech. and Found. Div. Proc. A.S.C.E. Vol. 94, SM2. March 1968 pp 497-526 with discussions and closure Vol. 95 SM6 Nov. 1969 pp 1541 - 1546.
5. Winchell, M. - A new method for the interpretation of fabric diagrams, American Mineralogist 1937, Vol. 22, pp 15 - 36.
6. Flynn, D. - On tests of significance of preferred orientation in three-dimensional fabric diagrams, J. Geol, 1958, Vol. 66, pp 526 - 539.
7. Vistelius, A.B. - Structural Diagrams, Permagon 1966, 176 pp.
8. Crow, E.L., Davis, F.A., Maxfield, M.W. - Statistics Manual, New York, Dover Publications, 1960, 288 pp.
9. Panet, M. - Discussion on Graphical Stability Analysis of slopes in jointed rock by K.W. John, J. Soil Mech. and Found. Div. Proc. A.S.C.E., Vol. 95, SM2, March 1969 pp. 685 - 686.
10. Wittke, W. - Verfahren zur Berechnung der Standsich er heit belasteter und unbelasteter Felsboschungen (A Numerical method of calculating the stability of loaded and unloaded rock slopes) Felsmechanic und Ingenieurgeologie Supp. 2, Safety in Rock Engineering, Springer,1963 pp 52-79.
11. Londe, P. Vigier, G. and Vormeringer, R.- Stability of Rock Slopes, A three-dimensional study, J. Soil Mech. and Found. Div. Proc.A.S.C.E. Vol. 95 SM1, January 1969, pp 235 - 261.
12. Hoek, E., 1970, Rock Slope Stability in Open-Cast Mining, Rock Mechanics Progress Report, Imperial College, No. 4, July, 1970, 71 pp.
13. Jennings, J.E. - A mathematical theory for the calculation of the stability of slopes in open-cast mines, Preprints, South African Symposium on Slope Stability in Open-Pit Mines, Sept.1970.
14. Wilson, S.D. - The application of Soil Mechanics to the stability of open-pit mines. Third Symposium on Rock Mechanics, Colo. School of Mines Quarterly Vol. 54, No. 3, 1959, pp 94 - 113.
15. Fisher, R.A. - Dispersion on a Sphere. Proc. of Royal Soc. of London, 1953, Series A. Vol. 217, pp 295.

Rock Mechanics Investigations for a Large Open Cut at Mount Isa

By

K. J. Rosengren, B.C.E., B.M.E., M.Eng.Sc., Ph.D., M.I.E.Aust., A.M.Aus.I.M.M.

(Senior Rock Mechanics Engineer, Mount Isa Mines Limited)

SUMMARY.- As part of a feasibility study of open cutting the outcropping portions of the Black Star lead orebodies at Mount Isa, a rock mechanics investigation into the stability of the proposed western batter has been carried out. Detailed structural measurements were made on oriented diamond drill core to determine the pattern of jointing in the area. Laboratory sliding tests were conducted on typical joint surfaces to provide data on frictional characteristics. Slope stability analyses, based on equilibrium of blocks and wedges formed by the joint systems, indicate that quite steep overall batter slopes are possible.

I.- INTRODUCTION

The Black Star lead orebody was one of the original outcrops discovered at Mount Isa in 1923. It proved to be very large, although of rather low grade, and mining commenced in 1931. The upper carbonate ore was mined by glory-holing to a depth of 100 ft. Below this depth the sulphide ore was mined by open stoping although the stopes were subsequently filled, mainly with surface overburden.

There is sufficient high grade ore remaining in pillars and lower grade ore not considered payable in the early mining to make open cut mining an economic proposition, using modern excavation techniques.

The orebody is tabular in shape, some 200 ft wide, striking north-south and dipping 65° west. The proposed open cut is fairly rigidly defined by existing surface structures and would be 2200 ft long x 1400 ft wide on the surface. It would be 550 ft deep and total excavation of ore plus waste would exceed 30 million tons.

Because of the major nature of this open cut it was considered essential to include a rock mechanics study of batter stability in the feasibility study. The only other large open cut operation at Mount Isa was situated in the Black Rock secondary copper orebody (Ref. 1). This open cut was completed some 40 ft short of its planned depth of 520 ft owing to instability of the western batter (Ref. 2).

The preliminary study was restricted to the western or hanging wall batter for the following reasons.

(i) In-stability of the western batter had caused premature closure of the Black Rock open cut some 2000 ft further south.

(ii) The longer sides of the open cut were more likely to show instability than the shorter sides, which gain support from their arch shape.

(iii) The eastern batter was unlikely to present a major problem, since the bench slope would coincide with the average bedding dip.

Since it is well established that the stability of slopes in hard unweathered rock is controlled principally by the distribution of structural defects in the rock (Ref. 3), the rock mechanics investigation was concerned primarily with the geology and structure of the rocks in the batter area.

II.- NOTATION

α	Angle of joint plane to horizontal
β	Angle of slope to horizontal
δ	Angle formed by stepped failure surface
γ	Unit weight of rock
H	Vertical height of slope
Z	Depth below surface of secondary failure plane
F	Factor of safety
c	Cohesion parameter for sliding on joint
ϕ	Friction parameter for sliding on joint

III.- GEOLOGY AND STRUCTURAL ANALYSIS

None of the mine openings penetrated the area and only meagre information was available from the logs of diamond drill holes put down some 40 years earlier. Further exploration was required and diamond drilling was selected as the most economical method. Since the bedding orientation in the Urquhart Shale and Spear Siltstone appeared reasonably uniform in the area, it was hoped that the diamond drill core could be oriented to give maximum information on structural defects.

To explore the structure in three dimensions, three mutually perpendicular drill holes are, ideally, required. There are, however, certain limitations on the drill hole orientations to ensure favourable intersections with bedding planes for core orientation purposes. After possible drilling sites had been

considered, two intersecting horizontal holes, denoted A and B were drilled from No. 4 level development (350 ft below surface) and a hole dipping east, denoted C, was drilled from the surface (Figs. 1 and 2). Each hole was approximately 800 ft long and drilled NMLC size with a triple tube core barrel and hydraulic feed drilling machine; this equipment is essential for successful structural drilling (Ref. 4). High core recovery was obtained and most of the core was ultimately oriented.

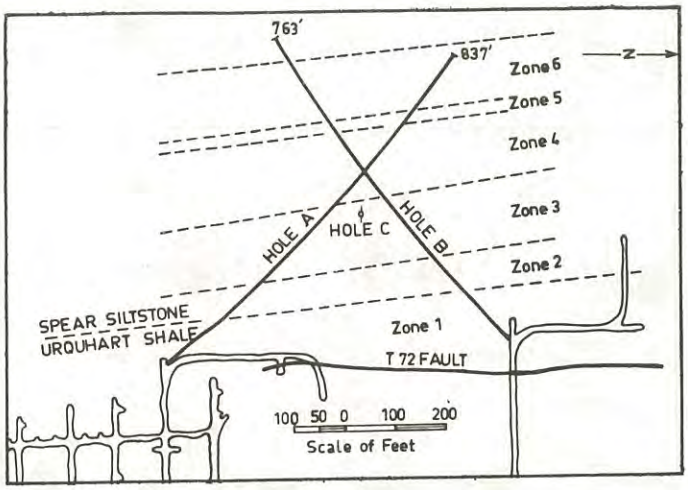

Fig. 1 Plan of No. 4 level horizon showing drill holes A and B and rock zones.

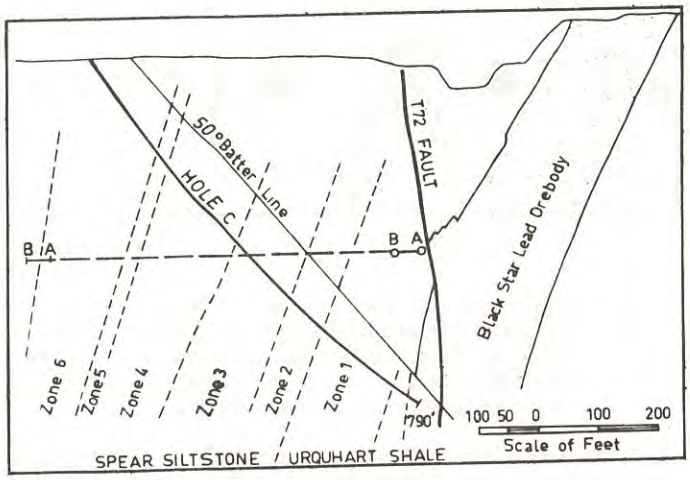

Fig. 2 Cross-section showing drill hole C and rock zones.

Six different rock zones were delineated by correlations of tuff marker beds and changes in rock type in the three holes. Briefly, these were

1. thin bedded Urquhart Shale with two sub-zones, one highly pyritic and the other non-pyritic;

2. coarse bedded dolomitic siltstone;

3. bedded gradation of siltstone, mudstone and slate;

4. intensely sheared black slate;

5. thin zone of sedimentary breccia;

6. thin bedded light grey slate.

All except zone 1 are part of the Spear Siltstone formation (Ref. 5).

The core was fitted together and a reference line drawn along it. The orientation of bedding planes and any breaks was measured relative to the core by two angles.

(i) angle between feature and core axis

(ii) angle between major axis of elliptical trace of the feature and the reference line, measured on the circumference of the core.

Breaks were classified as bedding or joints, and artificial breaks obviously caused by drilling were not counted (Ref. 6).

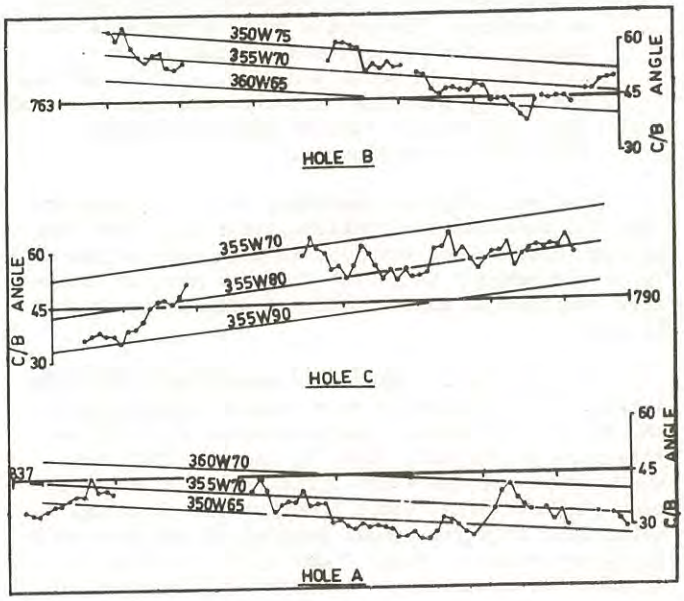

Fig. 3 Variation of the 10 ft average core bedding angle in the three exploratory holes.

The core bedding angle, defined as the angle between bedding trace and core axis was measured at 3 in. intervals, where possible. 10 ft average values are shown in Fig. 3 and there is only a relatively small scatter about the average 335° strike and W70° dip defined by the rock zone boundaries shown in Figs. 1 and 2. This proved that the bedding orientation is reasonably constant and that there is no major folding; thus the core orientation procedure should be successful.

The core was oriented in 10 ft sections by calculating the most likely bedding orientation from the average core bedding angle and rotating the core axis and bedding orientation to their true positions in space on a stereographic projection. The orientation of joints and other structural features in the core was then determined. A computer program

was developed which plotted contoured equal area projections of the joint poles and which automatically weighted the readings to compensate for the effect of drill hole orientation using the method of Terzaghi (Ref. 7).

Contoured equal area projections of the weakness plane orientations in the various zones are shown in Fig. 4. Three joint sets are evident.

(i) Bedding joints, striking north south and dipping 70° west are prominent in zones 1 and 2. Bedding is present, but is not a major weakness plane, in zones 3 to 6.

(ii) Microfaults, parallel to the cleavage in the slates, striking north south and dipping 70° to 80° east are most prominent in zones 3 to 6. Although shear features, these are typically discontinuous and are mainly breaks on chlorite filled veins.

(iii) In all zones there is a family of joints whose poles lie in a girdle containing the bedding plane; the joints are therefore perpendicular to bedding. The girdle usually contains two maxima defining joints described as set 1, striking north south and dipping 20° - 30° east, and set 2, striking east-west and near vertical. These joints are tension features and are typically discontinuous.

Analysis of joint spacings, including corrections for borehole inclinations, indicates that the average spacing for each set in each zone is generally in the range 1 to 2 ft. The rock mass is therefore composed of approximately equidimensional unit blocks.

No major fault zones were encountered although drill core cannot easily distinguish between minor and major structures. The pattern of faulting in this part of the mine (Ref. 5) is such that only north-south and east-west striking faults, both with near vertical dips, would be expected. Both types, determined from geological mapping of the mine workings, are shown in Figs. 1 and 2, but neither is oriented unfavourably with respect to the open cut batter.

IV.- STRENGTH PROPERTIES OF JOINTS

Sliding friction tests were conducted on typical specimens of the various joint sets using a modified triaxial cell which permitted large displacements on the joint plane (Ref. 6). Despite wide variations in surface roughness and surface coatings the frictional properties fell within a relatively narrow range. In nearly all cases the shear stress - normal stress plot gave a linear relation with an angle of friction ϕ in the range 25° - 35° and a cohesion intercept, c, in the range 50 - 200 lb/in.^{2}. Furthermore, these values were not significantly altered by pore pressure in the joint, provided that the results were calculated in terms of effective stresses.

V.- SLOPE STABILITY ANALYSIS

Because of the well defined bedding and jointing in the rock forming the batter, it was considered that limit equilibrium analysis of blocks sliding on these weakness planes was the most appropriate method of stability analysis for a preliminary study. The three major weakness planes determined by the structural analysis influence the stability as follows.

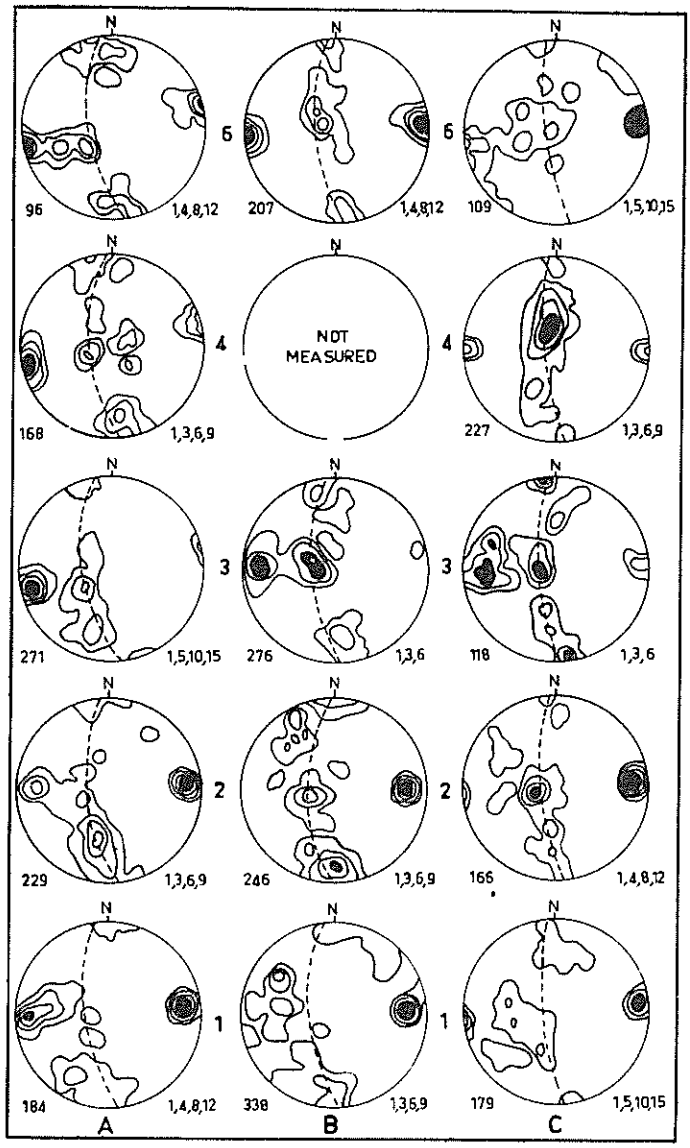

Fig. 4 Contoured equal area lower hemisphere projections showing weakness plane orientations as determined from oriented drill core. Numerals denote number of readings and contour intervals respectively.

(i) The bedding planes cannot be primary surfaces of failure since they dip into the batter. They can, however, be important secondary failure planes which separate blocks tending to slide on other planes.

(ii) The microfaults dip in general, from 70° east to vertical. Therefore they cannot be primary surfaces of failure, but will again be important secondary failure planes.

(iii) The joints normal to bedding are likely to be the most important primary failure planes in the batter. The east dipping joints will provide single planar failure surfaces. In addition, the wide range of orientation of the joints means that tetrahedral blocks of a variety of shapes will have questionable stability.

(a) Plane Failure

The simplest case of plane failure is that of a slope of height H and inclination β, containing a continuous joint plane with inclination α passing through the toe (Fig. 5(a)). The factor of safety (F), defined as the ratio of resultant available resisting force to the resultant force tending to cause collapse, is given by

$$F = \frac{\tan\phi}{\tan\alpha} + \frac{2c\sin\beta}{\gamma H \sin\alpha \sin(\beta-\alpha)} \qquad (1)$$

Therefore, for given values of α, c and ϕ the factor of safety is a function both of the height H and inclination β of the slope. For c = 0 the slope will be stable only if $\alpha < \phi$

The presence of bedding planes and microfaults makes this mode of failure, termed case A, rather unlikely. More likely failure modes are shown in Fig. 5(b) and 5(c) with secondary failure on bedding (case B) and microfaults (case C), respectively. However for both these cases the expression for factor of safety is identical with equation (1). Since the factor of safety is inversely proportional to H, the height of the sliding block, for any given slope the most likely sliding plane is that passing through the toe of the slope.

A more critical condition is shown in Fig. 5(d) where the secondary failure plane is located behind the top of the slope (case D). This is analagous to the case of a tension crack in slope stability analysis and the factor of safety is given by

$$F = \frac{\tan\phi}{\tan\alpha} + \frac{2c\left(1-\frac{Z}{H}\right)}{\gamma H \sin^2\alpha\left(\cot\alpha - \cot\beta - \left(\frac{Z}{H}\right)^2\cot\alpha\right)} \qquad (2)$$

where Z is the depth below surface of the secondary failure plane. The factor of safety in this case is a minimum when the secondary failure plane is approximately midway between the top of slope and trace of the primary failure plane.

TABLE I

VALUES OF COHESION NECESSARY TO MAINTAIN STABILITY

Slope angle degrees	Cases A,B,C lb/in.^{2}	Case D lb/in.^{2}
40	8	9
45	15	16
50	20	23
55	24	30

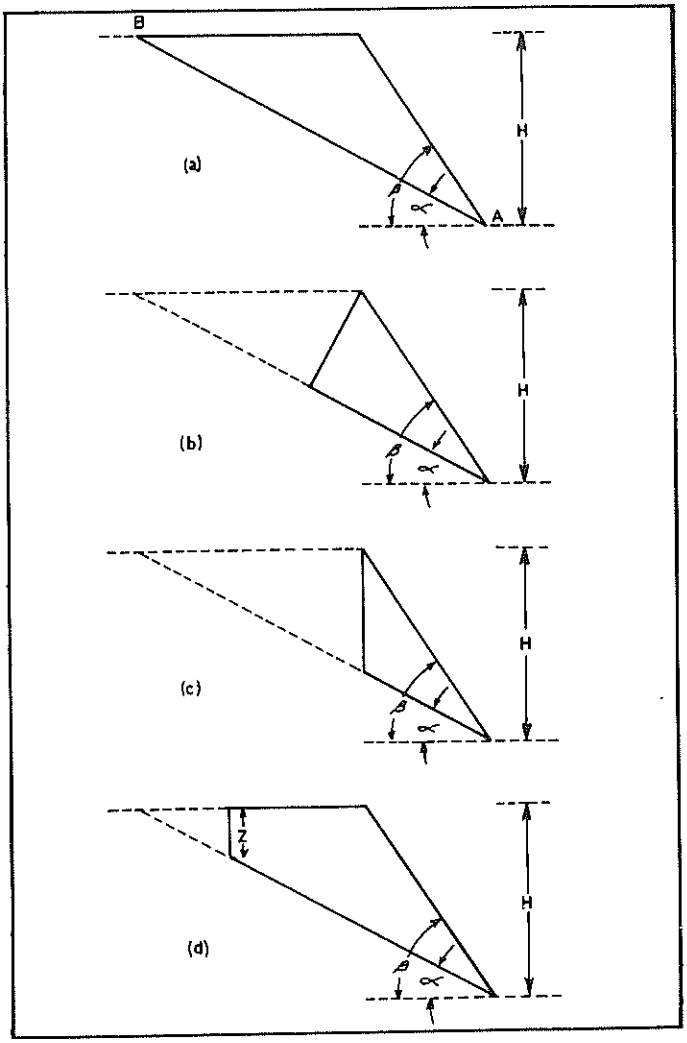

Fig. 5 Four possible cases of plane failure on east-dipping joints.

The joints are statistically normal to bedding which dips west 60° to 80° and the angle α is generally in the range 30° to 10°. Since ϕ normally lies between 25° and 35°, in most cases stability can be maintained by friction alone. Under certain circumstances, however, a joint with high angle may have low friction angle ϕ. The worst combination likely to occur is α = 35° and ϕ = 25°. For H = 550 ft and γ = 165 lb/ft^3 the values of cohesion c, required to maintain stability (F = 1.0) are set out in Table I.

These cohesion values are small compared with those measured in laboratory sliding friction tests on joints, which were in the range 50 to 200 lb/in.^{2}. Moreover the analysis is conservative, since the joints are characteristically discontinuous, and for failure to occur material bridges must be sheared or, alternatively, a continuous but stepped failure plane formed. In the latter case (Fig. 6) the stable slope for c = 0 is $(\alpha + \delta)$ where the angle δ is a function of the shape of the unit blocks formed by the joint sets. For equidimensional blocks, which approximate the present situation, δ = 26° and the

stable slope for $\alpha = 30^{\circ}$ is 56°.

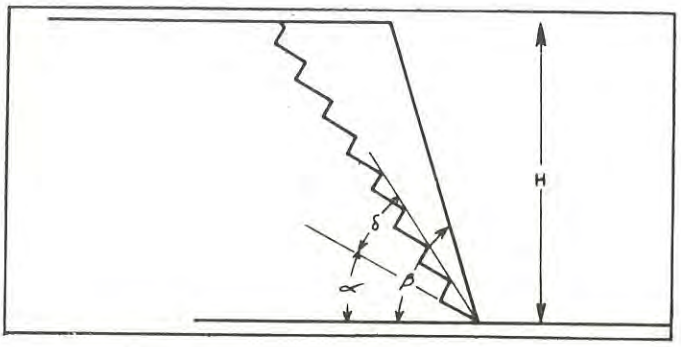

Fig. 6 Stepped failure surface resulting from a discontinuous joint set.

An additional factor which must be considered is the stability of individual bench faces, which would normally be designed with height approximately 70 ft and slope approximately 70°. Blocks formed by microfaults with dips less than 70° east will be inherently unstable, since very high cohesion values would be required to maintain stability. However, as shown in Fig. 4 the microfaults are normally steeply dipping and this situation would arise only in isolated cases.

Analysis of sliding on east dipping joints is identical with that given in equations 1 and 2. Cohesion values equivalent to those given in Table I for a 70 ft high 70° bench slope are 5 lb/sq.in. and 7 lb/sq.in. for cases A, B, C and case D, respectively. It is clear therefore that individual bench slopes should be generally stable with respect to the east dipping joints.

(b) Wedge Failure

The wide range of orientations of joints normal to bedding, makes it probable that in many cases the mode of failure will be by sliding of a tetrahedral wedge on two inclined joints. A typical situation is shown in Fig. 7(a); partial block failures, as in Figs. 5(b), (c) and (d) are similarly possible.

If contact is maintained on both joint faces during sliding, there is only one possible slip direction, which is the line of intersection of the two planes. Since the joint poles lie in a great circle girdle, the line of intersection of any combination of joints must be the pole of the plane containing the joint poles, which in this case is the pole of the bedding plane (Fig. 7(b)).

The analysis of stability of such a wedge follows exactly that given above for plane failure, except that the geometry is more complex. However, a method developed by John (Ref. 9) permits a rapid graphical appraisal of the situation. Considering frictional resistance only when the wedge is on the point of sliding, the resultant force on the wedge from each joint plane must lie in a plane containing the pole of the joint plane and the slip direction. When friction is fully mobilised the resultant forces, R_1 and R_2, must be located at ϕ degrees along

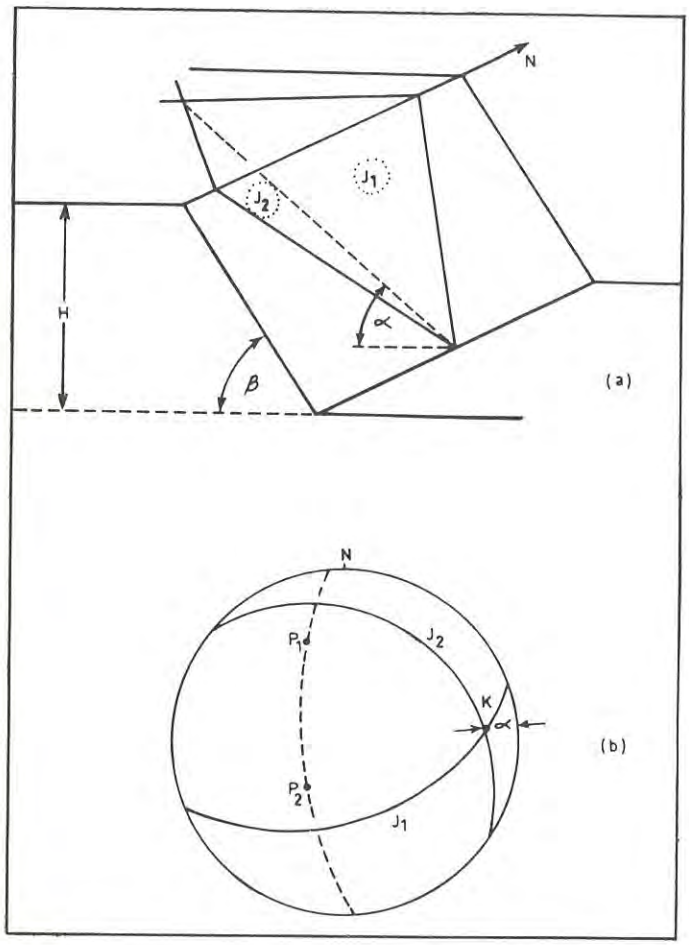

Fig. 7 Wedge failure on two incline joints with stereographic projection showing slip direction.

the great circles from the respective poles of the joint planes in the correct sense (Fig. 8 (a)). For equilibrium to be maintained, the plane containing the resultant forces R_1 and R_2 must also contain the direction of the resultant disturbing force on the wedge. If gravity is the only disturbing force, R_1 and R_2 must lie in a vertical plane. The case of different coefficients of friction on the two planes is easily included.

An example is shown in Fig. 8(b) for two joints intersecting to give $\alpha = 30^{\circ}$. In this case, the angle of friction mobilised on each joint plane to preserve stability is 22°. For a given value of α it can be shown that the angle of friction mobilised increases from zero to a maximum as the two joint poles move from the primitive of the projection (corresponding to two parallel east-west vertical planes) towards coincidence in a vertical plane normal to the batter (corresponding to a single failure surface shown in Fig. 5(a)). Therefore, wedge failure is not as critical as plane failure in this situation where the joints are normal to bedding. This is not necessarily so in the general case where there are no restraints on the orientation of the joint planes.

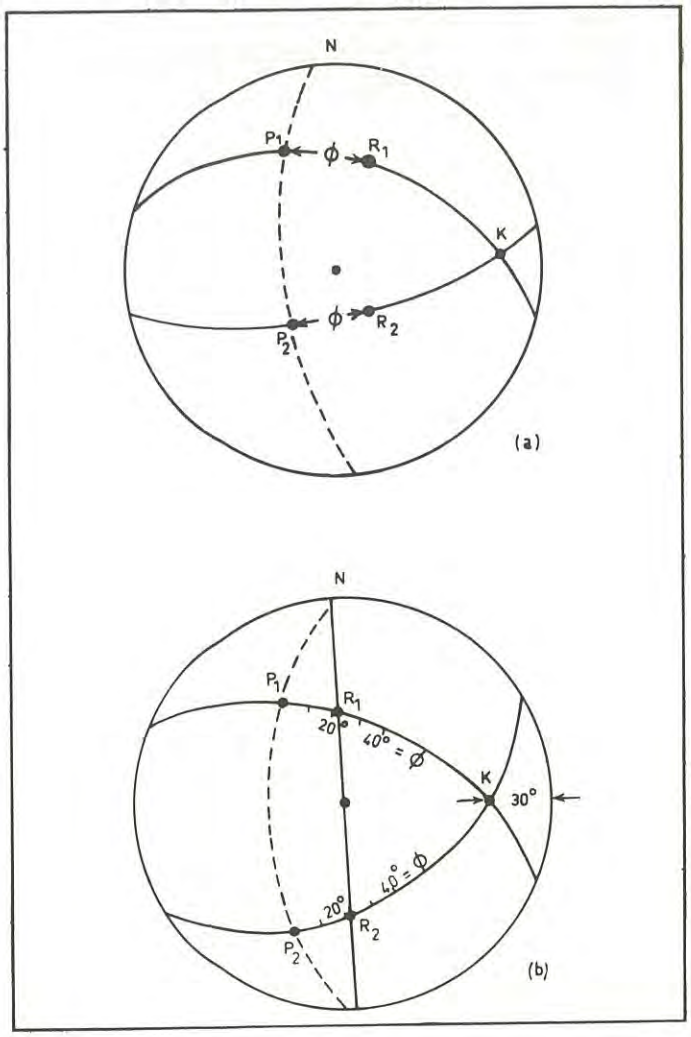

Fig. 8 Stereographic projections illustrating resultant forces on sliding wedge.

(c) Effect of Water Pressure

The whole of the above analysis has assumed that the slope is fully drained. In the present case this is a reasonable assumption since the slope directly overlies the worked out stopes of the 650 copper orebody (Ref. 1) and the water table in the area is likely to be well below the bottom of the open cut. In fact, considerable trouble was experienced with loss of water circulation during the drilling of the structural holes described in Section III.

However, high rates of precipitation occur in the Mount Isa area during the wet season and it is possible that significant transient cleft water pressures may occur under these circumstances. Since the stability of the batter is dependent primarily on frictional resistance of the joints, it is essential that the phreatic surface for seepage through the batter should be kept below the potential slip planes through the toe at each stage of open cut development. Adequate drainage provision and field piezometer installations will therefore be an integral part of open cut design and operation.

VI.- CONCLUSIONS

The simple calculations show that major sliding can occur only on the east dipping joints and that in the worst case stability can be maintained by small values of joint cohesion. Quite steep batter slopes are therefore theoretically possible. However since the various assumptions are largely untested on a large scale, an overall slope of 50° is considered optimum for initial design, provided adequate drainage measures are included; this represents an increase of at least 5° on what could be proposed from experience in the Black Rock open cut. In any case, a slope of this order will be near the maximum on geometrical grounds, allowing for minimum width berms and a spiral haul road.

Rock mechanics investigations will not cease at the conclusion of the feasibility study. The open cut will be continuously monitored during operation and the further information on structure and other variables obtained as excavation proceeds will permit progressive amendments to the design to suit the particular circumstances.

VII.- ACKNOWLEDGMENTS

The major part of this work was carried out between 1966 and 1968 during the tenure of a Research Scholarship at the Australian National University. The author is grateful to Professor J.C. Jaeger for his guidance and encouragement during this period.

The author wishes to thank Mount Isa Mines Limited for permission to publish this paper and Mr. K.E. Mathews, Mining Research Engineer, for his helpful assistance.

REFERENCES

1. DAVIES, E. - Mining Practice at Mount Isa Mines Limited, Australia. Trans. Instn. Min. Metall. (Sect. A: Min. industry), vol. 76, 1967, pp. A14-40.

2. EDWARDS, D.B. - Ground Stability Problems Associated with the Black Rock Open Cut at Mount Isa. Proc. Aust. Inst. Min. Met., No. 226, pt. 2, 1968, pp. 61-72.

3. TERZAGHI, K. - Stability of Steep Slopes on Hard Unweathered Rock. Geotechnique, Vol. 12, No. 4, December 1962, pp. 251-270.

4. MOYE, D.G. - Diamond Drilling for Foundation Exploration. Civ. Engg. Trans. I.E. Aust., Vol. CE9, 1965, pp. 95-100.

5. BENNETT, E.M. - Lead-Zinc-Silver and Copper Deposits of Mount Isa. Geology of Australian Ore Deposits, 2nd edition (ed. J. McAndrew) Melbourne, Eighth Comm. Min. Met. Congr., 1965, pp. 233-246.

6. ROSENGREN, K.J. - Diamond Drilling for Structural Purposes at Mount Isa. Aust. Diamond Drilling Assoc. Symp., Surfers Paradise, November 1969.

7. TERZAGHI, R.D. - Sources of Error in Joint Surveys. Geotechnique, Vol. 15, No. 3, Sept.,

1965, pp. 287-304.

8. ROSENGREN, K.J. - Measurement of Rock Friction in the Triaxial Apparatus. To be published, 1971.

9. JOHN, K.W. - Graphical Stability Analysis of Slopes in Jointed Rock. Journ. Soil Mech. Found. Div., A.S.C.E., Vol. 94, No. SM2, Proc. Paper 5865, March, 1968, pp. 497-526.

Geotechnical Investigations for Slope Stability Studies in Brown Coal Open Cuts

BY

C. S. GLOE, M.SC., A.M.AUS.I.M.M.
(Geologist-in-Charge, Planning and Investigations Department, S.E.C.V.)

J. P. JAMES, B.E. (Civil), M.ENG.SC., PH.D., M.I.E.AUST.
(Engineer, Fuel Department, S.E.C.V.)

AND

C. M. BARTON, B.SC., PH.D.
(Regional Geologist, Latrobe Valley, S.E.C.V.)

SUMMARY.- Major thermal power stations in the Latrobe Valley, Victoria, are fired with brown coal excavated from the large Yallourn and Morwell Open Cuts.

Batter stability problems arise because of such factors as the shape and depth of the open cuts, the geological structure of the coal seams, the presence of clay layers immediately beneath the coal seams, and from the piezometric pressures in the coal and underlying sand aquifers.

The paper describes some of the field investigations being carried out to aid assessment and prediction of batter stability in the Morwell Open Cut. These include the mapping of geological structures, the measurement of surface and sub-surface vertical and horizontal movements, the observation of piezometric pressures in coal seams and interseam sediments and the laboratory determination of physical properties of these materials.

Features of the work include the installation of piezometers and extensometers in boreholes to depths up to 720 feet, the development of extensometer anchors for brown coal, the sealing of piezometer and other installations by special chemical muds and the use of precise borehole inclinometers in difficult sub-surface conditions involving high water temperatures and pressures.

1.- INTRODUCTION

As with all open cuts, stability of batters is a major problem. The materials involved in the large brown coal open cuts of the Latrobe Valley consist of brown coals, clays and sands. About 80% of the permanent batters and most of the operating faces are made up of brown coal and, because of certain physical properties of this material, it has been found that stability and movement of batters are a geotechnical problem. Investigations of stability and of the factors likely to influence stability have been carried out for many years, and have included some unusual features.

During 1970, these investigations were intensified at Morwell in collaboration with Golder, Brawner and Associates Ltd. of Vancouver.

1I.- GEOLOGY

The Tertiary deposits of the Latrobe Valley Depression include up to 2,500 feet of fresh water sediments known as the Upper Latrobe Valley Coal Measures. These consist of three main groups of thick brown coal seams interbedded with clays and sands (Fig. 1, Ref. 1).

The sediments were deposited in a slowly subsiding basin in which swamp conditions prevailed and where the rate of subsidence of the floor of the basin coincided with the rate of accumulation of decomposing plant debris. Occasionally the rates were not precisely uniform and, as a result, the peat swamps tended to migrate causing two lower groups of seams to be split in several areas. At other times very minor changes in water level caused changes in the character of the developing peat and hence in the resulting peat. These variations can be seen in the banded character of exposed faces of coal. In some areas the formation of brown coal continued for very long periods of time and up to 750 feet of continuous coal has been proved in the Loy Yang field.

The interseam sediments of the Coal Measures include lensing beds of sand which contain water under pressure. Where ground levels are low the water is under sufficient pressure to flow at the surface. The intake areas for the various aquifers separating coal seams in the Yallourn-Morwell area are considered to be located along the south-west, west and northern edges of the basin. Some of the basalt flows which underlie the Coal Measures and outcrop to the west are also considered as probable intake beds.

Deposition of the Coal Measures ceased with the laying down of some hundreds of feet of clays over the youngest or Yallourn Seam. Subsequently, the sediments were uplifted and folded, much of the differential movement probably reflecting faulting in the Mesozoic basement.

Apart from the Loy Yang Dome and the Baragwanath Anticline, the major structural features are a series of more or less en-echelon monoclines. Separating these structures are gentle synclines and anticlines, mostly pitching in a northerly direction at about 2 to 4 degrees.

Drilling has not disclosed any major faulting in the Coal Measures. No faults at all have been observed in the Yallourn Open Cut but numerous small

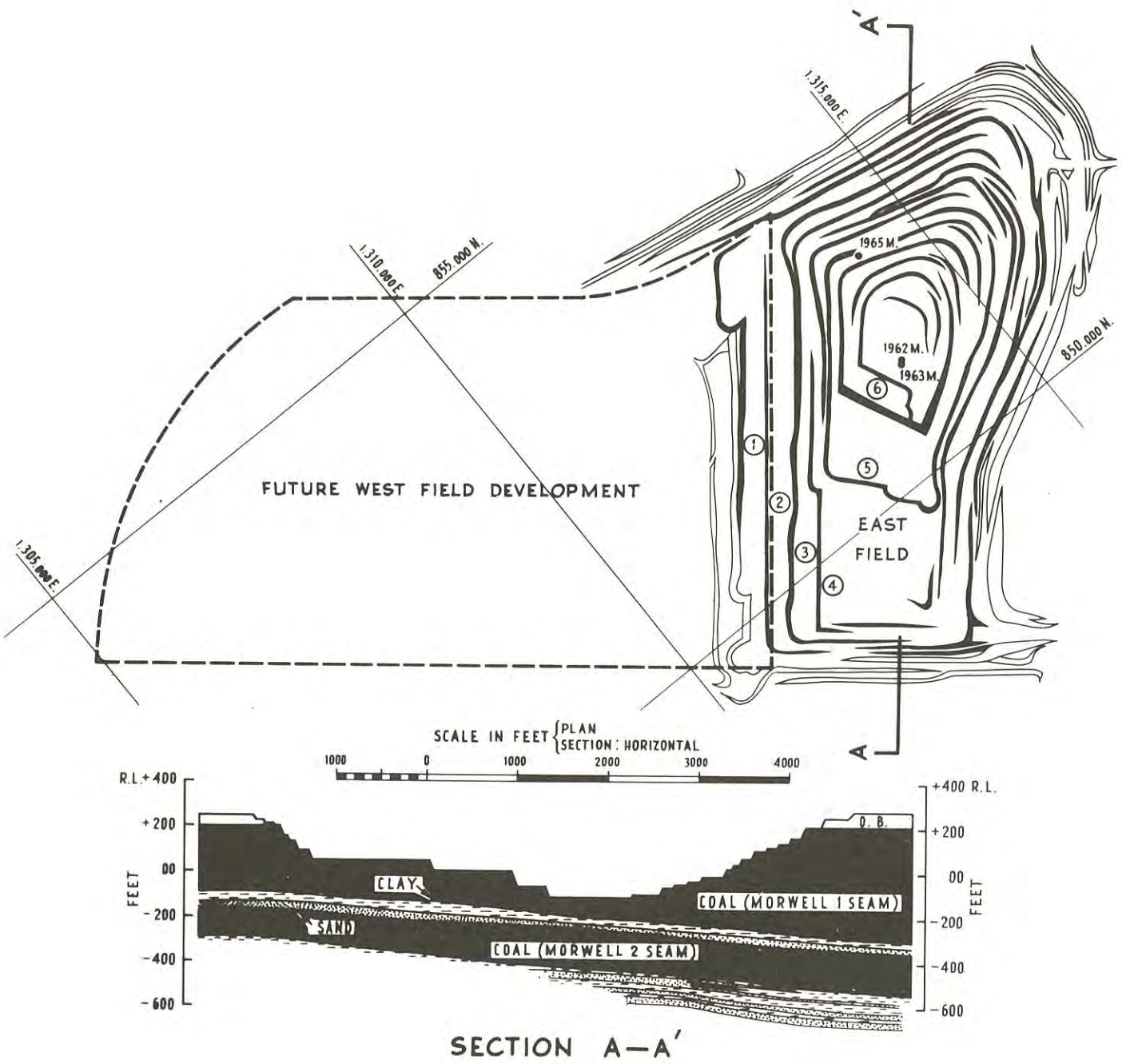

Fig. 1. Morwell Open Cut

step faults and occasional reverse faults, with up to 40 feet throw, have been exposed in the Morwell Open Cut. However, the coal in both open cuts is strongly jointed and the joint patterns clearly indicate their tectonic origin. At Yallourn the cracks, which have been traced for distances of up to half a mile and penetrate the full thickness of the seam, are generally wide apart, with the result that the seam is broken into huge blocks. The jointing is much more intense at Morwell and with the greater incidence of those having low and medium angled dips, the blocks tend to be smaller and much more irregular in shape.

Widespread erosion followed the uplift and folding, virtually to the stage of peneplanation. Later differential earth movements rejuvenated streams and up to 300 feet, but generally lesser thicknesses, of sands and clays were deposited on the eroded surface. In the major open cut areas this material forms the overburden and generally ranges from 30 to 60 feet in thickness. During this general period further earth movements put the coal seams in tension, resulting in the opening up of many cracks. Those which had

opened were subsequently filled with clays and sands from the overburden.

Geologically, the brown coals and interseam sediments are soft and unconsolidated. However, while normal consolidation, or what Edwards (Ref. 2) called compaction, occurred as the sediments accumulated, the subsequent folding and widespread erosion resulted in various coal seams now being located at shallow depths in different areas and each preconsolidated to varying pressures. It is also likely that in areas of more intense folding additional forces would have increased the normal preconsolidation pressures.

III.- OPEN CUT MINING OPERATIONS

Since brown coal has a high moisture content and hence is of a low grade, it must be excavated in large quantities at low cost in order to be economically used as a fuel. Open cut sites, therefore, are selected where relatively flat bedded thick coal seams underlie shallow overburden. Development is usually rapid in depth in order to establish sufficient operating faces to enable coal to be won at the high rate required by neighbouring power stations or any other uses. The coal and overburden is excavated by large bucket-wheel or bucket-chain dredgers which operate on faces ranging up to 90 feet in height and having slopes between 30° and 70° from horizontal.

Coal from Morwell Open Cut is expected to be won at rates of up to 60,000 tons per day during winter months and totals some 16 to 17 million tons a year. At such rates the shape and depth of open cuts alter rapidly.

The overall batter angle adopted averages about $3\frac{1}{2}$:1, but it is generally steeper towards the top of the cut and gradually flattens towards the base. As stated earlier, much of the permanent batters of the Latrobe Valley open cuts is made up of continuous coal. At Morwell the northern batter will develop to a height of 500 feet, of which 450 feet will be brown coal. As this height of coal batter is far in excess of that of any other brown coal open cut in the world, there is no previous experience of the long-term behaviour of such a height of coal in a permanent batter. Another important aspect is that while the flattening of the angle of the batter towards the base of the seam is likely to increase its stability, it is still not known whether many millions of tons of coal which could be cheaply won are needlessly tied up in this batter system.

Mention has already been made of the artesian water occurring in an aquifer located within a few feet of the base of the Morwell No.1 coal seam in the Morwell Open Cut (Fig. 1). It has been recognised from the commencement of operations that the piezometric pressure of this water has to be progressively reduced as the open cut is developed in depth. A series of aquifers occurring below the Morwell No. 2 coal seam, which is some 150 feet thick and about 50 to 75 feet below the Morwell No. 1 coal seam, also contain large volumes of water with a pressure head reaching approximately the same original height as that of the upper aquifer. The lowering of the piezometric surface of this lower water is equally important as is that of the upper aquifer.

A feature of the basin as a whole is the high temperature gradient within the coal itself and the variable but high temperatures of the artesian water. The latter range between 42°C and 58°C, and the above-normal heat, which is common in some coal fields, is considered to be due to autoxidation of the coal.

IV.- FACTORS INFLUENCING BATTER STABILITY IN THE MORWELL OPEN CUT

The development of an open cut, particularly a deep cut in soft rocks, invariably results in some movement of the batters and the floor of the excavation. These movements are mostly relatively small. It is only if these lead to a more sudden or larger movement, which would be called a slide, that the slopes should be considered unstable.

It is necessary to distinguish between a slide involving the whole of the batter and localized instability associated with structural planes of weakness within the coal. Some instances of localized instability have been reported previously (Ref. 3)

Since the commencement of the open cut in 1958, movements have been observed in both the batters and the floor of the cut.

Batter movements consist of a downward component and a horizontal component directed inwards towards the open cut. At the top of the northern and eastern batters (Fig. 1) the horizontal component has now amounted to about 5 feet and the vertical component to about 3 feet. Movements down the batters cannot be measured absolutely because of the progressive deepening of the cut. However, by projecting measured movements downwards, it is apparent that the vertical component of movement down the batters remains approximately constant but the horizontal component increases. It is inferred that the horizontal component of movement near the toe of the northern and eastern batters is up to about twice that at the top.

Factors which could contribute to the overall movement are:

Pressure relief;
Geometry or shape of the open cut;
Geologic structure of the coal deposits;
Subsidence due to increase in effective pressures arising from reduction in artesian and groundwater pressures;
Horizontal movement due to differential subsidence;
Block movements on clay layers triggered by water pressure in tension cracks;
Shear failure of the underlying strata.

(a) Pressure Relief

Pressure relief movements follow from the excavation of overburden and coal as the open cut is progressively developed. The removal of material disturbs the stress equilibrium and a stress readjustment occurs associated with movements within the open cut.

(b) Geometry Or Shape Of The Open Cut

Movements and batter stability are related to the length of unsupported faces and are aggravated by any "nose" structures in the open cut boundaries. Overall batter slopes similarly influence movements and stability.

(c) Geologic Structure Of The Coal Deposits

Planes of weakness, particularly joints, exist in the coal and are considered to contribute significantly to potential movement. A major crack pattern predominates, comprising near vertical cracks oriented mainly in a NNW-SSE direction (Ref.1; Ref. 4). There are in addition a number of low angled and intermediate angled cracks. Shear has frequently occurred along these low angled cracks but, despite associated movement on coal levels, this has not caused major instability of the operating coal faces.

(d) Subsidence Due To Increase In Effective Pressures Arising From Reduction In Artesian And Groundwater Pressures

The water pressures in the No. 1 and No. 2 aquifers have been considerably reduced - by as much as about 350 feet in the case of the No. 1 aquifer. In addition the groundwater table within the overburden and M1 coal seam has lowered with deepening of the cut and associated increased drainage of groundwater through the batter faces. This reduction in artesian and groundwater pressures gives rise to increased effective pressures and could induce strata subsidence.

(e) Horizontal Movement Due To Differential Subsidence

As subsidence increases towards the open cut, the strata will tip towards the cut and will also be in a state of tension. This could lead to the opening of existing cracks in the coal and to the development of high lateral hydrostatic forces as the cracks become filled with water.

(f) Block Movements On Clay Layers Triggered By Water Pressures In Tension Cracks.

Block movements of coal on the clay layer which underlies the M1 coal seam are theoretically possible because of the low residual strength of the clay and the high lateral hydrostatic forces in vertical tension cracks in the coal (Ref. 5). Movements which can occur due to these conditions appear to be of a start-stop nature. As the water pressure increases (perhaps due to heavy rainfall) movement will occur when the hydrostatic force exceeds the friction resistance at the base of the block plus the passive resistance of any coal remaining in the floor of the open cut. This movement is associated with the widening of the cracks but ceases as soon as the pressure is relieved. The passive pressure offered by the thickness of coal remaining in the floor of the open cut above the clay layer appears to be an important factor in resisting block movements.

(g) Shear Failure Of The Underlying Strata

A bearing capacity type failure of strata underlying the batters is a factor to be considered as the open cut is deepened.

... ...

In the floor of the open cut, heaves of up to 10 feet have been measured as each new level has been developed. Since survey pegs could not be established until after the coal was excavated, the actual heave would be even greater than the measured values.

Lateral pressure exerted by the batters and excess water pressures in underlying aquifers are additional factors which could contribute to heave of the floor of the cut.

At present the water pressure in the No. 1 aquifer has been reduced to a value which is less than the pressure due to the weight of overlying strata. However, the piezometric head in the No. 2 aquifer is now about 140 feet above the floor of the open cut and is sufficient to contribute significantly to the heave.

The heave is being controlled by lowering the artesian pressures in order to prevent material in the floor of the cut from becoming cracked and consequently weakened, thus avoiding migration of water from the aquifers into the base stratum and toe of the batters where the maintenance of stability is most critical.

Another concern is whether heave of the base is accompanied by lateral movements of clay and aquifer sand.

V.- FIELD INVESTIGATIONS AND INSTRUMENTATION

Vertical and horizontal movement of surface points in and around the open cuts have been obtained, over a period of 30 years, through regular precision surveys of bench marks and lines of pins.

Joints in the coal play a major role in block movements within the open cuts and, as a consequence, a succession of "crack surveys" has recently been carried out by geology vacation-students. From these field surveys, structural analyses have been effected (Ref. 4). Some areas of potential instability of wedges and blocks have been located, but these are not regarded as sufficiently large to constitute a major slide.

Present studies also include investigations of aquifer materials (Ref. 6), measurements of crack intensities, computerised plotting of crack-pole stereograms and detailed mapping of coal faces.

Over the past 10 years, the investigations have included detailed bore-hole instrumentation. Progressive improvements have been made in instrumentation and installation methods and, by 1970, the most modern available equipment was being installed by trained and experienced operators.

Investigations in recent years have been concentrated in Morwell Open Cut where stability problems are considered to be more complex than at Yallourn. The following section of this paper describes experience gained at Morwell during the installation of borehole monitoring sensors down to

720 feet below surface.

A rotary Failing 1500 rig was used for high speed drilling and coring operations while percussion equipment, of types Goldfields G33-34 and Ruston 22SW-60RL, was used for other controlled drilling and instrumentation. Four-inch and six-inch diameter cores, which were taken with Triefus 5 feet triple-tube core barrels, were retained in solid inner sleeves and treated on site to prevent initial loss of moisture or disturbance.

Instrumentation within vertical holes may conveniently be subdivided into extensometer, inclinometer and piezometer categories. Unusual techniques associated with installation within each of these categories are worthy of record.

(a) Extensometers

Preliminary tests on a recommended commercially available hydraulic extension anchor (manufactured by Slope Indicator Co., Seattle, Washington, USA) indicated that the standard anchor was unsuitable for penetration into Morwell brown coal. In order to counter this deficiency, prong terminations were sharpened, prong guide heads were enlarged to near actual bore diameter, and piston barrels were either increased from 1¼ to 2 inch od. or heavier gauge oil pressure lines were used. Subsequent installation at oil line pressures of up to 2,500 psi provided satisfactory prong penetration and anchorage.

As many as six anchors were satisfactorily placed at various positions within individual partially cased boreholes. Despite all feasible precautions, including the use of heavy drilling mud as a means of support, caving of the walls of some boreholes occurred during installation of anchors. These installations had to be either abandoned or modified.

(b) Inclinometers

Two accelerometer-type inclinometers are presently being used for bore surveys; an SEC Vic. - University of Tasmania Mark 2 instrument, with a designed accuracy of 1 part in 1,000, and a commercial probe ("Digitilt" inclinometer, manufactured by Slope Indicator Co., Seattle) with a designed accuracy of 1:10,000. The SEC instrument has been in continuous use over a number of years and the Digitilt for about six months.

Installation of aluminium inclinometer guide pipe for the "Digitilt" instrument necessitated the maintenance of accurately aligned, clean guide-wheel channels within the entire length of 3 inch id. fluted casing. Precision cradles were constructed to ensure accurate alignment of joined casing sections, while great care was exercised in ensuring a completely dirt and water-tight join. Excellent seals, selectively tested to 50 psi were obtained by butt-joining sand blasted pipe ends with a short pop-riveted aluminium sleeve and by liberally coating both inner and outer sleeve surfaces with Bond-O-Fil plastic filler paste.

(c) Piezometers

Perhaps the most intricate technical procedures were established during installation of up to 6 pore-pressure transducers (manufactured by Slope Indicator Co., Seattle) to depths of 720 ft within a single bore. Effective water seals between piezometers were achieved by the pumped introduction of a 30 ft + column of diesoline based mud formulated on the weight basis 14 diesoline, 5 cement, 10 bentonite. This so called "gunk" mud solidifies and slightly expands on contact with water held in the bore and ultimately sets into a very effective seal with an unconfined compressive strength of > 30 psi. Water and "gunk" cannot be allowed to mix within the delivery pipe and, in order to effect this essential separation, each measured volume of "gunk" is bracketed by diesoline slugs. A greased squash ball, punctured and weighted to give positive density, was found to be a cheap, extremely effective squeegee for isolating separate fluid slugs within the 1.5 inch diameter polythene delivery tube.

Other equipment includes two types of stress meter which also required considerable skill in their installation. No useful results have been obtained from these meters to date and this type of investigation has been temporarily suspended.

Comments on installations at Morwell Open Cut would not be complete without note of the recent establishment of approximately horizontal 6-inch diameter drainage holes driven 800 feet into brown coal and equipped with perforated pipe. The purpose of these bores is to assist in the stabilization of the toes of batters.

As indicated above, the coal seams have an unusually high temperature gradient and are underlain by hot waters under high pressures. The coal and the interseam sediments are relatively soft materials, liable to be disturbed at any time by earth movements. For this reason, the successful installation of multiple equipment down deep boreholes in the short time available while the hole remains open, in conditions of hot pressure waters, is a tribute to the skill of the operators.

VI.- INTERPRETATION AND SIGNIFICANCE OF DATA OBTAINED

Field measurements are being made first to determine the factors which contribute significantly to the movements and second to obtain data for aiding the prediction of movements associated with the development of existing and future open cuts. Extensive laboratory investigations of the properties of the various sub-surface materials (coal, clay and sand) have also been undertaken and, while these form an essential part of the overall stability problem, it is not proposed to cover the laboratory investigations in this paper.

In discussing the field measurements, it is proposed to direct main attention to the first of the two aspects mentioned above, because the accumulation of data necessary for improving predictions of future movements is a longer term project. For example, extensometer installations very quickly delineate the strata in which movements are taking place and hence satisfy the first aim at an early stage of the investigations. On the other hand, data on the amount and rate of consolidation of strata essential to the prediction of future movements are necessarily very limited in the short term.

Important data obtained from some of the extensometer, inclinometer and piezometer installations will be considered in turn.

(a) Extensometers

Absolute anchor movements for an installation at the floor of the open cut are plotted against time on Fig. 2. The positions of the anchors relative to the various strata are also indicated on this figure. In a six month period of observations from May, 1970, until October, 1970, over 2 feet vertical movement occurred in all strata, including the M2 coal seam which is located beneath the No. 1 aquifer. This indicates that the excess piezometric head existing in the No. 2 aquifer below the M2 coal seam is probably a significant factor in causing heave of the floor of the open cut.

It is possible that the seat of the vertical movement could even be at a lower level than the No. 2 aquifer; and the vertical extent of this aquifer and any possible underlying aquifers is under investigation.

The difference between individual anchor movements has been calculated and indicates that only minor compression of the M1 coal seam has occurred over the period of observations, whereas an expansion of almost 2 inches has taken place between the anchor in the clay and the anchor in the top of the M2 coal seam. This apparent expansion in the aquifer region could be due to pressure relief arising from excavation of coal coupled with a small increase in piezometric head in the aquifer which occurred over the period of observations. A satisfactory explanation of the apparent compression of the M1 coal seam has not been offered, but this in no way alters the important observation that the M2 coal seam is clearly moving upwards with the floor of the open cut.

It has been found that some caution has to be exercised in drawing conclusions from extensometer measurements if the borehole has deviated, or if the installation is subjected to differential horizontal movement or temperature variation. For example, temperature reduction and differential horizontal movement would be registered as apparent expansion.

(b) Inclinometers

Horizontal subsurface movements at a location in the southern part of the floor of the open cut are shown on Fig. 3. The measurements were made with the Mark 2 Inclinometer and on the figure cover a seven week period from early May, 1970. A comparison of the movement profile with the strata log given on the same figure indicates that there is some continuous shearing of the M1 coal seam on the underlying strata. However, the general movements are of a very complex character, there being some tilting and rotation of strata in addition to the shearing.

Perhaps the most interesting inclinometer measurements were made at a location on No. 5 level in the northern batters of the cut. The first inclinometer survey was made in this bore on 1st July 1970, upon completion of the installation. Some hours later severe movement occurred in the northern batters, as evidenced by the fracture of large diameter water mains. Further inclinometer surveys were made on 2nd July following the movements and surveys were then continued on a routine basis. Horizontal subsurface movements from 1st July, 1970, are shown on Fig. 4, which also includes a strata log.

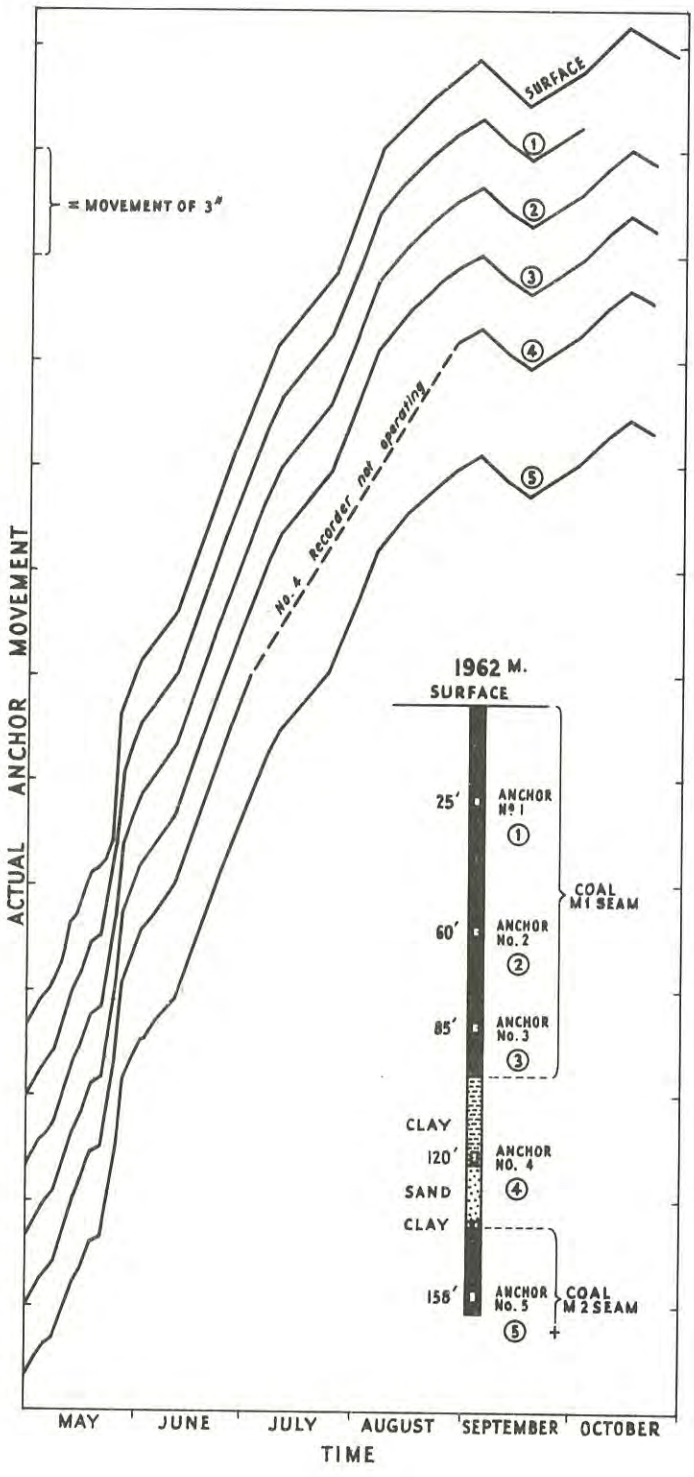

Fig. 2. Extensometer Measurements - Floor of Open Cut

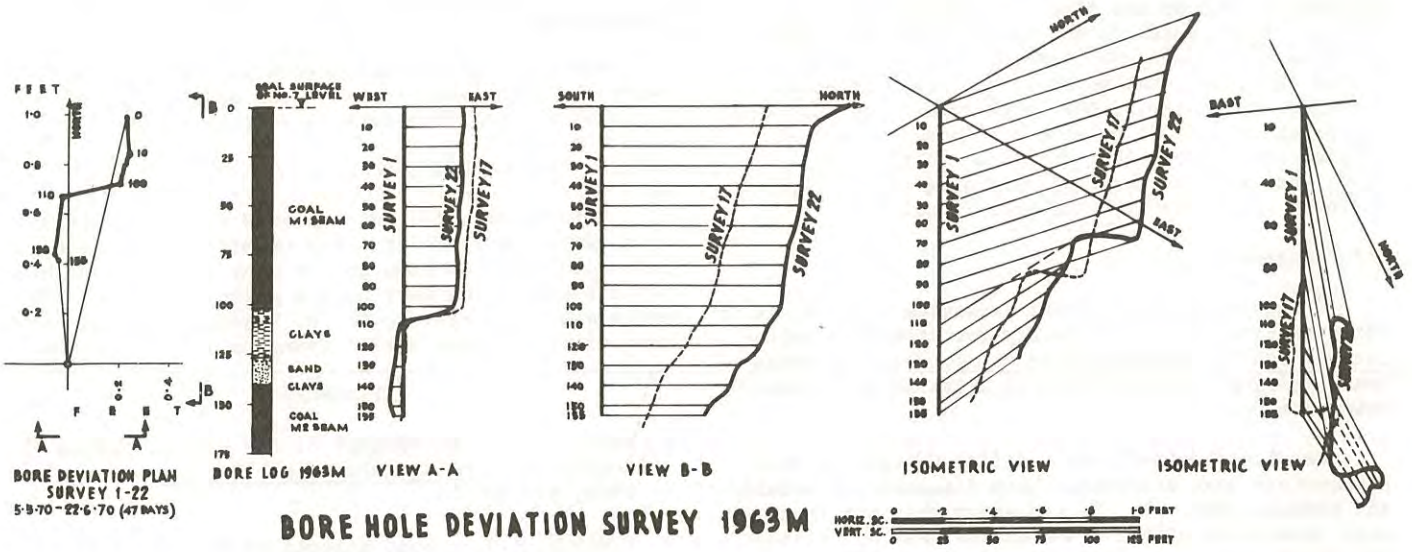

Fig. 3. Inclinometer Measurements - Floor of Open Cut

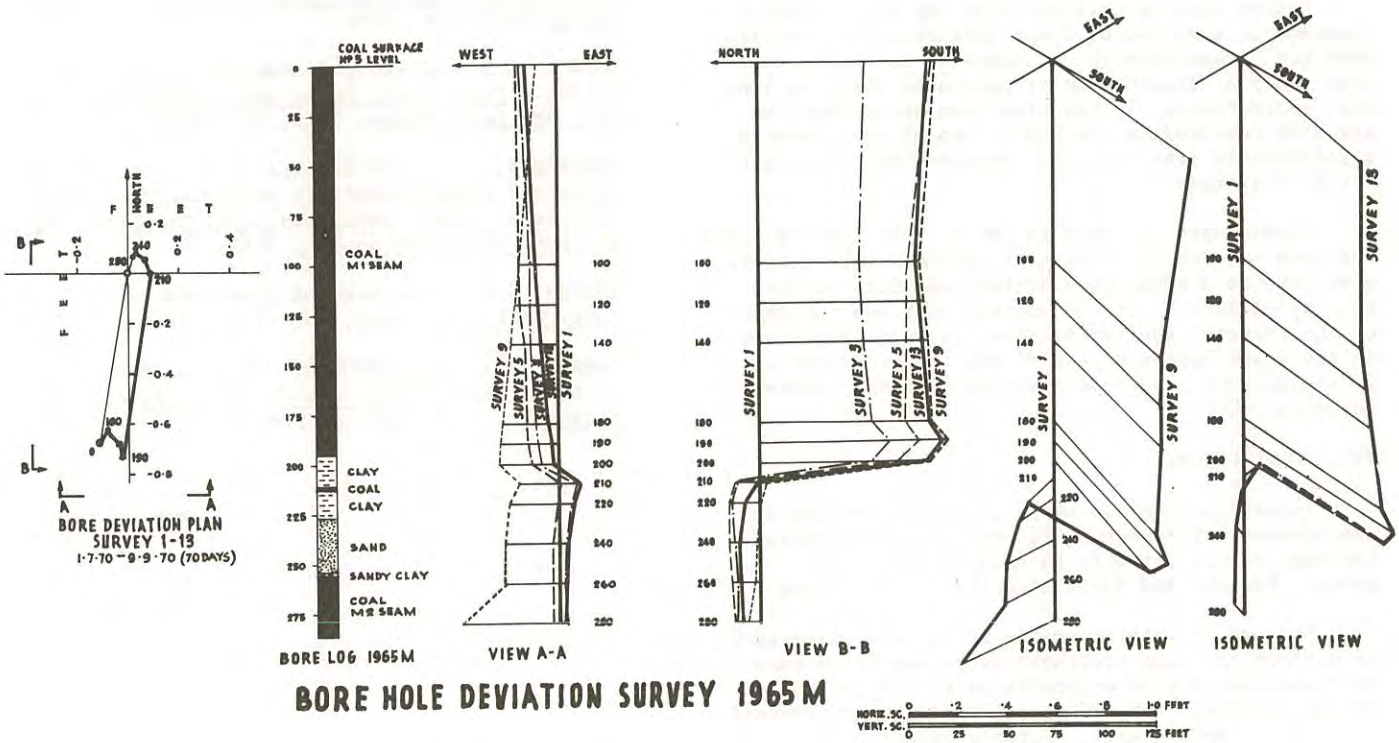

Fig. 4. Inclinometer Measurements - Northern Batters

It is noted that the movement involves a shearing of the M1 coal seam on underlying strata. The movement is directed inwards towards the cut and is at right angles to the northern batters. Compared with movements observed below the floor of the cut, movements at this location were not continuous, but virtually ceased a few weeks after 1st July. These observations are consistent with the concept of block movements of coal on the underlying clay layer being of a start-stop nature.

The overall shearing displacement is about 8 inches. Concurrently with these inclinometer measurements, pegs on the floor of the open cut on a line at right angles to the northern batters were surveyed. It was found that the pegs were stable up to 1st July, but then moved to the south by an amount 7 inches at the toe of the northern batters, decreasing progressively to an amount 4 inches at a coal lifting crack about 400 feet from the toe. This means that part of the coal remaining in the floor of the open cut moved with the batter coal.

(c) Piezometers

A knowledge of the water pressures existing in the various strata is necessary for stability calculations and for investigating the question of subsidence arising from reduction in artesian and groundwater pressures.

Results obtained with modified Casagrande type piezometers have previously been discussed by Donald and Krehula (Ref. 7). It was shown that the results were consistent with the assumption that unconfined groundwater flow - either through the coal or more probably along cracks - controls the water pressures in the upper layers of the M1 coal seam, whereas the aquifer pressure has an appreciable influence on the lower layers of the seam.

Recent results obtained with the pore pressure transducers supplied by Slope Indicator Co., confirm that the pressure-depth relationship in the M1 coal seam shows a distribution of pressures which is less than hydrostatic. It has also been noted that the pressure measured in the top of the M2 coal seam is significantly less than that measured in the base of the M1 coal seam.

Ground water seepage in the M1 coal seam towards the open cut would, because of curved equipotentials, give rise to a pressure distribution which is less than hydrostatic. It now appears that the influence of the changing aquifer pressure on water pressures in the lower layers of the M1 coal seam may not be so significant, and this question is being further investigated.

VII.- CONCLUSIONS

Investigations for slope stability studies in the Latrobe Valley open cuts have been in progress for many years, latterly in collaboration with Golder, Brawner and Associates Ltd. of Vancouver.

As part of this programme it has been necessary to develop or adapt instrumentation and techniques for installations in boreholes up to 720 feet deep in the difficult subsurface conditions which prevail at Morwell particularly. Notable examples are:

(a) the sealing of multiple piezometer installations with a mud formulation known as "gunk";
(b) the development of extensometer anchors for brown coal, based on an hydraulic anchor manufactured by Slope Indicator Co. of Seattle;
(c) the installation of sealed lengths of grooved "Digitilt" aluminium inclinometer casing.

Horizontal drains up to 800 feet long have also been introduced from the toes of batters to aid batter stability.

Geotechnical investigations as described in the paper are a necessary part of the development of the major brown coal open cuts in Victoria.

VIII.- ACKNOWLEDGEMENTS

This information is published with the permission of the State Electricity Commission of Victoria. Acknowledgement is made to the many officers who have contributed to the work over a period of years. The authors are grateful to Mr. M. Fajdiga who read the manuscript and made useful comments and suggestions.

REFERENCES

1. GLOE, C.S. - The Geology of the Latrobe Valley Coalfields. Proc. Aust. Inst. Min. Met. No. 194, 1960, pp. 57-125.

2. EDWARDS, A.B. - Some Effects of Folding on the Moisture Content of Brown Coal - Proc. Aust. Inst. Min. Met. No. 150-1, 1948, pp. 101-112

3. GLOE, C.S. - Case Histories of Slope Instability of Brown Coal Open Cuts - Engineering Geology, Melb. Group, Aust. Nat. Soc. Soil Mech. and Found. Engrg. Melbourne, 1969

4. BARTON, C.M. - Graphical Analysis of Fracture Planes. Proc. Rock. Mech. Symp. Aust. Inst. Min. Met. and Inst. Engrs. 1969, pp. 58-60

5. ROSENGREN, K.J., and KREHULA, F.J. - Earth Movements and Batter Stability in the Latrobe Valley Open Cuts - Aust. Inst. Min. Met. 8th Comm. Min. and Met. Cong., Melbourne, 1965

6. BARTON, C.M. - The Morwell Interseam "Sands" - Jour. Geol. Soc. Aust, 1971 (in press)

7. DONALD, I.B., and KREHULA, F.J. - Deep Piezometers in Brown Coal - Proc. 4th A.R.R.B. Conference, Melbourne, 1968, vol. 4, part 2, pp. 1862-1877

The Practical Application of Thermal and Freezing Methods to Soil Stabilization

By
T. Fujii
(Chief Engineer and Manager, Department of Engineering Development, Sanshin Kensetsu Kogyo Co. Ltd., Tokyo, Japan)

SUMMARY.- Principal practical methods for thermal soil stabilization are described, designed to strengthen the soil deep below the surface of a slope or under a foundation. Field data for two main types of heat treatment are compared.

For temporary stabilization of deep cuts, the so-called 'Quick-Freezing' method using liquefied gas is outlined, and exemplified from experience. Reference is also made to a newly developed injection technique using pressures higher than those of conventional grouting.

I.- INTRODUCTION

In recent years thermal soil stabilization has been attempted to prevent landslides in the U.S.S.R. and Rumania. This method aims at strengthening the soil deep below the surface of a slope or under a foundation.

The principle underlying this method is that structural changes of the clay minerals will produce stable soil particles when the temperature exceeds 400°C, and the strength obtained will not greatly diminish even under submerged conditions.

For the temporary stabilization of cuts which are deepened gradually, the so-called "alluvial grouting" technique has been used for about 10 years, to stop seepage through the gaps of the temporary timbering. However, conventional grouting techniques are not especially reliable for Japanese soils because these are often non-uniform. In contrast to these methods, the freezing method is the most reliable, except for a few cases. The conventional brine circulation method, though, is expensive and necessitates periods of relatively long duration to complete the desired freezing zone.

In this paper some practical applications of thermal soil stabilization and quick freezing by the use of liquefied gases are described. Also, a newly developed injection technique which uses pressures higher than those used in conventional grouting techniques is outlined.

II.- PRINCIPLES AND PRACTICAL APPLICATIONS OF THERMAL SOIL STABILIZATION

It is difficult to prevent local slope failures in fine grained soils with relatively high moisture content.

In recent years thermal soil stabilization has been attempted to prevent landslides and similar failures in the U.S.S.R. and Rumania. The principle involved in this method is that structural changes of the clay-minerals will produce stable soil particles at temperatures exceeding 400°C by the bonding of particles to each other, as is evident from Fig. 1. The increased strength obtained will not greatly diminish even under submerged conditions.

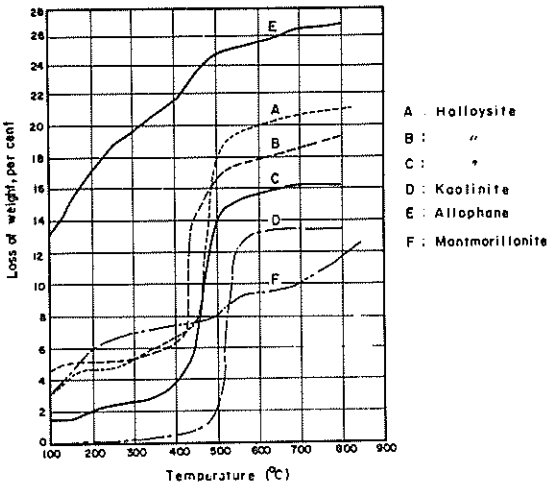

Fig. 1.- Loss of weight of various clay minerals

Practical application of the thermal treatment method is divided into two types:

The open (smoke-dust) type.
The closed (pressurized-burning) type.

The former is used in Rumania and consists of two bored holes connected together at the bottom. The burning equipment is placed over one of the two holes. The latter is commonly used in the U.S.S.R., and uses various fuels (gaseous, liquid or solid fuels) which are burned by means of a special burner placed over the closed hole with temperature controlled by keeping excess air pressures between 0.25 - 0.50 kg/sq cm. The heating of the soil is performed by infiltration

of the compressed heated air through the soil pores. The air temperature must not exceed the fusion temperature (about 1,200°C in general) of the soil.

(a) A Practical Example of Slope Stabilization of a Railway Embankment

Widening of the existing railway embankment was requested to accommodate another track near Kanazawa in 1964. The brown clay at the widening section consists of weathered shale, and its principal characteristics are as follows:

Grading: Sand (2 - 0.05mm) 23 - 38%
Silt (0.05 - 0.005mm) 49 - 58%
Clay (0.005mm or less) 13 - 28%

Moisture Content: w = 44 - 59%, w_L = 48 - 62%
w_p = 29 - 35%, I_p = 19 - 30%

Dry Density: γ_d = 1.21 - 1.51 g/cc

Because local failures or slides often caused the new track to settle, thermal treatment of the soil was planned to strengthen the deep soil of the new embankment as shown in Fig. 2. A total of 45 burning holes with a diameter of 200 mm were bored in the widening section. Holes with a total length of about 7.5m were spaced about 2m from each other.

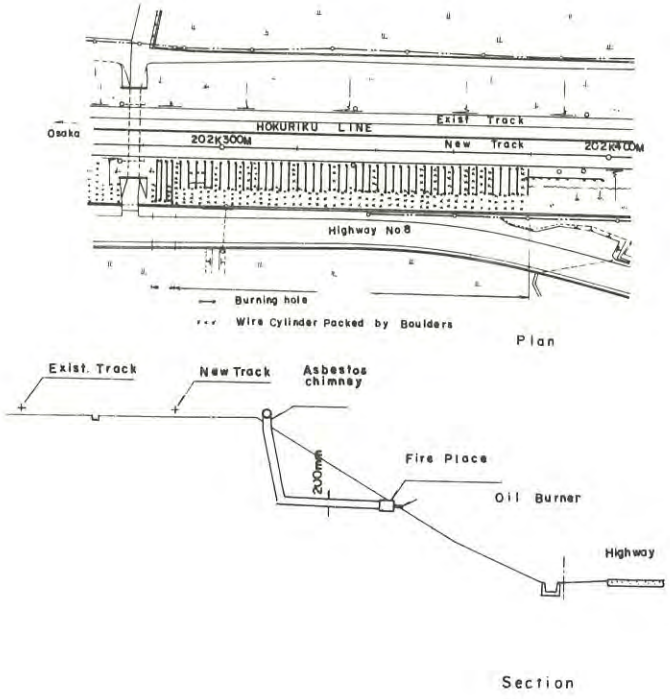

Fig. 2.- Thermal stabilization of the new embankment near Kanazawa

About 10 conventional type oil burners were fired at once by the use of heavy petroleum oil. Fig. 3 shows a typical diagram of the temperature change throughout each treatment. Treatment was continued until the temperature rose to 300°C about 30cm from

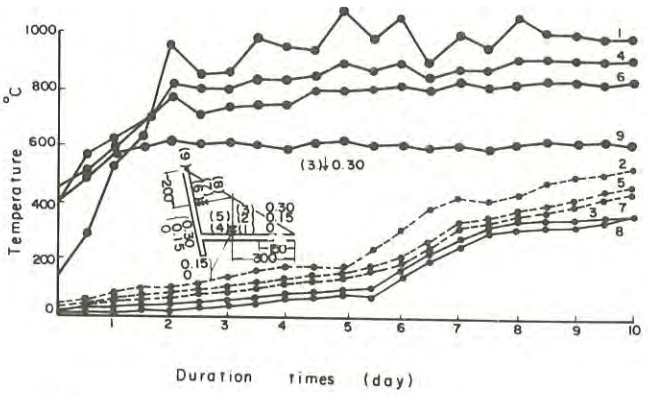

Fig. 3.- Typical diagram of temperature change during treatment

the center of the hole. In general it took about 10 days to reach the abovestated temperature. The fuel consumed amounted to approximately 5 l/hr, and the mean total quantity was about 1,200 l/hole.

The compressive strength of burned soil samples collected from each portion of the slope is shown in Fig. 4. As shown, the mean stabilized volume was about 7.4 cu m/hole, which consisted of burned soil from both the A and the B zones. Soil strength in the

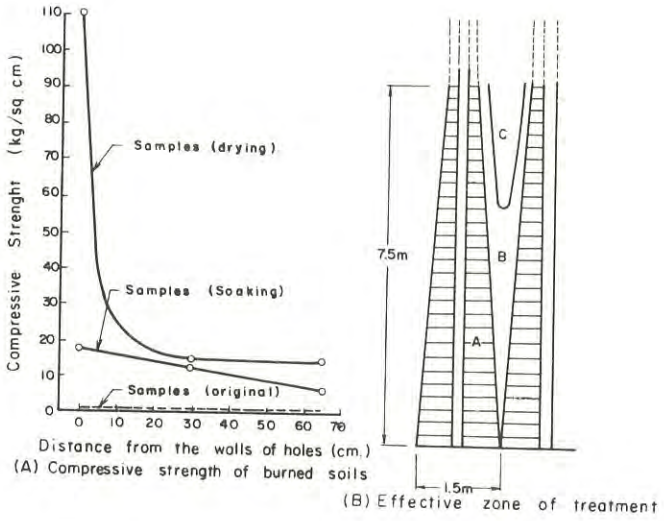

Fig. 4.- Compressive strength of each sample and effective zone of thermal treatment.

A-zone was about 10 to 20 times the original strength, even after total immersion. That of the B-zone was also higher than the original, whereas the strength of soil in the C-zone was reduced at once to the original by immersion.

(b) The Combustion Treatment of Ground Consisting of Disposed Waste

The closed type treatment is commonly used for gas-permeable "Loess" soils in the U.S.S.R.; however, this can hardly be used in Japan because Japanese

fine grained soils are mostly of too low a permeability for either water or gas.

Instead of thermal treatment of the soil, combustion treatment for waste was experimentally performed for ground in a part of the housing development area near Fukuoka, where waste had formerly been dumped.

The principal waste characteristics were as follows:

Water Content: w = 48 - 73%
Organic Content: 14 - 19%
Wet Density: γ = 1.03 - 1.23 gr/cc

A total of 227 burning holes with a diameter of 130 or 160mm were bored in the waste. The depths of these holes varied from 2 to 6m and were spaced 5m apart.

Fig. 5 shows the outline of the typical burning system. Principal equipment consisted of special type burners, a geared type oil pump and two rotary type air blowers. (head: 2,000mm water, delivery volume: 40 cu m/min, power: 30 kWh). Fuel oil piping (16mm dia., total 250m length) and air supply pipes (180mm dia., total 200m length) were used. A firing unit was placed over each hole and consisted of an iron cover plate, a reinforced fireproof concrete slab, and a furnace made of fire bricks. Treatment was continued until the burning had proceeded to a radius of about 1 m. It took about 7 to 15 days in general, and the mean total quantity of fuel was about 760 l/hole. The mean burned volume was presumed to be about 12.6 cu m.

(c) Thermal Calculations

Principal data for calculation of the thermal efficiency of the two treatments are shown in Table I.

TABLE I. PRINCIPAL DATA FOR THERMAL CALCULATIONS

Items	Open type (Kanazawa)	Closed type (Fukuoka)
Wet density kg/cu m	1800	1100
Moisture content %	50	60
Heat cap. of soils or wastes kcal/kg °C (C_s)	0.2	0.3
Heat cap. of water kcal/kg °C (C_w)	1.0	1.0
Latent heat of water kcal/kg (C_L)	540	540
Burned volume per hole cu m	7.4	12.6
Actual consumption of fuel per hole kg	1200	760
Ditto per unit volume kg/cu m	162	60

Theoretical consumption of fuel for these two treatments is as follows:

A. For slope stabilization by the open-type treatment

Dry soil weight (W_s) = $\frac{1800}{1 + 0.5} \simeq$ 1200 kg/cu m

Weight of pore water (W_w) = 1800-1200 = 600 kg/cu m

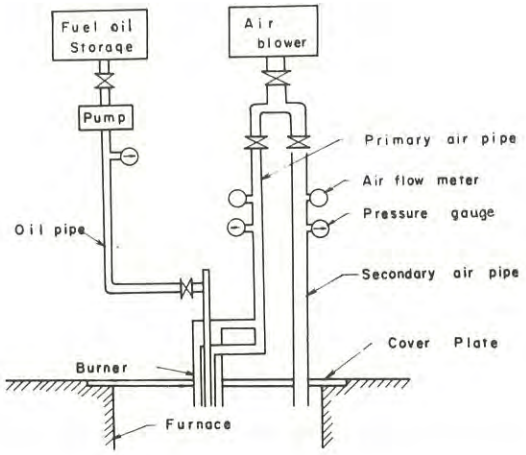

Fig. 5.- Closed type burning system

The maximum heating temperature is estimated at about 800°C.

Heat capacity of the soil (Q_s) = $W_s . C_s . T \simeq$ 192,000 kcal

Heat capacity of the pore water (Q_w) = $W_w . (C_w . T + C_L)$ $\simeq$ 384,000 kcal

Total heat capacity (Q) = $Q_s + Q_w \simeq$ 576,000 kcal/cu m

Theoretical fuel consumption = $\alpha = \frac{Q}{Q_o}$ = 57.6 kg/cu m

where Q_o represents the unit heating capacity of the fuel (about 10,000 kcal/kg).

B. Burning by the closed type treatment

Weight of dry wastes (W_s) = $\frac{1100}{1 + 0.6} \simeq$ 690 kg/cu m

Weight of pore water (W_w) = 1100-690 = 410 kg/cu m

Heat capacity of the wastes (Q_s) $\simeq$ 166,000 kcal

Heat capacity of the water (Q_w) $\simeq$ 263,000 kcal

Total heat capacity (Q) $\simeq$ 429,000 kcal/cu m

Theoretical fuel consumption = α = 42.9 kg/cu m

According to the above theoretical values and to Table I, the heat effect (defined by the percentage of the theoretical fuel consumption to the actual) may be calculated. In slope stabilization by the open type treatment, the heat efficiency was about 36%, and in burning by the closed type treatment about 72%.

(d) Some factors in Thermal Stabilization

As stated above, use of the closed type treatment will be desirable in thermal stabilization because its heating effects are more effective than those of the open type treatment in general; however, simultaneous control of many individual burners will necessitate very complicated techniques to adjust the combustion of each burning hole, especially for the closed type treatment.

Recently it has been sought to develop a heating air circulation system in which heating air would be

produced at a central furnace and circulated between groups of individual holes and the furnace by means of a closed circuit system.

The injection of some kind of inflammable and/or cooling material should also be investigated in order to keep a satisfactory combustion in the closed type of treatment.

III. THE PRINCIPLES AND PRACTICAL APPLICATIONS OF QUICK FREEZING

As stated earlier, freezing is a reliable method for temporary soil stabilization of deep cuts, including shaft sinking, shield or pipe thrusting, tunnelling, construction of frozen earth storages, etc.

Artificial freezing itself has a long history; about one century. But the conventional brine-circulation method is relatively expensive and requires a long time to accomplish the expected zone of freezing.

It is sought to overcome these difficulties by so-called "Quick Freezing", which aims at the effective usage of liquefied gases. Liquefied Nitrogen or Liquefied Carbonic Acid is chiefly used for these purposes, by means of freezing pipes as shown in Fig. 6. Recently a combined method which consists of a period of initial freezing by the use of liquefied gas, and another period by the brine circulation method simply to maintain the freezing condition has been tried. This is shown in Fig. 7.

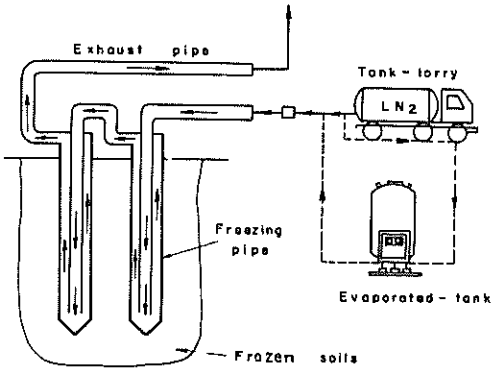

Fig. 6.- Quick freezing by liquefied gases

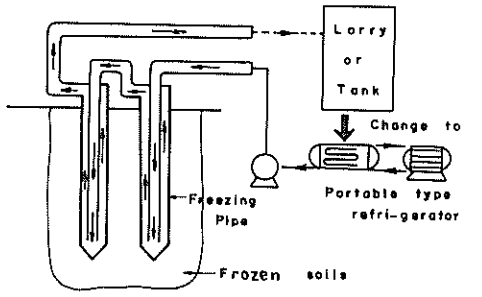

Fig. 7.- Combined method of quick freezing and conventional brine circulation

Comparisons of freezing time and unit cost as between conventional and quick freezing are shown in Figs. 8 and 9. The temperature difference between the freezing pipe and the surrounding soil is only about 40° to 50°C in the former method, whereas in the latter it will reach 100 to 150° or more. This is the principal reason for the great time reduction in quick freezing.

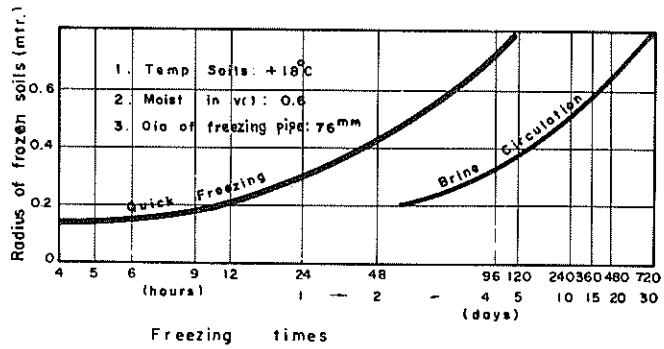

Fig. 8.- Comparison of freezing times for the quick and conventional freezing methods

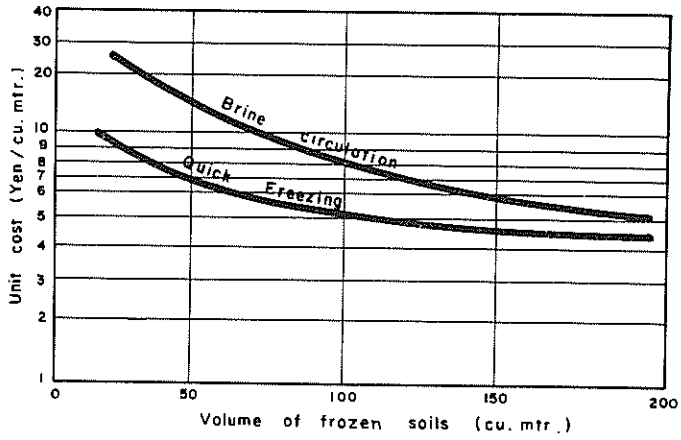

Fig. 9.- Comparison of costs for the quick and conventional freezing methods

Moreover, only a simple piping system is used in quick freezing and the gases are transported by tank or from the plant to the site; whilst a very complicated system, including refrigerator and heat exchangers must be used for the brine circulation method. Furthermore, legal authorisation must be obtained in Japan for the use of a high pressurized cooling medium (10 - 30 kg/sq cm).

Table II shows the thermal characteristics of liquefied gases. The cooling capacities of liquefied gases in the applied conditions are as follows:

A. Liquefied Nitrogen:

72.5 kcal/kg at -100°C, 1 atm
83.7 kcal/kg at -50°C, 1 atm

B. Liquefied Carbonic Acid:

about 74 kcal/kg at - 30°C, 1 atm

TABLE II. THERMAL CHARACTERISTICS OF LIQUEFIED GASES

Kind of Gas	Boiling point °C	Melting point °C	Latent heat at Boil. pt. kcal/kg
Carbonic Acid	-	-79	139
Oxygen	-183	-218	51
Nitrogen	-196	-210	48

By comparison, the freezing time of the former gas is faster than for the latter; however the temperature distribution of the former gas is non-uniform along the axis of the freezing pipe, whilst that of the latter is almost constant. But it is necessary to use special pressurized freezing pipes for the latter gas, as shown in Fig. 10. The internal pressure for these must be kept at about 6 kg/sq cm or more, because Liquefied Carbonic Acid will transform to the solid state under pressures less than 6 kg/sq cm.

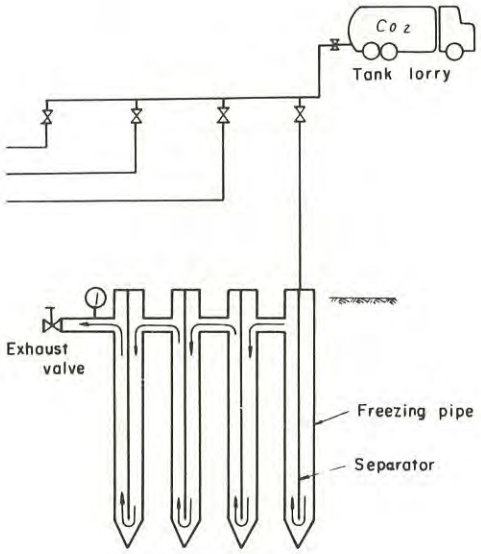

Fig. 10.- Pressurized freezing pipes for Liquid Carbonic Acid

Thermal characteristics of ordinary soils are shown in Table III. Therefore, necessary cooling capacities to freeze the soil unit volumes will be calculated by the following method:

Total cooling capacity = $Q = Q_1 + Q_2 + Q_3$ kcal/cu m

where Q_1 = cooling capacity necessary to lower the subsoil temperature (T_o°) to the freezing point (T_s°)

Q_2 = latent heat of freezing of the soil

Q_3 = cooling capacity required to lower the temperature of the frozen soil (T_f°).

$$Q_1 = \gamma_2 . C_2 . (T_s - T_o) \text{ kcal}$$

$$Q_2 = \frac{W' . L_i . 1000}{1} \text{ kcal}$$

where L_i = 79.5 kcal/kg (Latent Heat to freeze pore water).

$$Q_3 = \gamma_1 . C_1 . (T_o - T_f)$$

TABLE III. THERMAL CHARACTERISTICS OF SATURATED SOILS

Water in vol. in %	W'	0.3	0.4	0.5	0.6
Wet density kg/cu m	before freez	2.26	2.08	1.90	1.72
	after "	2.22	2.03	1.84	1.65
Specific heat kcal/kg °C	before freez C_2	0.32	0.37	0.43	0.49
	after " C_1	0.26	0.27	0.29	0.32
Heat conductivity kcal/m hr °C	before freez	1.87	1.62	1.41	1.22
	after "	2.63	2.52	2.41	2.31

(a) Quick Freezing for a Shield Starting

A shield with a diameter of 2.7 m will be started from a shaft near Yokohama as shown in Fig. 11. Soil at the site consists of very soft sandy silts which would be be squeezed out into the shield at starting after breaking the concrete wall of the shaft.

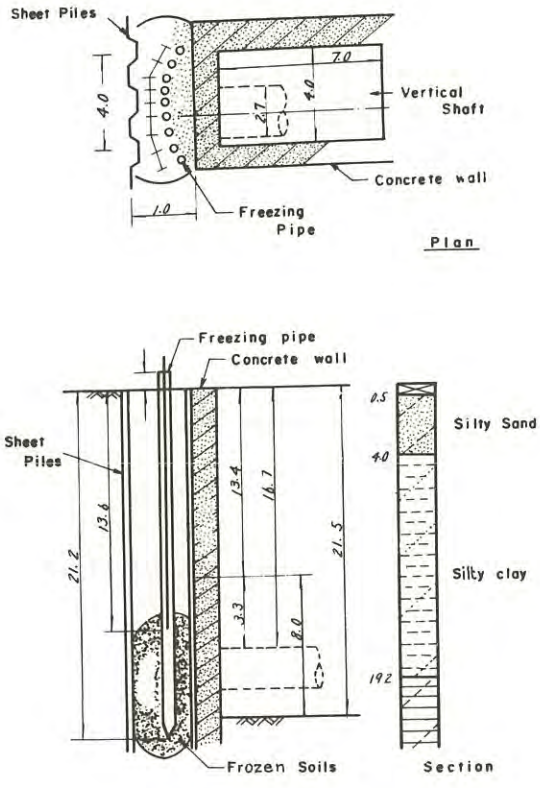

Fig. 11.- Quick freezing for shield starting

Freezing pipes with a diameter of 76 mm and a length of about 22 m were put in the ground at 0.5 m intervals. The expected volume of the frozen soil was estimated at about 53 cu m, and about 88 tons of Liquefied Nitrogen was supplied over a period of 6 days. The shield was started in safety 5 days after commencement of the gas-supply. Freezing pipes were cut out for the shield thrusting. The soil remained in a frozen condition for about 5 days after the end of the gas-supply.

(b) Quick Freezing for a Shield Thrusting

A small-scale shield with a diameter of 2 m was thrust in gravelly soil with plenty of seepage in the suburbs of Tokyo.

Freezing pipes with a diameter of 50 mm and a length of 5.5 m were inserted in a horizontal direction on the upper half of the shield as shown in Fig. 12.

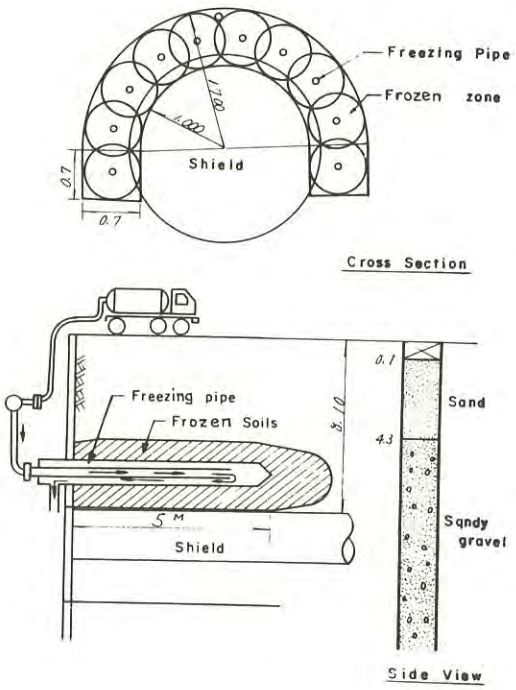

Fig. 12.- Quick freezing for shield thrusting

The volume of frozen soil was estimated to be about 21 cu m, and about 30 tons of Liquefied Nitrogen was supplied over a period of 4 days. The setting of the pipes and supplying of the gas was successively repeated, and the shield was safely thrusted except for a few cases.

Often grouting with cement suspension, combined with a silicate solution, was undertaken to protect against excessive seepage, especially at the base of the shield.

C. The combined method of initial quick freezing with subsequent brine circulation for a large-scale shaft.

A vertical shaft with an inside diameter of 9 m was sunk in the center of Tokyo for the construction of large-scale underground telephonic utilities, as shown in Fig.13. Soil at the site principally consisted of sandy soil with fine to medium grain size. Freezing pipes with a diameter of 76 mm and a length of 16.5 m were put in the ground and spaced about 0.5 m from each other (doubled rows).

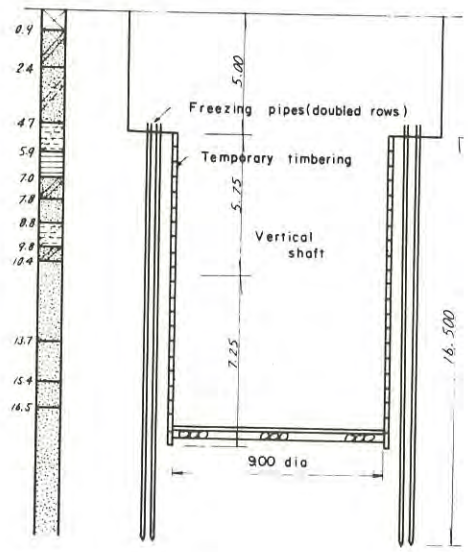

Fig. 13.- Quick freezing for shaft sinking

Initial quick freezing was combined with the brine circulation method. This was selected for the freezing method because of time saving, and because the working space of the site was too limited to install large-scale refrigerators.

The volume of frozen soil was estimated to be about 510 cu m, and about 606 tons of Liquefied Nitrogen was supplied over a period of 12 days for initial quick freezing. This was converted immediately into a brine circulation method to maintain the frozen condition. Two refrigerators with a capacity of 65,000 kcal per hour were used in this project over a period of 35 days, by which time the excavations were finished. In this case, if the conventional brine circulation method had been used throughout the whole working period, refrigerators with a total capacity of 260,000 kcal per hour and a working time of about 70 days or more might have been necessary.

(c) Some Considerations about Quick Freezing

As stated earlier, quick freezing is a more reliable method than the alluvial grouting technique as a temporary stabilization method for deep cuts. However, this method should be used only partially and on relatively small-scale projects because it is still too expensive to use on large-scale projects.

In the abovementioned "combined method", freezing times will be reduced to about 60 or 70% of the conventional brine circulation method, and the power of the refrigerators will also be reduced to about one half

of the latter. Therefore, the combined method is suitable for relatively large-scale works. Although further cost analyses are necessary, it may be reduced to about 70 to 80% of the conventional method.

Liquefied Carbonic Acid is everywhere more easily available than is Liquid Nitrogen. Also, the piping system for the former is simpler and more economical than the latter, as shown earlier.

Heating losses of the entire freezing system will reach about 30 to 60% in general for freezing. Those resulting from the use of Liquefied Carbonic Acid will be lower but more detailed research related to the use of Liquefied Carbonic Acid is necessary.

Also, further investigations are necessary to ensure uniform gas-supply to each freezing pipe, and also a more precise method of measuring subsoil temperatures throughout the treatment, than the chromel-alumel thermocouples used.

IV. OTHER METHODS FOR TEMPORARY STABILIZATION

As stated earlier, the conventional grouting technique is not especially reliable for non-uniform Japanese soils. Grouts will often escape to the weak points, which consist of lenses, seams, natural or artificial cavities, including any existing old ducts or pipes, etc. Packers and other special techniques used in rock grouting usually cannot be employed in alluvial grouting. R.H. Karol has described the effectiveness of a method which uses a shorter gel time with a long pumping time to realize the greatest degree of uniformity of penetration in stratified deposits. In this case, the grout is forced later into the opening previously left in the least pervious stratum. However, this method is used only for single polymeric grouting fluids.

A new injection technique which aims at the formation of waterproof grouted walls or films has been developed by the use of pressures higher than those used in conventional grouting techniques. Pressures of about 100 to 250 kg/sq cm are used. Grouted walls formed by this method have a width of about 1.2 to 2.6 m between injection holes, and a thickness of about 0.15 to 0.25 m, but this varies according to soil conditions.

This method can be performed more simply as well as more speedily (and the formation of grouted walls by this method are achieved more accurately as well as more reliably) than with the conventional grouting technique, although some problems still remain unsolved.

An epoch-making new grouting method named "TACSS" has been developed in recent years in Japan. "TACSS" means "Takenaka Aqua-reactive Chemical Stabilization System". A single fluid is injected into the soil and reacts directly with pore water to form an hydrophobic and unhydrated gel. Another important feature of the TACSS system is that this chemical grout itself expands during reaction. This enables the chemical grout to actively penetrate into the soil and enlarge its permeation zone without being affected by the underground seepage flow. There have already been some practical applications in overcoming seepages which had very high pressures of about 50 to 60 kg/sq cm or more. This special kind of work has been performed mostly in deep coal mines almost 500 to 600 m below the ground surface.

Some recent examples of temporary stabilization have included the use of in-situ piles of quick lime to prevent the heaving of very soft cohesive soils in deep open cuts; utilizing the water absorbing, thermal, osmotic and chemical hardening effects of quick lime.

Although there are many temporary stabilization methods for slopes and cuts, the most reliable (and, furthermore, the most inexpensive method) is a dewatering technique which consists of the wellpoint system, Siemen's wells or ejector-wells used together with temporary timbering. In general, however, these wells will often cause a loosening of nearby or soft soil.

Apart from temporary stabilization, the so-called "underground continuous walls", termed "concrete diaphragms" in European countries, have been used for about 5 to 10 years. Combined with anchoring techniques as a substitute for temporary timbering, they can be used subsequently as permanent walls for basement or underground utilities.

REFERENCES

1. FUJII, T. - On rational soil grouting. Soils and Foundations, Vol. 12, No. 4, p. 25, No. 5, 1964, p. 34.

2. HORN, A. - Basic factors of thermal methods of laying foundations. Baumaschine and Bautechnik, Vol. 16, No. 4, 1969, p. 169.

3. ISHIYAMA, K. and FUJII, T. - Chapter 5, Practice of freezing and thermal soil stabilization, Recent practice of soils and foundations. Japanese Society of Soil Engineering, Tokyo, 1967.

4. KAROL, R.H. - Chemical Grouting Technology. Proc. ASCE Structural Engineering Conference. Seattle Washington, 1967.

5. LITVINOV, I.M. - Fundamental requirements for design and practice of thermal soil stabilization. Construction Ministry of Ukrainian S.S.R., Kiev, 1959.

6. STAENDER, W. - Mathematical evaluation for calculathion of frost enlargement in still ground water in comparison with model-testing of freezing pipe arrangements for shaft and underground construction Technical University of Karlsruhe, Karlsruhe, 1967.

7. TAKASHI, T. - On freezing practice for soils. Freezing, Vol. 36, No. 408, 1961, p. 1.

8. YAMADA, G. - Strengthening cohesive soils by thermal treatment. Quarterly Report of the Railway Technical Research Institute, Japan National Railways, Vol. 2, No. 3, 1961, p. 19.

9. YAMAKADO, A. - Considerations on cutting practice high pressurized jet flow. Soils and Foundations, Vol. 16, No. 1, 1968, p. 21.

The Role of Progressive Failure in Clay Slopes

By
P. M. James, B.Sc., M.Sc.(Eng.), Ph.D., D.I.C.
(Senior Lecturer in Civil Engineering, University of Queensland)

SUMMARY.- Modes of time dependent weakening in clay slopes are discussed and evidence is quoted to show that the dominant pre-slip mechanism of time dependent weakening is a decay in cohesion, c', alone, while ϕ' remains at, or near to, the peak. That is, progressive failure (which may be defined as a simultaneous decay in both the c' and the ϕ' parameters) will be an untypical occurrence for the majority of clay slopes. Mention is then made of existing hypotheses of progressive failure which are suggested to provide an inadequate explanation of the process when it does occur. It is shown how large deformations, possibly of the order of feet, are necessary in the field in order to produce residual conditions along a potential slip plane and, neglecting landslides, such deformations can generally be satisfied only under a certain set of conditions. The common conditions which meet the requirements are non-homogeneous or localised straining associated with the non-homogeneous swelling of swelling soils present in a cutting or valley slope. Examples are given in support of this hypothesis.

I.- HISTORICAL BACKGROUND

The stability of slopes, especially in over-consolidated clays and clay shales, is a central problem in the Geomechanics field. Since the 1940's, the problem has received increasing attention, with particular attention being focused on the discrepancies between the laboratory strengths of formations and the much lower strengths at which slopes in such formations often failed in practice. Papers by Skempton (1948), Cassell (1948) and Binger (1948) cite quantitative examples of the divergence between laboratory and field, while the first mentioned paper suggests a rate of strength decay for the London Clay formation.

The above analyses, as with all prior to the mid 1950's, were necessarily confined to a $\phi = 0$ approach, using cohesive strengths alone. A more rational approach to stability analysis was made possible with the development of the effective stress method, and work by de Lory (1957) pointed to a more fundamental mechanism of strength decay, confined to the effective cohesion parameter, c', while the parameter, ϕ', was taken as sensibly constant. At that stage the possibility of a reduction in ϕ' was not envisaged in Soil Mechanics, and it was not until the early years of the last decade that reliable case histories were published where failure could not be explained even with a cohesion term c' of zero. In other words, some reduction in ϕ' was also needed to obtain a Factor of Safety of unity. Observations in the field by Gould (1960), and in the laboratory by Borowicka (1963) pointed to the fact that the angle of shearing resistance of clays, ϕ', was decreased permanently due to strain, but the problem was not fully resolved until the phenomenon of residual strength was formerly postulated and defined by Skempton (1964).

The concept of residual strength has possibly effected the most radical change in philosophy in Soil Mechanics during the past decade. Perhaps for this reason there has been a tendency, in most recent years, to over-emphasize the residual approach to the design of slopes; an over-emphasis since knowledge of the actual path from peak to residual in the field, i.e. the progressive failure mechanism, was largely hypothetical. Skempton (ibid) himself introduced an R (Residual) factor to describe the extent to which the strength of a clay had fallen from its peak towards its residual, since the evidence at the time pointed to an inevitable progression of this nature.

It should be pointed out that progressive failure is taken, in this paper, to mean a simultaneous, or quasi-simultaneous, decay in both the c' and ϕ' parameters preceding actual failure.

Several postulations to explain the mechanism of progressive failure have been put forward in recent years:- Skempton and La Rochelle (1965), where the effect of fissuring in over-consolidated clays is discussed; Bjerrum (1966), where the release of strain energy on weathering forms an important aspect of the hypothesis; and Yudbhir (1969) who considers the release of horizontal stresses in over-consolidated clays to be a dominant factor.

In an effort to establish the validity of these or other hypotheses, a large number of case histories were analysed by the author, James (1970). The formations studied were over-consolidated clays and clay shales and from the investigations a pattern was observed which suggested progressive failure was a most uncommon feature. Two dominant

phases were distinguished in the pattern of the development of natural slopes.

(i) A pre-slip stage. Here the loss in strength was found to be almost entirely due to a loss in terms of the parameter c', as suggested originally by de Lory (loc.cit) and quoted by Skempton (1970). During this phase the value of the parameter ϕ' remains at, or very near to, the peak value since the effect of weathering on this parameter within engineering time scales is generally negligible.

Such a decay in strength is also along the lines of the softening process outlined by Terzaghi (1936). Or, as Terzaghi suggested: on excavation of a cutting, fissures open due to the unequal lateral expansion towards the face; this allows ingress of water into the soil causing softening and swelling along the fissure planes, subsequent rupture of "intact blocks" and thereby production of further fissures. Ad infinitum or slope failure. Slopes failing due to this process are referred to as first time slips.

(ii) A post-slip stage. The necessary condition for this second stage is, obviously, a landslip. The catastrophic failure may have resulted from a general loss of strength outlined in the above paragraph (i); or, alternatively, from some form of progressive failure. In either event the clay is characterised by the presence of slip planes which have undergone considerable strain, and along which the angle of shearing resistance will have dropped some of the way from the peak to the residual value. It is sufficient to note, at this juncture, that the presence of slip planes does not necessarily imply the clay along the plane is at its ultimate residual strength, although it will generally be close to the condition.

Within the general group encompassed by this phase (ii) would be also included sites containing Pleistocene land slip zones, cambered valleys or periglacial shear zones.

For the purpose of design of slopes it is important to distinguish between first time slips in undisturbed material and reactivated slips or slips along some weak pre-existing shear zone as mentioned above.

It is suggested that if a slope in undisturbed material is designed for

$$\begin{cases} c' \rightarrow 0^{*} \\ \phi' = \phi' \text{ peak}, \end{cases}$$

then the slope will be stable from the long term point of view and, except under special circumstances, will not be subject to progressive failure. This is in contrast to the residual approach where the design could be based on the over-conservative parameters,

$$\begin{cases} c' = 0 \\ \phi' = \phi'_r \end{cases}$$

* The value of c' may be increased for cuttings required to be stable over a limited number of years, Skempton and James (in press).

It is the purpose of this paper to outline some of the circumstances which are believed to lead to progressive failure in undisturbed clays, and to suggest means of predicting such occurences. The criteria for a landslip caused by progressive failure is that (i) the landslip should be a first-time failure and not due to any pre-existing slip planes, and (ii) the slip should fail at a strength at or near to the residual, or at least substantially below the parameters given by $c' = 0$, $\phi' = \phi'$ peak.

II.- STRAINS REQUIRED FOR RESIDUAL CONDITIONS IN THE FIELD

Most hypotheses on progressive failure appear to contain the implication that residual conditions are developed rapidly on straining. However, before proceeding to discuss the subject, it is important to obtain some quantitative idea of the sorts of deformations needed to produce residual conditions along the slip plane of a landslide.

It has been found, Peck (1967), that residual conditions are reached slightly more rapidly under low stress levels than under high; and this is frequently observed in shear box tests. Since the majority of landslides in engineering works will occur under average effective normal stresses, (σ'_n), of around 5 lb/sq.in. or less, the tendency will favour a rapid reduction in strength on sliding. Alternatively, in larger landslides it may mean that the slip zone in the toe area will exhibit a lower strength than further back into the slipping mass where the stress level is higher. The orientation of the slip plane in relation to the bedding will also tend to favour an unequal development, James (1970).

However, laboratory work on the microscopic structure of clays under shear, Tchalenko (1967), suggests that for some considerable time after the peak has been passed the shear zone will not consist of a single plane but rather of multiple planes (reidel shears), one set of which is inclined at a small angle to the disturbing stress. Coalescence of these into a single, undulatory, shear plane, usually containing shear lozenges, requires a large degree of deformation; perhaps the equivalent of two or three travels in a repeated shear box test. Hence, reaching residual conditions can be a lengthy process and the effect of multiple shear zones might be expected to be even more marked under the characteristically less specific set of stresses in the field.

In order to compare the various effects of landslides a dimensionless factor, "field strain", may be introduced at this stage. This is taken as the ratio of the amount of slip movement occurring to the length of the slip plane or, more approximately, the ratio of the vertical drop in the head of the slip (height of scarp) to the height of the slip. Profiles of slopes before and after failure may be analysed to determine the strength required under both conditions, and the difference in strength can then be compared with the field strain. First time slips, only, give useful data.

Fig No. 1 shows such a relationship.

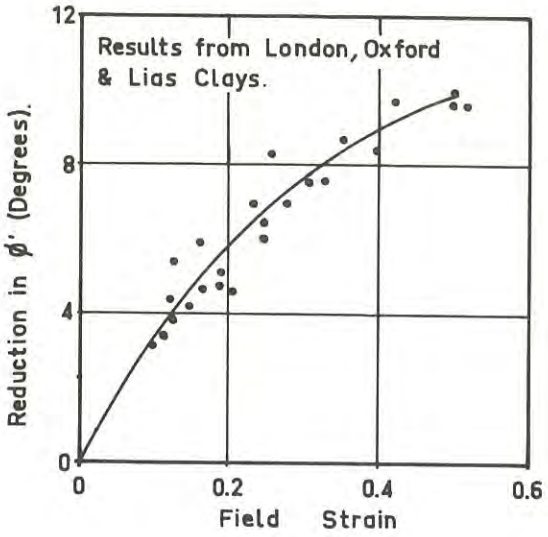

Fig. 1. Loss in strength related to field strain

For convenience, the strength drop is expressed in terms of the drop in ϕ' alone, i.e. the difference in the ϕ' required for stability in each case, assuming c' equals zero. In most of these cases, the value of c' represents less than 10% of the required total strength for stability.

It may be seen from the graph that a definite trend is present and also that considerable deformation is necessary in a first time slip in order to produce conditions which would approximate to the residual over the whole of the slip zone. For example, in a 30 ft high cutting in London Clay, a slip movement of around 7 ft (i.e. a field strain $\doteq 0.25$) would be required to give the necessary drop in ϕ' of 6^{o} between peak and residual. (ϕ' peak = 20^{o}, ϕ'_R = 14^{o} for London Clay). In less catastrophic slips it may be inferred that not the whole of the slip plane will exhibit the residual strength, while the average drop in strength will usually be less than occurs in one travel of the conventional shear box test.

In summary, it is seen that the average drop in the angle of shearing resistance of a clay will be approximately proportional to the degree of deformation undergone, with substantial strains being generally necessary to reach residual conditions. Further, residual conditions will, in most cases, tend to occur first near the toe of a slip, both due to bedding and also the lower stress levels usually applicable in this location. Nevertheless, it appears that movements of perhaps feet would be still necessary in the toe region to cause complete reduction in the angle of shearing resistance, particularly where multiple shear zones exist.

III.- MODES OF PROGRESSIVE FAILURE

The need for relatively great deformations to produce residual conditions may now be considered in the light of existing hypotheses on progressive failure, e.g. Bjerrum or Yudbhir. In both cases residual conditions are postulated to be the result of some form of expansion towards a cutting face or, alternatively, into an eroding valley. Little information regarding pre-slip movements is available in the literature, but in London Clay cuttings, de Lory (1957), it appears such movements due to high lateral stresses are small, of the order of inches. Experience in the behaviour of high faces in brick pit excavations confirms this order of magnitude of stable pre-slip movement.

Hence, it is suggested that unless the lateral movements or strains are very much localised, i.e. to one thin seam, such minor pre-slip movements would be insufficient to produce any substantial drop in the angle of shearing resistance of the clay. In other words, progressive failure is therefore unlikely in homogeneous clay slopes. London Clay, for example, would typically fall into the homogeneous category, except perhaps at the brown/blue interface, while compacted fills and many normally consolidated deposits will also be included.

It is also apparent that for a progressive failure mechanism to be effective, it must not only cause this localised straining in the vicinity of the toe of the slope, but also inwards for some distance into the slope. That is, the mechanism should be retrogressive. For most over-consolidated clays a mass lateral movement towards a cutting of several or more inches should be sufficient to release the high in-built horizontal stresses, thus depriving a progressive failure mechanism, due to this alone, of its disturbing influence. In the case of the release-of-strain-energy-due-to-weathering approach, while the rate of release can only be guessed at, there seems to be no reason for such a mechanism to extend with finite strains for any distance into a slope over engineering time scales.

Thus, from the above, it may be inferred that progressive failure, at least as a dominant mechanism of strength decay, requires a certain set of conditions for its implementation. And, in fact, reliable case histories of large seemingly initial movements, i.e. first time slides, at or near the residual strength are rare. Many instances of landslides originally thought to be first time slides at exceptionally low strengths have proved to be reactivation of older landslides, e.g. Walton's Wood, Skempton and Petley (1967); the Seattle Freeway landslides, Wilson and Johnson (1964); Portuguese Bend, Merriam (1960).

The Devon Rd Landslide, (Alberta), Broscoe and Thompson (1967), shown in Fig No. 2 is an initial slide. Slipping has taken place here along a

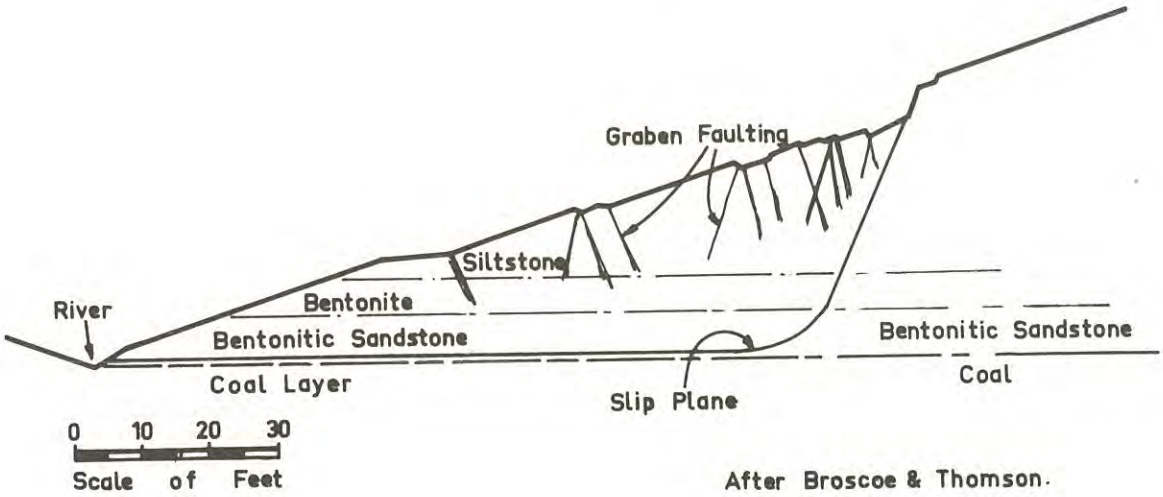

Fig. 2. Devon Rd Landslide, Edmonton

bentonitic layer in a bentonitic sandstone, at or near the junction with the coal layer. The valley in the area shows no signs of instability and the present slide was initiated by a small road cutting near the toe. Analyses indicate that the required angle of shearing resistance here could be as low as 5^{o}, Morgenstern (personal communication). Graben faulting on the surface of the slope also indicates that movement has been retrogressive, i.e. commencing at the toe and working inwards, and drilling behind the slipped area has proved that slickensiding also exists there, in the in-place bentonitic material just above coal. Thus relative deformations have occurred to quite some distance in from the toe. This site has all the attributes of progressive failure.

A mechanism which would here provide the relative deformation and slickensiding in the bentonite, i.e. the progressive failure, would be a non-homogeneous swelling mechanism. By this is meant a differential swelling of the swelling soil layer against the non-swelling layer with strains occurring in a fashion analagous to those at the interface of competent and incompetent beds during folding. Swelling in such a case might be initiated by stress releases during valley formations, and it is possible that swelling pressures up to several tons per square foot could be developed. Expansion would occur out towards the valley sides, thus releasing stresses interiorly, and thereby allowing the process to continue. Hence, non-homogeneous swelling has the attribute of extended retrogressive behaviour, while strains associated with the process will typically be localised to the interface with layers of different composition.

Few sites provide data as dramatic as the Devon Rd site. However, similar tendences have been observed in other sites with distinct non-homogeneities. For example, the tendency was observed to a lesser degree in several London Clay sites where the failure plane was observed to follow along the jucntion of the weathered brown with the unweathered blue clay, James (1970). It is reasonable to assume the reaction of the two forms of the clay to stress release and swelling would be different, thus providing a means whereby differential straining could occur along this brown/blue boundary. In the relevant cases, it was observed that, while the strength required for stability was still well above the residual, it was nevertheless significantly below that typical in a cutting of the same age in this formation. Thus, it is suggested that a small amount of progressive failure could have occurred in such cases. The London Clay contains minor but significant amounts of montmorillonite disseminated in the mass, thus providing a small to moderate swelling potential.

Obviously, there is scope for some detailed analyses and instrumentation of slopes and cuttings to provide further evidence for this non-homogeneous straining hypothesis, but it is the author's opinion that non-homogeneous swelling either after the construction of a cutting or during valley formation, will be the dominant if not the only mechanism for true progressive failure.

IV.- ACKNOWLEDGEMENTS

Much of the work on which this paper was based was carried out when the author was Research Assistant at Imperial College, London. The author is grateful to Professor A.W. Skempton for his help and advice during this time and likewise to Professor N.R. Morgenstern who also provided information on North American slides quoted herein.

V.- REFERENCES

Binger, W.V. (1948). Analytical studies of the Panama Canal slides. Proceeds 2nd I.C.S.M.F.E. Vol. 2.

Bjerrum, L. (1966). The mechanism of progressive failure in slopes of over-consolidated plastic clays and clay shales. 3rd Terzaghi lecture, A.S.C.E. Struct. Eng. Conf., Miami.

Borowicka, H. (1963). The Vienna method of shear testing. A.S.T.M. Spec. Tech. Publ. 361, p306-314.

Broscoe, A.J. & Thomson, S. (1967). The Devon Rd Landslide. Assn. of Engin. Geol. Meeting, Dallas, Oct 1967.

Cassel, F.L. (1948). Slips in fissured clays. Proceeds 2nd I.C.S.M.F.E. Vol 2.

de Lory, F.A. (1957). Long term stability in slopes in over-consolidated clays. Ph.D. Thesis, Univ. of London.

Gould, J.P. (1960). A study of the shear failure in certain tertiary marine sediments. A.S.C.E. Res. Conf. on Shear Strength, Boulder, p615-647.

James, P.M. (1970). Time effects and progressive failure in clay slopes. Ph.D. Thesis, Univ. of London.

Peck, R.B. (1967). Stability of natural slopes. Jnl. S.M. & F.E. Div., A.S.C.E., 93:4:403-418.

Skempton, A.W. (1948). The rate of softening in stiff fissured clays, with special reference to London Clay. Proc. 2nd I.C.S.M.F.E., Vol 2.

Skempton, A.W. (1964). Long term stability of clay slopes. 4th Rankine lecture, Geotechnique 14:2:75-102.

Skempton, A.W. (1970). First time slides in over-consolidated clays. Geotechnique 20:3:320-324.

Skempton, A.W. & La Rochelle, P. (1965). The Bradwell slip. Geotechnique 15:3:221-242.

Skempton, A.W. & Petley, D. (1967). The strength along structural discontinuities in stiff clays. Proc. Geotech. Conf., Oslo, Vol 2, 3-20.

Tchalenko, J.S. (1967). The influence of shear and consolidation on the microscopic structure of some clays. Ph.D. Thesis, Univ. of London.

Terzaghi, K. (1936). Stability of slopes in natural clays. Proc. 1st I.C.S.M.F.E. Vol 1, 161-165.

Wilson, S.D. & Johnson, K.A. (1964). Slides in over-consolidated clay along the Seattle Freeway. 2nd Annual Eng. Geol. & Soil Eng. Symposium Proc. p29-42.

Yudbhir (1969). Engineering behaviour of over-consolidated clays and clay shales with special reference to long term stability. Ph.D. Thesis, Cornell Univ., Ithaca, N.Y.

Effects of Anisotropy and Sample Disturbance on the "$\Phi_u = 0$" Stability Analysis

By
G. R. Martin, M.E., Ph.D. (Calif.)
(Senior Lecturer in Civil Engineering, University of Auckland)
AND
T. J. Kayes, M.E.
(Soils Engineer, Rendel Palmer and Tritton, London)

SUMMARY.- Studies have shown that undrained strengths of many saturated clays vary with the direction of the failure plane. As such strength anisotropy is not taken into account in the conventional "$\Phi_u = 0$" stability analysis for slopes in saturated clays, it has been suggested that the success of the "$\Phi_u = 0$" method is in some measure due to the compensating effects of strength anisotropy and sample disturbance. In this paper, the effects of strength anisotropy and sample disturbance on the "$\Phi_u = 0$" stability analysis are examined analytically, with a view to assessing their combined effects.

Using an idealized theoretical relationship to describe variations of undrained strength with direction, non-dimensional stability curves are presented for a range of slopes with varying degrees of strength anisotropy. The combined effects of strength anisotropy and sample disturbance are presented in chart form in terms of an "error factor", which gives a direct indication of the discrepancy between factors of safety as found in the conventional "$\Phi_u = 0$" analysis, and the insitu factor of safety taking into account strength anisotropy and sample disturbance.

It is shown that the effects of strength anisotropy and sample disturbance tend to be compensating for flat slopes of normally consolidated clays in particular, although in some cases where a marked degree of anisotropy exists, the conventional "$\Phi_u = 0$" method may overestimate the factor of safety. For heavily over-consolidated clays, the effects are additive, the conventional method being somewhat conservative.

I.- INTRODUCTION

The conventional "$\Phi_u = 0$" method of stability analysis is widely used for assessing the short term stability of cut slopes in saturated intact clays. The method, the basis of which is described by Skempton (Ref. 1), assumes the slip surface to be a circular arc, with the strength mobilized over the failure surface being assumed to equal the apparent cohesion c_u as determined in unconsolidated undrained triaxial tests on soil samples taken vertically in the field. The method has been justified for design purposes by the analysis of several failures (Refs. 2 and 3), where computed minimum factors of safety have generally been close to 1. Also recent research (Refs. 4 and 5), indicating that the stress changes associated with sampling have only a small effect on the undrained strength of vertical samples, would suggest the method is a valid approach.

Although from the above evidence, the "$\Phi_u = 0$" method would appear a reasonable design approach, several factors are not taken into account. In the first instance, it is implicit in the method that the soil is isotropic with respect to undrained strength. However many studies, several of which have recently been summarized by Duncan and Seed (Ref. 6), have indicated that clays are anisotropic with respect to undrained strength to varying degrees. Secondly, all laboratory samples are disturbed to some degree during sampling, transporting and laboratory preparation, which results in some loss of strength compared to insitu strengths. Both of the above factors must have an important bearing on the accuracy of the conventional "$\Phi_u = 0$" stability analysis. In addition, the strength used in the "$\Phi_u = 0$" analysis is half the deviator stress at failure, rather than the shear stress on the failure plane, and is based on triaxial rather than plane strain strengths. This could also affect the accuracy of the analysis. These factors when taken together, suggest that a computed minimum factor of safety of near unity for a slope failure, as has been noted in many instances, could be rather fortuitous if computed using the conventional "$\Phi_u = 0$" analysis. The effects of including the above factors on the "$\Phi_u = 0$" analysis are examined below, with a view to assessing the importance of their combined effects.

II.- NOTATION

The following symbols have been adopted for use in this paper:

- c' effective cohesion
- c_e true cohesion (after Hvorslev)
- c_u apparent cohesion as determined in triaxial test, $\frac{1}{2}(\sigma_1 - \sigma_3)_f$
- $(c_u)_i$ apparent cohesion with sample axis at angle i to the vertical
- f angle between failure plane and plane of major principal stress
- i angle between major principal stress and the vertical axis
- k degree of anisotropy $(c_u)_{i=0}/(c_u)_{i=90^\circ}$
- $\bar{A}_f$ pore pressure parameter (change in pore pressure/change in deviator stress) at failure

D	Depth factor
E_F	error factor ρ_D/ρ_A
F	factor of safety
H	vertical height of slope
N	stability number
α	geometric parameter
β	angle of slope to horizontal
γ	unit weight of soil
λ	geometric parameter
ρ_A	anisotropy ratio
ρ_D	disturbance ratio
σ_1	major principal stress
σ_3	minor principal stress
θ	geometric parameter
Φ_u	apparent angle of internal friction
Φ'	effective angle of internal friction
Φ_e	true angle of internal friction. (after Hvorslev)

III.- UNDRAINED STRENGTH ANISOTROPY IN CLAY

Most clay deposits are initially consolidated one dimensionally under an anisotropic system of stresses. Studies of clay structure, such as that presented by Mitchell (Ref. 7), have shown that there is a tendency for plate-like clay particles to become oriented with their flat sides parallel to the plane of the major principal stress during one dimensional consolidation. With such preferred particle orientation, it is not surprising that many clays have been found to be anisotropic with respect to undrained strength.

Variations of undrained strength with orientation of the failure plane may be investigated by simply trimming triaxial samples with their axes at different angles to the vertical axis of a field sample.

It has been shown by Duncan and Seed (Ref. 8), that assuming perfect sampling, the variation of strength determined in such a manner, should be similar to that occurring insitu. Results of such tests may be plotted in the form shown in Fig. 1.

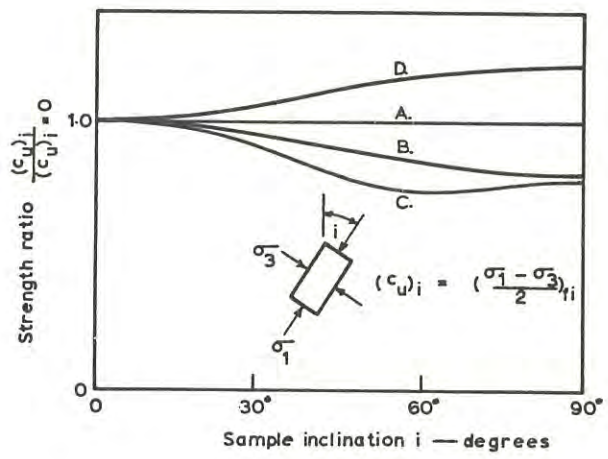

Fig. 1 Variation of undrained strength with sample orientation.

Tests on some clays have shown negligible strength variation with direction indicating isotropic properties as shown by line A. However many tests on normally consolidated or lightly overconsolidated clays have resulted in strength variations as shown in curves B and C (Ref. 6). Curve B is typical of soils which give minimum strengths for samples trimmed horizontally. However in some instances, minimum strength occurs when the failure plane is horizontal as shown by Curve C. For heavily overconsolidated clays, strengths of horizontal samples are greater than that of vertical samples as shown by Curve D. This may be related to the fact that for such clays, the insitu horizontal stresses are greater than the vertical stresses.

As discussed by Duncan and Seed (Ref. 6), variations of undrained strength such as shown in Fig. 1 may arise from several contributing sources. In terms of physical soil properties, anisotropy with respect to the shear strength parameters c' and Φ', (or c_e and Φ_e); and anisotropy with respect to the pore pressure parameter $\bar{A}_f$ could contribute to variations of undrained strength with orientation of the failure plane, both being related to the nature of the clay structure. Reorientation of principal stress directions during sampling and testing may also contribute to undrained strength anisotropy. Hansen and Gibson (Ref. 9) have shown that reorientation of principal stress directions during loading would result in variations of undrained strength even if the clay was isotropic with respect to all physical properties. Such reorientation will occur in the field during the construction of a cutting to varying degrees around a potential slip surface. Tests described by Duncan and Seed (Refs. 6 and 8) have suggested that anisotropy with respect to $\bar{A}_f$, and reorientation of principal stresses during loading are primarily responsible for undrained strength anisotropy, with anisotropy with respect to the shear strength parameters being of secondary importance.

IV.- EFFECT OF ANISOTROPY ON SLOPE STABILITY

The effects of undrained strength anisotropy on the conventional "$\Phi_u = 0$" stability analysis have been considered by Lo (Ref. 10) and Ranganatham et.al. (Ref. 11). In order to carry out a general stability analysis including the effects of anisotropy, it is necessary to establish a mathematical relationship between the undrained strength $(c_u)_i$ resulting from a triaxial test with the sample axis at an angle i to the vertical, and the angle of inclination i. It has been found (Ref. 10) that test results generally lie close to a theoretical curve given by

$$(c_u)_i = (c_u)_{i=90} + [(c_u)_{i=0} - (c_u)_{i=90}]\cos^2 i \quad (1)$$

Curves B and D shown in Fig. 1 have been drawn according to this relationship, which was first proposed by Casagrande and Carrillo (Ref. 12). In order to make use of the relationship given by equation (1), it is necessary to know the inclination of the principal stresses at failure over the length of the failure arc. Using the notation adopted by Lo as shown in Fig. 2, if f is the angle of the failure plane to the plane of the major

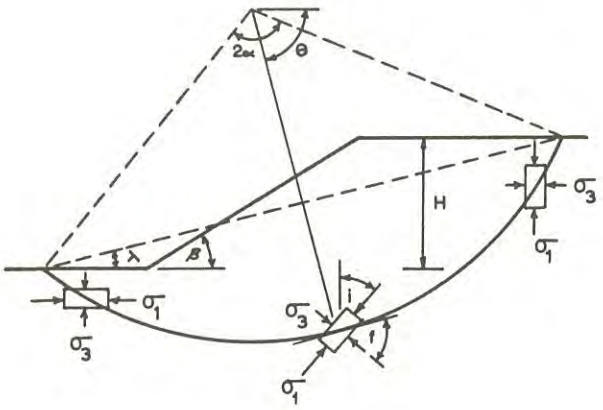

Fig. 2 Typical slip circle showing stress orientation at failure.

principal stress, then

$$i = f + \theta - \frac{\pi}{2} \qquad (2)$$

The results of strength tests on an anisotropic clay reported by Lo, suggest that f is relatively independent of i. As it is generally accepted that $f = 45 + \Phi_e/2$, this suggests that anisotropy with respect to Φ_e is relatively insignificant, as suggested by Duncan and Seed (Refs. 6 and 8).

Making use of equations (1) and (2) (assuming a constant value of f = 55°), Lo developed an analytical solution for the stability of the simple slope shown in Fig. 2, based on the "$\Phi_u = 0$" concept. By integrating equation (1) over the length of a potential failure arc, the average shear strength mobilized over the failure surface may be shown to be given by

$$(c_u)_{av.} = \frac{1}{2\alpha}[(1+k)(c_u)_{i=0}\alpha + \tfrac{1}{2}(1-k)(c_u)_{i=0}\, x \sin 2\alpha \cos(2f-2\lambda)] \qquad (3)$$

$$\text{where } k = \frac{(c_u)_{i=90°}}{(c_u)_{i=0°}} \text{ (degree of anisotropy)}$$

Defining the factor of safety F as being equal to the ratio of the resisting moment to the overturning moment, solutions may be conveniently expressed by the equation

$$F = \frac{(c_u)_{i=0}}{\gamma H} N \qquad (4)$$

where N is a stability number. Lo presents curves of the critical stability number (i.e. F=1) versus slope angle β for the general case shown in Fig. 2 and for toe circles, with values of k varying between 0.5 and 1. The case where strengths increased with depth was also considered.

Lo's results were extended by the authors, with values of k > 1 (typical of heavily overconsolidated clays), and circles tangential to a hard stratum being considered. Results are shown plotted in Figs. 3, 4 and 5. Critical circles were located with the aid of a computer program incorporating a search routine. The curves corresponding to values of k = 1.0 (isotropic case) are identical to the standard "$\Phi_u = 0$" solutions presented by Taylor (Ref. 13), except that the stability number N used is the inverse of that adopted by Taylor. From the above figures, it may be seen that the effects of anisotropy may have a significant effect on computed factors of safety. For example, for a 30° slope with D = 0.5H (Fig. 5), factors of safety computed assuming isotropy would be 11% less than the value calculated for a case where k = 1.2 and 9% greater than that for a case where k = 0.8. The difference in the position of critical circles for the anisotropic cases, compared to the position of the critical circles for isotropic cases, was found to be relatively small.

V.- COMPENSATING FACTORS

It has been suggested (Refs. 10, 14) that the effects of compensating factors as outlined in the introduction, and in particular sample disturbance, could possibly account for the success of the conventional "$\Phi_u = 0$" analysis, at least in the case of normally consolidated or lightly over-consolidated clays where k is less than 1. For such soils, Figs. 3-5 show that factors of safety computed assuming k = 1 are too high, and hence it is apparent that the effects of sample disturbance could compensate for the error.

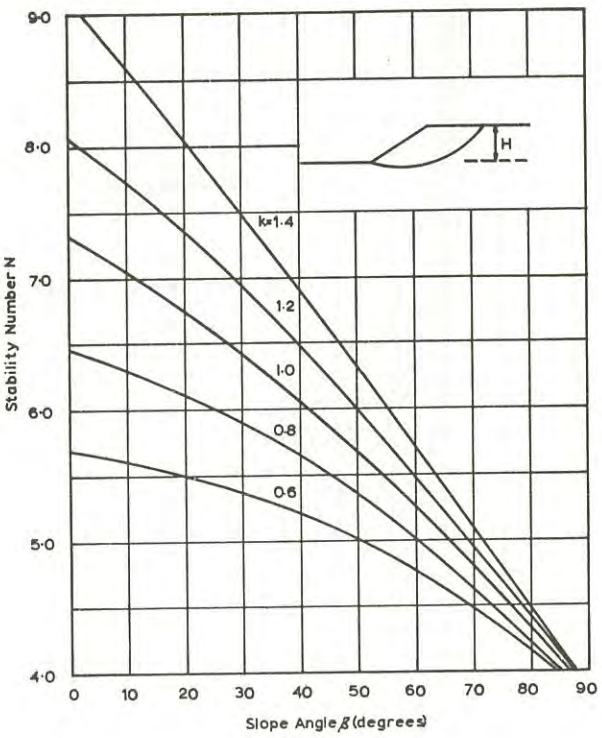

Fig. 3 Stability number vs. slope angle (toe circles).

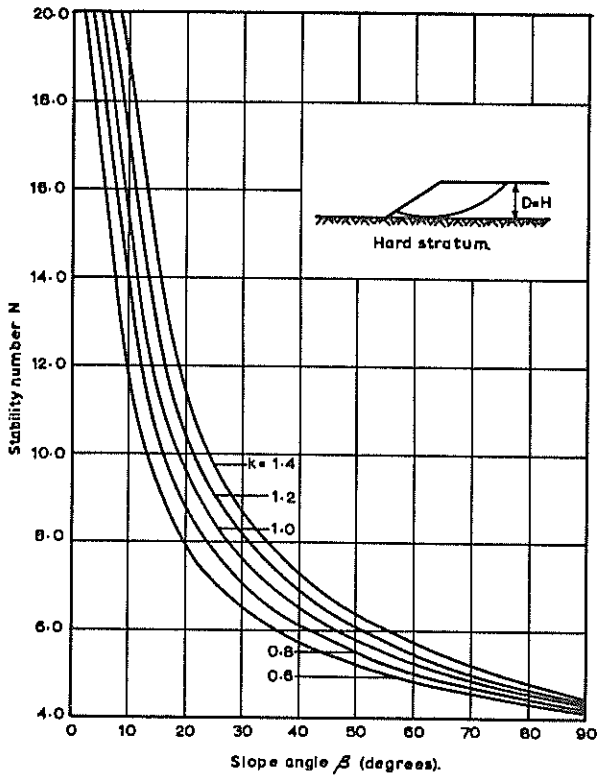

Fig. 4 Stability number vs. slope angle (D = 0)

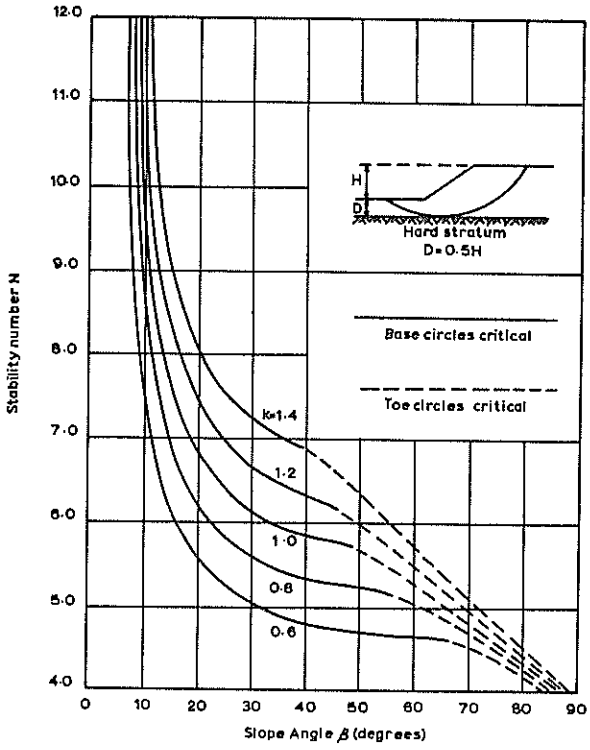

Fig. 5 Stability number vs. slope angle (D = 0.5H)

In order to illustrate such compensating effects, it is useful to make use of two non-dimensional ratios as defined by Duncan and Seed (Ref. 14), namely a disturbance ratio ρ_D and an anisotropy ratio ρ_A. The disturbance ratio is defined by the equation

$$\rho_D = \frac{c_u \text{ (from triaxial tests on vert. samples)}}{\text{insitu shear strength for vert. plane strain}} \quad (5)$$

The ratio hence reflects the difference between undrained strengths of disturbed vertical triaxial samples as determined in the laboratory, and insitu shear strengths for the same orientation of the failure plane, determined under plane strain conditions. For the purpose of this investigation a value of $\rho_D = 0.9$ is assumed. Duncan and Seed (Ref. 14), report a value of $\rho_D = 0.94$ for San Francisco Bay Mud based on lab tests on high quality samples subjected to minimal disturbance, and hence the value of 0.9 assumed would reflect good field sampling techniques. The anisotropy ratio is defined by the equation

$$\rho_A = \frac{\text{avge. insitu shear strength for plane strain}}{\text{insitu shear strength for vert. plane strain}} \quad (6)$$

Values of ρ_A hence reflect the effects of anisotropy on undrained strengths mobilized over a failure surface in the field. Assuming that the anisotropy ratio as defined above, is equal to the ratio defined with respect to undrained triaxial strengths, c_u, then from equation (3), we may write

$$\rho_A = \frac{1}{2\alpha}[(1+k)\alpha + \tfrac{1}{2}(1-k)\sin 2\alpha \cos(2f-2\lambda)] \quad (7)$$

Based on the above two ratios, one can define an "error factor"

$$E_f = \frac{\rho_D}{\rho_A} = \frac{c_u \text{ (from triaxial tests on vert. samples)}}{\text{avge. insitu shear strength for plane strain}} \quad (8)$$

As the factor of safety computed using the conventional "$\Phi_u = 0$" method of analysis is proportional to the shear strength used in the analysis, the "error factor" gives a direct indication of the discrepancy between the calculated factor of safety as found in the conventional "$\Phi_u = 0$" analysis (assuming isotropy), and the true insitu factor of safety. Using a value of $\rho_D = 0.9$, and critical values of ρ_A corresponding to slip circles giving minimum factors of safety as determined in the study described in the previous section, values of E_f were computed using equation (8), and are shown plotted against slope angle in Figs. 6, 7 and 8.

From the error factor curves, it may be seen that for values of k of the order of 0.8, which could be typical of many normally consolidated clays, the effects of anisotropy and sample disturbance tend to compensate, particularly for flatter slopes and deeper seated failure circles. However, for values of k less than 0.8, the conventional "$\Phi_u = 0$" method in some cases overestimates the factor of

safety. For values of k greater than one, typical of more heavily overconsolidated clays, the two effects become additive. For example, from Fig. 8, for a 30° slope where k = 1.2, E_f = 0.83. Therefore, if the computed factor of safety using the conventional "Φ_u = 0" analysis equals 1.0, then the insitu factor of safety would be 1.2. It should be noted that the discontinuities in Fig. 8 where the critical circles change from "base" to "toe" circles, indicate that although the factors of safety for the two circles are the same at the transition point, the actual circles are not identical. Also the trend for toe circles to approach an error factor of 0.9 (i.e. an anisotropy ratio of 1.0) as the slope angle increases, reflects the fact that the failure arc tends towards a straight line of slope f, failure being similar to that of a vertical sample

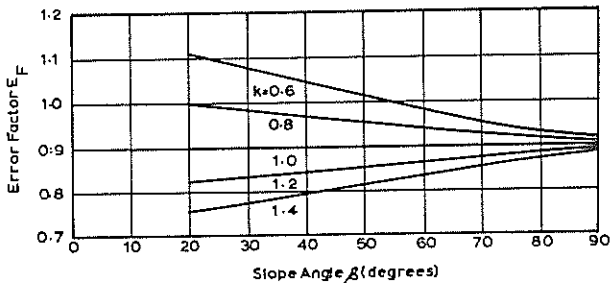

Fig. 6 Error factor vs. slope angle (toe circles)

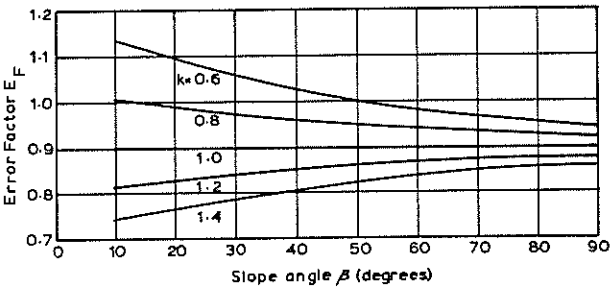

Fig. 7 Error factor vs. slope angle (D = 0)

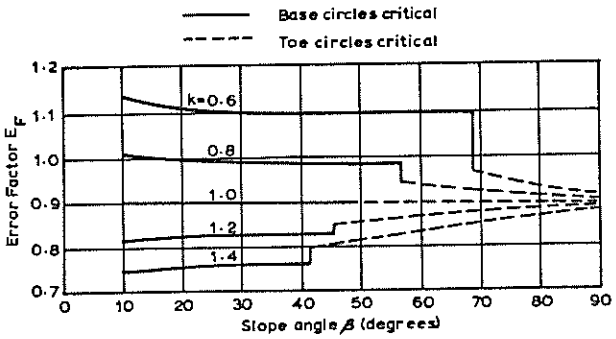

Fig. 8 Error factor vs. slope angle (D = 0.5H)

VI.- CONCLUSIONS

The combined effects of undrained strength anisotropy and sample disturbance on the conventional "Φ_u = 0" stability analysis for slopes, have been shown to be of significance. The two effects tend to be compensating, particularly for flat slopes in normally consolidated clays, where undrained strengths in the vertical direction are greater than those in horizontal directions. However, in some cases for marked degrees of anisotropy, the conventional method may overestimate the factor of safety. For heavily overconsolidated clays where vertical strengths are less than horizontal strengths, the two effects are additive, factors of safety computed by the conventional method being somewhat conservative.

For immediately after construction stability problems for slopes in intact saturated clays, the conventional "Φ_u = 0" analysis has proved simple and relatively reliable as a design tool, and no doubt will continue to be used. However, it is suggested that where economy or site conditions necessitate the use of a factor of safety of the order of 1.2 or less, the degree of anisotropy be determined by testing triaxial samples trimmed in both vertical and horizontal directions, and the combined effects of anisotropy and sample disturbance taken into account in assessing insitu stability.

VII.- ACKNOWLEDGEMENTS

The authors wish to thank Mr. P.W. Taylor for his helpful criticism during preparation of the paper.

REFERENCES

1. SKEMPTON, A.W., - The ϕ = 0 Analysis of Stability and its Theoretical Basis. Proc. Second Int. Conf. on Soil Mech. and Found. Engg., 1948, Vol. 1, pp. 72-78.

2. SKEMPTON, A.W., and GOLDER, H.Q., - Practical Examples of the ϕ = 0 Analysis. Proc. Second Int. Conf. on Soil Mech. and Found. Engg., 1948, Vol. 2, pp 63-70.

3. BISHOP, A.W., and BJERRUM, L., - The Relevance of the Triaxial Test to the Solution of Stability Problems. Proc. A.S.C.E. Research Conf. on the Shear Strength of Cohesive Soils, 1960. pp. 437-501.

4. SKEMPTON, A.W. and SOWA, V.A., - The Behaviour of Saturated Clays During Sampling and Testing. Geotechnique, Vol. 13, No. 4, 1963, pp. 269-290.

5. NOORANY, I. and SEED, H.B., - Insitu Strength Characteristics of Soft Clays. Proc. A.S.C.E., Vol. 91, No. SM2, March 1965, pp. 49-80.

6. DUNCAN, J.M., and SEED, H.B., - Anisotropy and Stress Reorientation in Clay. Proc. A.S.C.E., Vol. 92, No. SM5, Sept. 1966, pp. 21-50.

7. MITCHELL, J.K., - The Fabric of Natural Clay and its Relationship to Engineering Properties. Proc. Highway Research Board, Vol. 35, 1956,

pp. 693-713.

8. DUNCAN, J.M., and SEED, H.B., - Strength Variation along Failure Surfaces in Clay. Proc. A.S.C.E., Vol. 92, No. SM6, Nov. 1966, pp.81-104.

9. HANSEN, J.B. and GIBSON, R.E., - Undrained Shear Strengths of Anisotropically Consolidated Clays. Geotechnique, Vol. 1, No. 3, June 1949, pp. 189-204.

10. LO, K.Y., - Stability of Slopes in Anisotropic Soils. Proc. A.S.C.E., Vol. 91, No. SM4, July 1965, pp. 85-106.

11. RANGENATHAM, B.V., SANI, A.C., and SREENIVASULU, V., - Strength Anisotropy on Slope Stability and Bearing Capacity of Clays. Proc. Seventh Int. Conf. on Soil Mech. and Found. Engg., 1969, Vol. 2, pp. 659-667.

12. CASAGRANDE, A. and CARRILLO, N., - Shear Failure of Anisotropic Soils. Contributions to Soil Mechanics 1941-1953, Boston Society of Civil Engineers.

13. TAYLOR, D.W., - Stability of Earth Slopes. Contributions to Soil Mechanics 1925-1940, Boston Society of Civil Engineers.

14. DUNCAN, J.M., and SEED, H.B., - The Effect of Anisotropy and Reorientation of Principal Stresses on the Shear Strength of Saturated Clay. Univ. of Calif., Berkeley, Soil Mechanics and Bituminous Materials Research Laboratory, Report No. TE-65-3, 1965.

An Investigation of an Earth Pressure Problem using a Rod Model Analogue

By

R. Butterfield, B.Sc. (Eng.), D.I.C.

(Senior Lecturer in Civil Engineering, University of Southampton, England)

AND

K. Z. Andrawes, M.Sc., Ph.D.

(Research Fellow, University of Southampton, England)

SUMMARY.- The paper presents results obtained from a small rigid retaining wall rotating about its top into brass-rod fill material used to model a granular medium deforming in plane strain. Detailed measurements were made of the variation of the wall pressure distribution with wall rotation and the complete displacement and strain fields produced in the model. These are discussed and compared with published data obtained from similar walls rotating into sand backfill. Whereas similarity between both measured and predicted results suggests that in these circumstances the rod material is a viable analogue for a loosely packed granular medium their kinematic behaviour is disimilar. In contrast to a loose granular medium distinct velocity discontinuities develop in the rod material around which volumetric expansion occurs and changes of mean stress produce negligible volumetric strains.

I.- INTRODUCTION

In the investigation of plane strain models incorporating granular materials an unavoidable problem is introduced by the restraining forces which arise from the relative motion between the deforming material and the structure introduced to impose the plane strain boundary condition. There are two basic alternative approaches to this problem, either to use relatively wide models (Ref. 1,2) and by taking all measurements as nearly as possible on the centre plane of the model minimise the effect of the extraneous plane boundary forces or to use much narrower models (Refs. 3,4) across which any additional forces will be essentially uniformly distributed and accept the inherent errors that these will produce. Whereas measurements of stresses on the centre section of a long retaining wall (Ref.1), or foundation (Ref.2), is feasible detailed measurements of displacement and strain fields can, at present, only be made on the boundary planes of such models (Ref. 5,6). The two sets of data obtained this way will not therefore be strictly comparable. Use of a narrow model can ensure that the measured stress and strain fields do refer to the same plane and since both of these will be practically uniform across the width of the model the displacement field may be determined equally well either in the centre plane using X-ray techniques (Refs. 3,4) or on the boundary planes (Refs. 2,5,6). Since neither of the models mentioned is entirely satisfactory a number of workers have used a two dimensional rod-medium as an analogue of the granular material (Ref. 7 to 12). Such an analogue has immediate attractions in that the plane strain boundary condition is automatically and simply satisfied without using any confining structure and also, by using small diameter high density metal rods, relatively large forces can be generated in small models. The model size is then mainly governed by the requirement that the mean rod diameter must be statistically small in relation to the dimensions of any load cells or displacement measuring grids used. However any use of a "rod-analogue" makes the fundamental assumption that it is indeed a valid representation of a granular material deforming plane strain. This is an unavoidable requirement whether the analogue is to be used for obtaining data on either detailed or overall kinematic behaviour or detailed or overall stress distributions. This paper attempts to investigate the validity of a rod-analogue used in conjunction with a rigid model retaining wall rotating about its top into the fill by comparing in some detail the experimental results obtained with those obtained from similar models using sand. (Refs. 3,4,15)

II.- THE EXPERIMENTS

(a) The Rod Material

Brass rods of three sizes were used, (2.62, 1.56 and 0.71 mm diameter, by 73 mm long) combined in the ratio of 20% : 50% : 30% by weight respectively, which from detailed visual inspection appears to overcome the very strong anisotropy generated when single sized rods are used alone. It was found that hand packed rods, lightly tamped in place in the model, gave an equivalent specific gravity of 6.50 readily reproducible to within $\pm$ 2%. The converse of this attractive feature is that the achievable range of specific gravities is quite small being from 6.0 to 6.75. In order to satisfy the statistical requirements mentioned above minimum load cell dimensions of 25 mm and displacement grid dimensions of 15 mm were adopted. Biaxial tests on this material (Fig.1) using lubricated end plattens suggested that its Coulomb $\phi \approx 32^{\circ}$ at the low mean stress levels developed in the model, that it has a brittleness index = 0.9, that it is essentially incompressible under small spherical stress increments and that its friction angle on the mild steel wall = 7°.

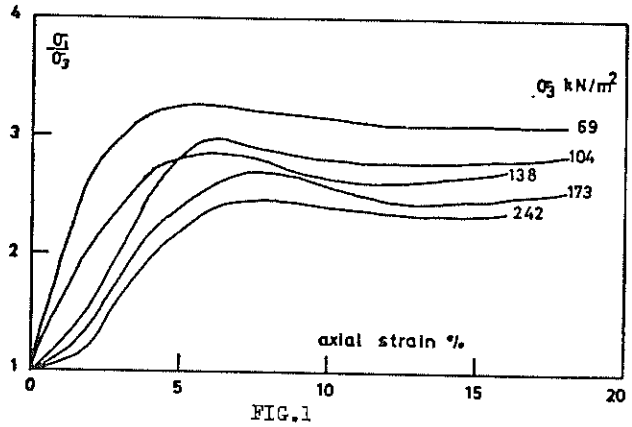

FIG.1

(b) The Retaining Wall Model

This is shown schematically in Fig. 2 the most important feature of which is the rigid model wall, 190 mm high (H), built entirely from seven small full-width (73 mm) load cells. They each had an active face height of 25 mm, were very stiff (1.5 KN/mm) and measured normal forces only up to 100 N on this face with a sensitivity of 0.4 N irrespective of the eccentricity of the force. The wall could be rotated in displacement controlled increments about an axle, 25 mm above top fill level, supported in a very stiff (10KN/mm) instrumented bearing designed to measure the vertical and horizontal reaction forces on the axle. The force in the cable rotating the wall via the quadrant at its top (Fig. 2) was also measured. These three forces therefore provided an independent check of the resultant forces acting on the wall.

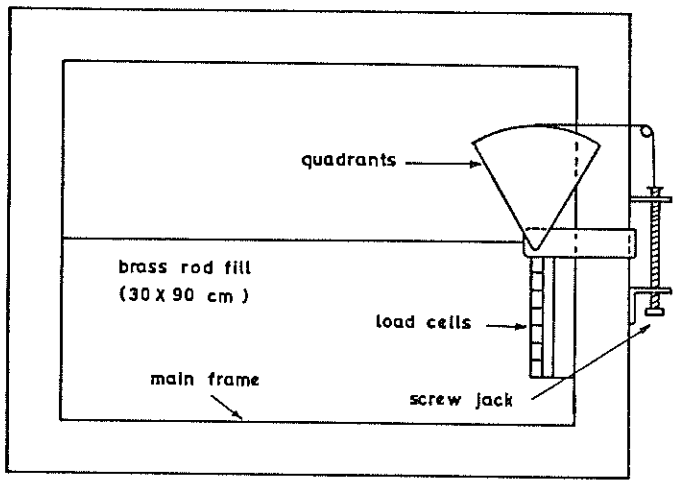

FIG. 2

III.-RESULTS

(a) Wall Pressures

Fig. 3 shows as full lines typical dimensionless wall pressure distribution $(\sigma/\gamma H)$ diagrams obtained as the wall was rotated into the fill progressively through angles of 0.2°, 0.4°, 0.8°, 1.5°, 3° and 6°, where $1\frac{1}{2}$° rotation corresponds to a wall toe movement of about 5 mm. The total normal force on the wall increased rapidly with wall rotation reaching a maximum at between 3° and 6° and only decreased by typically 10% as the rotation was increased to 10°. Its maximum value was 270 N ± 10 N acting at 0.28 H above the wall toe which is quite close to the total normal 'Rankine' force of 284 N calculated for a smooth wall and $\phi = 32°$.

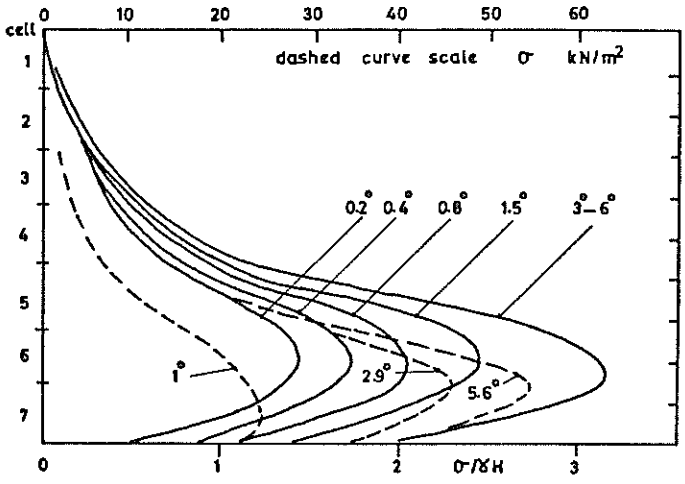

FIG.3

Also shown in Fig. 3 (dashed lines) are actual pressure distributions taken from Ref. 4, Fig. 19 for a similar model wall rotating into a loose sand ($e \simeq 0.70$, $\phi \simeq 35°$) through angles of 1°, 2.9° and 5.6° which are of a generally similar shape to those obtained from the rod model and also indicate a maximum total force occurring at about 6° wall rotation although the centre of pressure is rather lower on the wall at 0.21 H above the base. In this case the maximum wall force measured was 720 N whereas a smooth wall $\phi = 35°$ calculation gives 690 N and 720 N requires a wall friction angle of 2°. The similarity between the wall pressure distributions, the rotation to peak normal force on the wall and its small decrease with additional rotation in both the rod model and the loose sand model suggests that their behaviour is closely analogous at the low stress levels used. It should be noted that identical tests using a dense sand ($e = 0.53$) gave a peak normal wall force at 1.6° rotation which had dropped by more than two thirds at a rotation of 6° (Fig. 17a, Ref.4). Measurements made on a long wedge shaped body (60° apex angle) driven vertically into both sand and the same rod material (Ref.2) showed that again the penetration resistance varied similarly in the rod model and loose sand. Other experimental evidence (e.g. Refs. 10,11) also supports this conclusion.

Unfortunately the overall vertical friction forces acting on the walls could not be compared since the vertical force sensitivity of the axle support bracket in the rod model, proved to be inadequate although the summation of the load cell readings agreed almost exactly with the resultant horizontal force measurements.

(b) Displacement and Strain Fields

Photographs of the deforming model were taken with the intention of measuring the displacement of a marker grid (Figs. 4) (in this case the end point of a shadow cast by protruding rods) from which the incremental strain field could be obtained. This was attempted for a cumulative wall rotation from 0^{o} to 6^{o} by taking hand measurements from an enlarged projection of the photographic negatives, a method which proved to be not only very laborious but also insufficiently sensitive. At a later date we developed a stereo-photogrammetric displacement field measuring technique (Refs. 5,6) which does not require the use of a special marker grid and is equally applicable to either granular materials or rod models. This was used with the negatives of the two photographs shown in Figs. 4 (a,b) which refer to one small wall rotation increment of from $4\frac{1}{2}^{o}$ to 6^{o}. If these plates are viewed in an ordinary mirror stereoscope the three dimensional relief which was contoured to obtain the complete horizontal and vertical displacement field components shown in Figs. 5a, b will be clearly seen. In particular the major velocity discontinuity occurring along the bounding slip line is very evident.

The complete displacement contours were drawn very simply in about two hours using a Galileo-Santoni Mark II plotting machine as described in Refs. 5,6. Subsequently more precise "spot-height" measurements were made on the stereo model at points spaced 16 mm apart in the real model from which the incremental strain fields shown in Figs 6(a,b) were calculated. For this purpose the displacement components were measured to 10-micron sensitivity using the original 58 mm square roll-film negatives which were approximately a 1:5 scale reduction on the actual model size. Obviously larger scale photographs on plates can potentially produce much more precise information. The rotation increment of $1\frac{1}{2}^{o}$ (.025 radians) is almost exactly that used (.023 rads.) by workers at Cambridge to obtain the maximum shear strain contours published as Fig. 6 in Ref. 3, Fig. 25a in Ref. 4 and Fig. 19a in Ref. 15 for a wall rotating about its top into a dense Leighton Buzzard sand (e= 0.52 - 0.55).

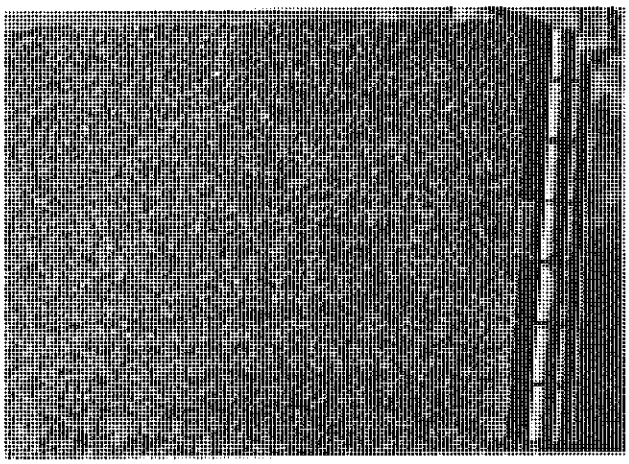

FIG. 4a

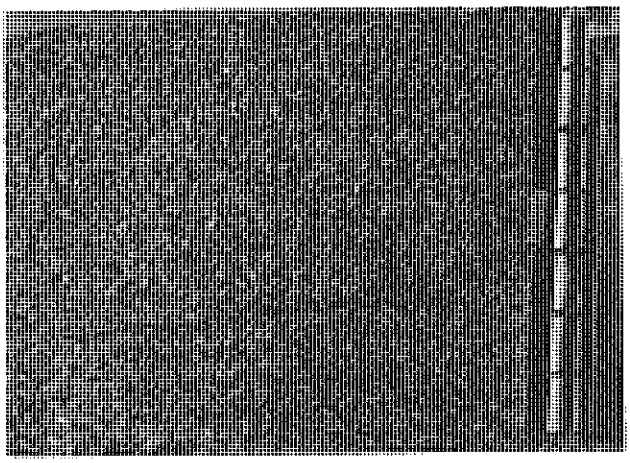

FIG. 4b

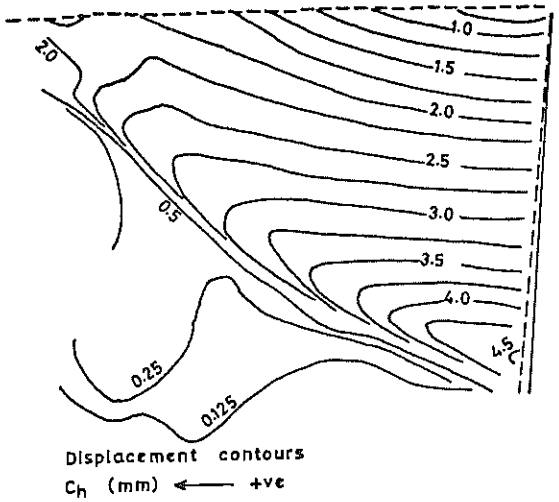

FIG. 5a

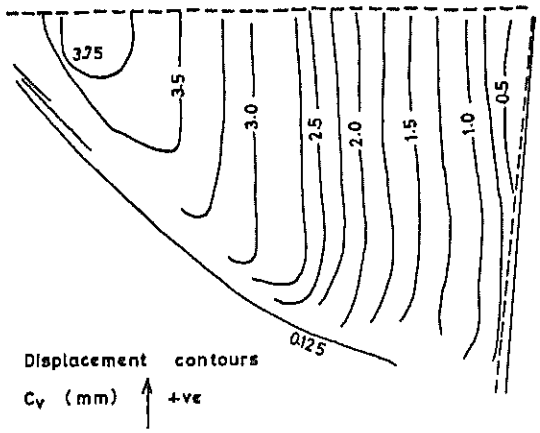

FIG. 5b

Comparison of the maximum shear strain increments shown in Fig. 6 (a) with any of the Cambridge figures illustrates two main features. Firstly that the sensitivity of the photogrammetric technique is comparable with that of the highly complex'X-ray' method used at Cambridge and secondly that the zones of intense shear distortion which occur around the major velocity discontinuity are rather more pronounced in the rod model than in the dense sand. By contrast measurements in loose sand, for example Figs 17 (a) Ref. 15 and Fig. 26(a), Ref. 4, show that no such zones are developed.

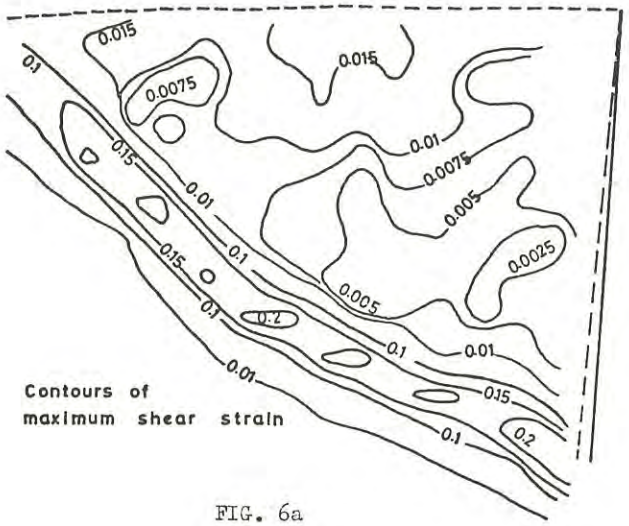

FIG. 6a

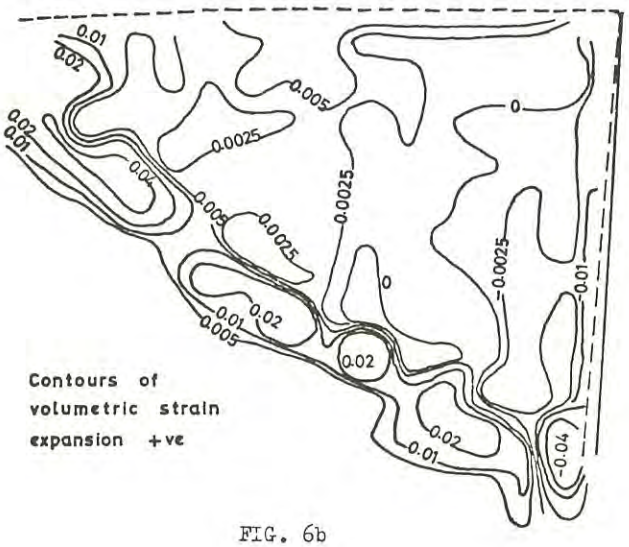

FIG. 6b

Fig. 6(b) is a plot of the volumetric strain increments which occur simultaneously with the maximum shear strain increments of Fig. 6(a). The former are seen to be confined exclusively to the zones of high shear strain and are obviously inter-related phenomena. The only comparable published data appears in Figs. 26 (c,d) Ref.4 which gives much less detailed information on a loose sand test. Here there was no zone of intense volume change although interestingly some decrease in volume was measured near the toe of the wall as shown in Fig. 6(b). However results for a dense sand Figs. 22, Ref.4, although related to a wall rotating about its toe, do indicate the development of volumetric strains associated with a velocity discontinuity much more closely analagous to the rod material behaviour.

These comparisons demonstrate quite conclusively that the rod analogue does not deform as a loose granular medium but that its kinematic behaviour is much more analogous to that of a densely packed granular material.

This statement is again supported by kinematic measurements made on the previously mentioned wedge penetration tests into rod material and sands (Ref.2)

(c) The Displacement Field

Although almost invariably in soil models displacement fields are measured and subsequently differentiated to obtain strain fields the displacement fields themselves have until recently (Refs. 2,13,14) received very little attention. Displacement (or velocity) field data is best summarised in a velocity hodograph. This is merely a diagram in which the radius vector to any point in it, measured from an origin in the diagram, uniquely represents the actual displacement (or velocity) vector of the corresponding point in the deforming field (Refs. 13, 14). In particular the hodograph of any field which is rotating as a rigid body will merely reproduce the field rotated through a right angle. Furthermore equal interval displacement contours of such a field will appear as equi-spaced orthogonal straight lines in diagrams such as Figs.5 (a,b.) A large area of these figures does appear to be approximately of this form and therefore a hodograph of the network of points shown in Fig.7(a) has been constructed (Fig. 7(b)) using the displacement components obtained from Figs. 5(a,b)

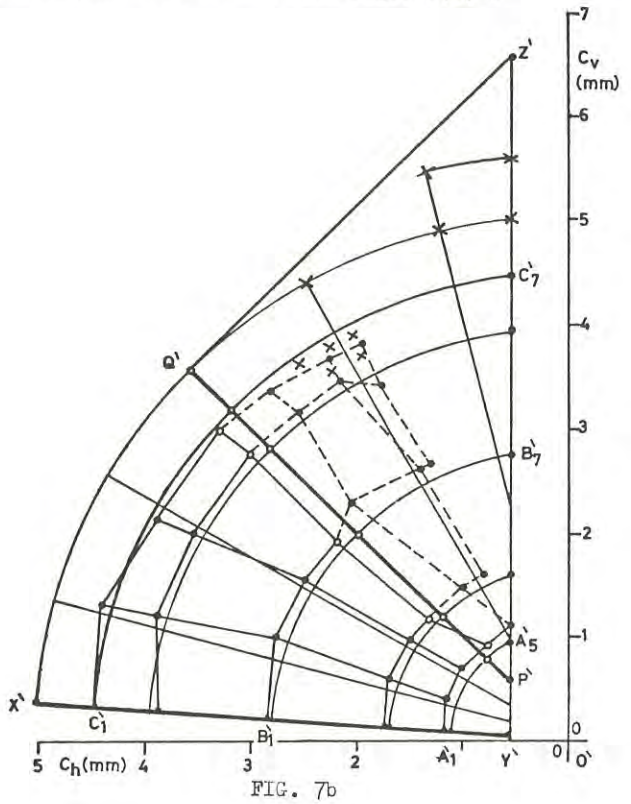

FIG. 7b

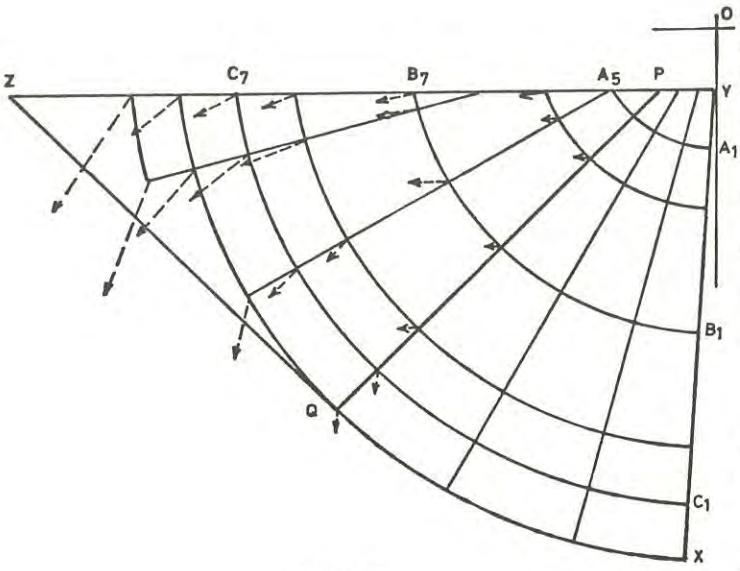

FIG. 7a

More specifically if the whole region XYZ in Fig 7(a) were rotating as a rigid body about the wall rotation centre 0 all points in XYZ (for example A_1-A_5, B_1-B_7, C_1-C_7 etc.) would map into the hodograph Fig. 7(b) as X'Y'Z' and the specific points mentioned above would appear at A'_1 -A'_5 , B'_1 - B'_7 , C'_1 - C'_7 etc. It should be noted that the displacement scale in the hodograph refers to the absolute displacement increments of the "soil" particles in mm and that the theoretical figure is plotted for a general rotation of the model of $1\frac{1}{2}^o$ (from $4\frac{1}{2}^o$ to 6^o away from the vertical). The comparisons being made therefore relate to predictions of extremely small displacement increments of individual "soil" grains. Fig. 7(b) also shows the less regular hodograph obtained by plotting the actual displacements of points A_1 ... C_7 etc. from the experimental measurements shown in Figs. 5(a,b). Within the zone corresponding to XYPQ (mapped at X'Y'P'Q' where PQ is at 45^o to the horizontal) the agreement between the two hodographs is quite remarkable which demonstrates that this region did indeed rotate essentially as a rigid body during the rotation increment. This is, of course, further substantiated by the fact that within this region in Figs 6(a,b) both the volumetric and maximum shear strain increments are very nearly zero.

In the regions PZQ and P'Z'Q' the two hodographs are of quite different form and it is of interest to discuss this briefly. The boundary conditions along the wall XY are kinematically determined as explained in Ref. 14 and therefore one limiting displacement field could be a simple rigid body rotation about 0 of the whole failing zone XYZ as discussed above leading to the X'Y'Z' hodograph. Alternatively, and more probably, the stress governed boundary conditions along YZ will govern the behaviour near this boundary and a further plausible kinematic solution allowing for this would postulate that within PQZ the velocity characteristics may form an orthogonal straight line network out-cropping at the consistent angle of 45^o along PZ and marrying up with the circular arc fan along PQ. Interestingly the bounding velocity discontinuities in Figs. 5(a,b) do outcrop at 45^o and conform very closely to the outer boundary of the figure just described. If now this whole region (XYZ) started to rotate about 0 the triangular zone (PQZ) could slip consistently in an "active" sense along planes parallel to PQ to maintain continuity of the body along ZQ. The resultant displacement field produced has much in common with those discussed in relation to retaining walls by James and Bransby (Ref.15). In particular the velocity hodograph for such kinematic behaviour would comprise only the region X'Y'P'Q' in Fig. 7(b) with the whole of the region PQZ "collapsing" onto P'Q' (Refs 13, 14).

The two alternative mechanisms described probably represent reasonable approximations to the extremes of kinematically admissable solutions and it is intriguing to note that the measured behaviour falls very neatly between them.

In Fig. 7(a) relative displacement vectors have been added (measured directly from Fig. 7(b)) attached to the points within PQZ. These show in magnitude and direction the measured displacement of each point relative to a basic rigid body rotation of the whole field of $1\frac{1}{2}^o$ about 0.

IV.- CONCLUSIONS

These relate solely to the preceeding comparisons of the measured behaviour of rod analogue material, deforming at low stress levels behind a fairly smooth rigid model retaining wall rotating about its top into the rod fill, with that of a similar model using sand backfill deforming in plane strain.

(a) Wall Pressures.

The rod material appears to be a reasonable analogue of a loose sand. This is supported by the facts that they both

(i) do not exhibit either peaks in their stress-strain behaviour or any appreciable decrease in apparent friction angle at high strains.

(ii) the total forces on both walls reached their maximum value at rotations of 5^o-6^o and decreased very little with further rotation of the wall.

(iii) In each case the total force could be approximated reasonably by conventional smooth wall passive earth pressure calculations using experimentally measured ϕ values.

(b) Kinematic behaviour of the backfill.

Here the rod analogue material behaves quite differently from a loose sand and more closely reproduces the behaviour of a densely compacted sand in that

(i) their volumetric compressibility under spherical effective stresses is relatively low

(ii) they can both form distinct velocity discontinuities which produce zones of intense shear distortion within which high

dilatancy rates can be measured.

(iii) detailed measurement and analysis of both strain and displacement increment fields shows that rigid body motions develop in the rod material which do not do so in a loose sand.

(c) The behaviour of the rod-analogue is therefore somewhat ambiguous and it does not appear to be suited to providing information on either the kinematic behaviour of loose granular materials or the stress distributions associated with dense ones.

The measurements made directly on the rod analogue model were obtained by Messrs. R.J. Reynolds and M.K. Chatterjee (1967) in connection with their student research projects.

REFERENCES

1. ROWE P.W., PEAKER K. - Passive Earth Pressure Measurements, Geotechnique 15, 1965, pp 57-58

2. ANDRAWES K.Z. - A contribution to plane strain model testing of granular materials. Ph.D. Thesis 1970, University of Southampton

3. ARTHUR J.R.F., JAMES R.G., ROSCOE K.H. - The Determination of Stress Fields during Plane Strain of a Sand Mass. Geotechnique 14, 1964, pp 283-308

4. ROSCOE K.H. - The Influence of Strains in Soil Mechanics Geotechnique 20, 1970, pp 129-170

5. BUTTERFIELD R, HARKNESS R.M., ANDRAWES K.Z. A Stereo-Photogrammetric Method for Measuring Displacement Fields. Geotechnique 20, 1970, pp 308-314

6. BUTTERFIELD R, ANDRAWES K.Z.- The Visualisation of Planar Displacement Fields. Roscoe Memorial Symposium, Cambridge 1971

7. BIAREZ J. - Contribution a l'Etude des Propriétés Mécaniques des Sols et des Matériaux Pulvérulents. Imprimerie Louis-Jean Gap 1961

8. BIAREZ J. BOUCRAUT L.M., NEGRE R. - Limiting Equilibrium of Vertical Barriers subjected to Translation and Rotation Forces Proc. 6th Int. Conf. Soil Mech. Found.Eng. 1965 Vol.2, pp 368-372

9. KENNERSON J.- Research on Retaining wall Pressures using a 2-D Analogy. Dept. Civ. Eng. M.I.T., Serial 79, June 1941

10. KREBS OVESEN N. - Cellular Cofferdams, Calculation Methods and Model Tests Danish Geo. Inst. Bulletin No. 14, 1962

11. KREBS OVESEN N. - Anchor Slabs, Calculation Methods and Model Tests Danish Geo Ints. Bulletin No. 16 1964

12. NAYLOR A.H., STUART J.G., EDU N.K. - The Stability of Embankments of Frictional Material Retaining a Low Friction Fill Geotechnique 11. 1961, pp 114-120

13. BUTTERFIELD R., HARKNESS R.M. - The Velocity Hodograph in Soil Mechanics. Dept. Civ. Eng. University of Southampton, 1969 Report CE/9/69

14. BUTTERFIELD R. HARKNESS R. - The Kinematics of Mohr-Coulomb Materials Roscoe Memorial Symposium, Cambridge 1971

15. JAMES R.G. BRANSBY P.L. - A Velocity Field for some Passive Earth Pressure Problems. Geotechnique 21, 1971 pp. 61-83

Instrumentation of Raft Foundations in Perth

By

C. M. Gerrard, B.E., M.Eng.Sc., Ph.D., M.I.E.Aust., A.M.Aus.I.M.M.
(Senior Research Scientist, Division of Applied Geomechanics, C.S.I.R.O.)

M. Kurzeme, B.E., M.Eng.Sc., Ph.D., Grad.I.E.Aust.
(Research Scientist, Division of Applied Geomechanics, C.S.I.R.O.)

D. C. Andrews, B.Sc., Ph.D.
(Research Scientist, Division of Applied Geomechanics, C.S.I.R.O.)

AND

R. Topp
(Senior Technical Officer, Division of Applied Geomechanics, C.S.I.R.O.)

SUMMARY.- The foundations of three multi-storey office buildings in Perth, Western Australia, have been instrumented by the CSIRO to investigate the performance of rafts over deep deposits of sands interbedded with clays and silts. The field observation program is one of the three interacting components of an Integrated Geomechanics Project, the others being the determination of initial conditions and material properties, and the prediction of raft performance.

The reinforced concrete rafts range in size from 100 ft by 100 ft by 4 ft thick to 200 ft by 100 ft and 7 ft thick. The variables observed are contact stresses on the underside of the rafts by means of earth pressure cells; pore water pressures on the underside of the rafts and at depth by piezometers; total settlement and deflected shape of the raft by precise levelling; settlement at depth by vertical settlement gauges; lateral movement at depth by lateral displacement gauges; stresses and strains within the rafts by concrete stress and strain gauges; and column loads imposed on the rafts by concrete stress gauges and bonded strain gauges.

The installation and calibration of the instrumentation is described and observations made during the construction phase of the projects are presented.

I.- INTRODUCTION

Instrumentation and field observations are needed for two main reasons (Ref. 1). Firstly, when undertaken during the construction phase, they permit the measurement of some soil response properties that could not be adequately assessed during the investigation and design phases. The data obtained can be used to improve construction practices. Secondly, observations of performance are an essential ingredient in the evolution of a more realistic and balanced synthesis of the inter-related aspects of investigation, design, and construction. This paper is concerned with this second reason as applied to raft foundations constructed over the deep deposits of interbedded sands of the Perth City area. The main purpose of these field observations are to examine the nature of the bending of the rafts, the total and differential settlements produced, and the stability of the rafts under seismic loading. This last aspect is important because, by Australian standards, the south west of Western Australia has relatively high seismicity. Reviews of raft foundation response to quasi-static and seismic loading have been presented elsewhere (Ref. 2, 3).

Relative to usual investigation costs, field measurement projects are extremely expensive to undertake, and it is important to examine their *probable* economic returns. The major factors are the reliability of the readings, the ease with which they can be interpreted, their relevance to design methods, the likely savings due to improved design, and the extent to which the particular project is representative of the type of structure under examination.

Although there has been a general increase in field measurements, the instrumentation of a specific type of geomechanics project is still very infrequent. This highlights the need for extreme care in conducting such projects, including installation and calibration of instruments, and interpretation of results. Carelessness can result in the adoption of erroneous data that may not be repudiated for some considerable time.

There appear to be few reported cases of comprehensive instrumentation schemes related to foundation rafts, although SCHULTZE (Ref. 4) discusses the results of pressure distribution measurements beneath buildings. In a more recent study, GOSBELL (Ref. 5) describes the instrumentation of a foundation raft in Perth, Western Australia, where readings of the interface soil pressures were coupled with column load measurements.

At this stage the Division of Applied Geomechanics, CSIRO, is undertaking the instrumentation of three raft foundations in Perth. The instrumentation work is part of the application of the *scientific method* in the form of an Integrated Geomechanics Project (IGP). The integrated approach applied to foundation response both under quasi-static and seismic conditions consists of three components: the determination of material properties and initial conditions relevant to the predictive model to be used; the use of an appropriate mathematical or physical model to predict the performance of a structure under the effect of estimated design loads; and field observations of the performance of the prototype structure.

Field observations are necessary to provide an estimate of the accuracy of the prediction and to indicate the validity of the method of modelling and the

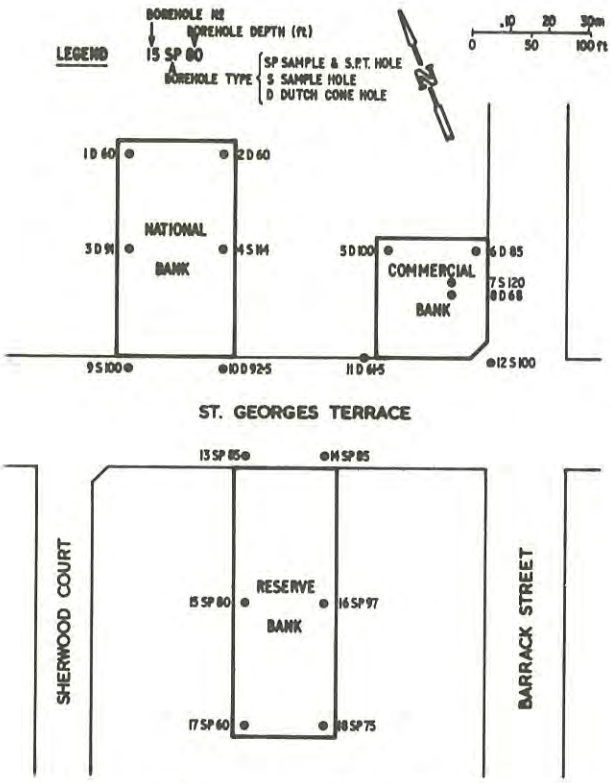

Fig. 1.- Locality plan.

relevance of the material properties and initial conditions that were measured. They provide a feedback indicating what modifications to the prediction method are necessary to improve its accuracy.

The paper describes the structural and foundation details of the buildings, the design of the instrumentation schemes, the details of the instruments and their calibration and installation, and the results of observations taken during the construction phases. Consideration is also given to the required site investigation and laboratory test data and the available predictive methods for quasi-static and dynamic loading conditions.

II.- DESCRIPTION OF PERTH PROJECTS

The buildings instrumented are the Reserve Bank of Australia, the C.B.A. House, and the N.B.A. House. As can be seen on the locality plan (Fig. 1), they form a closely spaced group. The Reserve Bank, situated on the south of St. George's Terrace close to Barrack Street, will be a structural steel-framed building founded upon a stepped reinforced concrete raft. The upper half of the raft is adjacent to St. George's Terrace and 17 ft above the lower raft section. The lower section of the raft is below ground water level and construction is facilitated by using a cast *in situ* diaphragm wall. The other two buildings form part of the St. Martins City Centre redevelopment and are both situated on the north of St. George's Terrace. Both structures will be of reinforced concrete construction. The relevant dimensions and loads of the buildings are given in Table I.

The area on which the three buildings are sited is an alluvial terrace of the Swan River, formed during the Quaternary Age, and subsequently covered by sand of aeolian origin. The area to the north of St. George's Terrace is relatively flat (RL 47), while to the south the ground slopes towards the river at a gradient of about 1 in 20. The cover of dune sand and sand fill averages 28 ft in thickness along St. George's Terrace and decreases in a southerly direction until at the river end of the Reserve Bank site it is only 15 ft thick. Generally, between 2 and 7 ft of this is recent sand fill. Beneath the

TABLE I

DIMENSIONS AND LOADS OF BUILDINGS

	Approximate Area of Raft (ft x ft)	Raft Thickness (ft)	Storeys	Height above Pavement Level (ft)	Founding Depth: Below Pavement Level (ft)	Founding Depth: RL (ft)	Average Estimated Raft Contact Stress (kips/sq. ft): Gross	Average Estimated Raft Contact Stress (kips/sq. ft): Net*	Date of Pouring of Rafts
C.B.A. HOUSE	88 x 94	4.0 - 4.5 (0.5 capitals) (top of slab)	B + G + 13	172	14.5	+31.2	4.3	2.6	15/ 8/70
N.B.A. HOUSE	99 x 102	4.0 - 5.0 (1.0 capitals) (bottom of slab)	B + G + 14	190	15	+31.8	5.5	3.8	8/ 8/70
RESERVE BANK	Upper 88 x 92	7.0	B + G + 10	154	19	+27.8	6.9	5.6	15/11/70
	Lower 85 x 116	7.5	2B + G + 10		36	+ 9.7	6.6	4.2	23/ 8/70

*Net = Gross - weight of excavated soil.

sand lies a bed of stiff grey-brown silty clay with pockets consisting predominantly of silt or fine sand. Consolidation data indicate that this soil has been preconsolidated. The silty clay varies in thickness between 10 ft and 31 ft. Underlying the silty clay there is an interbedded mass of sands, silts and clays, with the sand layers predominating until the thinly bedded calcareous shale bedrock is encountered at approximately RL -60. Ground water exists at approximately RL 27 over the area of the sites. The soil profile of a section taken along St. George's Terrace is shown in Fig. 2(Ref. 6), together with the levels of the undersides of the respective raft foundations.

The design of the three buildings is based on site investigation and laboratory testing data obtained previously by consulting engineers to the projects. This work involved the determination of field moisture content and density and the logging of soil profiles from bore holes, together with penetration testing using Dutch Cone and SPT. Various representative samples of the soil were subject to classification tests, consolidation tests and undrained triaxial tests. Since these investigations were performed for the purpose of routine design they do not completely serve the requirements of an IGP. The main additional elements required are the logging and sampling of the profile to bedrock, or to a depth at least equal to 1.5 times the raft width, and stress-deformation testing of the soils. The aim in these tests is to take full account of the initial stresses in the ground, the development of the quasi-static stresses produced by constructing the buildings, and the loads imposed by seismic events.

With regard to quasi-static conditions the 'stress path' methods of Lambe (Ref. 7) and Davis and Poulos (Ref. 8) appear to offer the best approach to laboratory testing with special attention on the secondary consolidation behaviour of the clays in the profile (Ref. 9). However, because of the difficulties in obtaining truly undisturbed samples, it is extremely desirable to complement the laboratory results with *in situ* measurements of the stress-deformation properties. It is proposed to conduct surface plate bearing tests and to examine the feasibility of using a device such as the helical plate discussed by Webb (Ref. 10), since this allows measurements to be made at various depths. An assessment of the quasi-static deformation properties of the soils under realistic stress paths will lead to improved estimates of total settlement. Also, more importantly, these measurements can be used to examine differential settlements and their effects on raft bending as well as to provide input data for theoretical predictions of soil-structure interaction. The finite element methods currently available (Ref. 11) allow the predictive methods to include realistic properties of both the soils and the structures.

In designing an instrumentation scheme for the raft foundations on interbedded sands it is important to consider not only the prime objectives of the study but the relationship between the field observations and the other two components of the IGP, i.e. gathering initial data and performance prediction. From a quasi-static point of view the main aspects are the bending and settlement of the rafts. Measurements of raft bending can be approached in three different ways and these can be checked against each other and against the bending for which the rafts were designed. The first, and perhaps most reliable, couples measurement of the contact stresses on the underside of the raft

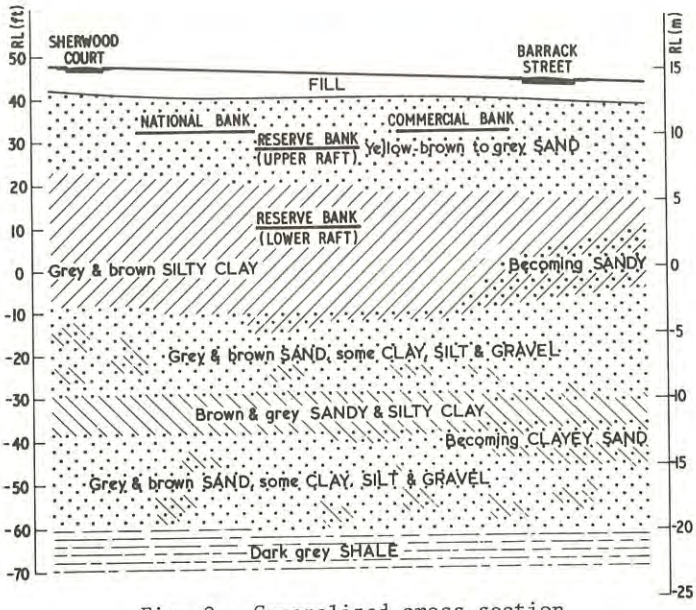

Fig. 2.- Generalized cross section.

with the column loads on top. In the second the stresses, strains and temperatures occurring within the raft are measured, and in the third the deflected shape of the raft is observed. A simplified theory indicates that the bending moments are given by the double differential of this shape.

With regard to settlement, the surface movement should be compared with the compression of each of the main layers comprising the soil profile, these being complemented by pore pressure measurements. The measurement of lateral movements is likely to indicate the more compressible layers and the effects of the construction on adjacent structures. Differential settlement measurements can also be coupled with contact stresses and raft bending.

The analysis of the seismic loading problem (Ref. 3) requires data from most of the above quasi-static instrumentation in order to define initial conditions. The seismic parameters that require to be measured in order to provide an input for and a confirmation of the analysis are the ground motions at the soil-rock interface, at the free soil surface, at the soil structure interface together with the motions induced in the structure. A comprehensive array of strong motion instruments is very expensive, and in the Perth environment there is no guarantee that any useful records will be obtained during the lifetime of the structures. Consequently, no seismic instrumentation has been installed in the buildings described, but the acquisition of strong motion records is being investigated on a regional basis. In the absence of strong motion records, an analysis of possible response may be made using idealized design spectrum curves as input.

III.- INSTRUMENTATION

The instruments installed to date in the foundation rafts can be considered in four categories according to the level of installation. The first, deep instrumentation, consists of vertical settlement gauges, a lateral movement device, and piezometers. Secondly, there are the soil-raft interface instruments consisting of earth pressure cells and piezometers.

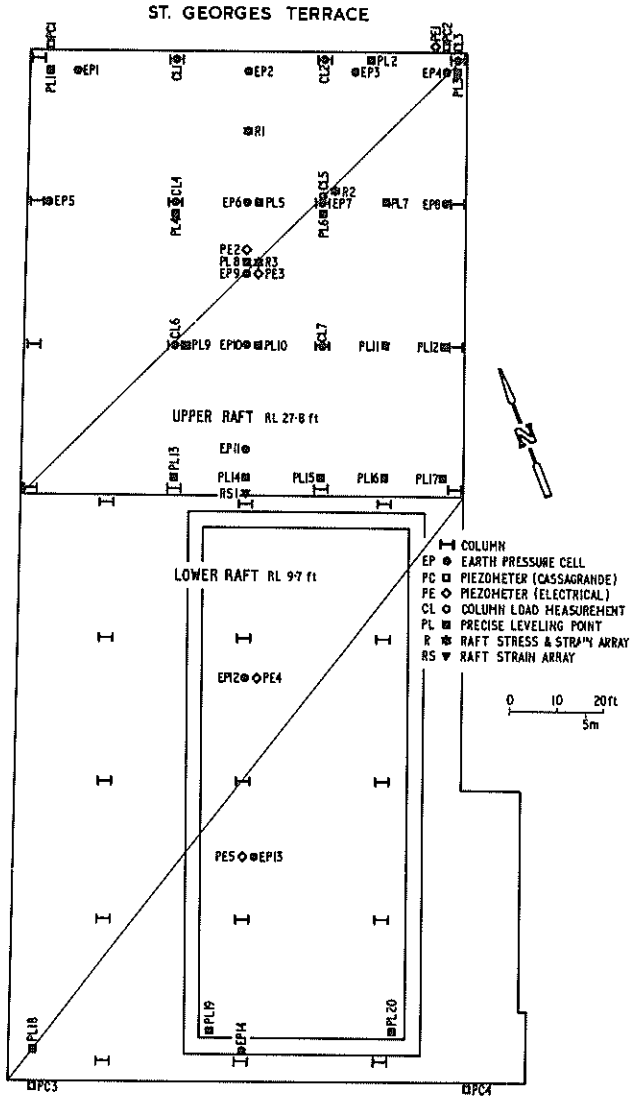

Fig. 3.- Instrument location - Reserve Bank.

Concrete stress, strain and temperature meters, placed within the raft, form the third category. Finally, there are column load measuring devices in the form of concrete stress meters, bonded electrical strain gauges on steel members, and 'Demec' points on the faces of concrete columns. At this stage the costs involved have not permitted the installation of accelerographs to measure seismic parameters.

Because of the very high cost of installed instruments, and the limited funds available, the layout schemes adopted on each of the three sites fell well short of the numbers of instruments that would be desirable from a statistical point of view. The actual schemes for the Reserve Bank, the N.B.A. House and the C.B.A. House are shown in Fig. 3, 4 and 5, respectively. A common feature on each site is the concentration of instruments within an area of interest, these being chosen because they contain relatively simple portions of the rafts. Instruments placed outside these areas were usually designed to examine conditions along particular axes. The most important aspect of the study, the relation between contact stresses and raft bending, was instrumented in greatest detail: measurements of raft contact stresses, column loads, and

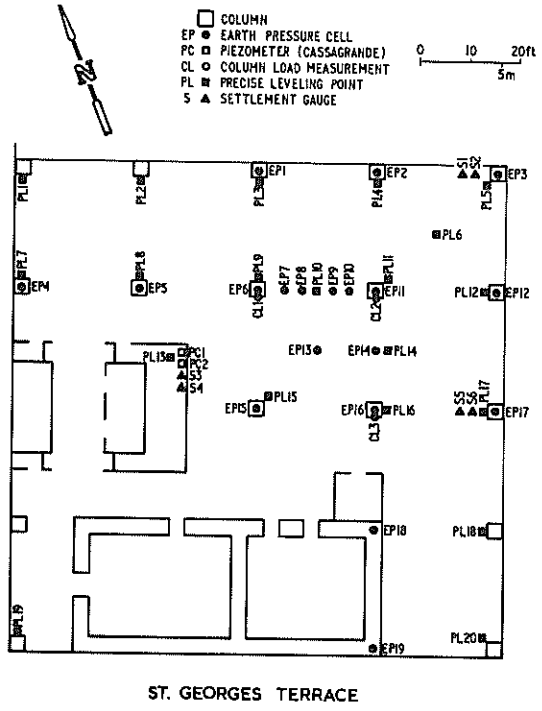

Fig. 4.- Instrument location - N.B.A. House.

the deflected shape of the rafts being undertaken on all three sites. Associated measurements of concrete stresses and strains were only undertaken on one site, the Reserve Bank, because of the difficulty of interpreting results. The conditions existing in the subsurface soil layers were examined on the other two sites (N.B.A. House and C.B.A. House) with measurement of vertical and horizontal movements at depth together with pore pressures.

The types and makes of instruments chosen to measure the variables depended not only on their technical suitability but also on expediency as dictated by the limited time expected between the availability of funds and the construction of the buildings. Details of the types of instruments used and their installation are given in Appendix A.

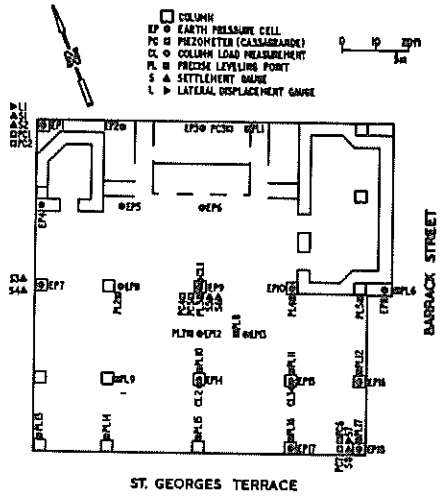

Fig. 5.- Instrument location - C.B.A. House.

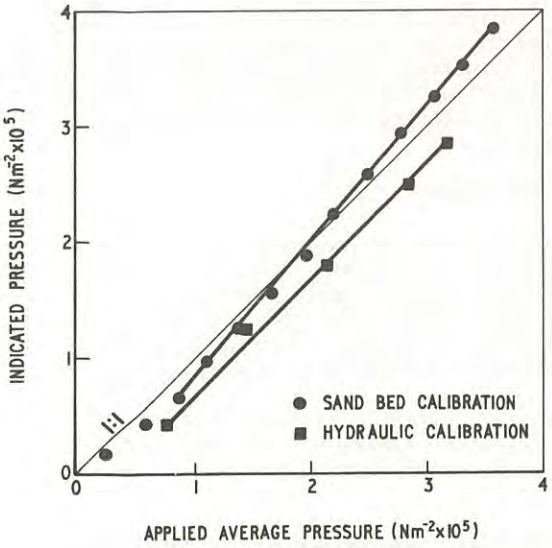

Fig. 6.- Typical calibration earth pressure cell.

IV.- CALIBRATION

To obtain the maximum benefit from the readings of the instruments it is essential to undertake careful calibration programs, particularly for those instruments measuring pressure or stress. Where it is expected that the calibration is likely to be a function of many of the field operational conditions the following philosophy has been adopted.

(i) A 'simple' and readily repeatable calibration involving the prime variable is performed on all instruments before installation. This gives a measure of the basic difference between individual instruments and provides a check on the manufacturers' data.

(ii) A 'comprehensive' calibration program involving a controlled simulation of field operational conditions is then performed on spare but typical instruments, the response of the instruments being expressed as ratios (calibration factors) of their 'simple' calibrations. The 'calibration factors' therefore reflect differences in various field operational conditions but not the individual differences between instruments.

(iii) The field operational conditions at each installed instrument station are then studied and the appropriate calibration factor selected and applied to the instrument reading.

As examples of the 'simple' type of calibration, fluid pressure was applied to the earth pressure cells and the electrical piezometers, while the concrete strain meters were strained in tension and compression by the application of load from a lead screw. The more 'comprehensive' type of calibration has been conducted on Kyowa and Gloetzl concrete stress meters (Hutchings and James, Ref. 12) by casting the meters in concrete columns and examining the response under short term and sustained loads. At the Division of Applied Geomechanics, CSIRO, 'comprehensive' calibration programs for the earth pressure cells, the concrete stress meters, and the concrete strain meters are currently in progress. Fig. 6 shows typical fluid calibration and concrete-soil interface calibration curves of earth pressure cell.

V.- OBSERVATIONS DURING CONSTRUCTION PHASE

The instruments were read twice weekly up to the time of the pouring of the rafts and thereafter on the basis of every half storey of construction. The read-out data are accompanied by a photographic record of building progress. Where applicable the instrument leads are terminated in gauge rooms situated in the basements of each of the three buildings. The recording, storage, and reduction of the data are simplified as far as possible. The readings are recorded manually in the field on computer data sheets using a standard format, thus allowing rapid transcription to punch card form. The data are then reduced to the desired form by the use of standard reduction programs specifically designed for the particular type of instrument.

Observations of instruments were initiated as soon as practicable after installation. Subsequent readings were made to coincide with construction progress or fixed time intervals, whichever was more applicable.

At the time of writing construction had not progressed significantly above the raft and superimposed loads were low so that the values of many of the variables being observed were at the limits of resolution of the measurement techniques being employed. However a preliminary interpretation is possible of the contact stresses as indicated by the earth pressure cells and the raft settlement profiles obtained by precise levelling.

The gross contact stress distributions for two conditions of loading on representative sections of the N.B.A. House and C.B.A. House are shown in Fig. 7 and 8, respectively. Superimposed are the calculated average contact stresses for the sections. These were obtained by summing the weight of the raft and all superimposed walls, columns, floor slabs, etc. in place at that time over a strip equal to one column bay width along the section of interest, and by dividing the area of the strip. Also shown are the settle-

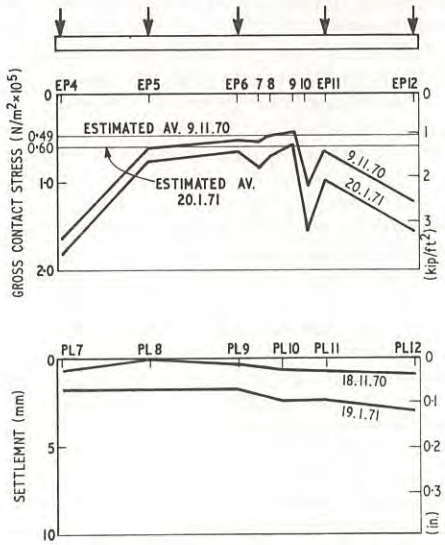

Fig. 7.- N.B.A. House - Contact stress distribution and raft settlement profile.

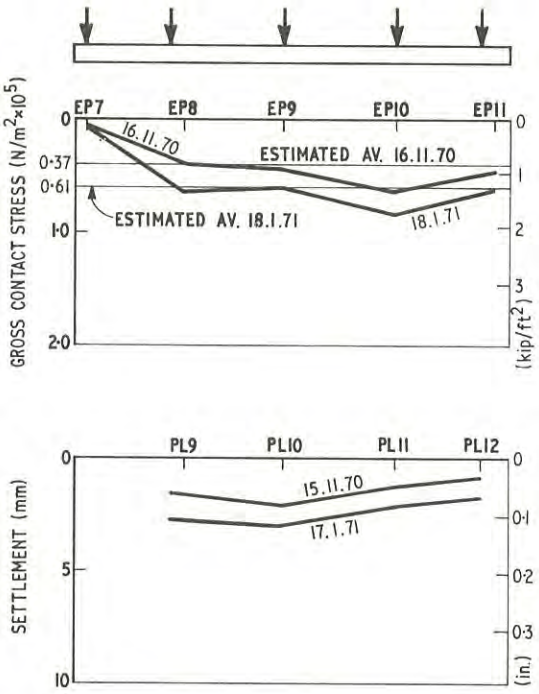

Fig. 8.- C.B.A. House - Contact stress distribution and raft settlement profile.

ment profiles of the rafts along closely related sections at approximately the same times. The data for settlements are the raft surfaces immediately after pouring and curing. The calculated averaged contact stress on the N.B.A. House raft (Fig. 7) appears to be rather less than that indicated by the earth pressure cells, but in the case of the C.B.A. House raft (Fig. 8) the correspondence is quite good.

The shape of the contact stress distribution is of interest even at this early stage of construction. The N.B.A. House raft (Fig. 7) indicates a contact stress distribution approximating that of a relatively rigid foundation on an elastic half space, the maximum contact stresses at the edges. This form of contact stress distribution was also observed by GOSBELL (Ref. 5). The settlement profile of the N.B.A. House raft indicates approximately uniform settlement over the entire raft, apparently confirming the relatively rigid behaviour. Although the contact stresses, as indicated by the closely spaced earth pressure cells EP7, 8, 9 and 10, are in general agreement with the stress distribution associated with relatively rigid behaviour they show some local variations. These cells were installed to obtain an indication of the effect on the contact stress distribution of local variations in the geometry of the raft produced by the inverted capitals.

The shape of the contact stress distribution of the C.B.A. House raft (Fig. 8) appears to be more uniform, being indicative of relatively flexible behaviour. The available settlement profile also appears to confirm this as settlements decrease towards the edges.

The available settlement at depth profiles, as obtained from the vertical settlement gauges, appears to indicate that the total settlement as observed at the surface has been contributed to by approximately equal vertical strains throughout the whole depth of the underlying soil. Piezometers, installed prior to raft construction, show no significant change in indicated pore pressures when the rafts were poured. This may indicate that the drainage paths from the clay layers or lenses (Fig. 2) are relatively short thereby preventing the build-up of excessive pore pressures.

VI.- CONCLUSIONS

Instrumentation has been installed to monitor the performance of the raft foundations of three multi-storey buildings in Perth, Australia. The variables being observed are the loads applied to the rafts and the stress-deformation behaviour of both the foundation material and the raft structures.

Careful planning of installation procedures and a high degree of supervision during installation has resulted in a negligible loss of planned monitoring capability.

The field observation of the performance of the rafts is one of the components of this integrated geomechanics project. However, because of the scarcity of comprehensive field instrumentation and observation programs, it assumes a relative greater importance than either the determination of material properties or the prediction of performance.

The observations presented are preliminary but appear to show trends of behaviour of the rafts which were previously subject to speculation.

VII.- ACKNOWLEDGEMENTS

This work has been made possible by the financial support provided by the Reserve Bank of Australia and St. Martins Properties (Aust.) Ltd. The collaboration and co-operation of the consultants involved on the projects, Commonwealth Department of Works, Cameron, Chisholm and Nicol, and Wood and Grieve, is gratefully acknowledged. The contractors for the various buildings, Leightons Contractors Ltd., and Dillinghams Constructions Pty. Ltd. have also been extremely helpful during the installation of the instruments.

APPENDIX A

(a) Vertical and Horizontal Movements at Depth

Vertical settlement gauges were installed in pairs at separate levels, corresponding approximately to the top and bottom of the layer of stiff grey-brown silty clay with some silt and sand (Fig. 2). Each gauge consists of a galvanized water pipe placed down a PVC cased borehole, the lower end of the pipe being secured in a bulb of concrete (Fig. 9). The pipe is restrained laterally by Teflon spacers. Settlement at depth is measured at the surface end of the pipe using a micrometer depth gauge. The settlements occurring in each of the three main soil layers can be deduced from the gauge readings and precise levelling surveys.

The lateral displacement device consists of an 11 kg cylindrical weight with spring loaded balls mounted in its peripheral surface to locate the weight within a 4.25 in. PVC cased borehole drilled to bedrock (approx. 120 ft). The weight is suspended from a stainless steel cable that passes through a grid ring (to which is attached a micrometer measuring head) over a pulley to a winch (see Fig. 9b). With the weight at the surface the cable datum position is measured at

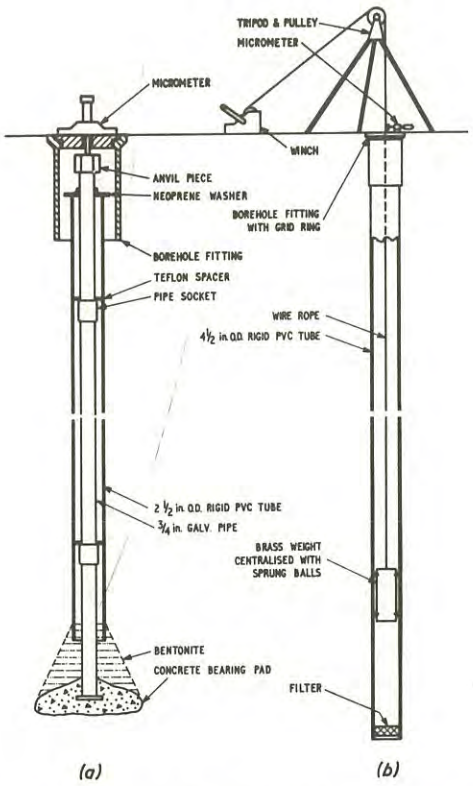

Fig. 9.- Displacement gauges: (a) vertical settlement; (b) lateral displacement.

two positions at right angles in a reference horizontal plane. Movements from this datum with the weight at predetermined depths enable the horizontal movement of the casing to be computed.

(b) Piezometers

To measure pore pressures two types of piezometers were used. An electrical type, complete with filter, (Kyowa Type CP IN) was used underneath rafts through which no access was permitted, the readout cable being laid along the subgrade beneath the blinding layer back to a gauge room. This and the other Kyowa instruments used are all of the unbonded strain gauge type, which are free of bonding material creep. Pressure is transmitted via a flat circular outer diaphragm through a film of mercury to a diaphragm of considerably smaller size. The deflection of this diaphragm activates the unbonded strain gauges. This type of instrument, used in conjunction with the Kyowa Universal Bridge, had temperature read-out facilities. The Casagrande piezometer was also used and despite its lengthy response time, was the preferred type because of its simplicity. In general the design and installation techniques were based on those used previously by the Division of Applied Geomechanics, CSIRO (Ref. 13), although in this case the filter tip was surrounded by sand held in place by wire mesh. The water level in the piezometer tube is detected by a 'dipmeter', although when high excess pore water pressures are encountered the tube may be capped at the surface and a pressure transducer fitted.

(c) Earth Pressure Cells

These were the Kyowa type CE4R and CE8R placed to measure contact stresses at the raft-soil interface. The two types correspond to measureable pressure ranges of 0-4 kg/cm^2 and 0-8 kg/cm^2. The cells having higher ranges are used near the raft edges where stress concentrations are expected to occur. The method of operation of the cells is very similar to that of the Kyowa piezometers. Following the techniques used by Gosbell (Ref. 5), the cells were installed in precast concrete blocks with reinforcing attached (Fig. 10). The diaphragms of the cells were exposed in the undersurface of the blocks that were laid directly on the prepared subgrade immediately prior to pouring the blinding layer. The readout cable is laid along the subgrade back to the gauge room.

(d) Raft Instrumentation

This consisted of Kyowa concrete strain meters, Kyowa concrete stress meters and Gloetzl concrete stress meters. In general, the stress meters were installed in compressive zones and the strain meters in pairs in corresponding zones of tension and compression. The aim was to measure sufficient variables to allow the raft bending moments to be simply computed. Because of the uncertainties in measurement and interpretation, the two types of concrete stress meters

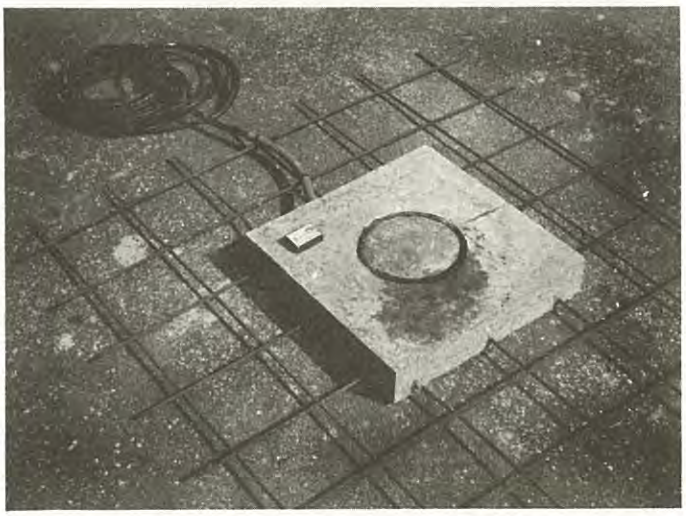

Fig. 10.- Earth pressure cell.

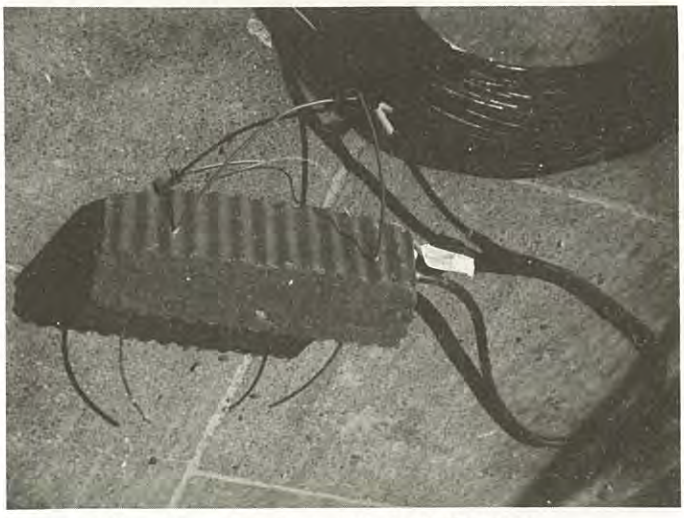

Fig. 11.- Strain meter in briquette.

were used as a check against each other. The Kyowa concrete stress meters (Type CR120G) operate in a similar way to the Kyowa piezometers and earth pressure cells, while the Gloetzl stress meters are hydraulically operated. The latter incorporate by-pass valves that operate when the pressure developed inside the meters equals that applied in the measuring lines. These lines are connected to a pump housed in the gauge room. The Kyowa concrete strain meters operate on an unbonded strain gauge principle and were cast into concrete blocks 12 hours before installation by attachment to reinforcing bars (Fig. 11). Installation took place immediately prior to pouring the raft and every endeavour was made to ensure a close similarity between the physical properties of the concrete in these blocks and those of the concrete in the raft.

(e) Column Load Instrumentation

On the Reserve Bank project the columns are steel and I-shaped in section. A configuration of six bonded electrical resistance strain gauges will be used on each instrumented column so that the axial load and the movements about both horizontal axes could be measured as well as providing several checks.

For the reinforced concrete columns of the C.B.A. House and the N.B.A. House the instrumentation consisted of concrete stress meters, bonded electrical resistance strain gauges and 'Demec' points to measure concrete strain. The concrete stress meters (Kyowa Type CR120G) were installed at the interface between the column and the raft, with the instrument diaphragm placed on the surface of the raft and the readout cable laid to the gauge room. The bonded electrical resistance strain gauges were cemented to the deformed reinforcing bars at points that were prepared by grinding flat. The gauges were placed on adjacent bars within several groups, these groups being so spaced within the columns to allow moments about two horizontal axes, as well as axial loads, to be measured. The steel strains measured by the bonded strain gauges were complemented by the measurement of concrete strains on the faces of the columns. A 'Demec' mechanical strain gauge was used to measure across 'Demec' points installed on a six point grid pattern on each face.

(f) Precise Levelling

A grid of points has been established on all three rafts to measure raft flexure, differential settlements and total settlements as well as to provide a reference for the measurements of vertical movements at depth. Two types of precise levelling points were used: a domed head stainless steel stud cemented into the raft surface, and a socket and pin type cemented in the column surface. Bench marks well outside the zone of influence of the buildings have been established and all reduced levels are based on the Metropolitan Water Supply Board Datum (RL) Low Water Mark Fremantle.

REFERENCES

1. TERZAGHI, K. and PECK, R.B. - Soil Mechanics in Engineering Practice, 2nd Edition, Wiley, New York, 1967.

2. GERRARD, C.M. - Foundation Response to Quasi-Static Loading, Proc. Symp. on Found. on Interbedded Sands. CSIRO, Aust., Div. of Applied Geomechanics, Melbourne, 1970.

3. KURZEME, M. - Foundation Response to Seismic Loading. Proc. Symp. on Found. on Interbedded Sands. CSIRO, Aust., Div. of Applied Geomechanics, Melbourne, 1970.

4. SCHULTZE, E. - Distribution of Stress Beneath a Rigid Foundation. Proc. 5th Int. Conf. Soil Mech. Fdn Engng, 1961, Vol. 1, p. 807.

5. GOSBELL, K.B. - The Design Instrumentation and Performance of the Perth Commonwealth Offices Raft Foundation. Proc. Symp. on Found. on Interbedded Sands, CSIRO, Aust., Div. of Applied Geomechanics, Melbourne, 1970.

6. ANDREWS, D.C. - Soils of the Perth Area - the City Centre. Proc. Symp. on Found. on Interbedded Sands, CSIRO, Aust., Div. of Applied Geomechanics, Melbourne, 1970.

7. LAMBE, T.W. - Stress Path Method. Proc. ASCE, Soil Mech. Fdn Engng Div., 1967, Vol. 93, No. SM6.

8. DAVIS, E.H. and POULOS, H.G. - The Use of Elastic Theory for Settlement Prediction under Three-dimensional Conditions. Géotechnique, 1968, 18, No. 1, p. 67.

9. WALKER, L.K. - Secondary Compression in the Shear of Clays. Proc. ASCE, Soil Mech. Fdn Engng Div., 1969, Vol. 95, No. SM1, pp. 167-187.

10. WEBB, D.L. - Settlement of Structures on Deep Alluvial Sandy Sediments in Durban, South Africa. *In situ* investigations in soils and rocks. British Geotechnical Society, London, 1969.

11. CLOUGH, R.W. - Comparison of Three-dimensional Finite Elements. Proc. of the Symp. on Application of Finite Element Methods in Civ. Engng, ASCE and Vanderbilt University, 1969.

12. HUTCHINGS, R. and JAMES, J.P. - Measurements with Concrete Stress Gauges, A.M.C.O.L.D. Bull., March, 1970.

13. INGLES, O.G., LANG, J.G., RICHARDS, B.G. and WOOD, C.C. - Soil and Water Observations in Flagstaff Gully Dam, Tasmania, CSIRO, Div. of Applied Geomechanics, Techn. Rep. No. 11, 1969.

An Infinitely Programmable Stiff Loading Frame

By

O. G. Ingles, B.A., M.Sc.

(Principal Research Scientist, Division of Applied Geomechanics, C.S.I.R.O.)

AND

R. C. Neil, B.E., M.Eng.Sc.

(Experimental Officer, Division of Applied Geomechanics, C.S.I.R.O.)

SYNOPSIS.- The modification of a 30-ton loading frame is described which, by instrumenting specimens in a simple manner with electrical output gauges, i.e. load cells, pressure transducers, linear transducers, etc., has been coupled to a small computer, controlling movements in the frame and the environmental conditions of the specimen, according to any pre-selected program.

This procedure increases the effective stiffness of the system for stabilized soils and soft rocks, and permits the testing of such materials in the brittle fracture range in such a way that transient changes of structure corresponding to new internal total stress states can be held and examined *in situ* under stress.

The procedure also permits not merely the usual dynamic or kinematic testing modes, but an infinite range of hybrid and other test modes, for instance, constant rate of volumetric strain, constant principal stress ratio.

I.- INTRODUCTION

It has long been recognized that material behaviour is directly related to material structure. For individual specimens, the effect of stress path and stress history is well known to be important to the material behaviour, and the most logical explanation for this is the occurrence of stress-induced structural changes in the fabric of the specimen. Such changes have been observed and reported (for instance, Ref. 1).

The methods hitherto adopted to observe these changes are still not satisfactory, however, especially for brittle materials. Sometimes the mechanical behaviour of a specimen changes too rapidly for any observation of structural change to be made, e.g. region 4, the region of sudden failure, described by Brace, *et al.* (Ref. 2). Sometimes phenomena occur at low stress levels, e.g. the 'matrix yield impediment' described by Trollope and Chan (Ref. 3) and by Herzog (Ref. 4) in a stepwise fashion for which the usual techniques of fabric analysis are quite unsuited, since they involve *destruction* of the specimen at some given point of its loading history; hence they will assume that similar specimens will behave identically. In addition, there are always objections to techniques which involve any stress relaxation in the specimen, or any drying and impregnation. The ideal way by which to examine the interrelationship of mechanical behaviour and structural change is to use *non-destructive* techniques for structure observation, and to ensure that the given stress state is maintained during the entire period of observation, even if that stress state is otherwise very difficult to hold, due to rapidly changing transient structural phenomena.

With conventional equipment, the more sophisticated stress states which are important, for instance, in modern pavement analysis are also difficult to examine. Solly (Ref. 5), for example, using Gerrard's analysis (Ref. 6), had to choose an arbitrary stress ratio from values which varied between 1 and infinity, because a more complex simulation of pavement stresses was beyond the capacity of his experimental research equipment. As a result, either point estimates are made of the mechanical behaviour of what are in fact substantial volumes, or alternatively a lumped estimate is obtained by methods which do not simulate the true situation at all points of the volume, and hence may bear no relation whatsoever to a true mean.

In an attempt to overcome these objections and to advance knowledge of the structural factors underlying material behaviour, a new type of servo-control has successfully been applied to conventional loading frames. Commercially available servo-control loading frames will at best give control programs only for dynamic or kinematic modes, and with a very few selected wave forms for fatigue or resilience testing. The machine now described permits testing in any chosen hybrid mode, and with an infinite number of time variations which need not necessarily take the form of a constant wave (with or without arrest intervals).

II. MACHINE PRINCIPLES

A first principle in the operation of any loading frame is that of releasing as little energy as possible from the stored energy of the frame itself into a rupturing specimen. This is especially important for strong, brittle materials, which often disintegrate violently. In principle, it seems that, if the frame energy is released rapidly into a much softer medium than the rupturing specimen, transient rupture phenomena can be held for study. Such a soft medium is the fluid of an hydraulic system, provided this fluid system can be gated at a large orifice at a speed comparable and in synchronization with the internal stress relief associated with the development of the failure

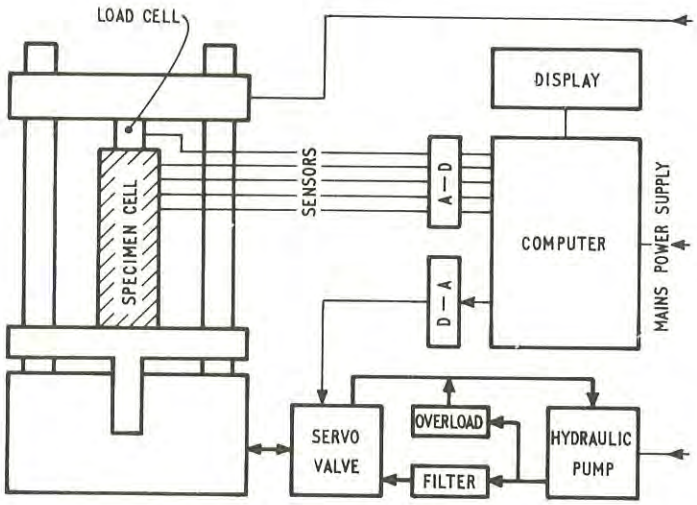

Fig. 1(a).- Test System - Schematic Layout.

surface(s).

Thus a sufficiently rapid means of conveying signals from a test specimen to the loading frame control system, and of executing the controls arising from such signals, would permit testing of materials by any preselected loading path. Modern computers and electronic signal devices provide such a means.

The control logic proposed for the present loading frame was therefore as follows. Test specimens must be fully instrumented by electronic signal devices of high sensitivity and instant response. This necessitates the use of load cells for pressure measurement, of linear transducers for strain measurement, and/or either pressure transducers or linear transducers for volumetric strains and pore pressures. An advantage of such devices is that large numbers can be installed on one specimen, and thus, for instance, radial strains may be measured at many points simultaneously.

These signals are taken by direct connection to a small computer for processing and storage in the memory bank. At this point, any preselected program can be applied to the input data, provided the computation time is very low. Examples will be given in detail presently, but one such example is the use of input axial stress-axial strain data for computing an elastic modulus to test the latter figure for significant changes, and to formulate a machine command accordingly. The preselected output command signal is then sent to the appropriate loading frame controls, which may be either the electrical circuit of a screw system, or the hydraulic valves or pump motor of an hydraulic system, or both. Because of inertia, the screw system is not favourable for rapid response control systems. A rapid response with simultaneous, high resolution flow control could be obtained with recently developed hydraulic servo-valves and was therefore selected for the mechanical control of the loading frame.

The loading frame is a simple, hydraulically-operated frame of standard type (Shimadzu RH 30). Flow in the continuously operating hydraulic pump circuit is diverted through the selected flow control valve referred to above, with a pressure overload device to ensure smooth, continuous operation in any hold-position of the valve, when only minute compensatory flows are required. The integrated system is represented schematically in Fig. 1(a), and the nature of the servo-valve in the form of a mathematical block diagram in Fig.1(b).

The basic specimen controls are thus either or both: (i) a fluctuating movement of the table;

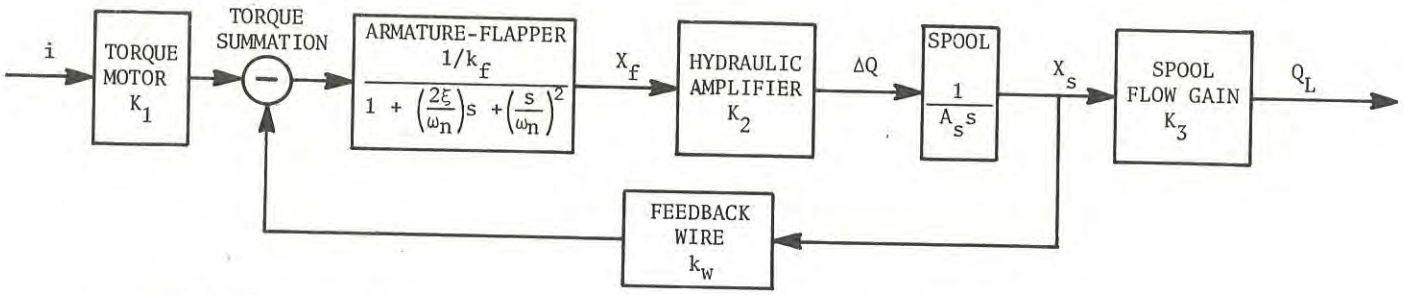

i = torque motor current
X_f = flapper displacement at nozzles
X_s = spool displacement
ΔQ = hydraulic amplifier differential flow
Q_L = servovalve control flow
K_1 = torque motor gain
K_2 = hydraulic amplifier flow gain
K_3 = flow gain of spool/bushing
A_s = spool end area
k_f = net stiffness on armature/flapper
s = input form parameter
k_w = feedback wire stiffness
b_f = net damping on armature/flapper
1_f = rotational mass of armature/flapper

$\omega_n = \sqrt{\frac{k_f}{1_f}}$ natural frequency of first stage

$\xi = \frac{1}{2}\frac{b_f}{k_f}\omega_n$ damping ratio of first stage

$K_v = \frac{K_2 k_w}{k_f A_s}$ servo-valve loop gain

Fig. 1(b).- Mathematical Block Diagram of Servo-valve.

(ii) a fluctuating pressure in the specimen cell; the latter can be servo-controlled directly from the computer to the hydraulic system of the specimen cell in precisely the same manner as for the machine table. In principle, of course, any number of lateral pressure control elements may be operated in this way on a single specimen, provided a servo-valve circuit is available for each element.

It is important to provide a visual monitor for any such servo-system. In the present instance, this is most conveniently given by x-y-t plotters directly linked to the computer. Thus the progress of any test may be followed instantaneously by any selected method, for example an axial stress-axial strain plot, or an axial strain-radial strain plot, or a volumetric strain-time plot, etc. Other data can be called back from the computer storage bank, as selected, at any subsequent time; or can be wholly extracted as punched tape for storage or processing on more advanced computers. A great advantage of the present system is that true curves can be plotted immediately, since corrections to the measured stresses and strains are easily incorporated in the printout program.

Fig. 2.- The Loading Frame and Accessories.

III.- CONSTRUCTION AND PROGRAMMING DETAIL

(a) The Loading Frame

The standard loading frame RH30 supplied by Shimadzu Seisakusho K.K. (Japan) has been used, with its standard hydraulic pump system, but without any controls other than the electrical connections for the hydraulic pump motor and the crosshead adjustment motor (the crosshead of this model operates on a screw system, and the table on an hydraulic system, Fig. 2).

The pump circuit is modified by replacing the standard mechanically-operated linear-proportioning valve by a Moog series 30 model 30S020 servo-valve, which operates to 3000 p.s.i. with a rated flow of 1.0 gal/min at 1000 p.s.i. and 1.7 gal/min at no load, having a null region less than 3 per cent. This valve must be protected immediately on the inlet by a 47 mm high pressure Millipore filter unit fitted with SCWP 8 micron filters, which are able to pass the maximum rate of oil flow without causing a pressure drop of more than 400 p.s.i. (28 kg/cm^2). Gauges, installed in the pipeline on both sides of the oil filter, permit any clogging to be detected, and an alternate filter circuit is provided in case of need. Since the standard mechanical, proportioning valve supplied with the hydraulic pump unit contains a built-in overload relief system, it is necessary to make a similar provision between the pump and the filter in the new system. This has been done by incorporating a Vickers ¼ in. pressure relief valve that returns to the oil reservoir, and is set at a level to protect the Moog valve from pressures in excess of 3000 p.s.i. (211 kg/cm^2).

Electrical cut-out sensors have also been installed on the columns of the loading frame to prevent the table and the crosshead from coming into contact, due to any control program and aberration.

(b) The Computer Circuit; Monitoring, Control and Output

The computer used is relatively small: a PDP8S with a 4K memory, type AF01A 64-channel multiplexer, and analog to digital converter which receive the input signal information. Data can be logged by this system at up to 4250 measurements per sec but, to ensure a smooth and continuous flow control at the servo-valve, a mathematical filter is currently applied to the actuating data such that the effective data usage for flow control is 50 measurements per sec. If required, the full 4250 measurements per sec can be taken out, for instance, to an x-y-t plotter, and indeed reveal a virtually imperceptible noise level. All specimen sensors are chosen to give a voltage output and hence can be directly connected to the multiplexer. Typical sensors at present in use include Kyowa and Shinkoh load cells, Schaevitz, Phillips and Intersonde displacement transducers, of which the unit with the least sensitive dynamic response has a negligible phase lag at 100 c/sec; but some sensors are capable of a dynamic response of 600 c/sec.

The computer control function is to process and store the input data in a form suited to the required response time. By using calculation programs based on measurement precision and sequential storage of actual measurements, a control program can be effected up to 25 times per sec. Using a 50-cycle mains clock

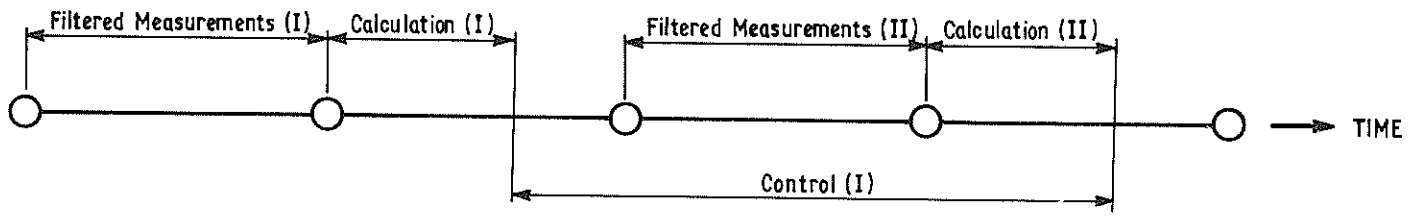

Fig. 3.- Time Sharing of Computer Functions (Intervals 0.02 sec).

for timing intervals, the time utilization in the computer is represented diagramatically in Fig. 3. This gives a control function period of 0.04 sec. However, if the mathematical filter were removed, the control function period would be reduced to about 0.002 sec for a calculation routine of moderate complexity. (Even at this level, it would still be possible to incorporate a much simplified mathematical filter.)

The control program utilizes the valve characteristic:

$$Q = K i \sqrt{P - \Delta P}$$

where Q = control flow $\propto$ to machine displacement

rate = $\frac{\text{sample load rate}}{\text{sample stiffness}}$

K = a proportionality constant

i = servo-valve current

P = supply pressure to servo-valve minus return pressure to sump

ΔP = pressure drop across the servo-valve control ports

= machine ram pressure minus return pressure to sump

To maintain control as the applied load and sample stiffness change during a test, and to compensate for servo-valve control drift, the value of K is continually recalculated by the computer in order to set the servo-valve current appropriate to both required and existing conditions. The control program is designed to maintain precise control corresponding to the last command within the time between successive executions (0.04 sec approx.). Hence the servo-valve setting is obtained from the filtered input completing the control loop. The control system described occupies not more than 15 per cent of the computer storage locations.

The computer output is directed into two channels, one operative and one storage and display. The operative commands are transmitted via a single-channel digital to analog converter* to the Moog valve, which has a phase lag of 25° at 50 c/sec at a ± 25 per cent rated current input. For rapid resetting (coarse adjustments) of any of the displacement sensors, a direct output is also provided to a stepping motor, Slosyn SS50-1001, which resets the sensors as directed by the program. The accumulated data stored in the computer may either be displayed during the test using either an oscilloscope or an x-y-t plotter or they may be retained for later recovery or more sophisticated processing at leisure. This information can be plotted, tabulated or punched on to paper tape or, if available, magnetic tape. If plotted or tabulated, the output data are displayed at 12 points per sec, but if an oscilloscope is used the output data are displayed at 2000 points per sec.

*Capable of being reset 6500 times per sec

The total system has an extremely fast response time of 0.0015 sec for a test, utilizing external electronic noise filters and small changes in servo-valve current. The use of a mathematical filter to give precise measurements, e.g. displacement measurement to within ± 0.5 micron, permits response times of 0.04 sec, at which flow changes will follow current input changes with no loss in proportionality and very small time delay. Thus, either the filter (if used) or the servo-valve at present limits the overall system response.

(c) The Sensors

Loads are detected with Kyowa and Shinkoh load cells, having a minimum sensitivity of 0.5 micro-strain per cent and a stiffness of $1.4.10^6$ kg/cm. Pore pressure measurement (not yet installed) will also be made by means of a load cell connected to a null point device.

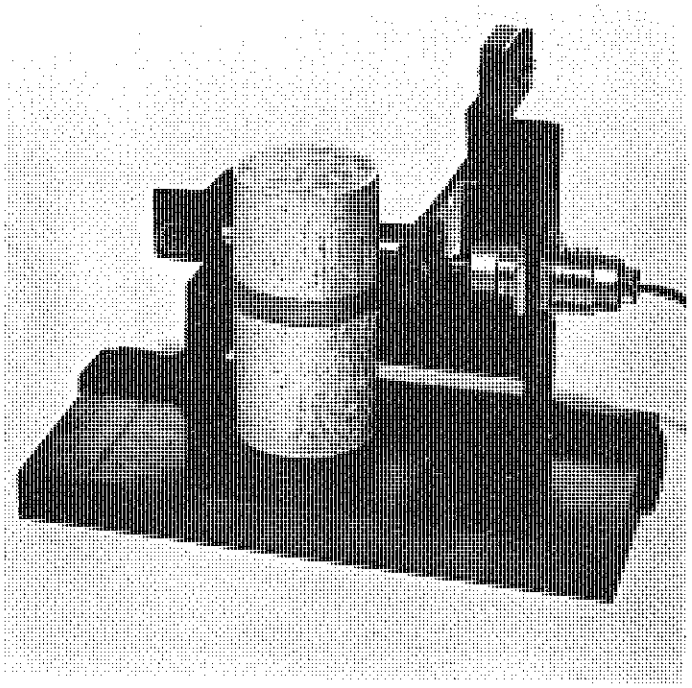

Fig. 4.- Radial strain recording device.

TABLE I.

Operational Programmes - Auto-Infinite Loading Frame

Control Mode		Simultaneous Output	Stored Output	Type of Test
No.	Description			
1	Constant rate of axial strain	Axial stress-axial strain	Axial strain v. time; Axial strain v. radial strain; Axial strain v. volumetric strain; etc.	Kinematic
2 (a)	Constant rate of radial strain	Axial stress-axial strain	Axial strain v. time; Axial strain v. radial strain; Axial strain v. volumetric strain; etc.	New
2 (b)	Constant rate of volumetric strain	Axial stress-axial strain	Axial strain v. time; Axial strain v. radial strain; Axial strain v. volumetric strain; etc.	New
3	Constant rate of load	Axial stress-axial strain	Load v. time Axial strain v. radial strain; etc.	Dynamic
4	Constant rate of strain to a preselected stress, followed by cycling between preselected stress levels at constant strain rates of equal magnitude in either direction	Axial stress-axial strain	Any strain v. time; Axial strain v. radial strain; etc.	Repeated Load (Symmetrical)
5	As above, but unequal strain rates in the cycling	Axial stress-axial strain	Any strain v. time; etc.	Repeated Load (Asymmetrical)
6	Constant rate of strain up to a predefined change of modulus, after which: (a) deformation is maintained constant for a preselected time interval, after which: (b) program returns to original strain rate and proceeds to the next change of modulus	Axial stress-Axial strain Axial stress v. axial strain; Load v. time; etc.	Any strain v. time; Axial strain v. radial strain; modulus v. load; etc. as above	New
7	Constant rate of strain to a preselected load, after which: (a) constant load is maintained for a preselected time after which: (b) program returns to original strain rate and proceeds to next preselected load	Axial stress v. axial strain Axial stress v. axial strain; any strain v. time	Any strain v. time Loan v. time; Axial strain v. radial strain; etc.	Stage Loading
8	Constant rate of strain for a preselected time with the strain cycled at a preselected rate and advancing by a preselected increment on each cycle	Axial stress v. axial strain	Load v. No. of cycles modulus v. No. of cycles; etc.	New
9	Constant rate of strain to a preselected modulus or change of modulus, after which: (a) immediate reduction to any preselected load, after which: (b) program returns to original rate of strain and continues to cycle as long as desired	Axial stress v. axial strain Axial Stress v. axial strain	Any strain v. time; modulus v. time; modulus v. any strain; etc.	New

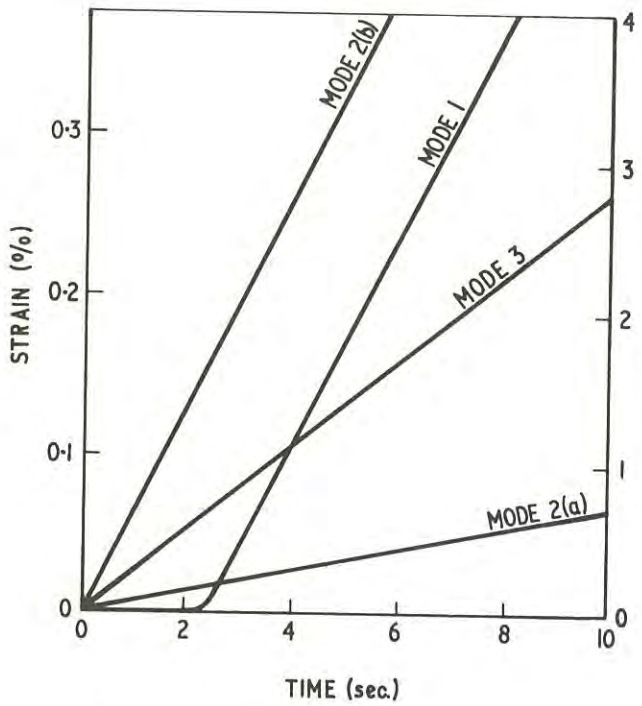

Fig. 5.- Machine Control Modes 1, 2, 3.

Displacements are detected by linear variable displacement transducers having a sensitivity of ½ micron and negligible friction. These are converted to strains in the computer. To measure radial deformations and convert them to radial strains, a frictionless band technique has been applied, which gives the circumferential (hence mean radial) strain over the whole circumference within the width of the band (see Fig. 4). A device for volumetric strain measurement (not yet installed) will rely on linear variable displacement transducer sensing the capillary displacement of the cell fluid, and computed to a volumetric strain from the known compressibility factors for cell and fluid. For both radial and volumetric strains the sensitivity is the same as for axial strain.

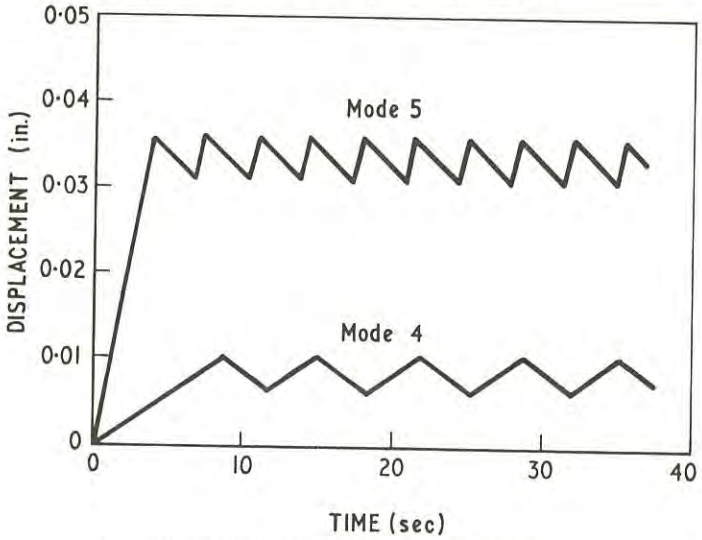

Fig. 6.- Machine Control Modes 4, 5.

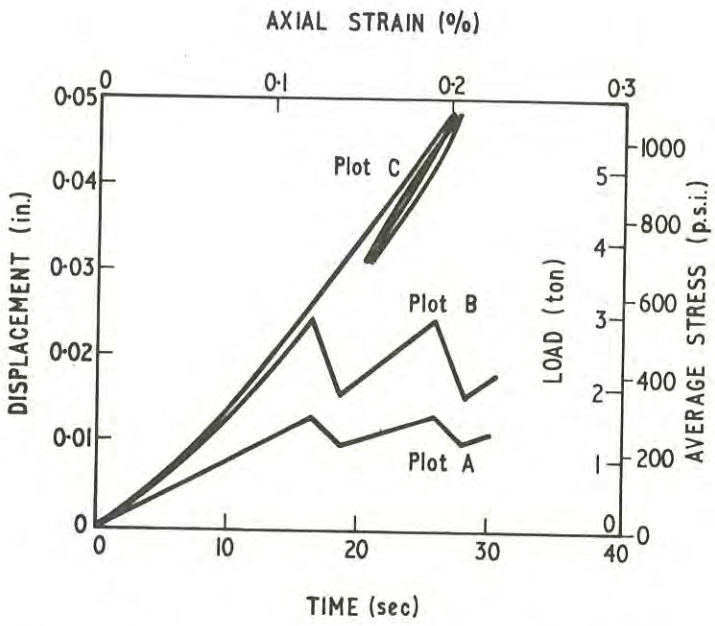

Fig. 7.- Machine Control Mode 5, various recall plots; A = Displacement (control parameter) versus Time; B = Load versus Time; C = Stress versus Strain.

IV.- OPERATION

Since operation of the machine requires the preparation of specific command programs, only a limited range of test procedures have as yet been performed; other more complex programs are in preparation. Those which have now been successfully performed under full automatic control cover a wide range of stress paths, and are summarized in Table I. Examples of the machine performance (showing the high level of signal to noise discrimination) are given as output traces for each case (Figs. 5-11).

A major concern in the operation of any loading frame is the stiffness achieved. To follow the falling branch of a load deflection curve it is essential that energy should not be released from the frame into the specimen. The rapid response of the present system allows a frame deflection of 0.05 cm, corresponding to a load of 30 tons, to be off-loaded in 0.002 sec. From photographic studies, Pomeroy (Ref. 7) has reported velocities of crack propagation in hard coals ranging from 10 to 2500 cm/sec. Thus for materials up to the strength of hard coal or equivalent soft rocks, the present system should be completely stiff, although in harder rocks it will possess no direct stiffness advantage over ordinary machines. However, since the discrimination in control is 10^{-6} in strain, (which can be operated by controlling lateral strain as easily as axial strain), and can be spread over any desired time interval, a virtually infinitely slow rate of strain is attainable, and failure conditions can be approached infinitely slowly for material studies. This is a considerable advantage over other comparable devices.

After mounting the specimen, and loading the chosen program, operation is essentially foolproof in as much as cutouts are provided to prevent any overload on the

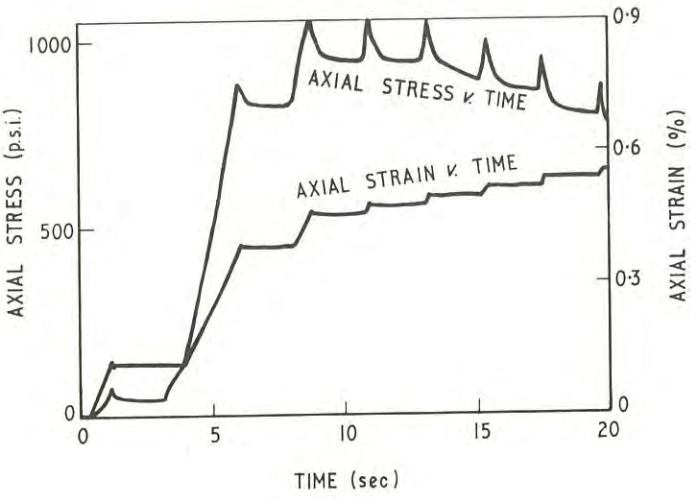

Fig. 8.- Machine Control Mode 6

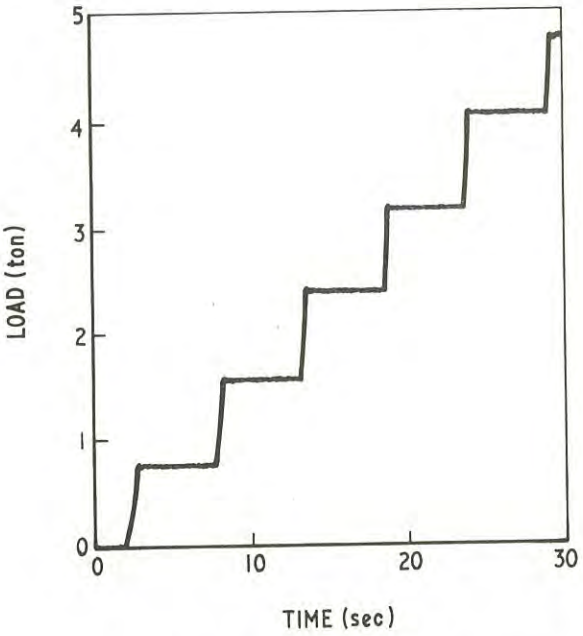

Fig. 9.- Machine Control Mode 7.

mechanical system. Stored data cannot be lost from the system, due to failure or aberration during the test; moreover, the specimen itself would be unloaded.

V.- POTENTIAL USES AND OVERALL COST

Table I gives only an indication of the full potential of this system. Amongst the important modes in which it may be operated for the testing of brittle materials, the following are a few of the programs which can be written and executed by currently known and straightforward mathematical and mechanical techniques.

(a) Non-destructive Examination of Structure under Constant Total Stress

The present technique permits a specimen to be immediately held, following any selected change of mechanical properties, e.g. a change of modulus or a change of strain ratio, and no relaxation phenomena will be interposed during the time required for examination of the structure of the specimen. Whilst the total stress state is thus maintained, non-destructive

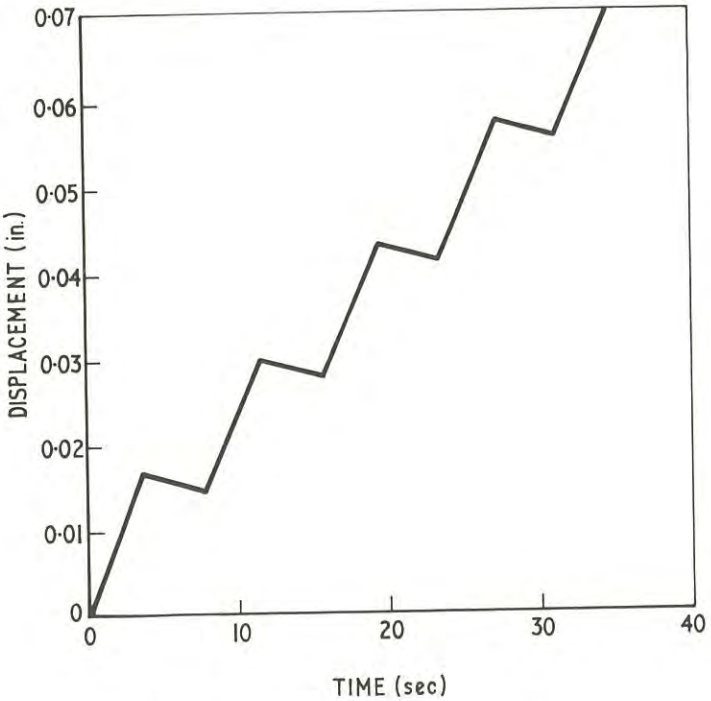

Fig. 10.- Machine Control Mode 8.

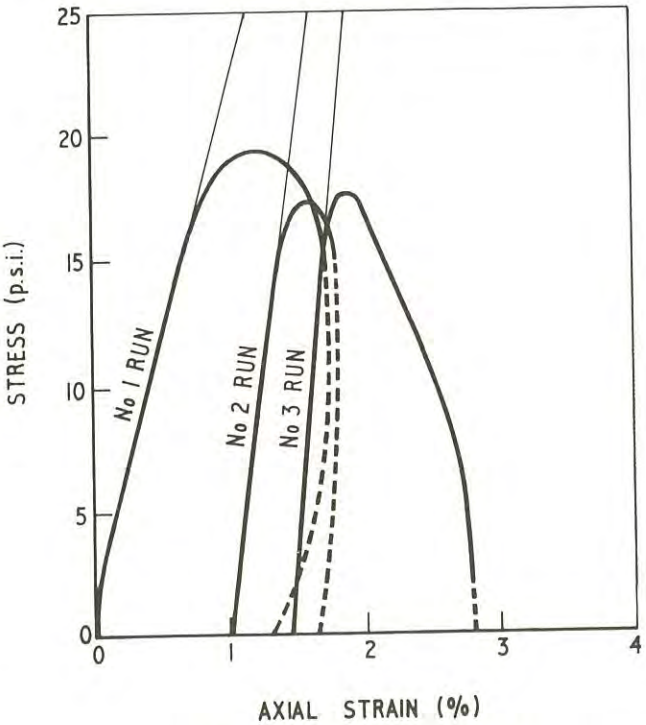

Fig. 11.- Machine Control Mode 9.

testing can be performed, the simplest of which is determination of permeability (Ref. 8). Axial permeability is readily determined; methods for measurement of lateral permeability within the loaded cells are in preparation. For brittle materials, this provides a sensitive measure of the progressive interlinking of microcracks into failure planes.

(b) Model Studies

Scale models of footings, piles and retaining walls can be accommodated on the loading table (which has a working area of 2500cm^2, a vertical movement of 200 mm and a maximum clearance between the crosshead and table of 800 mm). Preselected controls of such tests, as well as the measurement of significant parameters, can be effected over long time periods.

(c) Pavement Design

For pavement studies, it is possible to simulate readily any desired stress ratio without time lag, or to vary it during cycles of repeated loading. In particular, by the use of soft, segmented, lateral pressure controls, it becomes possible to simulate any chosen pattern of stress ratio distribution with depth, i.e. along the height of the specimen, and thus to simulate a full pavement layer and to examine regions of critical stress and strain in one test.

(d) Stress Path Studies

To examine the validity of mathematical models of material behaviour, it is possible to program specimens to follow complex stress paths to failure. In particular, the minimum energy criterion can be adopted, and stress-dilatancy theory incorporated as a controlling parameter for the evaluation of the structural basis of such theories.

(e) Tensile Testing

This may be performed either by direct or indirect methods (Brazilian) with the same order of control as for compression testing.

(f) Statistical Analysis

Any series of tests may be performed so that data are stored and processed to give all relevant statistical analysis on the test series as a direct output on completion of the series.

The overall cost naturally depends on the number and refinement of the sensors and output display devices chosen. Allowing only one output plotter and a simple basic range of load cells and linear transducers, but the full cost of a computer unit comparable to that described here, i.e. no time sharing, the estimated overall cost is approximately $A23,000.

REFERENCES

1. INGLES, O.G. and LAFEBER, D. - The Influence of Volume Defects on the Strength and Strength Isotropy of Stabilized Clays. Engg Geol. I, 1966, p. 305.

2. BRACE, W.F., PAULDING, B.W. and SCHOLZ, C. - Dilatancy in the Fracture of Crystalline Rocks. J. Geophys. Res., 71, 1966, p. 3939.

3. TROLLOPE, D.H. and CHAN, C.K. - Soil Structure and the Step-Strain Phenomenon. Proc. A.S.C.E., J. Soil Mech. and Fdn Div., SM2, 1960, p.1.

4. HERZOG, A. - The Structure of Clay Cement. Colloquium on Mechanisms of Soil Stabilization. CSIRO, Division of Soil Mechanics, Syndal, 1964.

5. SOLLY, R.H. - Repeated Loading on Cement Stabilized Crushed Rock. M. Eng. Sc. Thesis, Melbourne University, 1970.

6. GERRARD, C.M. - Tables of Stresses, Strains and Displacements in Two-layer Elastic Systems. A.R.R.B. Spec. Rept. No. 3, 1969.

7. POMEROY, C.D. - in "Mechanical Properties of Non-Metallic Brittle Materials". Walton (Ed), Butterworth's, 1958, p. 148, 374.

8. DUFFAUT, P. and HABIB, P. Progrès Récents en Mécanique des Roches, La Hovile Blanche, No. 7, 1965, p. 691.

Patterns of Strain in Strength Test Samples

By

W. M. Kirkpatrick, B.Sc., Ph.D.

(Senior Lecturer in Civil Engineering, University of Strathclyde, Glasgow, Scotland)

AND

J. S. Younger, B.Sc., M.S.

(Lecturer in Civil Engineering, University of Strathclyde, Glasgow, Scotland)

SUMMARY. - The paper presents internal strain data obtained using an X-ray Method from rectangular prismatic plane strain compression samples and on cube and cylindrical samples tested in triaxial extension and compression. The results show that homogeneous strain conditions develop in these samples as long as tests are performed using lubricated platens. The use of rough platens should be avoided since the severe distortions which are produced make the strain data of questionable value.

I.- INTRODUCTION

Reports by Kirkpatrick & Belshaw (ref.2) and Kirkpatrick & Younger (ref.3) describe investigations into the distributions of strain within cylindrical triaxial compression test samples in an attempt to establish the value of this test as a means of providing reliable stress-strain data. It was concluded in these reports that for drained sands at least, relatively uniform distribution of strain and hence homogeneous strain states are developed within the compression cylinder as long as adequate precautions are taken to reduce end restraints by providing satisfactory lubrication at the end platens. This condition is important since the usual practice of estimating strains from displacements measured at the sample boundaries is thus valid. Such practices cannot however be considered valid in cases where platen lubrication is not provided since the severe distortions induced in these cases result in large gradients of strain throughout the sample.

Since the publication of these reports the work has been extended and the present paper describes investigations into the conditions within cylindrical extension samples, cubical samples under direct extension or compression, and rectangular prismatic samples tested under plane strain deformation.

II.- EXPERIMENTAL WORK

Internal strains are determined from displacements of lead shot placed within the samples on a square grid at roughly 25mm spacing observed on radiographs exposed to an X-ray beam directed through the sample. The principles of the method and the experimental procedures have been described previously by Kirkpatrick and Belshaw (ref.2).

a) Cylindrical Samples

Cylindrical Samples where both rough and lubricated end platens were used were tested under conditions of triaxial extension. Rough sand paper discs were inserted at the sample ends to produce rough platens while end lubrication was achieved by placing two layers of greased latex over polished glass plates placed on top of heavy duralumin platens.

Samples in all cases had a diameter of the order of 220mm and a length to diameter ratio of 1. Conventional tests with rough platens are performed on samples with length to diameter ratios of the order of 2. For the convenience of testing in the present tests it was presumed that the strain conditions in a symmetrical half of such a sample could be reproduced in a sample with a length to diameter ratio of 1 tested with a lubricated platen at one end and a rough platen at the other. The adequacy of this simulation in which the lubricated platen is taken to represent the mid plane of the conventional rough platened sample has been shown for the compression test by Kirkpatrick and Younger (ref.3).

b) Cube Samples

Both compression and extension tests were performed on samples of cubical form. These samples had side lengths of approximately 190mm and were tested in all cases between lubricated end platens. A cube sample set up and ready for a compression test is shown in Fig. 1. The symmetry of deformation in cube tests was checked by comparing the lateral displacements measured across opposite faces of the cube with those measured on the diagonal between opposite corners by taking X-ray observations of lead shot placed in both of these planes. This was done in two ways. In the first case the lead shot was placed in both planes within the same sample and X-ray exposures were taken normal to each plane. This entailed unloading and rotating the sample for each observation. In the second case the lead shot grids were set up separately in pairs of samples, a diagonal grid being formed in one while the grid across the faces was set up in the other. Both samples in the pair were prepared to have closely comparable initial porosities and the X-ray observations were taken at the same boundary strain values in each test. The symmetry checks were thus made without needing to unload the samples. Symmetry checks were not made in the tests on cylindrical samples since previous observations in this test (Kirkpatrick and Belshaw ref.2) indicated that a high degree of symmetry can be expected. X-ray observations in the cylindrical tests were only made therefore while the sample was

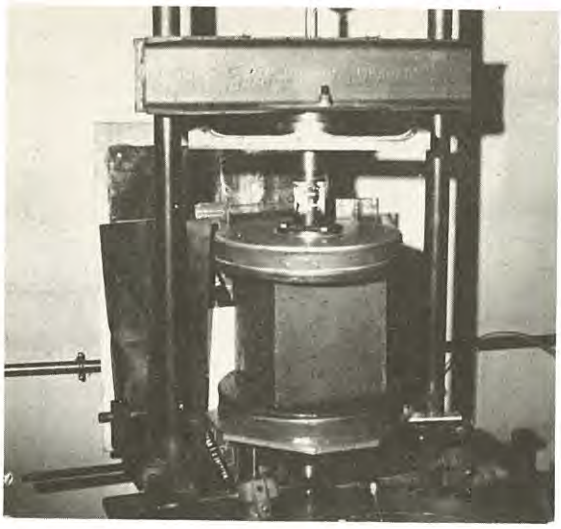

FIG. 1 CUBE COMPRESSION SAMPLE

in the loaded state.

c) Plane Strain Samples

These samples had breadths of approximately 200mm and length to breadth ratios of 1 or 2 depending whether they were tested with lubricated or rough end platens. The plane strain condition $\varepsilon_2 = 0$ was obtained by testing the samples between rigid perspex plates giving a thickness of sample in the 2 direction of about 75mm. This thickness was chosen to allow clear radiographs to be obtained with X-ray equipment available at that time although it was not considered ideal from the point of view of stress measurement. A double layer of greased latex was provided between the sample membrane and the perspex plate to cut down side friction. Although the side friction cannot be entirely eliminated it is presumed that the displacements at the centre of the sample will not be influenced by the side restraint. Allowance was made for friction for the calculation of the stresses by assuming that $\sigma_2 = \frac{1}{2} \times (\sigma_1 + \sigma_3)$ and taking the value of 0.1 for the coefficient of friction between the greased latex and the perspex plate.

III.- SOIL PROPERTIES AND TEST CONDITIONS

The material used in the tests was the proportion of Leighton Buzzard sand passing No. 14 B.S. sieve and retained on No. 25 B.S. sieve. The limiting porosity range for the material is 0.33 to 0.44 and the method of placement as described in Belshaw (ref.1) gave porosities in the order of 0.36.

The sand was tested in a dry condition and confining pressures were induced by vacuum applied to the inside of the samples. This lead to the most efficient use of X-rays since the outer casing and cell water used in normal procedures were no longer required. The effective confining pressure on all the samples was of the order of 77 kN/m^2 (11 p.s.i.) Vertical axial loads were applied through non tilting platens. The confining pressure was kept constant during each test, the axial stress being increased in a compression test and decreased in the extension test. The procedures used initially in preparing the extension test samples was identical to that used for compression samples. It was found however that the use of the enlarged platens, required in the case of the compression tests to allow the lubricated samples to spread latterally over their ends, were not satisfactory for the extension tests. Difficulty was found in preparing the tops of the samples when these enlarged platens were used since it was not possible to ensure that gaps did not develop between the top of the sand and the base of the top platen. This apparently did not adversely affect the samples tested in compression but in the extension test the presence of these gaps seemed to allow the sample to loosen non-uniformly at the top so that failure occurred prematurely due to localised necking which developed in the sample immediately below the top platen. In the extension tests the diameter reduces as the strains increase so that oversized platens are not necessary. The difficulty with the gaps was overcome therefore by using slightly undersized platens which fitted inside the former supporting the sample during preparation so that the platen could be made to rest positively on top of the sand.

IV.- RESULTS

a) Cylinder Extension Tests

Figure Nos. 2 and 3 relate to a cylindrical extension test in which lubricated platens were used at both ends of the sample. In this test the peak stresses occurred at a boundary axial strain of about 8% so that the data presented is for prepeak conditions. In Figure 2 the radial displacements u, for each row of lead shot are plotted on bases corresponding to the initial vertical position of the row in the sample as illustrated. A high degree of symmetry is observed in the upper two thirds of the sample while in the lower third there is a tendency for the left side to deform more rapidly than the right. Also the lateral displacements are slightly greater at the top than near the base. Despite this slight non uniformity it can be said for practical purposes that a homogeneous state of lateral strain existed over most of the sample and in view of the linearity of the relationship between radial displacement and radial distance, r, from the centre of the sample the condition of equality between the radial and tangential strains ($\varepsilon_r (= \partial u / \partial r) = \varepsilon_\theta (= u/r)$ generally assumed in the interpretation of such tests held true.

Fig. 3 shows the axial displacements of the columns of shot measured in the same test. Only slight differences in behaviour were observed between the left side and the right side of the sample and there was little to distinguish between the individual columns on respective sides. For the sake of clarity therefore only the right side data is shown. There was a tendency for the axial strain, defined as $\varepsilon_z = \partial w / \partial z$, represented by the slope of the displacement curves, to be smaller at the base and larger at the top than the average strain measured over the platens. The strain over the centre half to two thirds of this sample was however, approximately equal to the average strain.

Data for a simulated half of a rough ended sample are shown in figs. 4 and 5 where displacements from an extension test in which a lubricated top platen

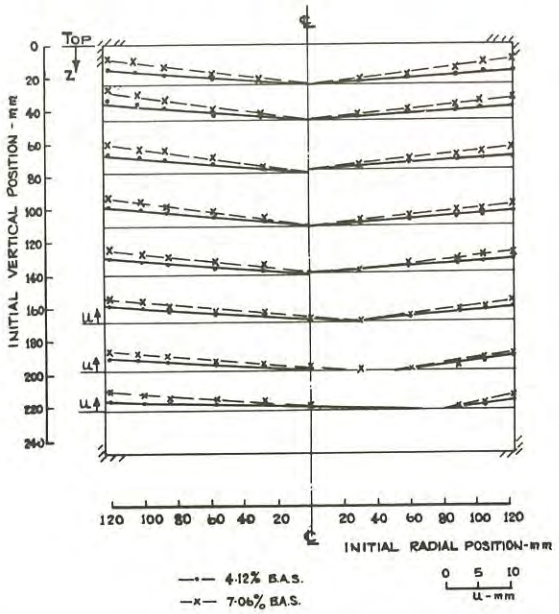

FIG. 2 CYLINDER EXTENSION LUBRICATED ENDS 1 : 1
RADIAL DISPLACEMENTS TEST 101.

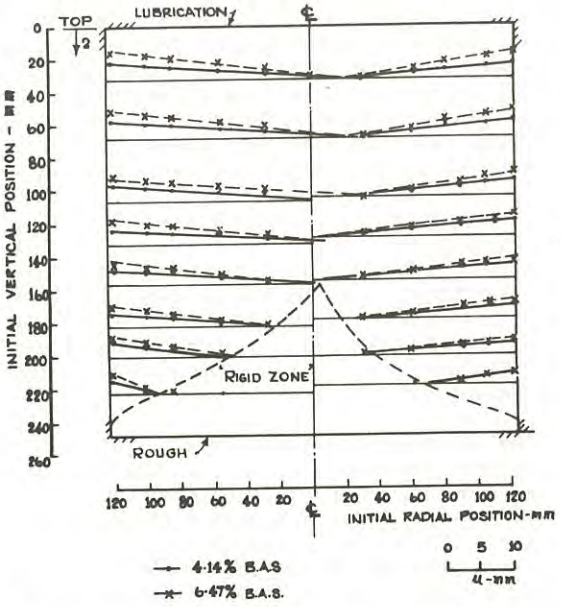

FIG. 4 CYLINDER EXTENSION - LUBRICATED ROUGH 1 : 1
RADIAL DISPLACEMENTS TEST 102.

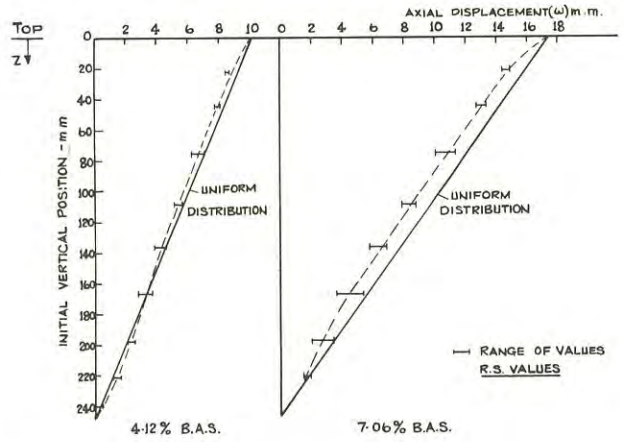

FIG. 3 CYLINDER EXTENSION LUBRICATED ENDS 1 : 1
AXIAL DISPLACEMENTS TEST 101.

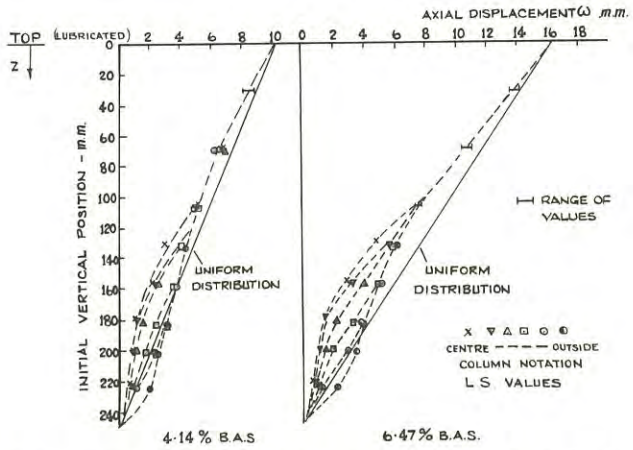

FIG. 5 CYLINDER EXTENSION LUBRICATED/ROUGH 1 : 1
AXIAL DISPLACEMENTS TEST 102.

was used in conjunction with a rough platen at the base. Observations were taken at two boundary axial strain (B.A.S.) values the latter of which was close to the peak strain which was somewhat smaller than the peak strain in lubricated samples.

The radial displacements shown in Fig. 4 are fairly symmetrical about the geometric centre line of the sample. A rigid zone in which the displacements are zero or too small to be measured is seen to have developed near the rough base and as a result of this a homogeneous state of strain cannot be claimed to exist in the sample. This conical shaped rigid zone has a height equal to about 0.35 x diameter and is appreciably smaller than that (=0.5 x dia.) developing near rough platens in the compression test. Although the base angle of the circumscribing straight sided cone at 35° is on the correct side of the 45° line compared with the compression test it is appreciably greater than the angle of $27° (45° - \phi/2)$ predicted for the failure plane by the Mohr Coulomb theory. Within the height of the sample containing the cones the lateral tangential and radial strains are not equal since $u/r \neq \partial u/\partial r$.

Lack of uniformity is also evident in the axial displacements plotted in Fig. 5. This non-uniformity is most pronounced near the rough base where the data indicate appreciably larger axial strains for the columns of lead shot near the outside of the sample than for those near the centre.

The distortions within samples with rough platens

in the extension test are much less severe than those of the compression test over much of the stress strain curve. Another disadvantage of the rough platened extension test under normal conditions lies in its tendency to form local necking in the sample at stresses close to peak. This clouds the accuracy of the stress determinations at these stages. Necking was not detected in the present tests but rather a reduction in diameter which was greatest at the lubricated platen. This difference in behaviour compared with that more generally reported for conventional rough platened extension tests with length to diameter ratios nearer 2 may be due to the inexact simulation of the mid height conditions provided by the lubricated platen in the present tests. The conditions at the rough platens should however be representative.

The strain conditions in the lubricated cylindrical extension test are in contrast reasonably uniform and only slightly less ideal than those already proved for the lubricated compression cylinder. These conditions are appreciably better than those provided by samples tested with rough platens and the benefits of using platen lubrication is therefore readily apparent.

b) Cube Extension Tests

The stress-strain behaviour of the cube samples in extension was very similar to that of the cylinders. In Fig. 6 the axial displacement data

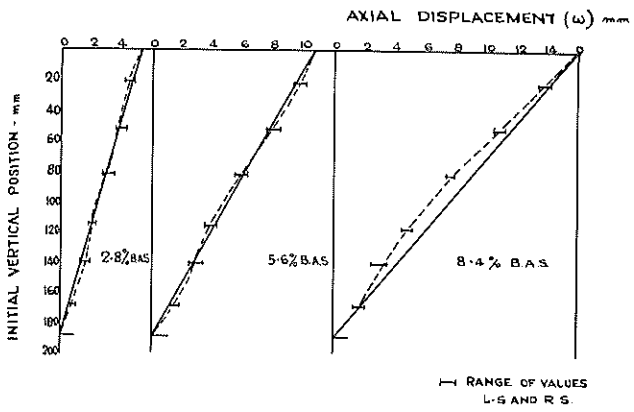

FIG. 6 CUBE EXTENSION AXIAL DISPLACEMENTS TEST 201

for an extension test shows that uniform strains develop throughout the sample up to high strain values. Lateral displacements measured across a diagonal plane between opposite corners are shown in Fig. 7. These indicate a high degree of symmetry about the geometric centre line of the sample. The distributions of lateral displacement are linear from the centre line outwards. A high degree of homogeneity is thus seen to exist up to strains beyond the peak stress conditions which occurred at boundary axial strains (B.A.S.) slightly below 8%.

The shape of the sides of the sample at various axial strain values are also shown in Fig. 7. The sides are seen to have moved inward uniformly up to

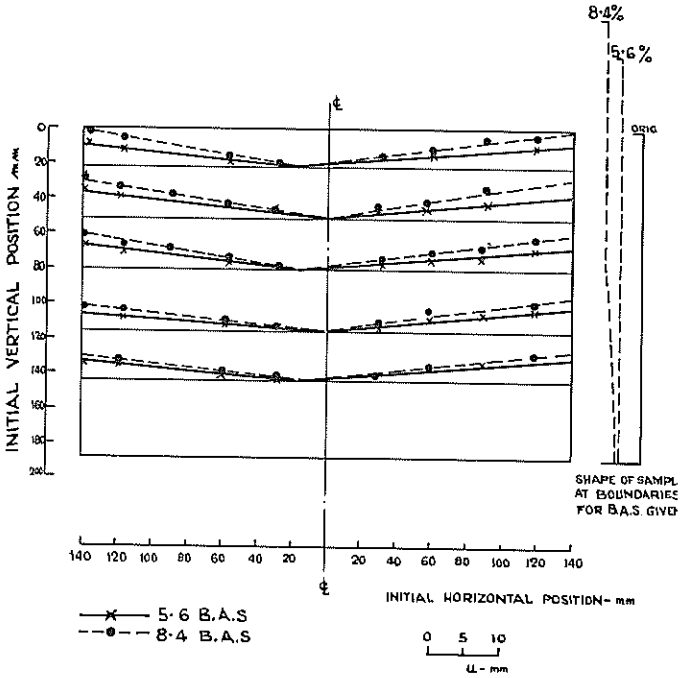

FIG. 7 CUBE EXTENSION LUBRICATED LATERAL DISPLACEMENTS ACROSS OPPOSITE CORNERS TEST 203

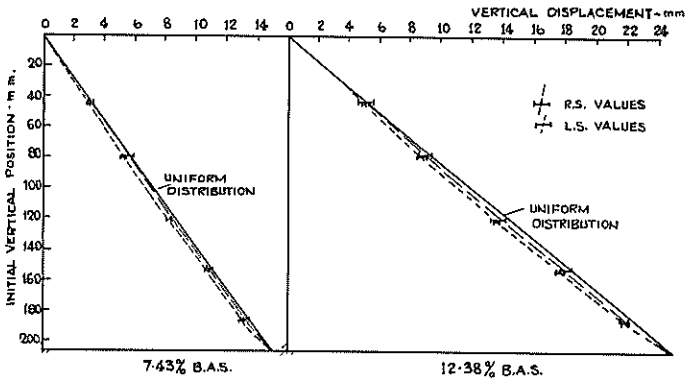

FIG. 8 CUBE COMPRESSION LUBRICATED AXIAL DISPLACEMENTS BETWEEN FACES TEST 107

boundary axial strains of about 6%. Beyond this stage the base of the sample shows no further movement while movement has continued at the top. Shear planes developed at about 10% axial strain but no localised necking occurred in any of the samples. This slight lack of uniformity also occurred in the cylinder extension tests as indicated previously. It is suspected that this behaviour has been caused by the sample having a tendency to come to failure first in the zone near the top where under the slight gradient of body stress due to the weight of sand the stress deviator $(\sigma_1 - \sigma_3)$ will be slightly greater than at the base. The effect which is exaggerated in the present tests involving large samples at relatively low confining pressures was not so noticeable in the more normal type of extension test performed on 100 mm x 100 mm sized samples at confining pressures of the order of 420 kN/m^2 (60 psi). It is claimed

however that the present tests show highly homogeneous strain states although tests performed under more normal practice would be even more ideal. Since failures by localised necking did not occur estimates of sample cross section areas to be used in the calculation of axial stresses should be relatively accurate.

A comparison of the lateral displacement data measured in diagonal planes between opposite corners with that measured in the planes normal to opposing faces allows a check on the symmetry of lateral deformation to be made. In all cases the strains, (measured as the slope of the displacement curves) were uniform and equal irrespective of the direction in which the strain was measured.

The equality of the lateral strains and the general homogeneity of the strain state development in the cube extension test leads to the acceptance of the method at least from the point of view of strain conditions as being equally as good as the cylindrical extension test. Non-uniform strain conditions due to "corner effects" have not been detected in the cube extension tests and hence such effects cannot be the reason, as suggested by Procter & Barden (ref. 4) for the different strengths measured by some investigators in the cube and cylindrical extension test.

c) Cube Compression Tests

In cubical samples tested in compression highly homogeneous strain conditions developed throughout the sample. Axial deformations are plotted in Fig.8

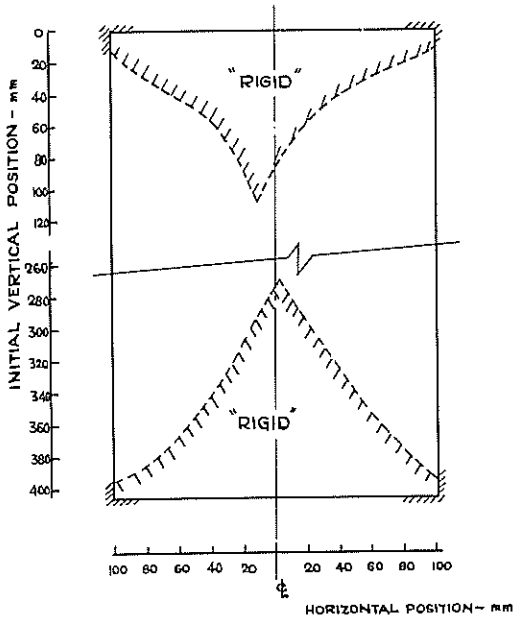

FIG. 9 PLANE STRAIN COMPRESSION 'RIGID' END ZONES ROUGH PLATENS TEST 150

and show that the displacements measured throughout the entire sample lie close to a uniform distribution. As in the case of the cube extension sample lateral strains were found to be equal irrespective of the direction of measurement and corner effects were again absent. It is again seen therefore that accurate estimates of strain can be obtained from displacements measured at the boundaries and that the lubricated compression cube can be accepted along with the other lubricated cubical and cylindrical extension and compression triaxial samples as relatively ideal test forms.

d) Plane Strain Compression Tests

The influence of the end restraint conditions provided by rough and lubricated platens observed on cylindrical triaxial samples was also noted in the plane strain compression tests. Fig. 9 shows the 'rigid' wedge shaped zones identified from lateral displacement measurements, which developed in a plane strain sample tested with rough platens. These zones extend into the sample to distances of about 0.6 x the width. The wedges thus occupy 60% of the height of the 2:1 length to width ratio sample tested and are somewhat more extensive than the rigid cones developing in the 2:1 length to diameter ratio cylindrical rough ended compression samples. These "rigid" zones develop early in the test and do not appear to vary as the strain increases.

The severely non homogeneous strain conditions noted from the lateral deformations are also reflected in the data shown in Fig. 10. In this figure the

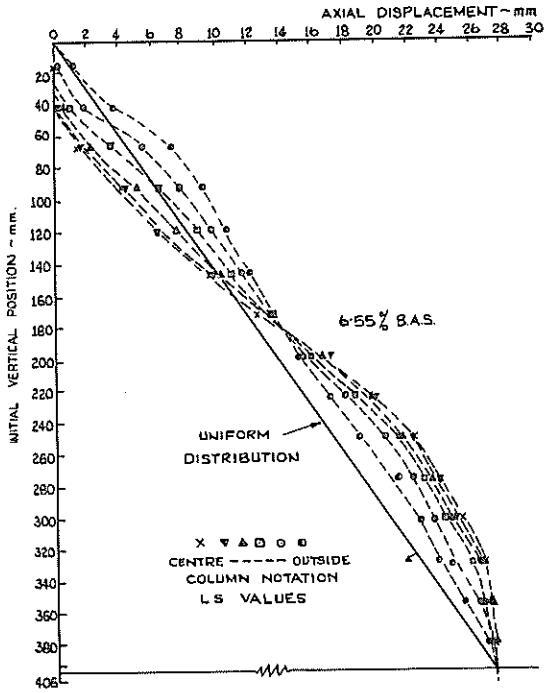

FIG. 10 PLANE STRAIN COMPRESSION - AXIAL DISPLACEMENTS ROUGH PLATENS TEST 150

axial displacements for the lead shot in the various columns are plotted. The distribution is nearest uniform for the columns near the outside edge of the sample while the columns near the centre show zero or near zero strain at the platens and very high strains at mid height.

Strain patterns for plane strain tests using lubricated platens on the other hand were largely uniform and the advantages of lubricated platens over rough platens in providing homogeneous strain states was again illustrated. The lateral and axial displacement data, not shown, are similar to that provided by cube compression tests.

V.-CONCLUSIONS

The following remarks summarise the findings obtained from the tests which were performed under drained conditions on medium-dense Leighton Buzzard sand.

The tests show that the use of lubricated end platens has the desirable feature of producing homogeneous strain states in the cubical and cylindrical triaxial extension test samples, also in the cubical triaxial compression test sample and in the prismatic plane strain compression test sample.

The use of rough platens on the other hand results in the development of highly non-uniform strain states in these tests and should be avoided in situations where reliable stress-strain information is required.

These conclusions are identical to those reached previously in relation to the use of lubricated and rough platens in the cylindrical triaxial compression sample.

Extension samples behaved well as long as the end platens were of the same size or slightly smaller than the initial diameter of the sample. In these cases the sides of the sample deformed relatively uniformly so that a reasonably accurate estimate of the cross sectional area could be obtained for use in the calculation of axial stress. The use of enlarged end platens led to the development of localised necking failures which resulted in inaccuracies in the estimation of cross sectional areas and would give errors in the calculation of stress.

REFERENCES

1. BELSHAW, D.J. - The Conditions of Strain in Sand under Triaxial Compression. Thesis (M.Sc.) University of Strathclyde, Glasgow, 1967.

2. KIRKPATRICK, W.M. and BELSHAW, D.J. - On the Interpretation of the Triaxial Test. Geotechnique, Vol. 18, No. 3 (1968) pp.336-350.

3. KIRKPATRICK, W.M. and YOUNGER, J.S. - Strain Conditions in Compression Cylinder. Journal of the Soil Mechanics and Foundation Division ASCE., Vol. 96, SM5, 1970, pp.1683-1695.

4. PROCTER, D.C. and BARDEN, L. - Correspondence to Geotechnique, Vol. 19, 1969, pp.424-426.

Simple Cantilever Beam Instrumentation for the Determination of Creep Behaviour in Rocks

By

L. M. L. Klingmueller, Geol. E., M.Sc., S.Aus.I.M.M.
(Fulbright Fellow (Macquarie University), University of Arizona, U.S.A.)

AND

M. J. Wallace, B.Sc., S.Aus.I.M.M.
(Senior Research Assistant, School of Earth Sciences, Macquarie University, N.S.W.)

SUMMARY.- Time-dependent deformation or creep in rocks is of significance in mining engineering. The design and construction of apparatus for cantilever bending creep tests is described. Using this simple, inexpensive, reliable and accurate system, multiple tests can be conducted for up to sixteen rock samples. Rectangular beams as small as 4 cm. x 1 cm. x 0.2 cm. are used for the tests. The end displacement of each cantilever beam is measured with a micrometer screw gauge. An electrical circuit detects the contact between the gauge and a stainless steel ball cemented to the beam. This system allows quick and precise measurements to be made. Reproducibility of readings for different operators is within 0.003 mm. The overall accuracy of the micrometer measuring system is approximately 0.5%. Characteristic load-deflection curves, unloading and creep curves for sandy dolomite and diapiric breccia are included as examples. The results are in accord with the expected behaviour of these materials.

I.- INTRODUCTION

The study of time-dependent deformation or creep in rocks is of significance to mining engineering. Time-dependent tests are useful not only in rock mechanics but also in structural geology. Creep tests are relevant in the design of underground openings, the study of failure mechanisms in rocks, and in determining the rheological properties of rocks. Creep studies, of necessity, involve extensive periods of time. This requires long-term stability of both loading and deformation measurement equipment. In addition creep testing equipment should preferably be simple in design, without loss of reliability or accuracy. The apparatus designed allows multiple tests to be conducted concurrently. The equipment is small in size, uncomplicated and relatively inexpensive. Long-term constancy of loading is achieved by the use of a simple dead weight loading system. The measuring system using micrometer screw gauges as described below, is similarly stable in time. Small samples of rock cut in rectangular beams are used. Cantilever bending tests on coal have been conducted by Pomeroy (Ref. 1). Other systems using bending of beams, rather than cantilevers, have been developed by various workers. A useful review of creep studies in rocks is provided by Robertson (Ref. 2).

II.- SAMPLE PREPARATION

The preparation of parallel-sided cantilever beams with a constant thickness, (approximately 6.0 cm. x 1.5 cm. x 0.3 cm.), can be a tedious and time consuming task. Consistent results are obtained by cutting a rectangular block of rock to the desired length and width. This block is then cemented with Canada Balsam to a glass plate. Beams are cut with a thin-bladed diamond saw to the desired thickness (Fig. 1). An adjustable hydraulic-feed saw, similar to that used for trimming petrological slides, can be used for this purpose with highly satisfactory results.

Frequently the rocks being tested are sampled by drill core. If a beam is to be cut in the bedding plane of a horizontally layered rock, its length will be limited by the diameter of the drill core.

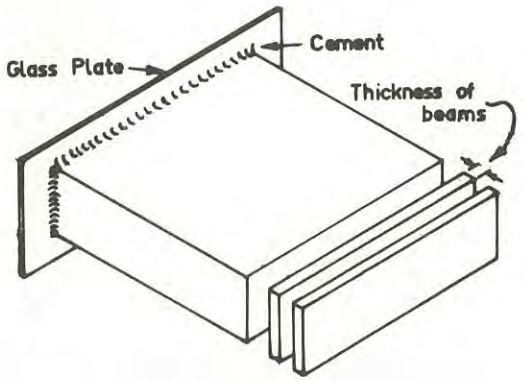

Preparation of beams

Fig. 1.

In order to obtain greater sensitivity for these short beams (three to four cm.), a rigid aluminium extension section is clamped to the free end. A stainless steel ball, the electrical contact-point and a loading bar are glued to the free end of the beam with a suitable cement. This modification allows accurate and reliable tests to be conducted on small samples of rock.

III.- CANTILEVER TEST APPARATUS

This apparatus allows concurrent testing of sixteen cantilever beams and the overall arrangement is illustrated in Plate 1. The beams are loaded using lead

shot in small plastic containers. Care is exercised to ensure that the load is vertically beneath the leading bar glued to the rock specimen. The load was applied quickly but gently to prevent impulse effects. The position of the loading point can be adjusted to suit the individual rock specimen - a weaker rock will require the loading bar to be moved closer to the bearing plate, while for stronger rocks the reverse applies. A microammeter is used to detect the electrical contact between the micrometer and the stainless steel ball cemented onto the specimen (Fig. 2). This electrical circuit system for the detection of contact has proved to be very effective. An earlier method, using dial gauges was found to be unsuitable, because of the friction associated with the gauges. The accuracy of the electrical contact system is limited by the quality of the micrometers used, the reproducibility of a given reading, both for a single operator and for various operators, and the cleanliness of the contact surfaces. The micrometers enable measurements to be made to 0.0001 cm. Reproducibility for a single operator is within 0.0002 cm., while for two operators the accuracy is 0.0003 cm. The system is very sensitive and an increase of 0.1% in a 1 kg. load can be detected.

Creep tests on rocks are best conducted in a controlled environment where temperature and humidity are constant. The accuracy of the system was found to be unaffected by the thermal expansion and contraction of the rig due to temperature variations. A steel control beam was tested simultaneously with the rock beams and over a five-month period the effect of temperature changes in the experimental room was negligible. Variations in humidity results in accelerated creep and even negative creep for some rocks. Details of humidity effects on the rocks tested are provided in a study by Wallace (Ref. 4).

In order to test the force applied on the beam (steel ball) when the contact is closed, an electrical strain gauge was cemented to a steel control beam. This applied force could not be detected by the strain gauge. The strain gauge system was also used to measure strain in the steel beam during early calibration tests. Strains measured in this way were compared with the strain calculated from the cantilever deflection using the elastic bending theory. Average variations measured were found to be less (0.5%) for the electrical micrometer system than for the strain gauge (1.2%). Factors such as air flow, floor vibration and movement of people in the room were found to interfere with the readings. Such effects were reduced to negligible proportions by the use of a large concrete block resting on several layers of thick felt as the support for the apparatus. The overall accuracy of the cantilever system for deflection measurements is approximately 0.5%.

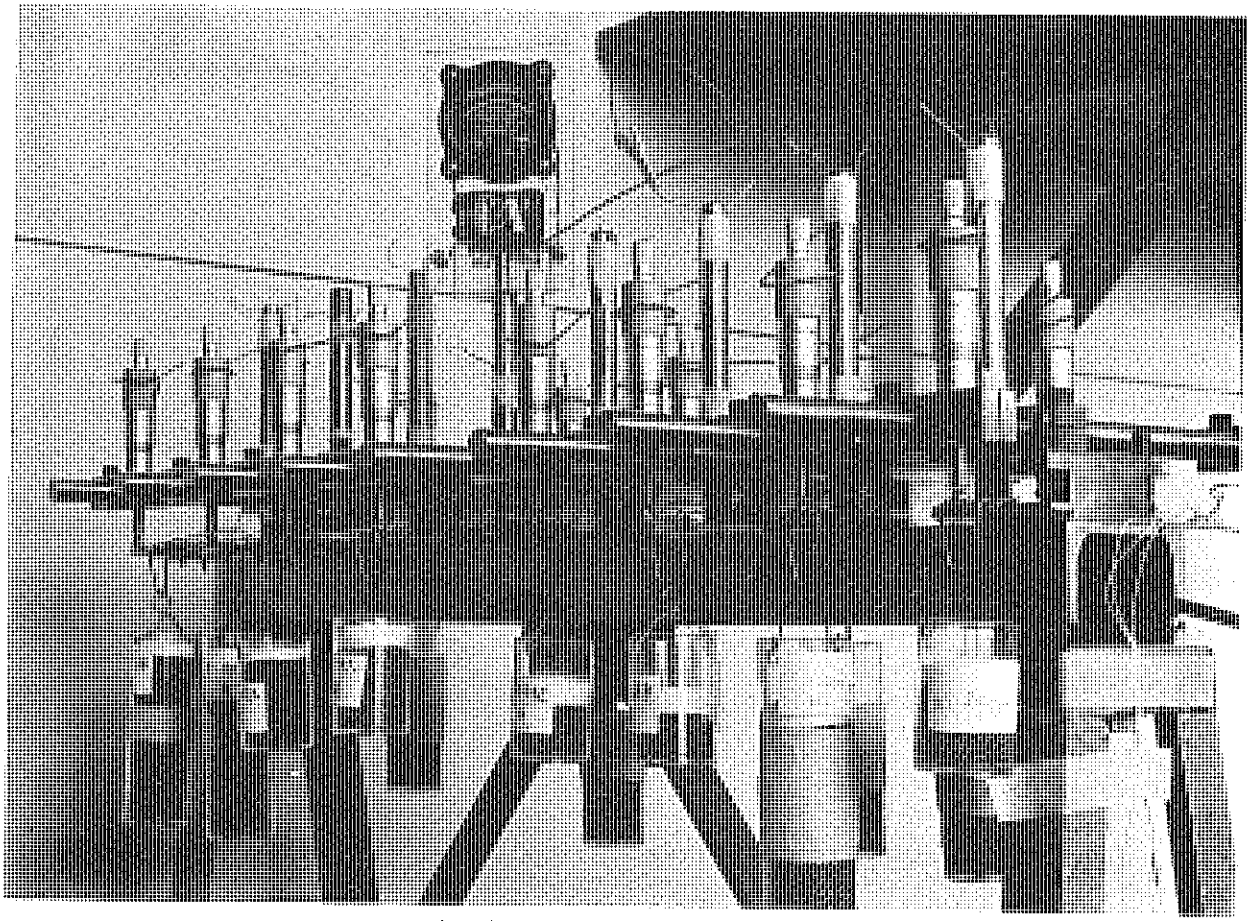

Cantilever Test Apparatus

Plate 1.

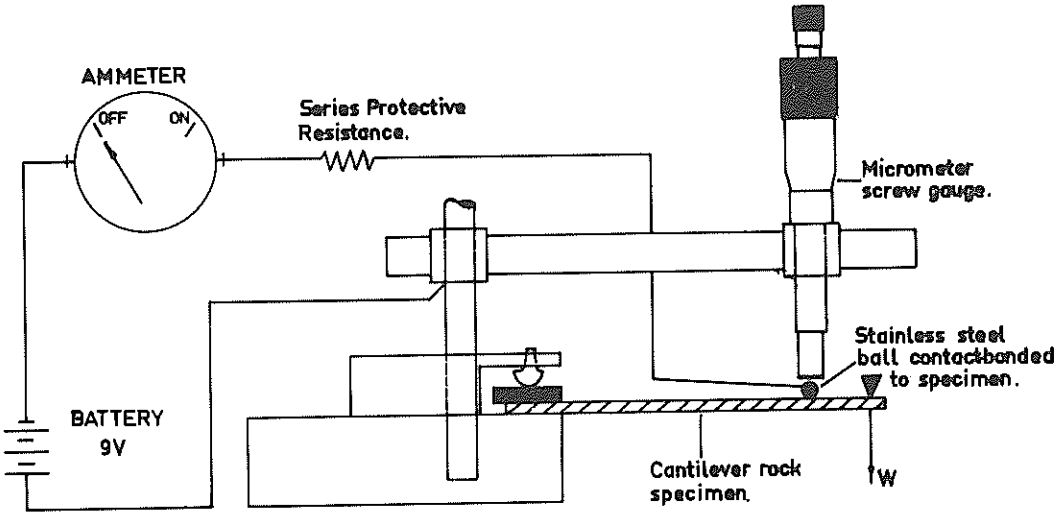

Schematic diagram of electrical measurement system

Fig. 2.

IV.- CHARACTERISTIC EXPERIMENTAL RESULTS

Three types of results can be obtained with this apparatus. Time-independent tests are used to investigate the tensional characteristics, rupture strength and hysteresis. For example, the sandy dolomite in Fig. 3, Curve A, behaves almost like an elastic material. In contrast, the diapiric breccia (cold intrusive rocks), Fig. 3, Curve B, not only has a much lower rupture strength, but also shows "interim or partial failures" (arrows, Fig. 3).

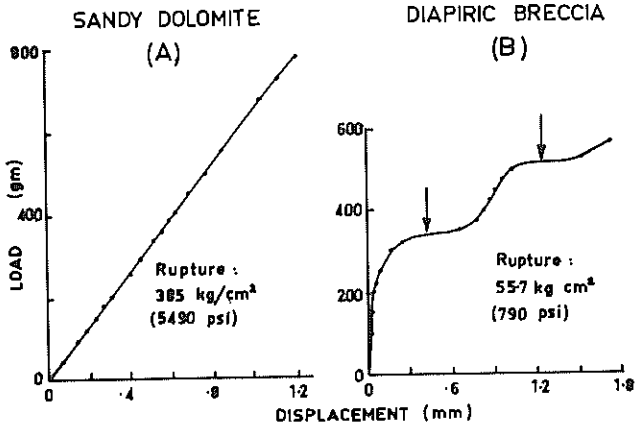

Load vs. Displacement curves

Fig. 3.

Beams loaded to 50% of their rupture strength reveal that the amount of permanent set or hysteresis is also larger for the breccia than for the dolomite (Fig. 4).

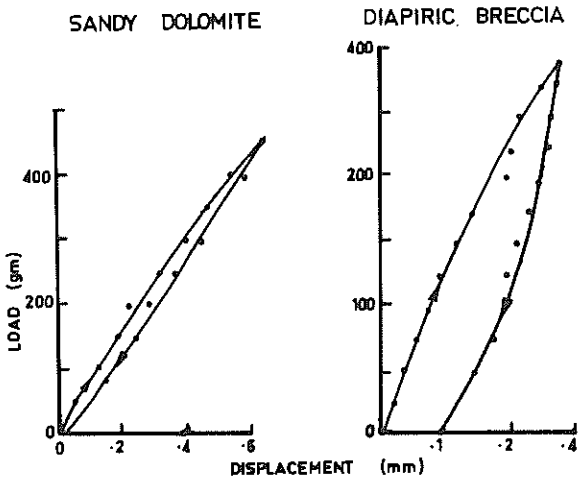

Unloading curves

Fig. 4.

Again comparing the breccia and the dolomite, Fig. 5 shows that the amount and nature of creep is markedly different for these rocks. The primary (Fig. 5, Curve A, Zone 1), secondary (2), and tertiary (3) creep zones can be identified for the breccia. For the same duration the dolomite remained in the secondary creep region.

The end displacement of the beam (y) follows Grigg's (Ref. 5) empirical creep equation. For the sandy dolomite (Fig. 5, Curve B) the co-efficients are $y = 24.197 + 0.010 \log t + 1067t$ when t is in days and y in cm x 10^{-3}. These coefficients were determined by a computer-based regression analysis (Ref. 4). The standard error in y for the above results is 0.173 indicating that the Griggs empirical equation is valid for the sandy dolomite.

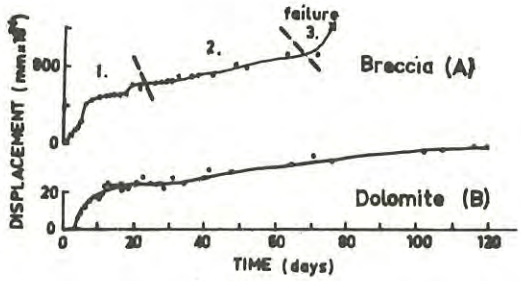

Creep curves

Fig. 5.

V.- CONCLUSIONS

The apparatus described enables simple, reliable and accurate measurements of time-dependent deformation in cantilever beams of rock. The instrumentation is a logical development from earlier methods and allows progress in rock mechanics, mining engineering and structural geology using materials previously considered difficult to test. The characteristic load-deflection curves, unloading and creep curves for rocks are easily obtained. The results obtained are acceptable in that they correlate adequately with expected results obtained in general from far more expensive instrumentation. The simple apparatus described in this paper is therefore considered to be satisfactory. The apparatus allows concurrent testing of sixteen rock samples. A comparative study of creep behaviour for various rocks is thus possible. Variations in humidity were shown to affect creep behaviour.

VI.- ACKNOWLEDGMENTS

The experiments described in this paper were conducted in the School of Earth Sciences at Macquarie University. The authors are grateful to Mr. W.A. Caw, Senior Research Scientist, C.S.I.R.O. Division of Physics, for his suggestion of an electrical contact system of measurement. The study received financial support from Australian Iron and Steel Pty. Ltd. The interest and encouragement provided by Dr. K.L. Burns, Senior Lecturer in Earth Sciences at Macquarie University, and Dr. A.J. Hargraves of Australian Iron and Steel Pty. Ltd. is acknowledged.

REFERENCES

1. POMEROY, C.D. - Creep in Coal at Room Temperature, Nature, 178, August, 1956.

2. ROBERTSON, E.C. - Viscoeleasticity of Rocks, in State of Stress in the Earth's Crust. New York, Elsevier, 1964.

3. KLINGMUELLER, L.M.L. - Geology of the Eastern Parts of the Burr Diapir, Flinders Ranges, S.A., unpublished Ph.D. thesis, University of Arizona, 1971.

4. WALLACE, M.J. - Time-Dependent Deformation in Rocks, unpublished M.Sc.(Hons.) thesis, Macquarie University, 1971.

5. GRIGGS, D.T. - Creep of Rocks, Journal of Geology, 47, 225, 1939.

Psychrometric Techniques for Field Measurement of Negative Pore Pressure in Soils

By

B. G. Richards, B.E., M.S.

(Principal Research Scientist, Division of Applied Geomechanics, C.S.I.R.O.)

SUMMARY.- Results from field trials show that the psychrometric techniques described in this paper permit the measurement of negative pore pressure over the range normally encountered in engineering practice in Australia, viz. 0 to -1500 p.s.i. suction (pF 0 to 5.0), with an accuracy in routine use of ± 10 per cent (lower limit ± 5 p.s.i.) in the laboratory, or ± 50 per cent (lower limit ± 25 p.s.i.) in the field. These figures are better than those achieved previously by any other method, and are sufficiently accurate for field use.

I.- INTRODUCTION

In the drier areas of Australia and indeed of the world, engineering structures are commonly founded on or built from unsaturated soils. For these soils, present techniques of soil mechanics are generally not applicable; consequently, new techniques are being developed. One such technique is the measurement of a useful soil water variable in unsaturated soils.

The advantages of measuring negative pore water pressure, soil water potential or soil suction (defined as being equivalent), are given in Ref. 1. Experience in using this variable over many years suggests that, for most Australian conditions, soil suctions lie in the range of about 5 to 1500 p.s.i. from the surface to often considerable depths. The psychrometric technique (Ref. 2 to 11), viz. a precise wet and dry bulb thermometer technique, is, at the present time, the only satisfactory method for measuring soil suctions of these magnitudes for engineering application. Further developments, (Ref. 12 and 13), have indicated the advantages of this method over other available techniques. This paper extends this earlier developmental work by attempting to evaluate the use of this technique for determining effective and useful values of soil suction in the field, and particularly *in situ* soil suction.

II. NOTATIONS (in order of appearance)

h = soil suction (p.s.i.)
R = universal gas constant ($8.3.10^7$ erg/mol/°K)
T = absolute temperature (°K)
g = acceleration due to gravity (981 cm/sec^2)
M = molecular weight of water = 18.02
H = relative humidity
C = heat capacity of junction including any condensed water (cal/°C)
θ = junction temperature relative to initial chamber temperature (°C)
t = time (sec)
H_a = sensible heat flux to the junction through air (cal/sec)
H_r = radiant heat flux to the junction (cal/sec)
H_w = heat flux through thermocouple wires to the junction (cal/sec)
L = latent heat of vaporization of water (585 cal/g)
q = rate of evaporation of water from junction (g/sec)
i = current (mA)
J = Joule
P = Peltier coefficient
θ_e = junction temperature during evaporation phase (°C)
θ_c = junction temperature during condensation phase (°C)
E = psychrometer output (micro-Volts)
τ = maximum theoretical wet bulb depression (°C)

III.- THEORY

(a) Relationship between Free Energy and Relative Humidity

The thermodynamic relation between the free energy of the soil moisture and the relative humidity is given in eq. (1).

$$h = \frac{RT}{gM} \log_e H \qquad \ldots(1)$$

From this relationship it can be shown (Ref. 13) that in order to determine soil suction below 400 p.s.i., it is necessary to measure relative humidity very precisely.

(b) Wet Bulb Depression

The relative humidity H can be measured by the psychrometric techniques. The instrument described below (often known as the Spanner psychrometer) uses probes consisting of a single thermocouple (Fig. 1). The dry bulb or 'zero' reading can be made by reading the output from the thermocouple in a humid atmosphere in equilibrium with the soil sample. By passing a current through the thermocouple in such a direction that the junction is cooled below dew point the thermocouple can then be transformed into a wet bulb. Evaporation of condensed water then lowers the temperature of the wet bulb. The maximum difference between wet and dry bulb reading occurs when the vapour pressure of the free water on the wet bulb is lowered to that of the ambient humid atmosphere; but in practice the maximum depression will never be obtained due to the

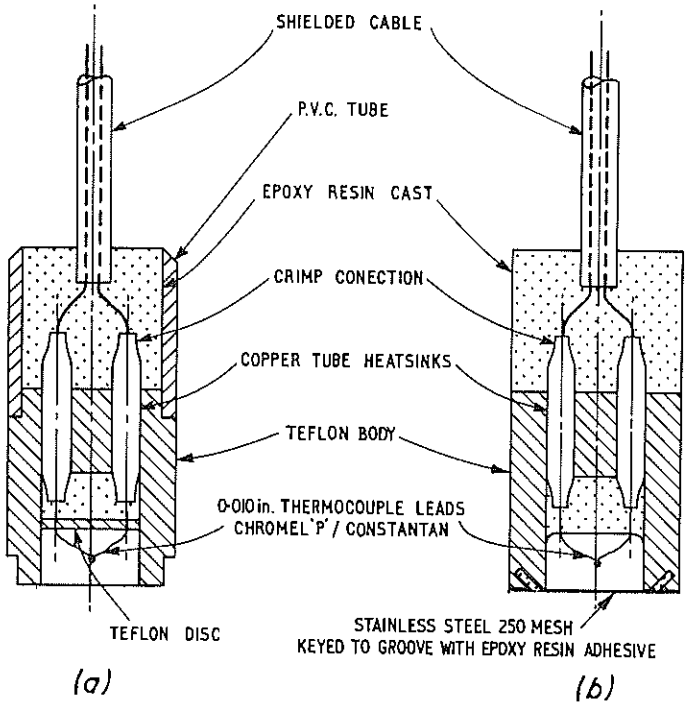

Fig. 1.- Schematic diagram of thermocouple probes: (a) laboratory probe; (b) field probe.

heat transfer from the surroundings to the wet bulb. Equilibrium is reached when the heat lost by mass transfer equals the heat gained.

Peck (Ref. 14) has made the most recent and comprehensive analysis of the Spanner psychrometer. He assumes that, before the passage of the constant cooling current through the junction, temperature and water vapour concentration are uniform throughout the psychrometer chamber. At all subsequent times, temperature and water vapour concentration are constant at their initial values on the walls of the chamber, which are assumed concentric with and very much larger than the thermocouple junction.

For convenience, the junction was assumed to be a spherical bead of fused metal, radius r_j. Evidence also suggests that convective transfer of heat from a sphere in air is negligible in comparison with thermal conduction, provided the Raleigh number (Ref. 14) is less than about 0.1.

Heat is transferred to the junction by conduction through the air (H_a) and the thermocouple wires (H_w), and by net radiation from the chamber walls (H_r). Heat is lost from the junction by evaporation of water (Lq). The junction energy balance gives:

$$C \frac{d\theta}{dt} = H_a + H_r + H_w - Lq \qquad \ldots(2)$$

Applying eq. (2) to the probes used by the author (Fig. 2), and using the expressions and data from Ref. 14, the following expression for the wet bulb depression at 20°C can be obtained.

θ_c = 0.000289°C/p.s.i. (0.00000419°C/cm water) soil suction

For Chromel-P Constantan thermocouples used in this paper, this is equivalent to:

E = 0.01676 micro-Volts/p.s.i. soil suction

i.e. the calibration between psychrometer output and soil suction is linear. Calibration of the probes in the laboratory is also approximately linear (Fig. 2). However, the line does not pass through the origin (zero offset). But field evidence suggests that the field calibration curve is linear through the origin and parallel to the laboratory curves, as discussed below. The mean slope of a large number of these experimental calibration curves is given by:

E = 0.0182 micro-Volts/p.s.i. soil suction

which compares favourably with the theoretical expression.

(c) Peltier Cooling

By including the transfer through the thermocouple wires to the junction of heat generated by Joule heating (i^2R) of the wires themselves and heat lost from the junction by the Peltier effect (Pi/J), shown in eq. (2), the following expression can also be obtained for the probes during the condensation phase, viz.:

$$\theta_c = -19.7i - 2.89.10^4.h - 1.01.10^2.i^2 \qquad \ldots(3)$$

For a given value of h, this is a quadratic equation in i, and shows a maximum degree of cooling when the current equals 97 mA ($\delta\theta/\delta i = 0$). In practice, the current actually used varies depending on time of

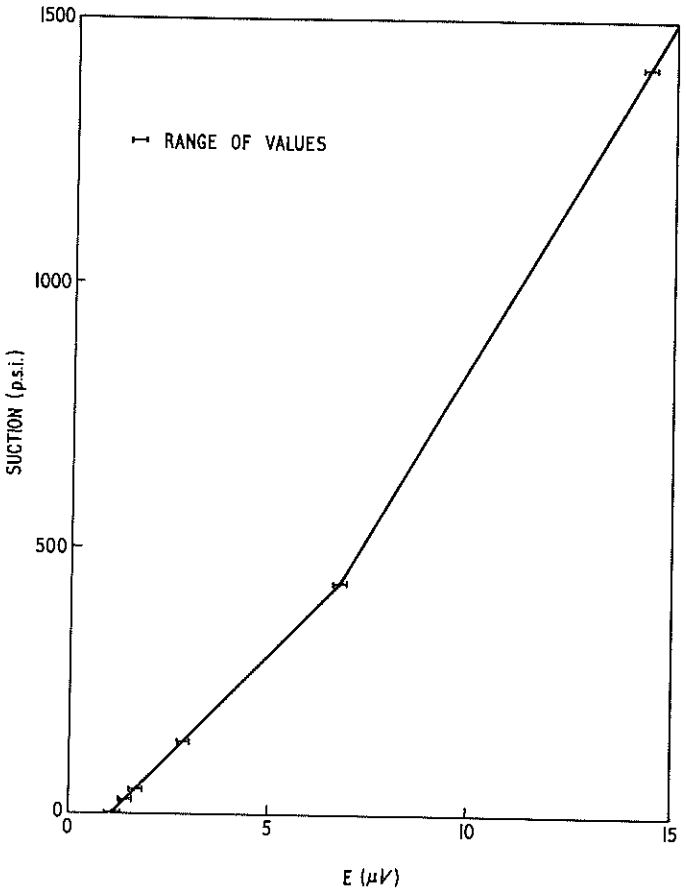

Fig. 2.- Calibration curve of a typical laboratory probe.

reading, etc., but at present 120 mA for 180 sec is giving satisfactory performance.

(d) Temperature Control

If the temperature changes sufficiently slowly to allow both the wet bulb and the sample temperatures to change at the same rate, then the humidity change is negligible. The calibration factor will change slightly with ambient temperature, but this can be incorporated into the calibration curves (Ref. 1 and 5).

The most serious errors occur where the wet bulb, the dry bulb and the sample temperatures differ over a significant length of time. The author (Ref. 12) showed that the error in the maximum theoretical wet bulb depression at 20°C is:

$$\tau \text{ error} \simeq 19\Delta T \qquad \ldots(4)$$

where ΔT is the temperature difference between sample and wet bulb.

To obtain a sensitivity of less than ± 5 p.s.i., τ error must be less than 0.076°C and ΔT less than 0.004°C. This can be achieved in the laboratory by maintaining a temperature control better than ± 0.001. In the field, the temperature variations in the ground at depth are sufficiently slow and small to meet these requirements. However, the depth above which these probes becomes too inaccurate for engineering purposes is not known, but experience has shown that sensible results can be obtained to within about a depth of 1 ft from the surface in many cases.

IV.- APPARATUS

The equipment used in this work is basically the same as that already described in Ref. 13. The laboratory and field probes have been modified as shown in Fig. 1. The laboratory instrument, consisting of a constant temperature bath and an automatic scanning read-out unit, has undergone slight modifications to permit up to 28 samples to be handled simultaneously. The temperature controller and the design of the bath have also been improved so that a temperature control within ± 0.0002° can still be achieved with smaller temperature gradients within the bath.

The manually operated field read-out unit has not been altered, but a new portable automatic scanning field unit has been built, and shows a similar performance to the laboratory unit.

V.- LABORATORY MEASUREMENTS

Using the previously described technique (Ref. 13) for laboratory measurements, in which the probes are individually calibrated against standard sodium chloride solutions, excellent accuracy and reproducibility can be achieved on 'intact' samples. A typical calibration curve is shown in Fig. 2. With reasonable care, an accuracy of about ± 2.5 p.s.i. or ± 5 per cent (whichever is greater) can usually be obtained.

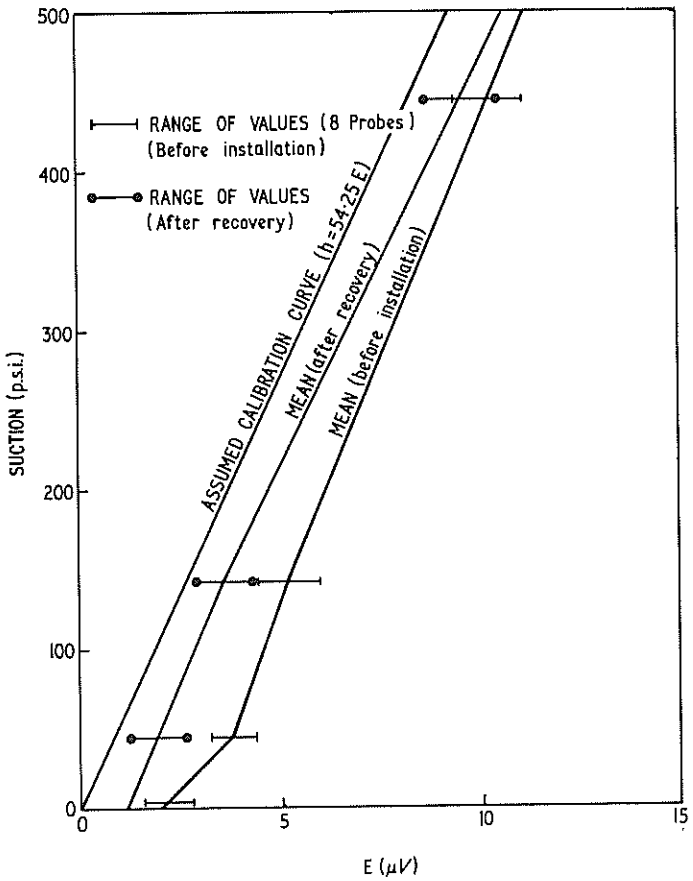

Fig. 3.- Mean calibration curve and range of readings from field probes before and after installation.

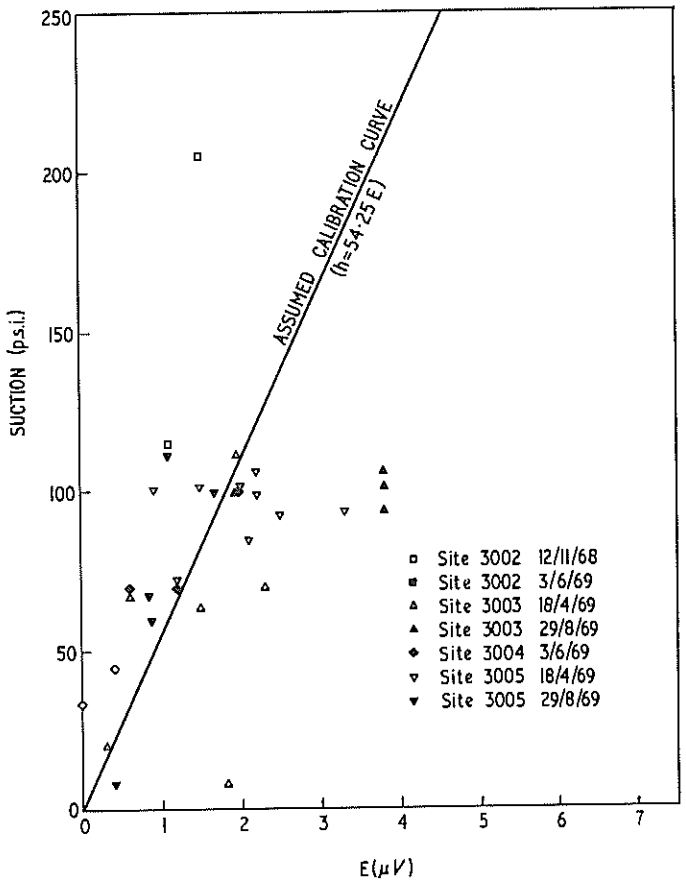

Fig. 4.- Field calibration curve.

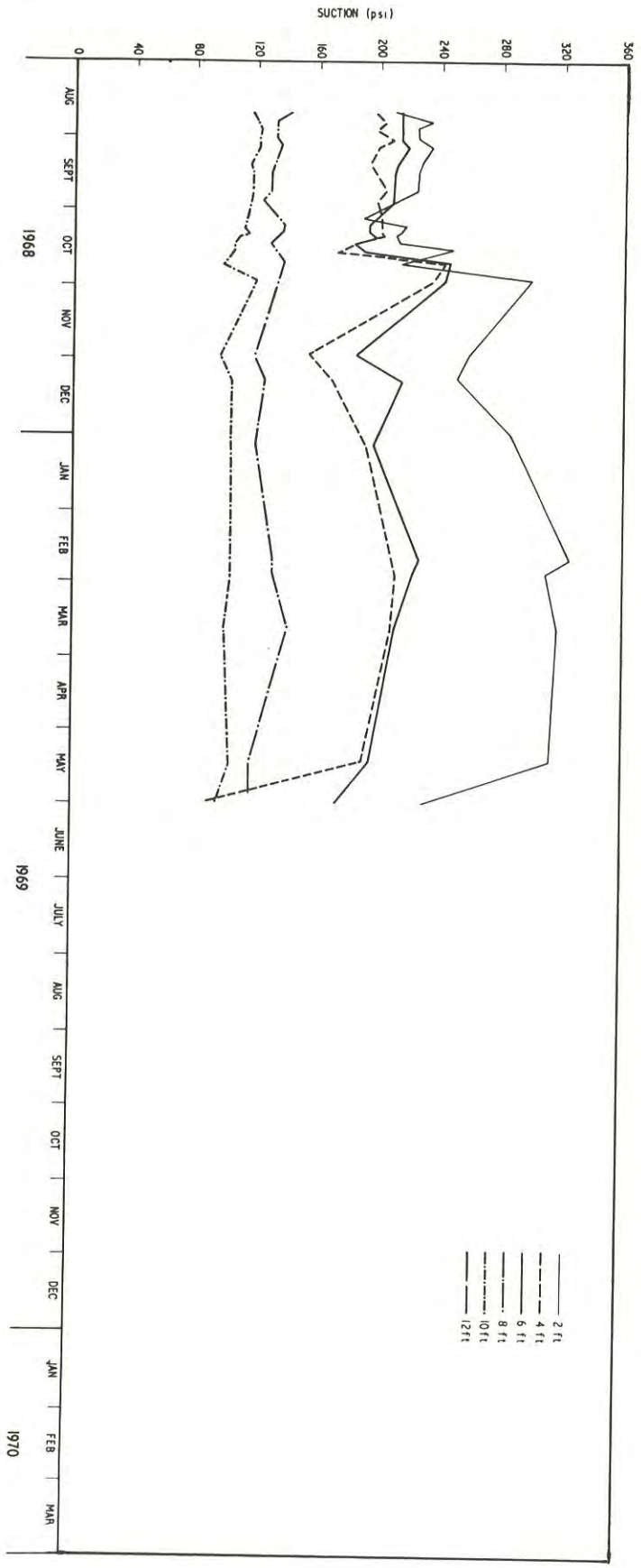

Fig. 5.- *In situ* suctions and rainfall plotted versus time. Rainfall.

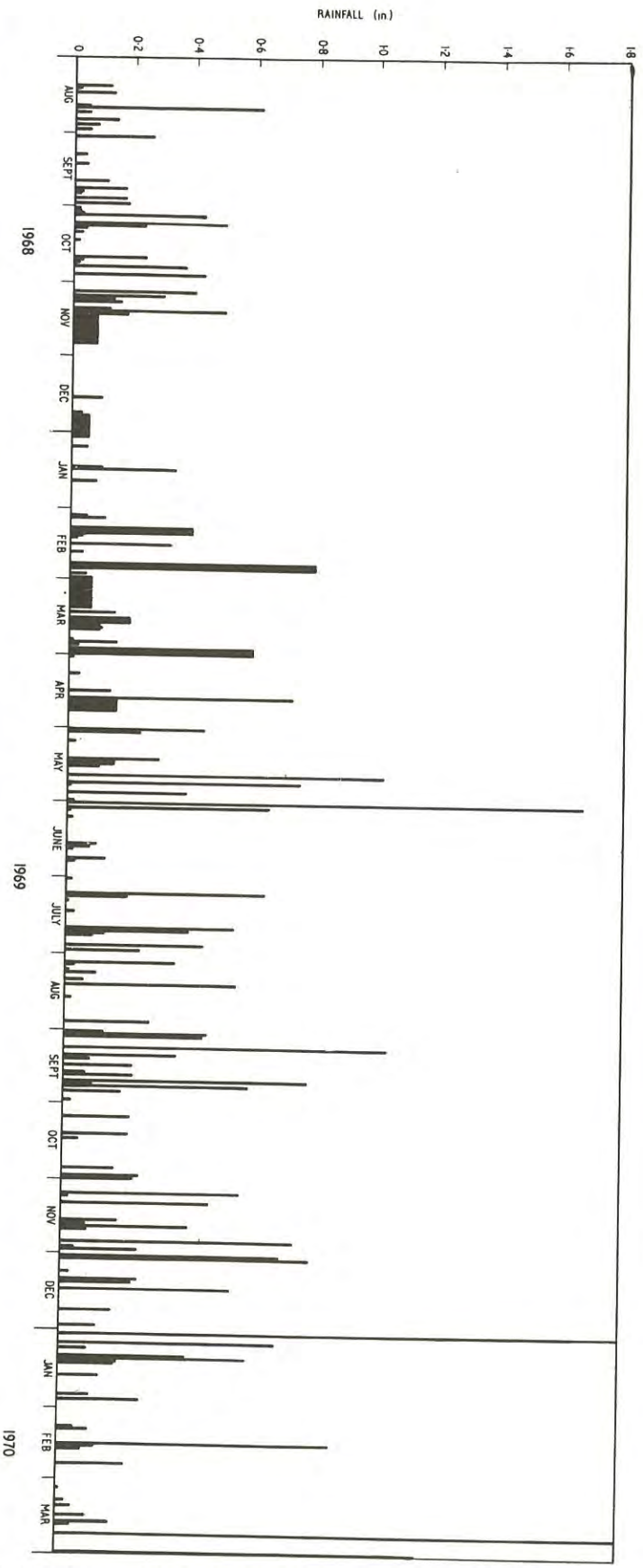

Fig. 5.- *In situ* suctions and rainfall plotted versus time. Site 3001.

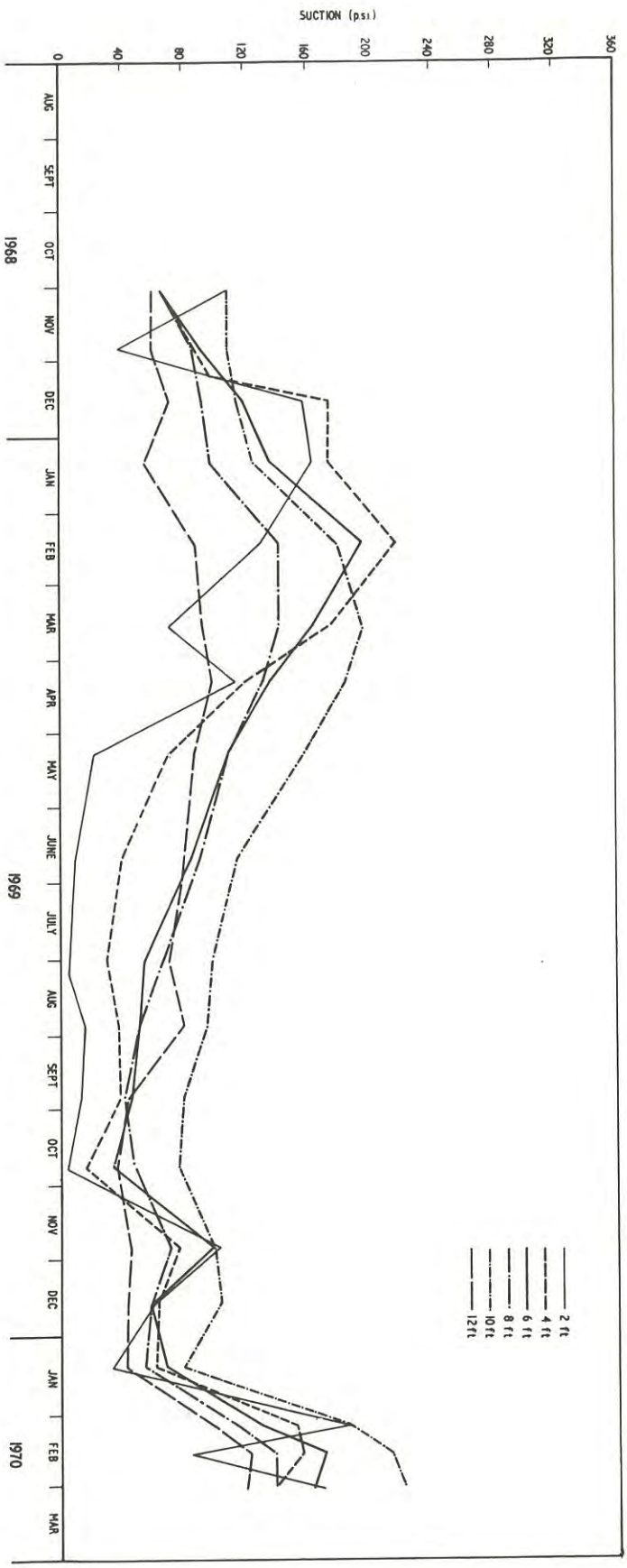

Fig. 5.- *In situ* suctions and rainfall plotted versus time. Site 3004.

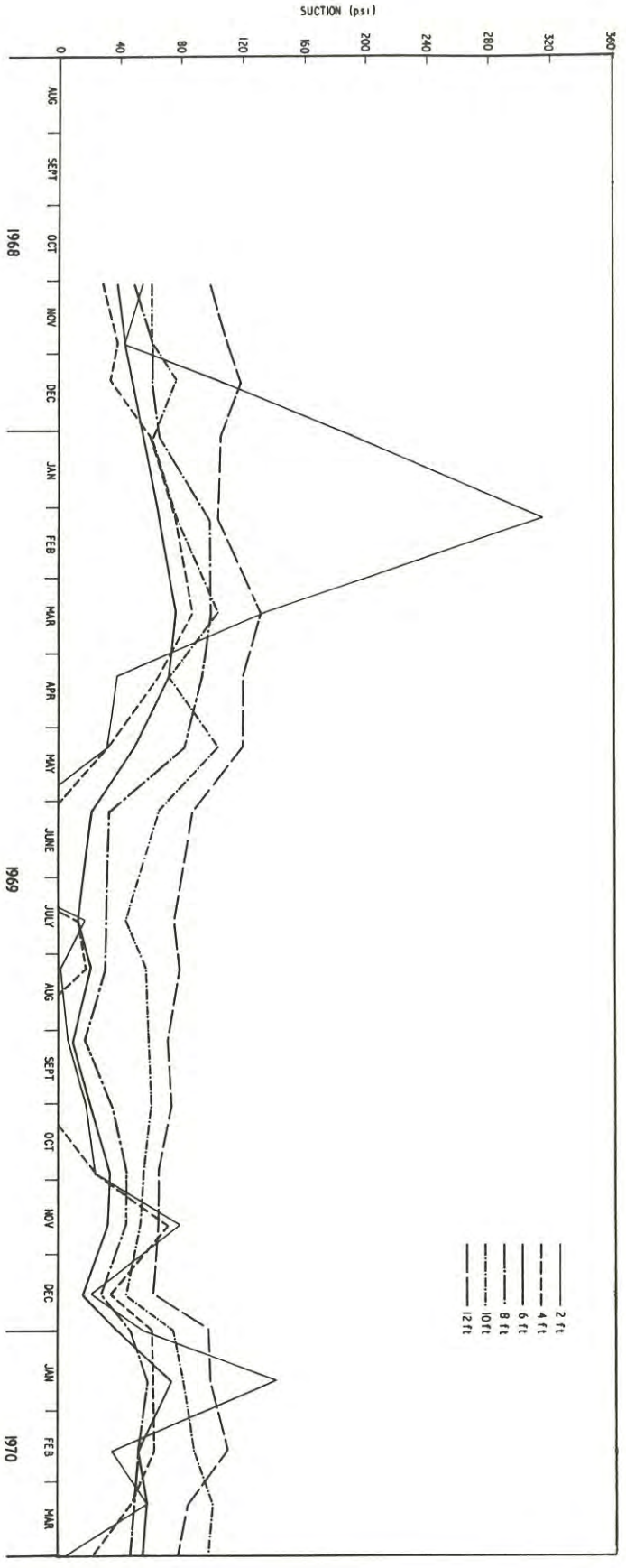

Fig. 5.- *In situ* suctions and rainfall plotted versus time. Site 3005.

However, in routine production testing, an accuracy of ± 5 p.s.i. or ± 10 per cent (whichever is greater) is probably a better estimate.

VI.- FIELD CALIBRATION

In order to evaluate the field probes shown in Fig. 1, some 30 probes were installed in the grounds of the Division of Applied Geomechanics, CSIRO, Syndal. A random selection of eight of these probes was calibrated in the laboratory unit before installation. After approximately 12 months in the ground, a number of probes were successfully recovered and subsequently recalibrated. The results, shown in Fig. 3, indicate that the curves, derived from the original laboratory curves, had not changed greatly during the 12-month use of the probes in the ground, and were essentially similar to the curves derived for laboratory probes (Fig. 2), that is, there has been no significant drift in the calibration curves during the 12-month period. However, using these calibration curves (Fig. 3), the readings from the probes in the ground gave soil suction values which experience suggested were consistently too low. This indicated that the calibration curves obtained for these probes in the laboratory might not be applicable to use *in situ*, and should be closer to the origin. An assumed calibration curve was then drawn through the origin parallel to the mean obtained in the laboratory, this also approximates to the theoretical calibration curve (Fig. 3). Subsequent 'intact' sampling on the circumference of a circle of 3 ft radius centred on the respective probes gave soil suction values that were considered more reasonable. These values were then plotted against the readings in micro-Volts from the corresponding field probes (Fig. 4). Because the correlation between the assumed curve and the field calibration points, as plotted in Fig. 4, was considered acceptable, this curve was subsequently used to determine soil suctions from the field probes.

In accordance with the theory presented by Peck (Ref. 14), that was unfortunately not available until after these probes were built and installed, four factors could result in the zero offsets observed in the laboratory calibration curves, viz.:

(i) inadequate heat dissipation in the massive junctions or heat sinks,
(ii) changes in effective junction size due to uneven deposition of condensed water, e.g. a water repellent junction,
(iii) incorrect interpretation of the transient temperature changes during the wet bulb reading, and
(iv) temperature gradients down the probe, e.g. due to heat conduction along the leads to the probe.

Due to the large thermal mass of the soil surrounding the probe *in situ*, it is considered that the zero offset resulting from (i) and (iv) above could be greatly reduced in the field. Further investigations into these important factors are now being carried out and should lead to improved probe design and calibration procedures.

VII.- FIELD MEASUREMENTS

The 30 probes were installed, in sets of 6 placed at 2 ft intervals, in five holes (subsequently referred to as sites). Site 3001, installed in July 1968, was located under the 48 ft wide concrete slab of the laboratory, 22 ft from the north wall. Site 3002, installed in September 1968, was located 12 ft from the north wall of the laboratory under an open sloping lawn and site 3003, installed in August 1968, 48 ft from the north wall under grass covered with native Australian trees up to 30 to 40 ft in height. During October 1968, following 'intact' sampling at sites 3002 and 3003, sites 3004 and 3005 were installed in the sampling holes, drilled 3 ft from sites 3002 and 3003 respectively. After having recovered the probes, sites 3002 and 3003 were destroyed during 1969.

Readings were taken more frequently than monthly but, for clarity, approximately only one reading per month is shown in the plots of suctions versus time (Fig. 5) for the probes at sites 3001, 3004 and 3005. The combined rainfall plus garden sprinkling at site 3004 is also shown in this Figure.

The results of six 'intact' sampling programs are plotted as suction profiles in Fig. 6, and the comparable field suction profiles are shown for comparison. Although the laboratory profile for site 3001 was obtained from 'intact' sampling only during installation useful comparisons were possible, due to the stability of moisture conditions under the floor (see Fig. 7).

VIII.- CONCLUSIONS

The results from the field probes in Fig. 5 and 6 are very encouraging. As expected, the probes near the natural surfaces at sites 3004 and 3005 indicate reasonable, seasonal variations in soil suction that decrease with depth. The long term stability over 18 to 24 months appears to be satisfactory. This is clearly indicated by the stable conditions under the slab floor at site 3001 as shown by the envelope in Fig. 7.

The comparisons between field readings and those determined on 'intact' samples in the laboratory are also satisfactory, particularly when considered in relation to the wide range of readings that can occur in the field. They certainly enable readings to be made in the field with far more confidence than previously possible.

Finally, the envelopes of all readings taken from the three sites were plotted against depth (Fig. 6). These plots clearly indicate, vertically, the extent of seasonal variations, particularly the influence of the trees at site 3005, creating both higher suctions and larger variations in suction at depth than those under the well-watered lawn at site 3004. The results from site 3001 are in good agreement with both theory and previous experience.

The above results have been presented in some detail, to enable the reader to draw his own conclusions. The results are considered satisfactory and suggest that the techniques described will be extremely useful in most soil engineering applications in the drier environments commonly found in Australia.

As a conservative guide, it can therefore be suggested that this technique will permit the measurement of negative pore pressures or soil suction over the range normally encountered in engineering practice in Australia, viz. 0 to 1500 p.s.i. suction (pF 0 to 5.0) with an accuracy in routine use of ± 10 per cent (lower limit ± 5 p.s.i.) in the laboratory, or ± 50 per

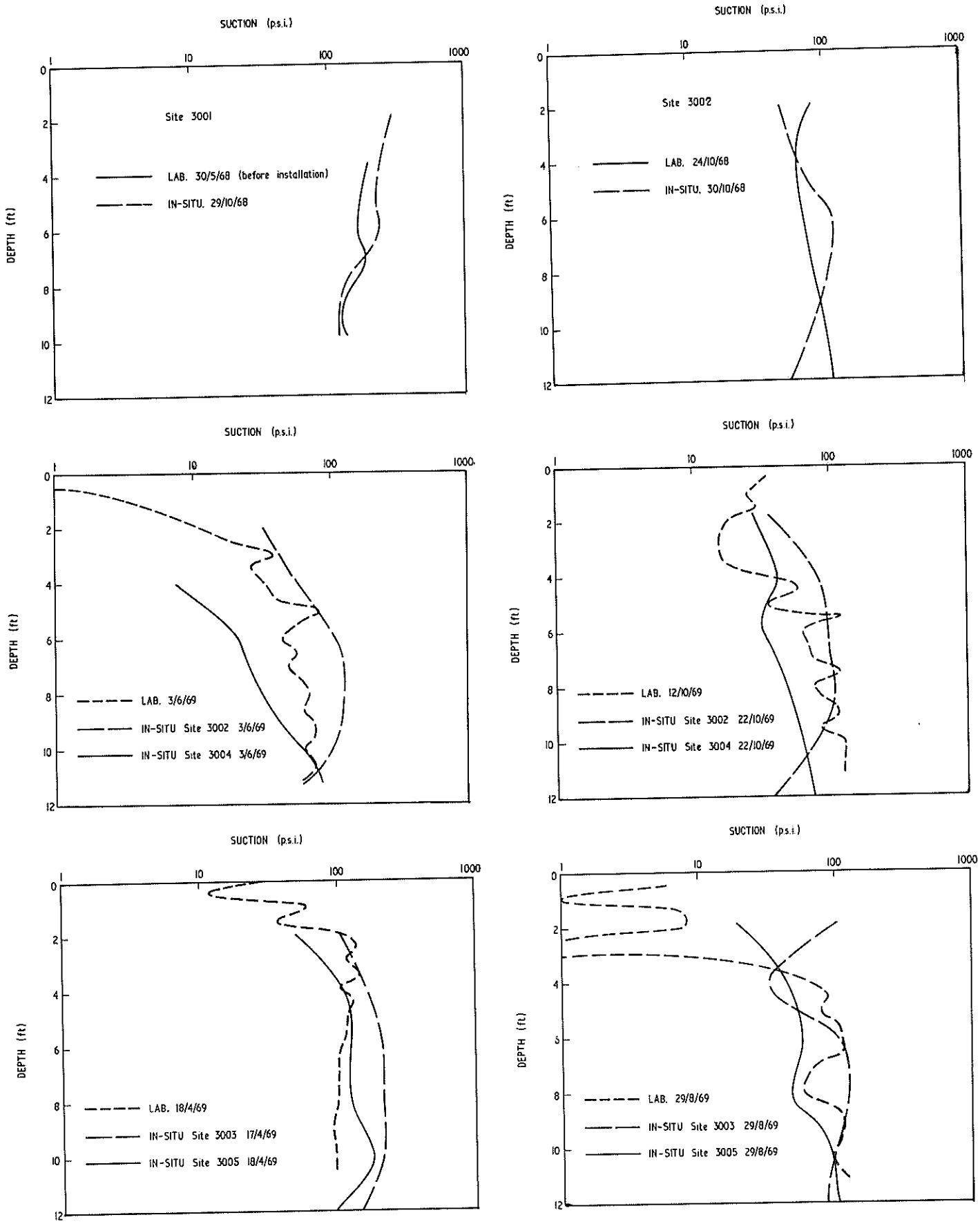

Fig. 6.- Suction profiles - compaction between intact sample and *in situ* values.

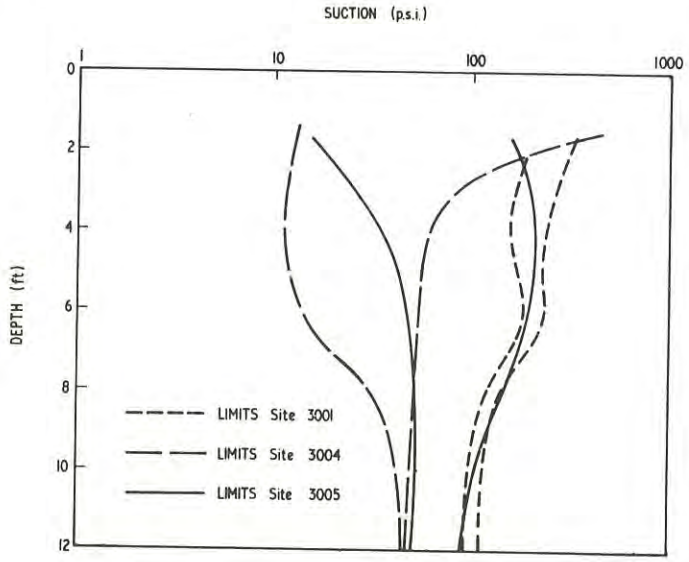

Fig. 7.- Maximum and minimum limits of *in situ* suction profiles.

cent (lower limit ± 25 p.s.i.) in the field.

IX.- ACKNOWLEDGEMENT

The author would like to acknowledge with thanks the work of Mr. Stephen Matthews who constructed and operated the instruments mentioned in this paper.

REFERENCES

1. RICHARDS, B.G. - Review of Measurement of Soil Water Variables and Flow Parameters. Proc. 4th Conf. A.R.R.B., 1968, Vol. 4, Pt. 2, pp. 1843-1861.

2. HILL, A.V. - Proc. Roy. Soc., A 127, 1930, 9.

3. BALDES, E.J. - Biodynamica No. 46, 1939.

4. BALDES, E.J. and JOHNSON, A.F. - Biodynamica No. 47, 1939.

5. BRADY, A.P., HUFF, H. and McBAIN, J.W. - Measurement of Vapour Pressures by Means of Matched Thermistors. J. Phys. Colloid Chem., 55, 1951, pp. 304-311.

6. SPANNER, D.C. - The Peltier Effect and Its Use in the Measurement of Suction Pressure. J. Exptl. Bot., 2(5), 1951, pp. 145-168.

7. MONTIETH, J.L. and OWEN, P.C. - A Thermocouple Method of Measuring Relative Humidity in the Range 95-100 per cent. J. Sci. Instr., Vol. 35, 1958, pp. 443-446.

8. RICHARDS, L.A. and OGATA, G. - A Thermocouple for Vapour Pressure Measurement in Biological and Soil Systems at High Humidity. Science, Vol. 128, 1958, pp. 1089-1090.

9. KLUTE, A. and RICHARDS, L.A. - Effect of Temperature on Relative Vapour Pressure of Water in Soil: Apparatus and Preliminary Measurement. Soil Sci., Vol. 93(6), 1962, pp. 391-396.

10. LANG, A.R.G. and TRICKETT, E.S. - Automatic Scanning of Spanner and Droplet Psychrometers having Outputs up to 30μV. J. Sci. Instr., Vol. 42(11), 1965, pp. 777-782.

11. RAWLINS, S.L. and DALTON, F.N. - Psychrometric Measurement of Soil Water Potential without Precise Temperature Control. Proc. Soil Sci. Soc. Am., 31, 1967, pp. 297-301.

12. RICHARDS, B.G. - Measurement of the Free Energy of Soil Moisture by the Psychrometric Technique Using Thermistors. In "Moisture Equilibria and Moisture Changes in Soils Beneath Covered Areas", Ed. G.D. Aitchison, Butterworths, Sydney, 1965, pp. 39-46.

13. RICHARDS, B.G. - Psychrometric Techniques for Measuring Soil Water Potential. Div. of Soil Mech., CSIRO, Tech. Rept. No. 9, 1969.

14. PECK, A.J. - Theory of the Spanner Psychrometer, 1. The Thermocouple. Agricultural Meteorology, Vol. 5, No. 6, 1968, pp. 433-447.

Laboratory Shear Testing of Weakness Planes in Diamond Drill Core

By
E. P. Waghorne, B.E. (Mining), S.Aus.I.M.M.
(Engineer, S.E.C.V.)

SUMMARY.- The importance of the frictional properties of joints in determining the stability of mine openings in rock has been well documented. Both in situ and laboratory testing are at present being used to estimate these properties, but often these methods require considerable specimen preparation. Diamond drill core taken for geological or geomechanical purposes offers readily prepared specimens on which a great number of tests could be conducted. To this end a machine was designed and constructed in the Mining Department of the University of Melbourne, enabling shear testing of cores up to 3.5 inches in diameter. Both open and intact joints through the core can be tested for peak and residual strengths, providing the angle of intersection between the joint plane and core axis is greater than 30°. Also, testing can be conducted along the joint plane in any direction relative to slickensiding. Calibration testing using teflon and brake lining specimens has been conducted, and the results of joint samples tested are discussed.

I.- INTRODUCTION

In recent years considerable interest has been shown in the frictional properties of the joints and weakness planes within rock. Where these planes are unfavourably oriented to the excavation, failure is more likely to occur along these weaknesses than through the rock matrix. Normal testing techniques use intact specimens which may not represent a rock mass dissected by weakness planes. However, this deficiency can be partially overcome by shear testing for peak and residual frictional resistence along particular weakness planes. These measurements, combined with a knowledge of the orientation and the surface properties of the joint, will enable stability predictions to be made.

Several shear testing techniques are in use at the present time. Triaxial apparatus can be used on solid cores with weakness planes within them, providing the planes intersect the core axis at angles between 30° and 60°. Direct shear testing has been conducted on joints or weakness planes both in situ and in the laboratory. In situ tests involve considerable time, expense and effort to arrange, but can be of real value where sampling would influence the results. Laboratory direct shear tests can be conducted under uniform conditions and at a lower cost than in situ tests. Well designed machinery is necessary to allow shear movement and riding over any surface irregularities which may occur, whilst preventing rotation. Specimens are usually chosen from surface outcrops or exploratory openings and require careful preparation before testing can be conducted. Tests on artificial surfaces are used to predict modes of failure rather than absolute values of friction.

These Direct Shear Testing methods involve time consuming work reducing the numbers of specimens which could be economically tested. Also, selecting samples from near excavated openings could impose restrictions on the results achieved. Machinery could be designed to improve testing of frictional properties of selected surfaces while overcoming the deficiencies of these methods.

II.- AIMS OF EQUIPMENT

(a) Rapid testing of a large number of samples, enabling statistical analysis.

(b) Testing of exploration drill cores.

(c) Testing of various diameter core.

(d) Loading to simulate in situ conditions.

(e) Testing in any direction to striations or slickensiding along joints intersecting the core.

(f) Separation of joint surfaces if riding over asperities occurs.

(g) Measurement of the loading applied and the resulting deformation to the specimen will determine the peak and residual strengths along the tested plane.

III.- DESIGN AND MANUFACTURE OF THE UNIVERSITY OF MELBOURNE DIRECT SHEAR TESTING MACHINE

The machine was designed and constructed within the Mining Department with the manufacture of major items being conducted by engineering firms. The loading capacity of 20 tons allows pressures of up to 10,000 p.s.i. to be applied to the surface area of the joint. Tests can be conducted on various core diameters to a maximum of 3.5 inches, with an allowable shear displacement of 1 inch in each direction and a normal displacement of .5 inch. A photograph of the machine is shown in Fig. 1.

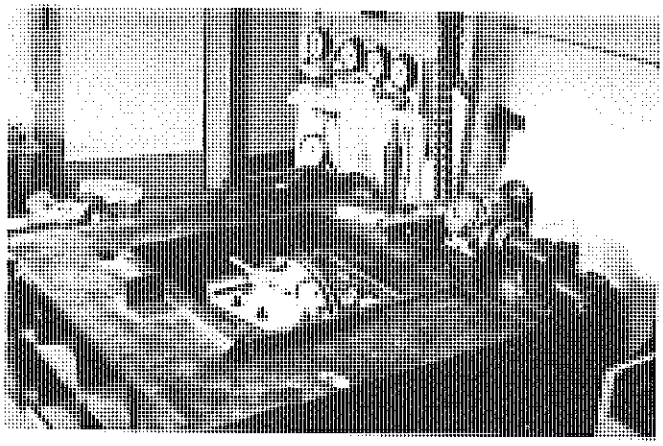

Fig.1 The Shear Testing Machine.

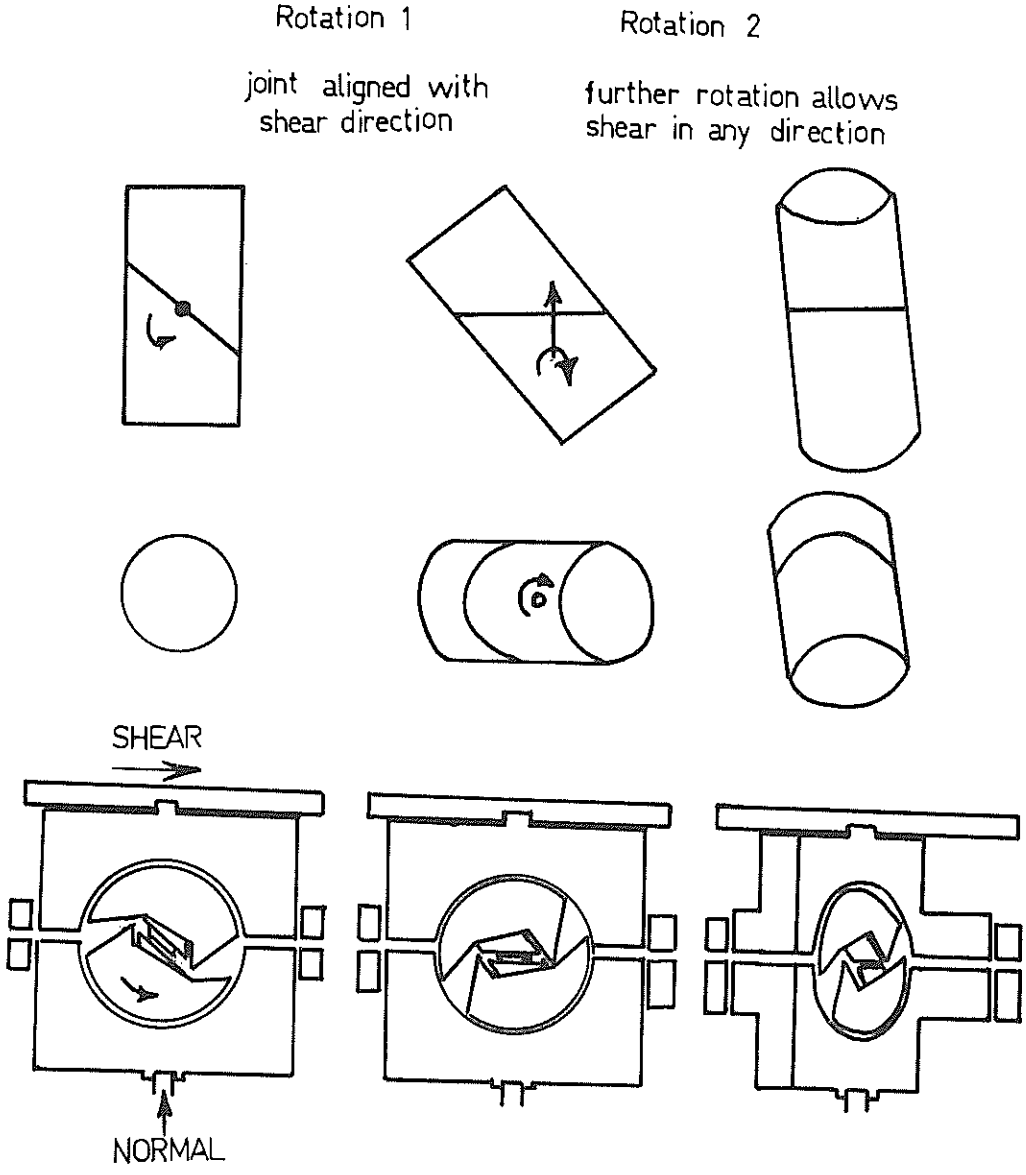

Fig.2 Rotations required prior to a test which aligns the joint with the shear direction.

The design is such that:

(a) Prior to a test the core specimen can be rotated relative to the loading points. This allows testing in any direction along the joint plane, providing the joint intersects the core at angles greater than 30°. Two rotations are required. The first is around the line perpendicular to the core axis and parallel to the joint plane. This aligns the joint with the direction of shear loading. Secondly, rotation around the line perpendicular to the joint plane allows shearing movement in any direction on that plane. These pre-test adjustments are shown in Fig.2.

(b) The core is rigidly held in sleeves, ensuring uniform loading to the specimen on each side of the joint plane. The sleeves are of various sizes to allow testing of core up to 3.5 inches in diameter. Also, the ends are cut at angles between 30° and 90° to the core axis so that specimens with weak plane intersections in this range may be tested with support to within .25 inch of the joint plane. The core and sleeve are held neatly in the specimen holder with packers and a screw adjustment. (Fig. 3). A keyway in the holder prevents axial rotation.

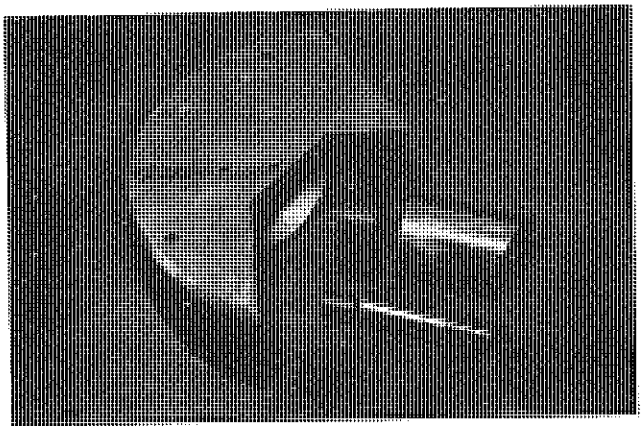

Fig. 3 The specimen holder and sleeve, showing the specimen location.

Each specimen holder is clamped between the upper and lower parts of one of the two universal loading frames. The specimen holder and the universal loading frame have circular mating surfaces for rotation prior to testing to orient the joint surfaces. (Fig. 4). Flat teflon-surfaced bearings on the outside of the universal loading frame control the movement of the two sides of the specimen. One frame can move parallel to the joint with the other perpendicular to this direction, so that riding over irregularities may occur.

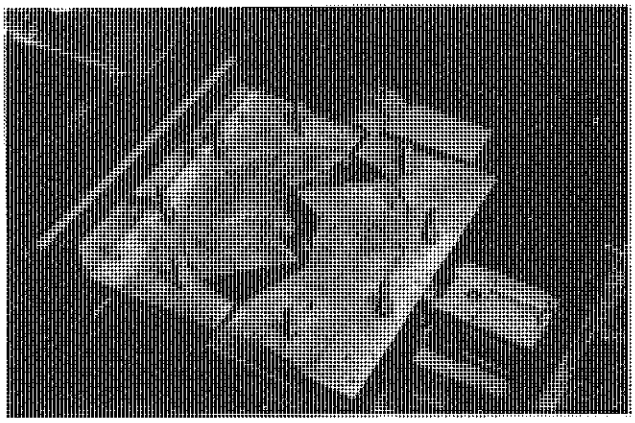

Fig.4 The Universal Loading Frame and the Specimen Holders, showing how rotations can be conducted.

(c) Shear loading can be applied in either direction to allow reversal of the test, and reach the residual strength. Loading is applied by hydraulic rams between the main frame and the universal loading frames. A constant normal load was applied by using a loaded lever arm, while a constant volume displacement oil pump provided the shear load. The shear system allowed pressure to build up at a uniform rate, reaching the resisting strength developed along the weakness plane before failure occurred. This compares with the situation found in situ where the forces causing sliding are thought to build up after each slip. The hydraulic circuits are shown in Fig. 5.

(d) Measurement of the loading applied to the specimen was made using pressure gauges in the hydraulic circuits. Displacements of the specimen were measured by using Linear Variable Differential Transformers (L.V.D.T.'s) between the two universal loading frames. The loading and resultant displacements were recorded using a four track Watanable continuous recorder.

(e) Using an overhead block and tackle system, it was found that a specimen could be tested and replaced within two hours.

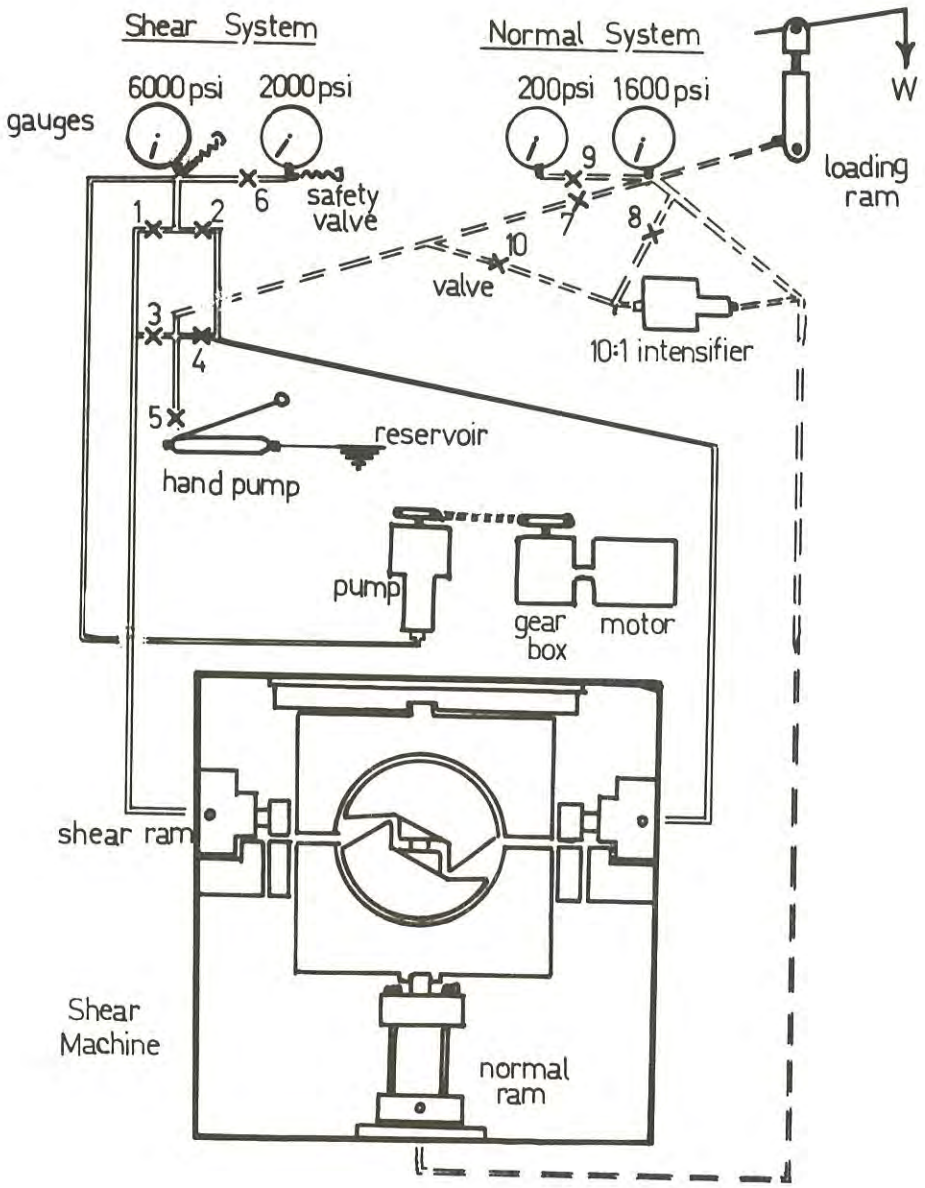

Fig.5 Shear and Normal loading circuits

IV.- CALIBRATION AND TESTING

Calibration was considered necessary because of the large component weight and the friction at the bearings. Samples were prepared of teflon against teflon and of cast iron against brake lining material, as both have relatively consistent frictional properties. It was found that a reduction of 320 lb. to the shear load produced accurate repetitive results. A more complete assessment could probably be achieved by using loadcell devices but this test has not been conducted at this stage.

Testing has been conducted on core provided by King Island Scheelite (1947) Ltd., Western Mining and the M.M.B.W. Both intact and open joints have been tested, and these have shown that the peak and residual shear properties can readily be achieved. A tested joint is shown in Fig.6.

The reversing procedure will show a different shear resistance if the failure surface is not accurately aligned with the load application. Correction for this error can be applied by averaging the forward and reverse values. An example of the results of two tests is shown in Fig. 7. Of the hornfels rock samples tested, the residual friction depended greatly on the surface properties on the line of failure. For example:- bedding plane joint (smooth, slightly curved surface) -: 40° to 45°.
smooth flat joints -: 38° to 42°.
rough joints -: 45°.

Fig.6 A tested specimen showing joint surfaces.

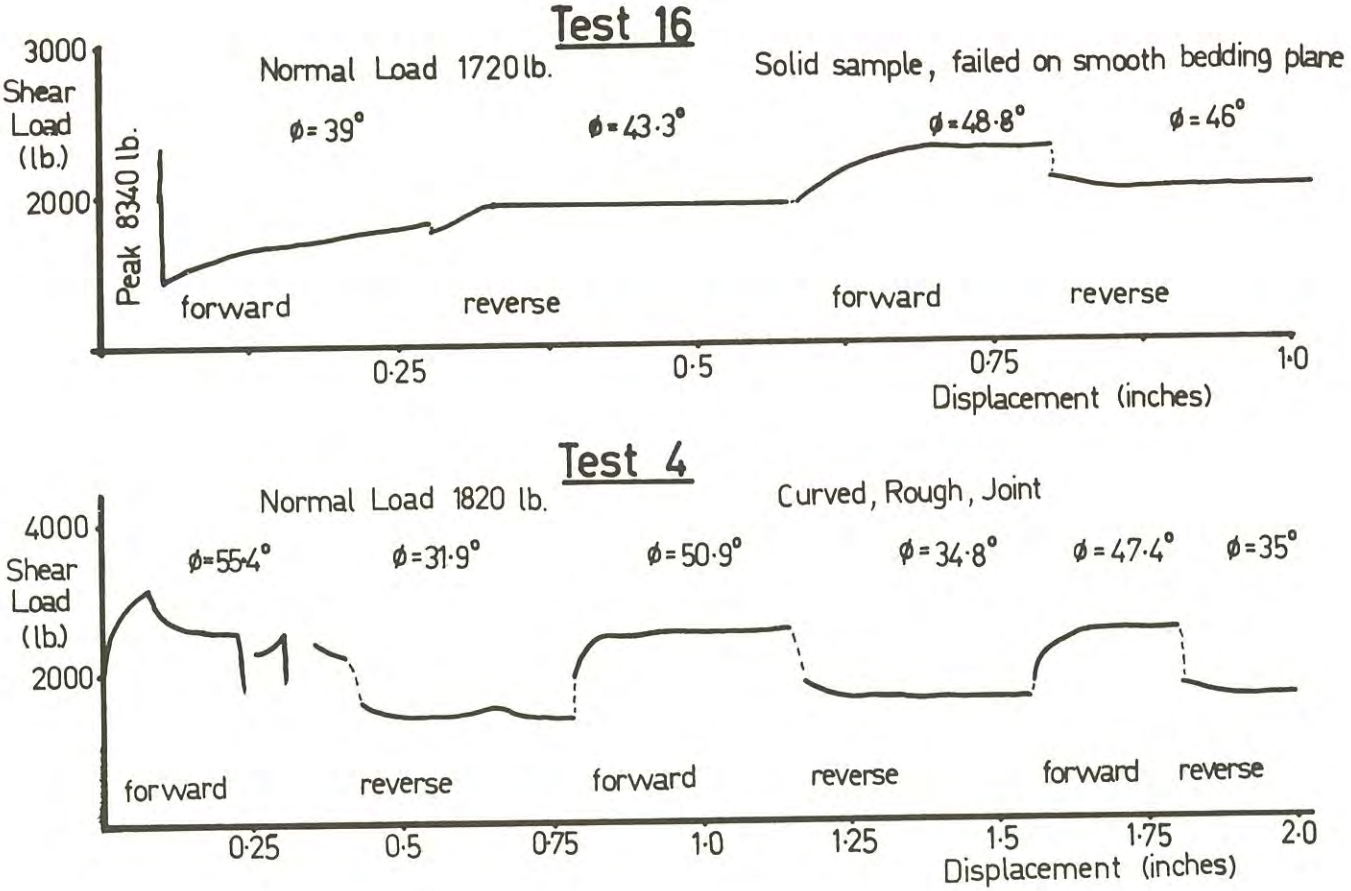

Fig.7 Load-displacement Curves for two tests.

V.- CONCLUSIONS

It is considered that this machine has fulfilled the requirements of providing measurements of peak and residual frictional properties of joints. The design has accomplished a degree of rapidity and versatility not present in other testing machines, allowing core samples from depth to be tested.

VI.- ACKNOWLEDGEMENT

The machine was designed and constructed with considerable aid from the academic and technical staff at the University of Melbourne. In particular, acknowledgement should be made to Messrs. Bamford, Dyson, Lawson and Ogden; and also for the generous assistance provided by King Island Scheelite (1947) Ltd., and the Western Mining Corporation.

VII.- BIBLIOGRAPHY

Bennet, A.G., 1971 Effect of Joints on the stability of a Machine-bored Tunnel, presented for a Ph.D.Thesis, Mining Dept., University of Melbourne. (unpublished)

Dyson, L.A.D., 1971, A Basic Rock Mechanics Survey and its uses in the Design of Underground Structures at the Kambalda Nickel Mine, presented for M.Eng.Sc.Degree, Mining Dept., University of Melbourne. (unpublished)

Waghorne, E.P., 1971, Rock Mechanics Applied to Open-Pit Mine Design at King Island, presented for M.Eng.Sc.Degree, Mining Dept., University of Melbourne. (unpublished)

Terrain Evaluation as a Basis for Engineering Geology

By

K. Grant, B.Sc.

(Principal Research Scientist, Division of Applied Geomechanics, C.S.I.R.O.)

Classification 20-50c / sq. mile

Evaluation $25 / " "

SUMMARY.- Engineering geology and terrain evaluation are complementary to each other. The one collects information about natural materials whilst the other provides methods for processing the information. Geotechnical information can be processed and stored for subsequent retrieval and can be extrapolated from one area to another by relating it to the terrain from which it was gathered. For this purpose terrain must be capable of classification at various defined significant homogeneous levels. Such a system of terrain classification can be based upon the principle that terrain is the result of the interaction of geology and climate with time as the operator.

I.- INTRODUCTION

Engineering geology has developed from the necessity for increasing specialization within the discipline of engineering as larger and more complex tasks were demanded from engineers by an increasingly affluent and educated society. Civil Engineering has always used the materials provided by the natural environment in constructing buildings, access ways, bridges, etc. The science of the occurrence and properties of these natural materials, including both soil and rock, falls within the ambit of geology. Engineering geology interprets the occurrence and estimates, both quantitatively and qualitatively, the properties of materials with regard to their situation within the environment in such a way that engineers with only a minimal training in earth sciences can sensibly design structures to be supported upon these materials and to use them within the structure.

Terrain evaluation, on the other hand, has developed from a desire and, indeed, a necessity to rationalize the collecting of information significant for engineering purposes and to collate, store and retrieve this information as the need arises. This necessity has arisen not only in those countries that require development but also in the most highly developed and affluent countries. These latter countries are demanding even more sophisticated engineering projects. There is a demand for information derived on a regional level as a prelude to planning and as the complexity of structures increases there is a necessity for increasingly detailed geotechnical site information. Engineering geology and terrain evaluation are, therefore, completely complementary to each other. The one collects information on natural materials and the other provides methods for processing this information. Both topics require similar skills for their successful implementation.

II.- PRINCIPLES OF TERRAIN EVALUATION

The basic principle upon which terrain evaluation rests can be stated simply as: *"products such as terrain with all its attributes (soil, rock, etc.) that have evolved from similar starting materials through similar geologic processes in similar climatic environments possess similar properties"*. This principle derives from the proposition that terrain as it exists is the product of the interaction of geology and climate with time as the operator.

Based upon this principle, although not always so stated, numerous systems of terrain classification have been proposed as the basis for terrain evaluation for various purposes. Those with engineering implications were reviewed by Aitchison and Grant (Ref. 1). The same authors (Ref. 2) realized that any system of terrain evaluation proposed for engineering must, for ease of interpretation, be not only within the understanding of specialist earth scientists such as geologists, but also of engineers who are not necessarily specialists in earth sciences. They therefore suggested a scheme based upon easily recognizable natural criteria that reflect geomorphic attributes rather than on those attributes themselves.

The basis of the scheme is that any area of land can be uniquely defined in terms of its topography, i.e. slope characteristics, underlying lithologic and tectonic characteristics and soil and vegetation characteristics; by defining intervals at suitable, significant levels for each characteristic, valid naturalistic terrain classes may be erected. The scheme, known as the P.U.C.E. Programme, operates at four levels of generalization, defined as follows:

(a) Terrain Component

A terrain component, apart from microtopography and certain other features which are defined below, has along each of a pair of lines, parallel to the major and minor axes of the slope (the principal axes), a constant rate of change of curvature always in the same sense, i.e. either convex or concave but not concavo-convex. Moreover, within assigned limits the maximum angles made by the principal axes with the horizontal are constant. It has, without exception, a consistent association of soils as expressed in terms of the Unified Soil Classification and at the subdivided primary profile form level (Ref. 3). Also, it has without exception a constant vegetation assoc-

iation, i.e. while more than one species or genus may be present, the species or genera always occur in the same relationship to each other and there is no discontinuity in their occurrence.

"The major axis of a slope can be regarded as the line on the surface, ignoring minor irregularities, that joins the highest and lowest points of the particular slope. As such, it will usually be at right angles to the contours in general sense."

"The minor axis of a slope may be regarded as the line of maximum extent on the surface, ignoring minor irregularities, bounding a vertical plane cutting the surface and set at right angles to the major axis of the slope".

Features not to be considered when rate of change of slope is determined are as follows:

(i) Microtopography which consists of small-scale natural topographic features, i.e. an inherent part of the particular piece of landscape and *not* of foreign material introduced accidentally into that particular piece of landscape from another part of the general landscape. It is considered arbitrarily that any such topographic feature with a relief amplitude of not more than 3 ft and an areal extent of not more than 600 sq ft falls into this category.

(ii) Rounded, angular, or irregular rock outcrop. Such outcrop may be of any size, but mostly will not be of large dimensions.

(iii) Elements such as rocks, boulders, cobbles, etc. derived from another part of the general landscape and introduced accidentally into the particular piece of landscape. Such elements may be of any size, but mostly will not be of large dimensions.

While elements of microtopography, rock outcrop, or accidental introduction as defined above are specifically excluded from slope considerations in the recognition of terrain components, they must enter into the descriptive phase of terrain component recognition as surface features. In these circumstances, a terrain component with any of these features will be essentially different from one similar in all other respects but containing either no, or different, surface features.

The exclusion of these features from slope considerations is based upon the principle that in any form of terrain classification that is to be workable, arbitrary lower limits must be placed upon the amount of variation allowed in any of the recognition criteria for each class. If all possible variations on a continuously varying medium are considered separately, an infinite number of varieties is possible; any system so based must be unworkable.

(b) Terrain Unit

A terrain unit is the area covered by a single physiographic feature of geomorphic significance having characteristic soil and vegetation associations.

The terrain unit so defined can be regarded as being composed of a limited number of terrain components which always recur in the same sense within the terrain unit. The characteristic slopes and soil and vegetation associations of the terrain unit will be those produced by a synthesis of those of the terrain components associated to form the terrain unit.

Topographically, the terrain unit will fall into classes and, within each class, will have a characteristic association of slopes and a consistent local relief amplitude. The classes so far recognized are listed as follows, but the list is not exhaustive.

(i) Surfaces, flat or with varying degrees of undulation, i.e. undissected, dissected, and/or eroded. These surfaces are not necessarily tied to specific erosional or depositional surfaces, i.e. the same terrain unit may occur on more than one erosional or depositional surface; such occurrences will be separated by a terrain unit classified under (ii) below.

(ii) Slopes between surfaces as in (i) above; gentle, steep or escarpment-like.

(iii) Isolated hills, ridges, etc., except those with flat tops; in the latter case the flat tops and surrounding slopes have been given independent terrain unit status in accordance with (i) and (ii) above respectively.

(iv) Drainage lines, lakes, etc.

The characteristic soil association of the terrain unit will be dominated by one of the following textural types:

Rock outcrop, pockets of shallow soil or gravel

Clay soils (Ug)*	Sand over clay soils (D)
Clay soils (U or G)	Sandy soils (U or G)
Clay soils (D)	Stratified soils
Silty soils	Organic soils
Sand over clay soils (G)	

* The symbols refer to the classification system of Northcote (Ref. 3).

The characteristic vegetation formation will be dominated by one of the following vegetation classes:

Bare, sparse grass, occasional tree or shrub

Grassland	Woodland
Shrubland	Forest
Open woodland	Rain forest
Savannah woodland	Fresh-water swamp forest
	Salt-water swamp forest

(c) Terrain Pattern

A terrain pattern is an area of constant geomorphic association containing recurring topography and soil and vegetation associations. The terrain pattern can be regarded as being composed of a limited number of recurring terrain units always associated in the same sense, and should be coincident with the area represented by a pattern on an aerial photograph of suitable scale.

Criteria for the delineation and recognition of terrain pattern boundaries are as follows:

(i) the continuous terrain unit or group of units changes;

(ii) terrain units included within the continuous terrain unit or group of terrain units change;

(iii) the continuous terrain unit or group of units and included terrain units do not change, but relative dominance of continuous and included terrain units changes;

(iv) type or density of the drainage net changes significantly; and

(v) local relief amplitude changes significantly.

(d) Province

A province is an area of constant geology at the group level and is composed of a limited number of recurring terrain patterns always associated in the same sense. When there is a change of province, the entire terrain association also changes.

The details of the scheme were elaborated by Grant (Ref. 4) and its application in the engineering sense by Grant (Ref. 5). Grant and Lodwick (Ref. 6) suggested the rudiments of an automatic data storage and retrieval system to operate as part of the scheme.

III.-THE USE OF TERRAIN EVALUATION IN THE PROCEDURES OF ENGINEERING GEOLOGY

Engineering geology is concerned essentially with geotechnical information gathered as part of the site investigation process. Terrain evaluation does not replace site investigation but supplements it by offering a rational system as a basis for the investigation. Geotechnical information may be gathered at two levels: (a) on a regional basis to determine the best location for a project, and (b) in a detailed site investigation when the site of the project has been determined. Terrain evaluation can operate at both these levels.

The first stage in any procedure using terrain evaluation is to classify the terrain. The methods of conducting this phase have been discussed by Grant (Ref. 5).

The level to which terrain is classified is dependent upon the scope of the investigation. Classification to terrain unit level is sufficient for regional studies. Classification to terrain component level is necessary for detailed site investigation. In general, classification to terrain unit level will be done by mapping terrain patterns at a scale of 1:250,000 and describing each terrain pattern in terms of the recognizable characteristics of its constituent terrain units. An example of part of such a description of a terrain pattern of widespread occurrence in the Melbourne area is shown in Fig. 1. A complete description of the Melbourne area (Ref. 7) at a scale of 1: 250,000 is in course of publication. The work was conducted in association with the Town and Country Planning Board, Victoria, as part of a project for the urban and rural planning of the Port Phillip District, Victoria. Classification to terrain component level will usually be done only in close proximity to the known project site. Terrain units may be mapped at a 1:50,000 scale, or terrain components at larger scales. At this level, each terrain unit will be described in terms of the recognizable characteristics of its constituent terrain components. An example of part of such a description of a terrain unit is shown in Fig. 2. The terrain unit described appertains to the terrain pattern in Fig. 1. It was described as part of a project conducted in association with the Country Roads Board, Victoria, for an experimental site investigation based upon terrain evaluation along the route of the proposed deviation of the Hume Highway between Wallan and Broadford, Victoria. A portion of the terrain component map for this project is shown in Fig. 3. The classification to terrain component level of a limited area such as along a road centreline in this particular project is a logical extension of a regional terrain classification as conducted in the Port Phillip District. It can be seen that the regional terrain classification, although originally conducted as a basis for urban and rural planning, remained valid as a basis for the more detailed classification necessary for the road construction purpose.

When the terrain has been classified, information gathered during the geotechnical processes can be attributed to the appropriate member of each class of terrain; general information may be appropriate at terrain pattern or terrain unit level, detailed information may be appropriate at terrain component level only, although some of this type of information may be appropriate at terrain unit level. Examples of general geotechnical information, attributed to terrain pattern and terrain unit level relevant to some aspects of railway construction, are given by Grant (Ref. 5), (Tables 4 and 5) and appropriate levels for expression of some factors of engineering significance are included in Grant (Ref. 8). The list given in the latter paper is by no means exhaustive, but it is not a difficult procedure to determine the appropriate level in the classification for each relevant factor of engineering significance. Thus all geotechnical information significant for engineering purposes can be tied to the terrain itself by the use of a system of terrain classification.

If it is presumed, in accordance with the basic principle of terrain evaluation, that all occurrences of each member of each class of terrain are essentially homogeneous, the geotechnical information collected for any one terrain class member can be extrapolated over all occurrences of that member. Using this hypothesis a facility can be incorporated into engineering geology for the advance prediction of material location and geotechnical properties over an area as extensive as that over which the terrain has been classified. In addition, the geotechnical information tied to the terrain base is in a convenient form for efficient and, if necessary, automatic data storage. Once stored, the information may be retrieved for use on subsequent similar projects to which it is appropriate, conducted in similar areas.

Terrain evaluation is thus a tool in the engineering geology process; it effectively rationalizes the collection of geotechnical information, proposes a system for storing this information for subsequent retrieval, and provides a basis for the extrapolation of information from one area to another and a facility for the advance prediction of material situation and properties.

REFERENCES

1. AITCHISON, G.D. and GRANT K. - Terrain Evaluation for Engineering. In Land Evaluation, G.A. Stewart, Ed., Melbourne, Macmillan, (1968), pp. 125-146.

TERRAIN PATTERN No.14

PROVINCE No. 33.001
Silurian-Devonian

LITHOLOGY - Siltstone, claystone, sandstone, minor conglomerate

OCCURRENCE - Widespread in areas underlain by Silurian-Devonian rocks; areas of lower relief

TOPOGRAPHY - Undulating terrain containing smooth sloped isolated hills

INCLUSIONS - Terrain pattern 36, province 33.001, terrain pattern 06, province 51.009, terrain pattern 03, province 52.010

CHARACTERISTIC CROSS-SECTION SHOWING TYPICAL LOCATION OF TERRAIN UNITS

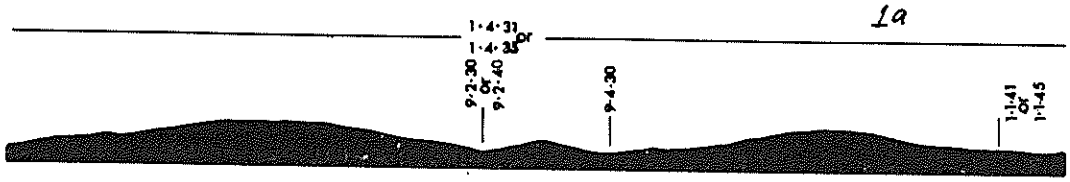

Vert. scale = twice horiz. scale

0 0.25 0.50
Miles

TERRAIN UNITS

Number	Terrain Pattern Area (%)	Occurrence	Description of Dominant		
			Topography	Soil	Land use
1.1.41	5	Discontinuous; floodplains adjacent to drainage	Flat surface	Uniform light grey or grey-brown deep clayey silt (ML;Uf)	Melbourne area, parkland; other areas pasture, some agriculture
1.4.31 or 1.4.35	80	Continuous; extensive	Undulating surface crests: rounded, linear to 5° slopes: convex to 10°	Duplex light grey clayey silt to 10 in. over yellow mottled heavy-textured clay (ML/CH;Dy) over decomposed rock at variable depth	Melbourne area, urban development; other areas pasture, some agriculture
3.5.31 or 3.5.35	5	Sometimes leading to drainage	Dissected slope slopes: convex to 10°	Duplex light grey clayey silt to 10 in. over yellow mottled heavy-textured clay (ML/CH;Dy) over decomposed rock at variable depth	Melbourne area, urban development; other areas pasture, some agriculture
4.3.31 or 4.3.35	10	Inclusive in undulating surface	Complex hill crests: rounded, convex to 10° slopes: convex to 10°	Shallow duplex light grey or grey-brown clayey silt to 4 in. over yellow mottled heavy-textured clay to 3 ft (ML/CH;Dy) or crests and upper slopes: light grey or grey-brown clayey silt to 4 in. over decomposed rock with some rock outcrop lower slopes: duplex light grey clayey silt to 10 in. over yellow mottled heavy-textured clay to 3 ft (ML/CH;Dy) over decomposed rock	Melbourne area, urban development; other areas pasture
4.8.31 or 4.8.35	5	Inclusive in undulating surface	Elongated rounded hill crests: rounded, convex to 5° slopes: convex to 10°	Shallow duplex light grey or grey-brown clayey silt to 4 in. over yellow mottled heavy-textured clay to 3 ft (ML/CH;Dy) or crests and upper slopes: light grey or grey-brown clayey silt to 4 in. over decomposed rock with some rock outcrop lower slopes: duplex light grey clayey silt to 10 in. over yellow mottled heavy-textured clay to 3 ft (ML/CH;Dy) over decomposed rock	Melbourne area, urban development; other areas pasture
9.2.41	<1	Drainage often artificially covered and controlled in the Melbourne area	Minor stream channel, often depressional slopes: concave to 10°	Uniform or stratified dark brown, grey-brown or occasionally yellow mottled silty or clayey fine sand or silty clay, some angular gravel towards stream heads (SM-ML-SC-CL) some GM-CC;Um	Unused

Fig. 1.- Typical description of a terrain pattern in terms of terrain units

TYPICAL DRAINAGE NET OF TERRAIN PATTERN

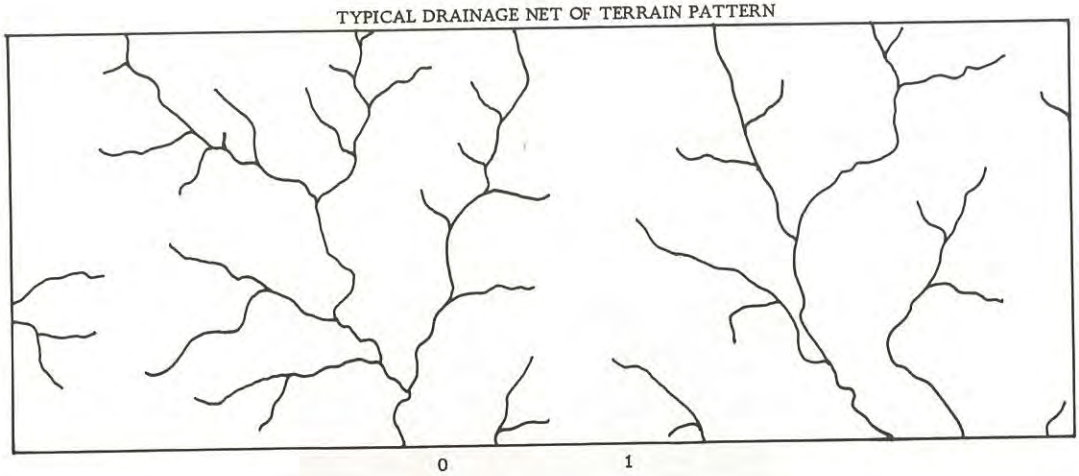

Stream Frequency per Mile						Drainage Type
Order	1st	2nd	3rd	>3rd	Total	
N-S	1.0	0.5	<0.5	<0.5	1.5	Coarse dendritic
E-W	1.0	0.5	<0.5	<0.5	1.5	

Vegetation	Inclusions	Terrain Parameters			
		Terrain Unit No.	Max. Local Relief Amplitude (ft)	Length of Terrain Unit	Width of Terrain Unit
Mostly cleared, grassland, short grass, scattered trees, messmate, manna gum or cultivated	Terrain pattern 03, province 52.010	1.1.41 or 1.1.45	3	2 miles	500 yards
Built up or mostly cleared, grassland, short grass, scattered trees; some areas woodland, south of the ranges: messmate, long leafed box, peppermint, occasional manna gum, north of the ranges: grey box, yellow box, some areas cultivated	Terrain pattern 36, province 33.001, terrain pattern 06, province 51.009	1.4.31 or 1.4.35	200	Extensive	Extensive
Built up or mostly cleared, grassland, short grass, scattered trees; some areas woodland, south of the ranges: messmate, long leafed box, peppermint, occasional manna gum, north of the ranges: grey box, yellow box, some areas cultivated	-	3.5.31 or 3.5.35	100	5 miles	1000 yards
Built up or mostly cleared, grassland, short grass, scattered trees; some areas woodland, south of the ranges: messmate north of the ranges: grey box, yellow box	-	4.3.31 or 4.3.35	200	1000 yards	1000 yards
Built up or mostly cleared, grassland, short grass, scattered trees; some areas woodland, south of the ranges: messmate, north of the ranges: grey box, yellow box	-	4.8.31 or 4.8.35	200	1 mile	500 yards
Grassland, short grass, manna gum, peppermint, long leafed box, sometimes fringing	-	9.2.41	10	Extensive	50 yards

DIAGRAMMATIC REPRESENTATION OF TOPOGRAPHY AND ARRANGEMENT OF TERRAIN UNITS WITHIN TERRAIN PATTERN

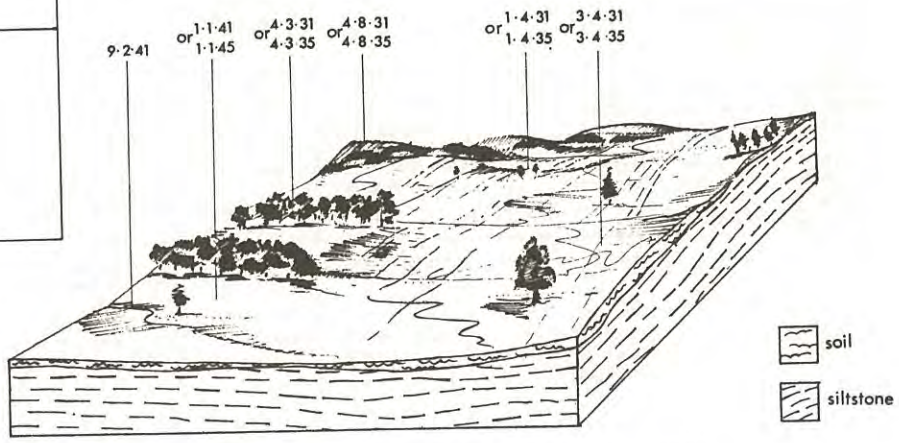

Fig. 1 (cont.).- Typical description of a terrain pattern in terms of terrain units

TERRAIN UNIT No. 1.4.31

PROVINCE No. 33.001
TERRAIN PATTERN No.14

LITHOLOGY - Siltstone, claystone, sandstone, minor conglomerate

OCCURRENCE - Continuous, extensive

TOPOGRAPHY - Undulating surface

INCLUSIONS - Terrain pattern 36, province 33.001, terrain pattern 06, province 51.009

TERRAIN COMPONENTS

Terrain Component No.	Dominance	Occurrence	Slope		Soil Description
			Parallel to Major Axis	Transverse to Major Axis	
120 022 01	Low	Lower slopes to drainage	Planar to 2°	Flat	Dark brown clayey silt to 6 in. over light yellow-grey clayey silt to 2 ft over yellow mottled medium to heavy-textured clay to > 3 ft
131 022 02 or 421 022 02 or 431 022 02	Dominant Low Low	Slopes of interfluves between crests and drainage	Planar to 5° or Concave to 2° or to 5°	Planar to 1°	Dark brown clayey silt to 6 in. over light yellow-grey clayey silt to 2 ft over yellow mottled medium to heavy-textured clay to > 3 ft
141 052 02 or 441 052 02	Very low Very low	Steep slopes of interfluves between crests and drainage	Planar to 10° or Concave to 10°	Planar to 1°	Dark grey-brown to pale grey gravelly fine sandy clayey silt to 1 ft over yellow mottled medium-textured gravelly clay to 3 ft over rock
233 042 01 or 234 042 01	Very low Very low	Minor drainage floors	Planar to 5°	Concave to 5° or to 10°	Grey-brown to yellow-grey clayey silt or silty clay to 8 in. over stratified yellow mottled gravelly clay to > 6 ft over rock
243 022 01	Very low	Steeper minor drainage floors	Planar to 10°	Concave to 5°	Dark brown clayey silt to 6 in. over light yellow-grey clayey silt to 2 ft over yellow mottled medium to heavy-textured clay to > 3 ft
313 002 02	Low	Sub-linear crests of ridges	Planar to 1°	Convex to 5°	Decomposed rock with areas of rock outcrop, pockets of duplex dark brown to light grey clayey silt to 4 in. over yellow mottled gravelly clay to 18 in. over rock
322 012 01	Very low (local)	Broad gently sloping crests of interfluves	Planar to 2°	Convex to 2°	Grey-brown to yellow-grey clayey silt or silty clay to 1 ft over yellow mottled heavy-textured clay to 4 ft over gravelly clay (decomposed rock) to 5 ft over rock
323 032 02 or 332 032 02 or 333 032 02 or 334 032 02	Sub-dominant (locally) Low Sub-dominant Low	Broad sloping interfluves	Planar to 2° or to 5°	Convex to 5° or to 2° or to 5°	Grey-brown clayey silt to 8 in. over yellow mottled medium to heavy-textured clay to 3 ft over rock
343 002 02 or 344 002 02 or 943 002 02	Very low Very low Very low	Steeper sloping interfluves	Planar to 10° or Convex to 10°	Convex to 5° or to 10° or to 5°	Decomposed rock with areas of rock outcrop, pockets of duplex dark brown to light grey clayey silt to 4 in. over yellow mottled gravelly clay to 18 in. over rock
522 012 01 or 532 012 01 or 533 012 01 or 543 012 01	Very low Very low Low Very low	Depressions between interfluves	Concave to 2° or to 5° or to 10°	Concave to 2° or to 5°	Grey-brown to yellow-grey clayey silt or silty clay to 12 in. over yellow mottled heavy-textured clay to 48 in. over gravelly clay (decomposed rock) to 5 ft over rock
623 002 02 or 633 002 02	Low	Saddles	Concave to 2° or to 5°	Convex to 5°	Decomposed rock with areas of rock outcrop, pockets of duplex dark brown to light grey clayey silt to 4 in. over yellow mottled gravelly clay to 1 ft over rock
751 052 02 or 761 052 02	Very low (local)	Steep slopes of gently sloping interfluves	Convex to 20° or to 40°	Planar to 1°	Dark grey-brown to pale grey gravelly fine sandy clayey silt to 1 ft over yellow mottled medium-textured gravelly clay to 3 ft over rock

Fig. 2.- Typical description of a terrain unit in terms of terrain components

DIAGRAMMATIC REPRESENTATION OF TOPOGRAPHY AND ARRANGEMENT OF TERRAIN COMPONENTS WITHIN TERRAIN UNIT

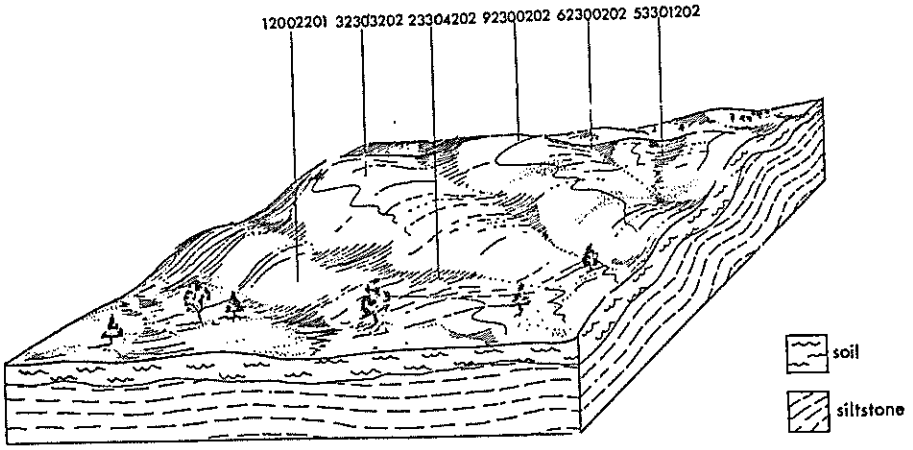

Parameters of Terrain Unit

Local Relief Amplitude to (ft)	Length to	Width to
200	Extensive	Extensive

USC	PPF	Land Use	Vegetation				Terrain Parameters		
			Description	Spacing to (ft)	Tree Height to (ft)	Girth Diam. to (in.)	Local Relief Amplitude to (ft)	Length to	Width to
ML	Dy	Pasture (mostly unimproved)	Grassland, tussock grass, bracken fern	-	-	-	50	500 yards	1000 yards
ML CH	Dy	Pasture (mostly unimproved)	Grassland, short grass, occasional trees, peppermint, yellow box, grey box, messmate, occasional black wattle	Scattered	40	18	100	1000 yards	500 yards
ML-GM GC	Dy	Pasture (mostly unimproved)	Grassland, short grass, occasional trees, peppermint, yellow box, grey box, messmate, occasional black wattle	Scattered	40	18	100	500 yards	100 yards
ML-CL GC	-	Pasture (mostly unimproved)	Grassland, tussock grass, bracken fern	-	-	-	100	1000 yards	50 yards
ML CH	Dy	Pasture (mostly unimproved)	Grassland, tussock grass, occasional trees, peppermint, yellow box, grey box, messmate, occasional black wattle	Scattered	40	18	100	1000 yards	50 yards
ML GC	Dy	Pasture (mostly unimproved)	Grassland, short grass, occasional trees, peppermint, yellow box, grey box, messmate, occasional black wattle	Scattered	40	18	20	500 yards	100 yards
ML-CL CH / GC	Dy	Pasture (mostly unimproved)	Grassland, tussock grass	-	-	-	20	1000 yards	500 yards
ML CL-CH	Dy	Pasture (mostly unimproved)	Grassland, short grass, occasional trees, pappermint, yellow box, grey box, messmate, occasional black wattle	Scattered	40	18	100	1000 yards	100 yards
ML GC	Dy	Pasture (mostly unimproved)	Grassland, short grass, occasional trees, peppermint, yellow box, grey box, messmate, occasional black wattle	Scattered	40	18	100	500 yards	100 yards
ML-CL CH / GC	Dy	Pasture (mostly unimproved)	Grassland, tussock grass, bracken fern	-	-	-	100	500 yards	100 yards
ML GL	Dy	Pasture (mostly unimproved)	Grassland, short grass, occasional trees, peppermint, yellow box, grey box, messmate, occasional black wattle	Scattered	40	18	20	500 yards	100 yards
ML GC	Dy	Pasture (mostly unimproved)	Grassland, short grass, occasional trees, peppermint, yellow box, grey box, messmate, occasional black wattle	Scattered	40	18	50	1000 yards	20 yards

Fig. 2 (cont.) - Typical description of a terrain unit in terms of terrain components.

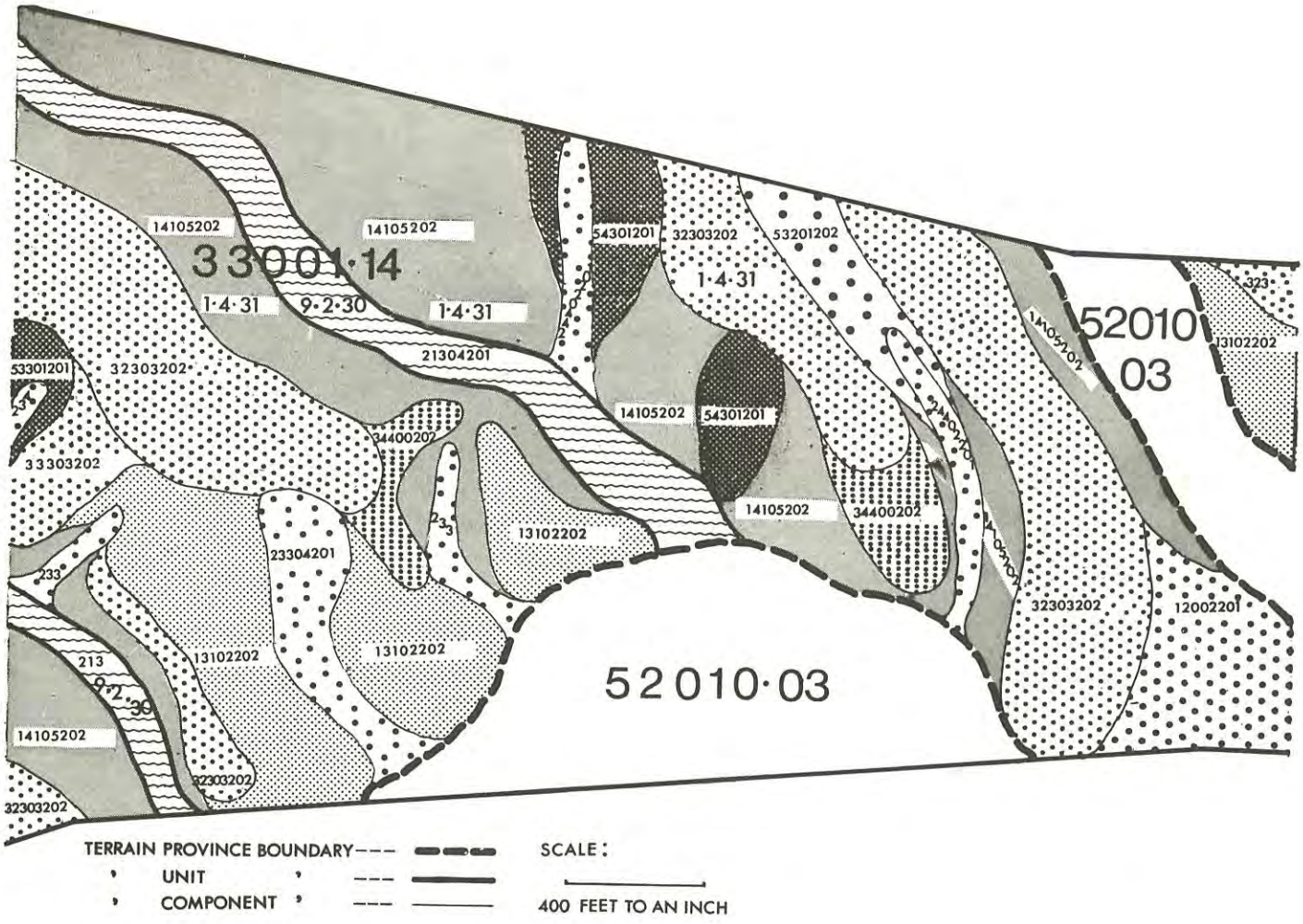

Fig. 3.- A portion of a typical terrain component map drawn along the projected centreline of a highway.

2. AITCHISON, G.D. and GRANT, K. - The P.U.C.E. programme of terrain evaluation. Proc. Fourth Reg. Conf. for Africa on Soil Mech. and Found. Engg., Cape Town, 1, 1967, pp. 1-8.

3. NORTHCOTE, K.H. - A factual key for the recognition of Australian soils, 2nd Ed. CSIRO, Aust. Div. Soils, Divl. Rep. No. 2/65, 1965.

4. GRANT, K. - A terrain evaluation system for engineering. Tech. Pap. No. 2, Division of Soil Mechanics, CSIRO, Aust. 1968.

5. GRANT, K. - Terrain evaluation for engineering purposes. Symposium on Terrain evaluation for Highway Engineering, Townsville. Special Rept. No. 6, A.R.R.B., Melbourne, 1971.

6. GRANT, K. and LODWICK, G.D. - Storage and retrieval of information in a terrain classification system. Proc. Fourth Conf. A.R.R.B., 1968, Melbourne 4(2), 1969, pp. 1667-1676.

7. Royal Australian Survey Corps Australia - 1:250,000 Melbourne, SJ55-5, Edition 1, Series R502, 1960.

8. GRANT, K. - Terrain evaluation for engineering. In Engineering Geology. I.E. Aust., 2 - 1-40, Melbourne, 1969.

? RQD

Underground Investigation for Large Excavation at Victorian Arts Centre

By

R. M. Johnson, B.C.E., S.M. (Harvard), F.I.E.Aust.

(Senior Partner, Milton Johnson and Partners, Melbourne)

I INTRODUCTION

The North End of the Victorian Arts Centre in St. Kilda Road Melbourne has been planned as one large building housing a complex of auditoria and related facilities. The Architect has placed the building underground, utilising the whole $1\frac{3}{4}$ acres available down to an average depth of 90 feet. An initial general site investigation had revealed the following underground strata in order of depth:-

Filling - of clay, rubble and gravel to an average depth of 25 feet.

Soft Organic Silty Clay - ranging from 40 - 48 ft. in thickness at depths of 40 - 100 ft. below ground.

Sand, Gravel and Cobble Aquifer - present only at the southern half of the site, thickness ranging from 0 - 25 feet.

Silurian Mudstone Bedrock - ranging in depth below ground from 75 ft. at the northern end to 100 ft. at the southern end. Some Basalt rock and some stiff clayey silt are also present overlying this bedrock at the northern end (See Fig. 4).

The nature of these materials, together with an arrangement of the auditoria that prohibits retaining wall supports at intermediate heights, has meant that the building must be housed within a massive perimeter retaining wall spanning between a strutting frame at the surface and the bedrock at the bottom.

Several types of wall and construction methods have been assessed. The detailed solution for each system requires a knowledge of specific water, soil and rock parameters, and this investigation has been planned and implemented to provide this data.

This paper will describe the various wall systems studied, details of the site investigation and its application to the analysis of forces acting on the structure.

II INITIAL INVESTIGATION

The general investigation for this portion of the Victorian Arts Centre site - the North End, was carried out in 1966 with the objective of determining general soil stratum profiles and properties for use in assessment of various foundation and excavation alternatives.

The investigation consisted of 11 boreholes of $3\frac{1}{2}$" diameter averaging 105 ft. depth including "N" size coring of Silurian rock for a minimum of 10 ft., and associated soil testing. The qualitative results of the investigation are summarised above.

III WALL SYSTEMS

Figs. 1 and 2 show just two of the various retaining wall/excavation systems devised to produce the large excavation space.

The following possible wall construction methods were then considered:-

For interlocking caissons, wall excavation would be by caisson sinking assisted by ground freezing and/or pressure grouting.

For a Solid or Cellular Insitu Wall, the construction method could include -

a) Soil excavation within sheeting formed by frozen ground or temporary concrete walls placed by bentonite displacement.

b) Soil excavation by mining techniques within sheet piling, assisted by ground freezing and/or pressure grouting.

Tenders were called for construction of the large excavation in August, 1970 allowing each Contractor to select one or other of the above methods, or any variations of his own initiative. At the time of preparation of this paper, the method had not been finally determined.

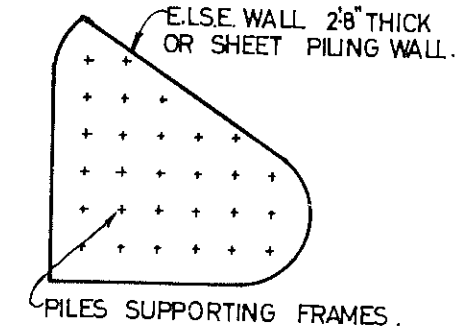

Result:- Walls would break & bottom heave up when excvn. to 50 ft.depth.
Hence: Reject system.
FIG.1. THIN WALL, THREE FRAMES

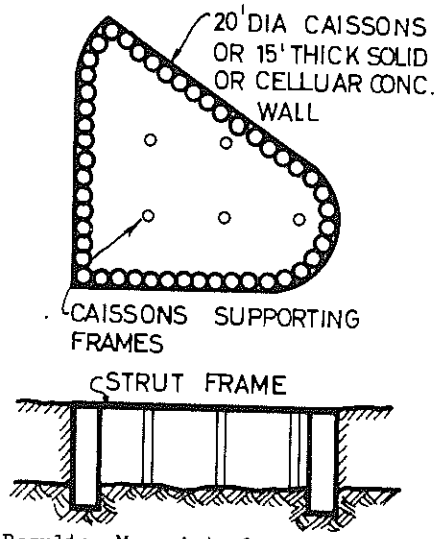

Result:- Max. int. free space for theatres.Ret.walls built first so no int. heave.
Hence: Method adopted.
FIG.2. THICK WALL,SINGLE STRUT FRAME

IV SPECIFIC UNDERGROUND INVESTIGATION

OBJECTIVES

The objectives of this investigation were to determine:-

1. The rock surface beneath the site, particularly on the perimeter.
2. The properties of the rock, i.e. dip and strike of bedding planes, jointing orientation, frequency and extent of clay filling, strength, density and permeability.
3. The properties of the insitu soil, e.g. strength, permeability and earth pressures.
4. Some properties of the frozen soil, e.g. strength compressive and tensile creep.

Total value $20M

SCOPE

In order to obtain maximum value for the investigation expenditure of $150,000, the work was divided into four separate contracts as described below, each being suited to one special function. The whole was co-ordinated and supervised by M.J & A. and took place between June 1969 & July, 1970.

Perimeter Drilling by Soil Mechanics Ltd.

Thirteen boreholes spaced at approx. 100 ft. centres were drilled around the perimeter of the site, as shown in Fig. 3 and penetrated 40 ft. into the Silurian bedrock. 4½" diameter undisturbed samples were taken of the organic clay stratum for laboratory testing and 5½" diameter rock cores were taken for detailed description and permanent record purposes.

Caisson Sinking by McDougall-Ireland Pty.Ltd.

Two 5'-9" dia. steel-lined shafts approx.100 ft. deep were sunk. One of these shafts, the North Caisson, penetrated the rock a distance of 0 - 2 ft. A chamber 11 ft. diameter was excavated below this level for conducting insitu rock strength tests and to permit wall tenderers to evaluate the rock en masse. The South Caisson was sunk to the surface of the rock to determine water flows in the sand stratum at that level. It also enabled the placement of pressure cells and piezometers.

Observation Wells by W.L. Sides & Son Pty.Ltd.

Four eight inch diameter boreholes with filter screens were drilled around the South Caisson to observe water levels.

Testing by Soilmech Pty.Ltd. in conjunction with Dr. J. Morgan, Reader, Department of Civil Engineering, University of Melbourne. Some specialised tests were also carried out by Professor Davis and Dr. Lee of the Department of Civil Engineering, University of Sydney.

A comprehensive programme of ambient and frozen temperature soil laboratory tests was conducted on undisturbed samples. Insitu horizontal shear strength tests on rock were performed in the North Caisson. Pressure cell installation and pump tests were made in the South Caisson.

FIELD WORK - DRILLING, SAMPLING, CORING AND TELEVISION INSPECTION

The 13 boreholes were sunk by the cable drop tool method inside 10" and 8" diameter casing. The sequence of strata revealed is summarised in Fig. 4. The 7 ft. above the location of any undisturbed sample was excavated by hand augering.

38 No. undisturbed samples were recovered in 4½" O.D. x 10g. x 3'-6" long sample tubes.

Diamond drilling was carried out with 2 - 7½" O.D 5½" I.D., 5 ft. long triple tube core barrels.

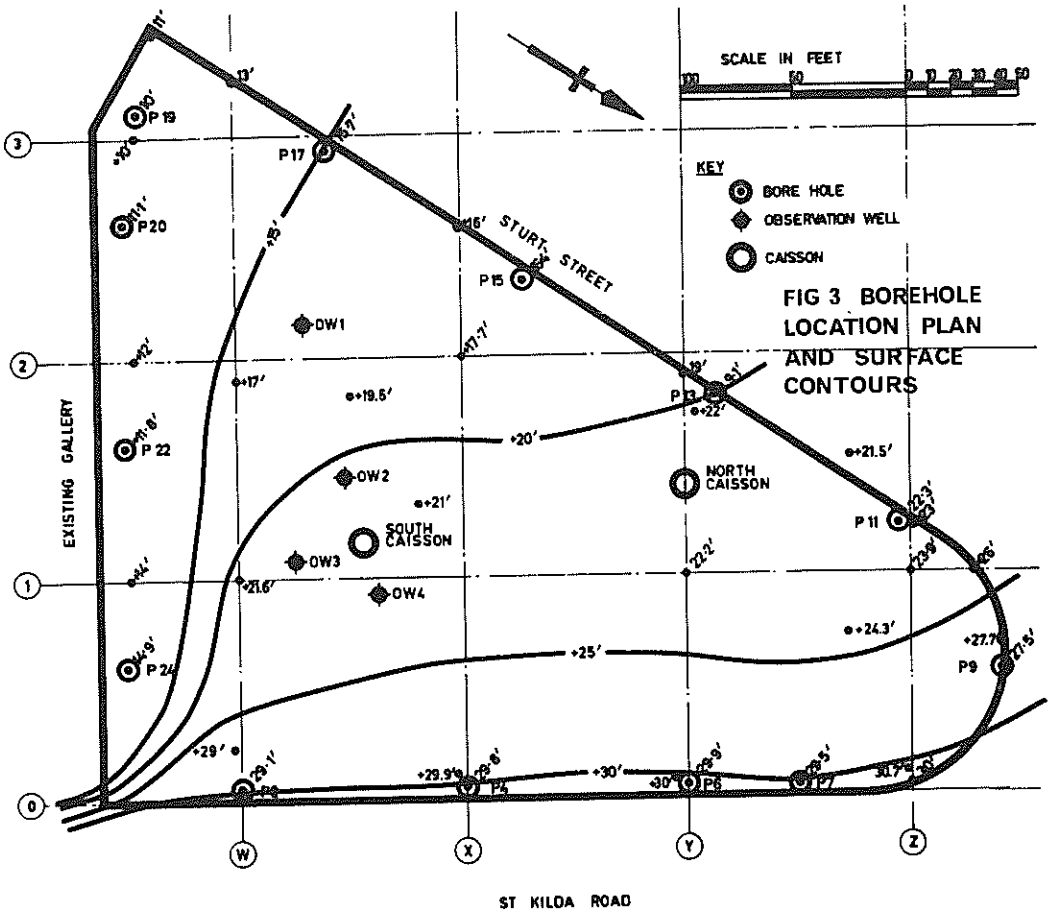

FIG 3 BOREHOLE LOCATION PLAN AND SURFACE CONTOURS

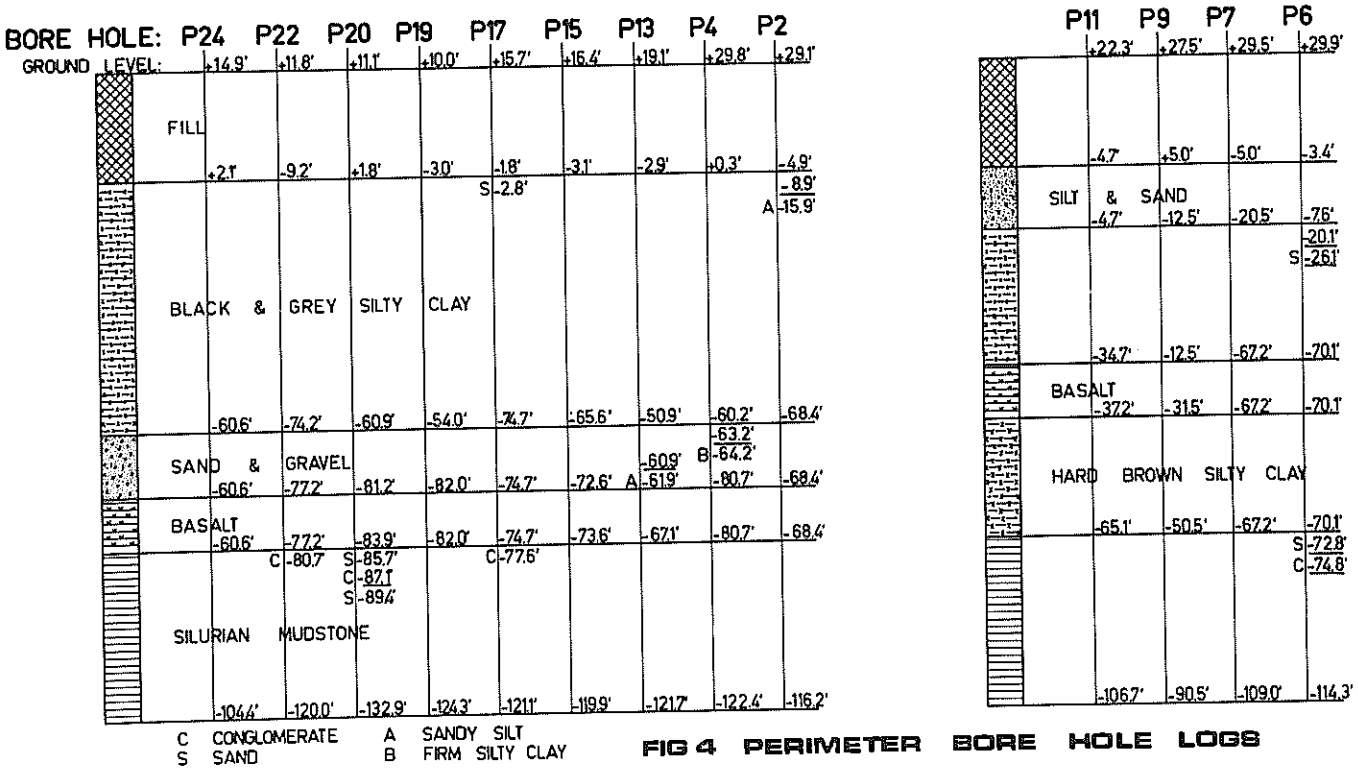

FIG 4 PERIMETER BORE HOLE LOGS

In order to determine the direction of dip of the Silurian rock bedding planes, an underwater television camera installation was developed specifically for this project and used in 8 representative boreholes.

The camera, which was 5¾" dia. and 2'-8" long was designed to operate underwater at depths up to 160 ft. Lighting was built into the camera. The camera lens was fixed, but side viewing in all directions was obtained hy means of a metallic mirror which could be rotated about the longitudinal axis of the camera by remote control from the surface.

Directional orientation was obtained by a magnetic compass built into the camera. 6½" and 23" television screens were provided in the control caravan for picture monitoring and for photographing results.

LABORATORY TESTING AND STRATUM PROPERTIES

These tests were performed to provide information to design and evaluate any construction method.

Black/Grey Silty Clay

The samples were predominantly stiff grey and black silty clays, but did include clayey sands, sandy silty clays and these materials with lenses of fine sand. The group symbols were predominantly CH, Cl and OH with some CL and SC.

The programme of laboratory testing included the following tests. Typical results only are quoted, the detailed results appearing in Reference No. 1.

Tests on insitu samples:-

Water content 48% Bulk density 113 lb.per cu.ft.
Liquid Limit 81% Plasticity Index 55%.
Undrained Triaxial C_u 8 p.s.i., ϕ_u 4 deg.
Constant Axial Stress Triaxial Type P, Initial K'0.56
E_{min} 900 p.s.i., E_{max} 6700 p.s.i.
Consolidated Undrained Triaxial C' 2.5 p.s.i., ϕ 32 deg
A(1) 0.31 A(3) 0.08
K'_o 0.45
Consolidation M_v 0.016 ft^2/T at ½ - 1 T/ft^2.

Tests on Frozen Samples:
Creep tests - tensile strength ranges from 10 k.s.ft. to 25 k.s.ft. for temperatures of 14 deg.F and -4 deg.F at rates of strain between 0 and 1.5 x 10^{-4} in/min.

Creep tests - compressive ranges from 10 k.s.ft to 33 k.s.ft. at 14 deg.F for 0 to 1.5 x 10^{-4} in/min rate of strain and 47 k.s.ft. to 77 k.s.ft. at -4 deg. F for 0 to 0.5 x 15^4 in/min rate of strain.
E_u 65,000 p.s.i.

Heave test 2% weight and height increase with vertical stress applied - Test of short term duration.

Silurian Rock.

The salient features revealed by the cores are as follows:-

a) General Description of Rock Cores.

This general description was prepared by Mr. J. L. Neilson, Senior Geologist, Victorian Mines Department.

"Recent drilling at the site to test for the proposed peripheral retaining wall has found unusually fresh and hard Silurian mudstone (with lesser fine sandstone) extending down at least 40 ft. from the topographic upper limit of the Silurian bedrock. The rock is hard and mostly sound; very few unstable shear zones were discovered, and clay bands are rare.

Dip and strike of the beds are fairly constant over the site, and bedding planes contain small-scale irregularities which would make slip on them difficult. The beds intersect the line of the wall at large angles, which also inhibits slip. Only at the south-west corner of the site will beds dip into the excavation and strike along the wall alignment; there, care will be necessary, particularly if any clay seams should be present.

Jointing is not intensive and is confined to high-angle joints. It is low-angle joints (from horizontal to 30°) which would be of most significance in foundation failure of the wall by horizontal stresses, and such joints are tight and always irregular, never completely planar, which in addition would make failure along them more difficult. Some joints were limonite (iron oxide) cemented, and none was clay filled.

Several shear zones of unknown orientation do not appear to be serious weaknesses but should be carefully considered."

b) Core Recovery.

100% recovery was obtained in all boreholes.

c) Dip of Bedding Planes.

Apart from a few isolated occurrences the dip ranged from 15° to 40°. The dip at the north-west end of the site was $35^{\circ}\ ^{+5^{\circ}}_{-10^{\circ}}$ (i.e. in boreholes P11,P13 & P15).

The dip for the remainder of the site perimeter was $25^{\circ} \pm 10^{\circ}$. The direction of dip was $355^{\circ} \pm 20^{\circ}$ rel. to mag. north.

d) Rock Quality Designation.

R.Q.D. is defined as:-

$$\frac{\text{The Aggregate Length of Core Pieces} \quad 4\text{" long}}{\text{Total Length Drilled}} \times 100$$

This varied considerably within any one borehole in quite a random manner (e.g. 15% to 70% typical). The total range for this site was 0% to 100% with approximately 30% of the 0-33% R.Q.D. present, and approximately 30% of the 33-67% R.Q.D. present.

e) Rock Strengths.

13 unconfined compression strength tests ranged from 420 to 10,300 lb/in^2 with an average of 3,600 lb/in^2. The planes of weakness were flatter than 34° and failure generally was by vertical splitting.

Two undrained triaxial compression tests were done. These were stage tests on single samples and produced the following results:-

C = 34 lb/in^2 ϕ = 30^o(clay on failure plane at angle of 48^o).

C = 0 lb/in^2 ϕ = 30^o(clay on failure plane at angle of 47^o).

f) Density of Rock.

The average bulk density of the rock core samples tested in the laboratory produced the following results:-

= 160 lb/ft^3 with a range of 151-171 lb/ft^3.

Insitu Stresses.

In order to obtain some indication of the insitu stress conditions of the rock, it was decided to adopt a programme of direct measurement of forces in rock excavation struts at the time of excavation for the wall. This was influenced by the knowledge that the Railway Construction Board had used flat jacks in slots in the rock to measure these stresses in test shafts for the City of Melbourne Underground Railway, but in spite of reasonable techniques, did not arrive at any conclusive results.

Aquifer.

Tests conducted on disturbed samples taken during caisson sinking revealed material including silty, clayey fine sand, silty fine to medium sand, gravelly coarse sand, cobbles (3" to 8" size) with fine to coarse sand.

Analysis of ground water samples taken from the North and South Caisson included the following results. Sulphate (SO_4) -1,400 parts/million, Chloride(Cl) -12,400 parts/million which were acceptable for normal dense concretes. During the sinking of the South Caisson, gases, principally H_2S, SO_3 and CO_2 were released from the ground water.

INSITU ROCK SHEAR TESTS.

The purpose of these tests was to carry out insitu large-scale horizontal loading shear tests of clay seams between bedding planes in blocks of Silurian rock, to give design data for specifying the depth of penetration of the base of the North End Wall.

The North Caisson rock chamber shown in Fig. 3 was excavated and a 3' x 3' x 3' (nominal) block was left intact on each of two floor levels for load testing. The test arrangement also included a steel framework for supporting the dial gauges used in monitoring vertical, horizontal and rotational movements. A "skate" was located below the vertical jack to ensure uninterrupted vertical loading as the movement of the upper block occurred.

Both tests were conducted in three stages as represented in Fig. 4; each stage involving an increase in horizontal load in 2T increments with a simultaneous reduction in the vertical load. The horizontal load being maintained constant until the movement ceased. The stage was terminated when the horizontal movement reached 0.1 in. or when the vertical load became zero.

The failure pattern and shear strength relation for the second block test is shown in Figs. 5 & 6.

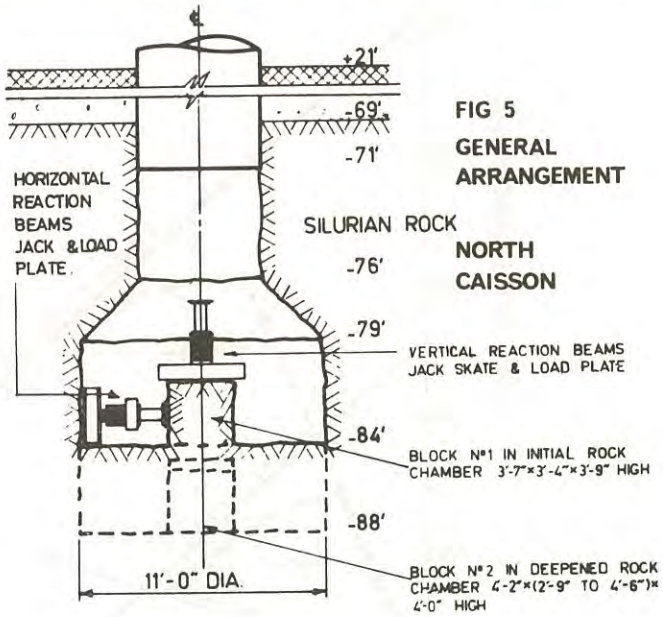

FIG 5
GENERAL ARRANGEMENT
NORTH CAISSON

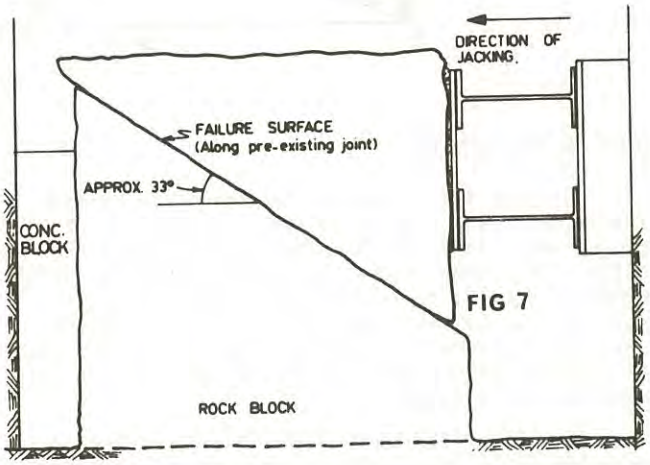

FIG 7

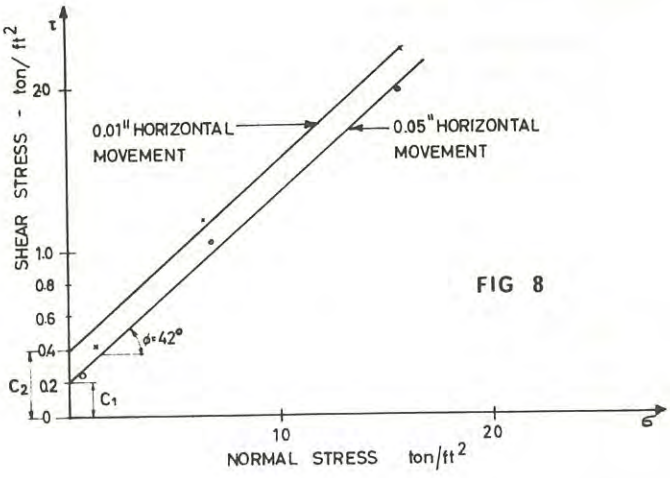

FIG 8

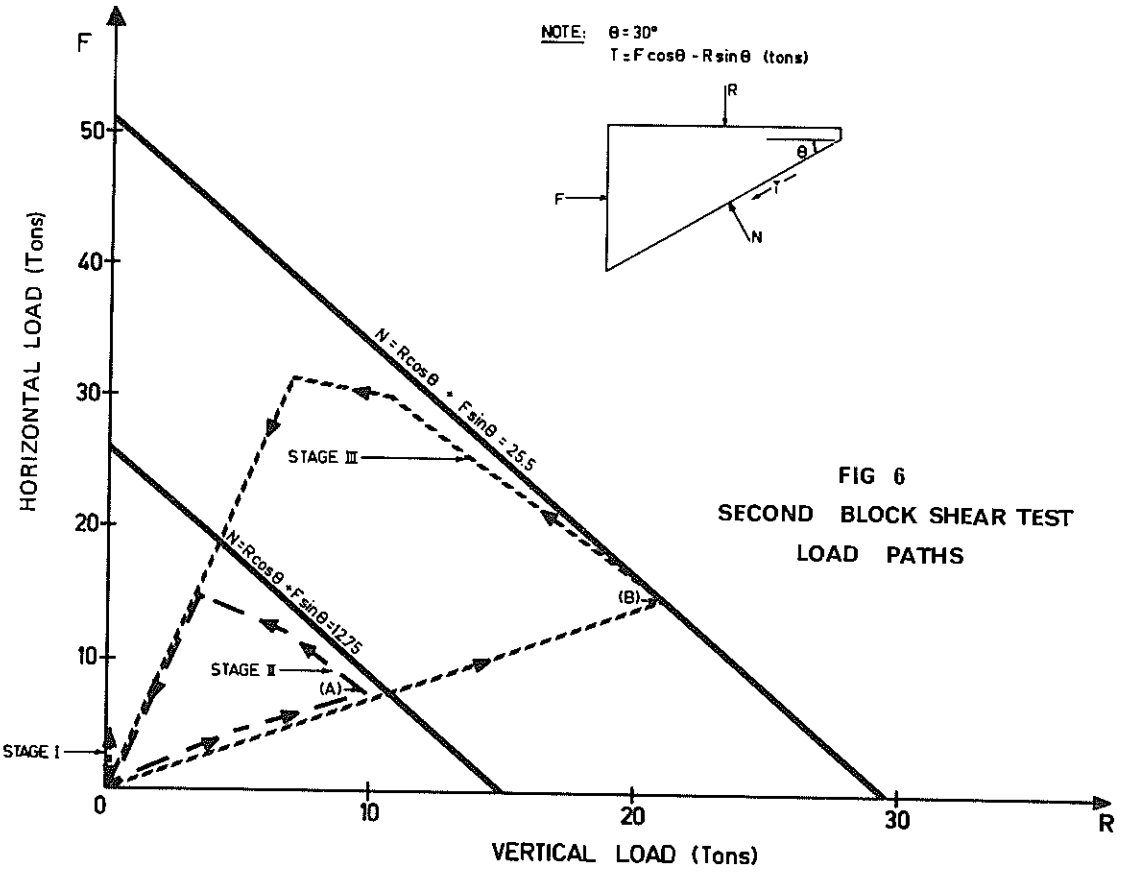

FIG 6
SECOND BLOCK SHEAR TEST
LOAD PATHS

FLOW IN THE AQUIFER

The pump test conducted in the South Caisson involved the observation of rate of drawdown of ground water level in the four surrounding observation wells. This enabled the average permeability of the confined aquifer to be computed. Observation of water levels without pumping enabled the maximum velocity of water to be computed. This information is required before the feasibility of freezing this stratum can be assessed.

The test arrangement included the pumping well, i.e. the 5'-9" dia. steel-lined South Caisson with its open base with a graded filter penetrating the aquifer to RL-70 ft., and four observation wells located as shown in Fig.1.

The graded filter to the South Caisson consisted of, from bottom to top -

3 ft. of $\frac{1}{4}$" screenings.
3 ft. of 2" - 3" screenings.
2 layers of A.S. No. 300 fabric.
Steel joists at 8" c/s welded to sides of caisson.

The four observation wells were $8^{9}/_{32}$" I.D. steel cased. The screens were of phosphor bronze material $5\frac{5}{8}$" I.D., 7" O.D. with holes ranging from 0.123" to 0.036" diameter.

A submersible pump was located at RL 62' and connected by a 6 inch P.V.C. delivery pipe to a section of steel pipe at the top of the caisson. This section contained a control valve, pressure gauge and $1\frac{1}{2}$" orifice plate and manometer. The discharge pipe was approximately 500 feet long and drained into a stormwater manhole in Sturt Street.

On the basis of previous trials, the discharge control valve was set at 55 gallons per minute and maintained constant for the duration of the test.

The permeability k of the aquifer was found to be:-

6.1×10^{-3} cm/sec. +30% - 20%.

The maximum velocity of water was found to be 0.7 ft/day which will not affect freezing in the aquifer.

V ANALYSIS OF ROCK STABILITY

Fig. No. 9 shows typical pressures acting on the external face of the perimeter wall together with the horizontal reactions provided by the top strut and the rock at the base of the wall.

For unit length of any wall e.g. Sturt Street, St. Kilda Road, etc. the horizontal resistance provided by the rock has been considered as being supplied by a reaction wedge bounded on its underside by joint planes parallel and perpendicular to the bedding and oriented in the most adverse manner possible (i.e. to give minimum capacity). Fig. 10 shows the forces acting on this wedge which are consistent with the following assumptions:-

1. Failure will not occur across intact rock since joints will be assumed to exist in the most adverse configuration.
2. The rock mass is assumed to be cut by three sets of orthogonal joint planes at any spacing.
3. One set of joint planes is assumed parallel to the bedding plane.

4. The other two sets of joint planes are defined by their intersection with the bedding planes being parallel and normal to the wall under consideration.
5. The shear force transmitted from the wall to the rock is limited to the buoyant weight at the wall; this force always being less than the shear strength of the joint, i.e. $V = P - U$.
6. Seepage forces on the underside of the failure wedge have been ignored.
7. The most adverse measured values of Dip and Strike for any particular wall have been adopted for the determination of the depth of penetration.
8. Hydrostatic uplift U under the wall is based on a flow net assuming homogenous rock.
9. Shear strength law on a typical joint plane is of the form –
$$\tau = K + \sigma_n \tan \phi$$
where K = constant
σ_n = normal stress
ϕ = angle of internal friction.
10. All soil and rock properties, dip, strike, etc. are based on the test results of the Underground Investigation, dated July, 1970.
viz: $K = 0.45$ K/Ft^2.
$\phi = 38$ degrees $\gamma_b = 85$ lb/ft^3.

Critical Dip and direction of Dip of joint planes

Name of Wall	Dip Deg.	Angle between Dip & Wall
St. Kilda Road	20	55
Gallery	44	75

The capacity of the wedge to resist horizontal forces imposed by a wall was computed upon our G.E. 265 Computer E.D.P. for varying values of depth of penetration. This enabled the appropriate depth to be selected to satisfy the following criteria:-

i) Wedge capacity to equal 1.5 (F of S) times the working reaction of the wall, as supplied by the wall designer.
ii) A maximum of 25 ft., but if the factor of safety associated with this depth is less than 1.5 then the additional horizontal capacity is supplied by rock anchoring the wedge to the underlying rock.
iii) A minimum of 15 ft., to provide sufficient water cut off and to limit horizontal deflections.

The results of these analyses led to the adoption of penetration of 15 ft. for the Gallery wall and 25 ft. for Sturt Street and St.Kilda Road, with 20% of the horizontal load capacity at St.Kilda Road being provided by rock anchoring through the reaction wedge.

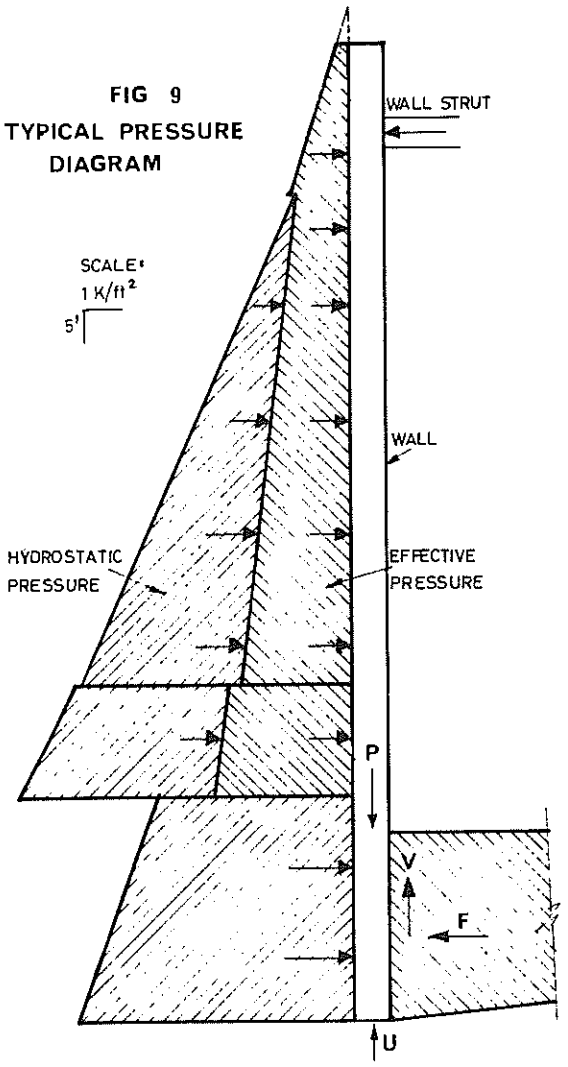

FIG 9
TYPICAL PRESSURE DIAGRAM

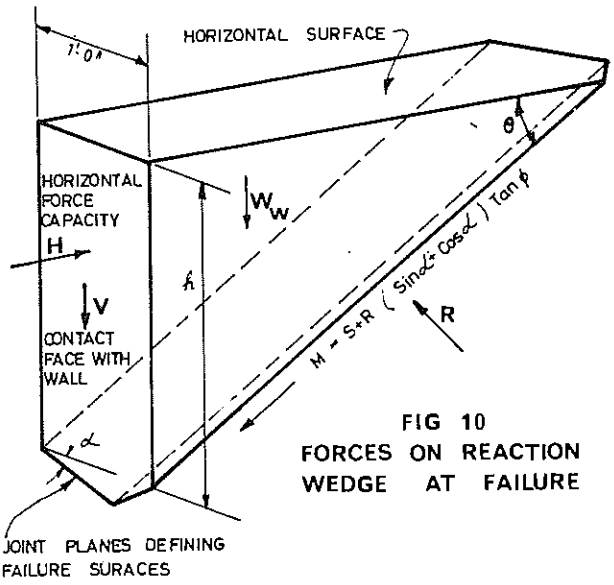

FIG 10
FORCES ON REACTION WEDGE AT FAILURE

VI ACKNOWLEDGEMENTS:

The Author records his thanks to Sir Roy Grounds and Mr.John Connell for granting permission to publish this paper, and to Mr.T. Langley for assistance in its preparation.

VII REFERENCE:

MILTON JOHNSON & ASSOCIATES
Victorian Arts Centre - North End,Underground Investigation Report, July, 1970.

Preliminary Geological and Foundation Investigations for a Nuclear Power Station at Jervis Bay, N.S.W.

By

J. P. MacGregor, B.Sc., D.I.C., A.M.Aus.I.M.M.

(Engineering Geologist, The Electricity Commission of New South Wales)

SUMMARY. The investigation to determine the optimum site location for the power station is described in this report. The work has included geological mapping, land and marine geophysical surveys, auger and diamond drilling, water pressure testing, field ripping tests and laboratory testing of samples. In addition it has been necessary to evaluate the possible seismic risk as a result of fault movement in the area.

The paper demonstrates how the various techniques contribute to an understanding of the geology of the area and shows the limitations of certain methods of investigation. This work has resulted in the selection of the area with the highest quality foundation material as the preferred site and has enabled a comparison to be made of different circulating water arrangements. The engineering properties of the rock are discussed in relation to the possible effect of loading by the station structures.

I. INTRODUCTION

In 1969, the Australian Atomic Energy Commission sought the assistance of the Electricity Commission of New South Wales to investigate sites suitable for the construction of a nuclear power station in Commonwealth Territory on the south-eastern shores of Jervis Bay. After the examination of several possible sites, work was concentrated on an area close to Murrays Beach. This paper describes the geological and geophysical investigations which have been carried out in order to determine the site with the optimum foundation conditions for the station and also to compare the geological aspects of the possible circulating water configurations which have been proposed. It is emphasised that this has been a preliminary study and further detailed work will be required for design.

II. TOPOGRAPHY

The area chosen for detailed investigation is located on the east coast of New South Wales about 120 miles by road south of Sydney (Fig. 1). Murrays Beach is situated immediately west of Governor Head which, with Bowen Island, forms the southern entrance to Jervis Bay. The site lies on the northern shore of the Bherwerre Peninsula which constitutes the Commonwealth Territory, Jervis Bay. The peninsula is dominated by a north-west/south-east trending ridge covered by low scrub and reaching an elevation of 550 feet above sea level. This ridge is flanked on either side by lower country which is densely wooded.

Murrays Beach is a small inlet about 1500 feet wide formed in the sheltered area west of Governor Head and south-west of Bowen Island. To the west and south-west of the beach the ground gradually rises to an elevation of 90 feet above sea level. This wooded area has been chosen as the proposed site. Between the site and the Tasman Sea lies a north-south trending ridge which reaches a height of 205 feet with cliffs averaging 130 feet in height on the ocean side.

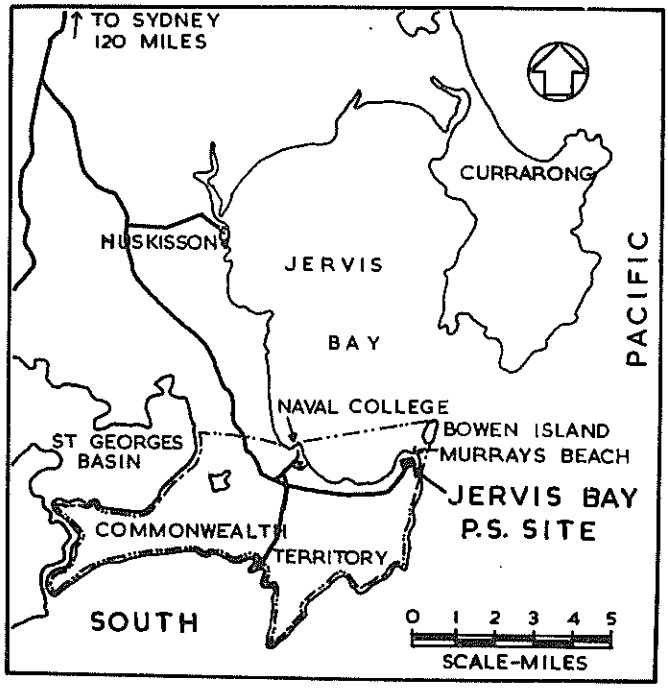

Fig. 1
Location of Power Station Site, Murrays Beach

III. REGIONAL GEOLOGY

Jervis Bay is located on the southern side of the Sydney Basin, which is composed of rocks of Permian and Triassic age. The Bherwerre Peninsula is underlain by a thick series of medium to coarse grained sandstones which are considered to belong to the

Permian Conjola Formation. In the area the Conjola Formation is believed to have a thickness of about 1400 feet (Ref. 1). With the exception of deposits of recent dune sand and soil, the Conjola Formation sandstones are the only rock-types which have been recognised close to the station site.

In the Jervis Bay area there is superimposed on the general structure of the Sydney Basin a series of broad folds. An anticlinal axis forms the south-east trending ridge along the centre of the Bherwerre Peninsula and another anticline follows the east coast.

IV. PREVIOUS INVESTIGATIONS

The first geological study of the Commonwealth Territory, Jervis Bay, was carried out by Perry & Dickins (Ref. 2) and Twist (Ref. 3) has reported on a reconnaisance study of the Nowra-Jervis Bay area. Jackson (Ref. 4) has examined the engineering geology and economic resources of the Territory. Prior to the investigation at Murrays Beach, work was carried out by the Electricity Commission of New South Wales on a site at Scottish Rocks about one mile south-west of the Murrays Beach site (Ref. 5).

V. FIELD INVESTIGATIONS

Rock exposures in the area of Murrays Beach are limited to outcrops along the coast and a few rocky knolls protruding through the sandy overburden on the ridge to the east and south of the site. Geological mapping of all accessible outcrops was carried out on a scale of 1:1200. The cliff-forming coastline south of Governor Head was mapped from the sea as part of the investigation of the geological structure of the area (Ref. 6).

In order to determine the level of bedrock in the proposed station area and to give an indication of the relative properties of the sub-surface materials, a seismic survey was carried out by a geophysical party from the Bureau of Mineral Resources led by E.J. Polak and P. Hill. This survey used two 24-channel seismic refraction sets with a 10 foot geophone spacing (Ref. 7). Seismic traverses were in general at a spacing of 200 feet.

The nature of the materials underlying the floor of Jervis Bay west of Murrays Beach was examined by a marine sparker survey carried out by Messrs. Carter, Albani and Johnson of the University of New South Wales.

A total of 49 N-size diamond drill holes supported by 67 auger holes to refusal have been drilled in the Murrays Beach area. The location of these holes was based on the results of the geophysical surveys, possible location of proposed structures and specific geological problems which emerged during the investigation. In overburden and unconsolidated material too weak to core, standard penetration tests were carried out at regular intervals and in rock several holes were water pressure tested in order to determine joint tightness and the extent of possible water inflows into excavations. All cores were logged in detail and photographed in colour.

A bulldozer was used in conjunction with a single channel engineering seismograph to estimate the depth of rippable material in the station area.

Several possible sources of construction materials were examined as a result of a survey by the Geological Survey of New South Wales (Ref. 8).

VI. LABORATORY INVESTIGATIONS

At an early stage of the investigation, photo-geological interpretation of the area was carried out using both black and white and colour aerial photographs. Selected core samples were petrographically examined with special emphasis placed on their engineering properties and core samples were tested for their resistance to simulated accelerated weathering, unconfined compressive strength and sonic velocity. The elastic moduli of several samples were determined by the laboratory of the School of Civil Engineering, University of Sydney. Some limited testing of soil samples was carried out.

VII. SITE GEOLOGY

(a) Lithology

The field and laboratory investigations revealed that the geology of the area around Murrays Beach is essentially simple, consisting of a series of sandstones and silty sandstones dipping to the north-west at 3° to 4° to the horizontal. Although the rocks all belong to the same formation, they can be divided for the purpose of this investigation into three horizons which have been called the Upper White Sandstone, the Intermediate Grey Silty Sandstone and the Lower Light Grey Sandstone. The bedrock is overlain by sand, some of which is derived from the underlying rocks and the remainder is dune sand. Over most of the area the average thickness of sand is 10 feet but south of Murrays Beach up to 69 feet of sand was encountered. The greater depth is thought to be due to the decomposition of the silty sandstone bedrock where it is close to and above sea level.

The Upper White Sandstone is exposed along the shoreline west of Murrays Beach and forms the upper section of the cliff at Governor Head. The top of the band has not been recognised but the greatest thickness encountered was 69 feet. The sandstone is almost pure white containing 80-90% of quartz. In some places 10-20% of fine dark interstitial material in the rock close to the base of the formation has produced a buff colour. The quartz grains form an interlocking mosaic and consolidation has been achieved by pressure welding - a slight recrystallisation of the grains along their boundaries under pressure. The uniform size and shape of the quartz grains has produced a rock with poorly developed bedding. The rock tends to be friable and the rounding of sharp corners by wave action has produced a characteristic knobbly weathering pattern close to sea level. The contact between the Upper White Sandstone and the underlying rocks is exposed in the cliffs south of Governor Head and this contact was also located in 25 of the diamond drill holes. Stratum contours of this contact are given in Figure 2. In most cases the contact is quite sharp with a distinct change in colour from white or buff to mid-grey accompanied by a general decrease in grain size.

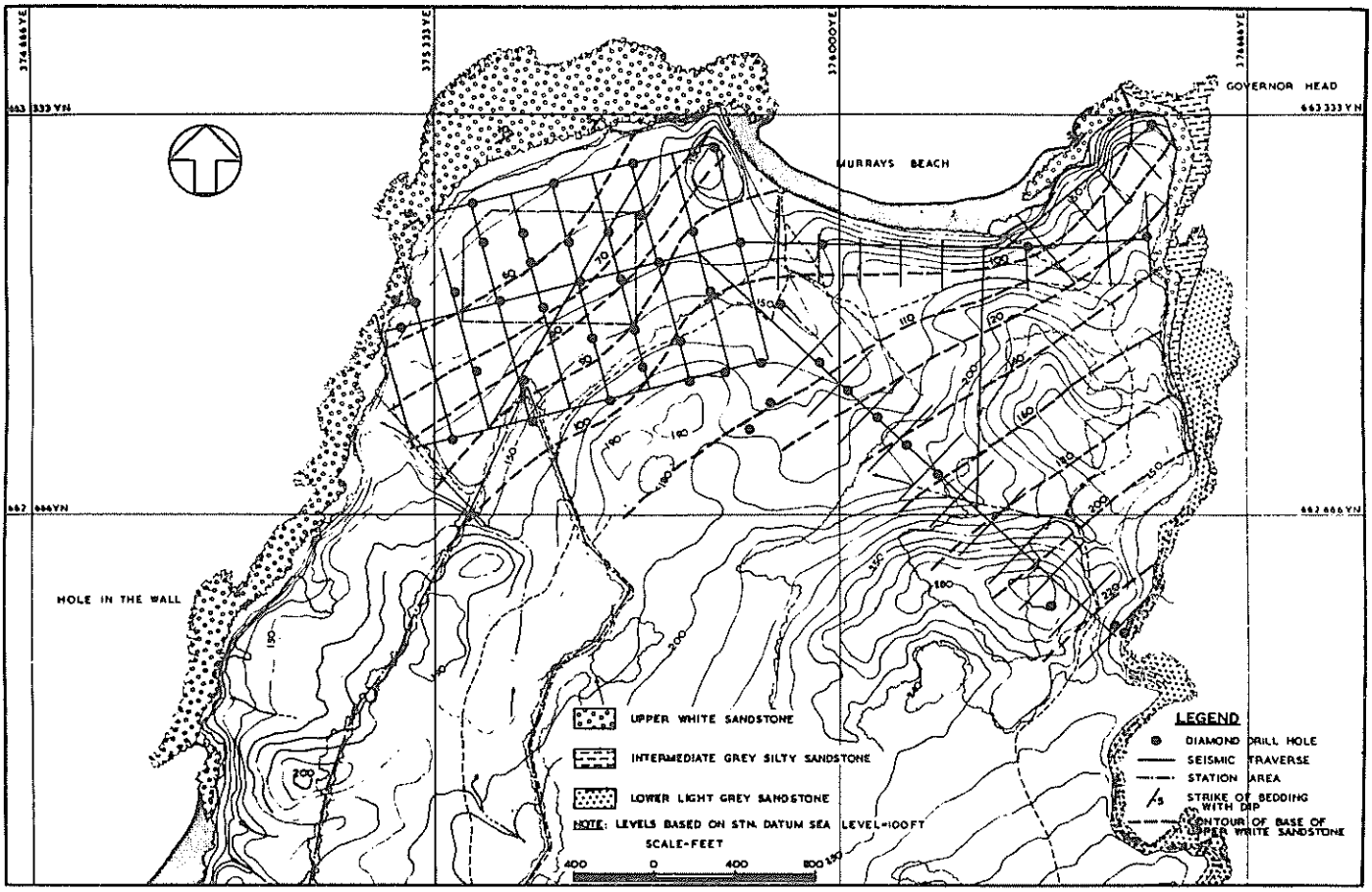

Fig. 2
Location of Site Investigation and Simplified Geology

In the cliffs south of Governor Head, the Upper White Sandstone is underlain by a massive mid-grey coloured, medium-grained silty sandstone band. This band has also been located in 34 diamond drill holes. Where the contacts above and below this stratum were recognised the thickness of the band ranges from 29 feet to 56 feet. The Intermediate Grey Silty Sandstone generally contains a higher silt content than the sandstones lying above and below, but there is considerable variation within the band with the content of clay minerals ranging from 10-70%. This band ranges in colour from light grey to dark grey and obviously represents a period of deposition in which there were some variations in local conditions. Petrographic examination shows that the quartz grains are separated by clay minerals. Although these minerals (kaolinite and illite) have low expansive properties, the band is not strong and loose blocks of silty sandstone disintegrate rapidly.

The base of the cliffs at Governor Head and most of the cliffs on the ocean coastline to the south are made up of a light grey, medium to coarse-grained sandstone which underlies the Intermediate Grey Silty Sandstone. The thickness of the Lower Light Grey Sandstone is not known but at least 150 feet have been penetrated in drilling. The rock is uniform, light to mid-grey in colour with large scale banding more strongly developed than in the other rocks. These rocks contain up to 10% of alkali feldspar and 15% of iron oxide minerals. The presence of the feldspar and the iron has resulted in a much stronger bond between the individual grains and also a strong matrix. Some pressure welding is also evident.

(b) Structure

The uniform nature of the rock types has resulted in poorly developed bedding over most of the area. However, on the cliffs where the rocks have been exposed to weathering, the bedding planes are more prominent. On Bowen Island, there is uniform dip to the west of 2° to 3°, while south of Governor Head the westerly dip increases to 15° and then decreases to an anticlinal crest about 1.4 miles south of Governor Head. Beyond the crest, the sandstone dips to the east and at Steamers Beach the anticlinal axis is again found.

The proposed station area is therefore on the western limb of an anticline whose axis trends north-east. In the drill cores bedding is not well developed but, by plotting the levels of the contacts between the rock types, the general bedding attitude shows a general north-westerly dip of between 3° and 6° to the horizontal. Some very gentle subsidiary folding may be present.

Widely spaced high angle jointing is developed throughout the Bherwerre Peninsula. The joint directions indicated on the aerial photographs and measured on the ground in the Governors Head/Murrays Beach area show azimuth maxima between 325° and 025°

and between 065° and 115°. Joints are normally tight with no infilling. No extensive area of close jointing was located by the drill holes.

The Ulladulla 1:250,000 geological map shows the geological structures on the south-western side of Jervis Bay to be truncated by a major fault which crosses the ocean coastline about one mile south-east of the proposed station site. In order to assess the significance of this fault and associated fractures on the proposed station site, a detailed examination was made of the faulting in the area (Ref. 6). This study found that, although a number of faults can be recognised in the cliffs south of Governor Head, the fault planes are narrow, the displacement along individual faults is less than 10 feet and the movement has had little effect on the surrounding strata. These faults in general strike north-east, dip to the west at between 35° and 50° to the horizontal and in almost every case in which movement can be measured, the faulting is reverse, i.e., compressional. The faulting is parallel to the anticline in this area and it is considered that any movement is of a minor nature and that it took place under the regional compressional stresses that caused the folding in this area during the Jurassic period. No faults were found which would significantly affect the structural level of the geological formations in the station area.

VIII. ENGINEERING PROPERTIES OF ROCKS

The power station structures will be founded on the Upper White Sandstone. This material proved to be relatively easy to drill and core recovery was good. Seismic velocities in the Upper White Sandstone ranged from 3,000 feet per second to 10,000 feet per second. With the exception of a thin upper layer of highly weathered rock which was extremely friable and not suitable for testing, it was found that the Upper White Sandstone could be divided into two groups as shown in Table I.

TABLE I

STRENGTH OF UPPER WHITE SANDSTONE

	Unconfined Compressive Strength p.s.i.	Secant Modulus* p.s.i. x 10^6
Samples taken from above the lowest 10 feet of the stratum	1822-9300	0.12 - 1.5
Samples taken from the lowest 10 feet of the stratum	390-2050	0.12

* At 318 p.s.i. (approx. 20 tons per square foot)

The ripping tests showed that a D9 bulldozer could probably rip this rock in areas where the seismic velocity was below 6000 feet per second. During the test the ripped material broke up into its component grains and both these conclusions have been confirmed during the excavation of the site.

Four core samples of the Upper White Sandstone withstood 300 cycles of simulated accelerated weathering without appreciable effect but two samples gave losses of 55% after the sodium sulphate soundness test and there was a loss of up to 88% after the Los Angeles abrasion test.

The Intermediate Grey Silty Sandstone is of variable lithology and generally has a lower strength than the Upper White Sandstone. Due to the higher velocities in the overlying white sandstone, it was not possible to define the extent of the Silty Sandstone layer by seismic methods.

The silty sandstone is soft enabling rapid drilling but core recovery in this material was relatively poor, probably due to the presence of hard chert pebbles which caused grinding in the friable silty matrix.

The unconfined compressive strength of samples from this band ranged from 360 p.s.i. to 8,130 p.s.i. Sixty percent of the samples gave strengths below 2,000 p.s.i. Secant moduli values ranged from 0.10 - 0.60 x 10^6 p.s.i. at a loading of 318 p.s.i.

Weathering in the Intermediate Grey Silty Sandstone is moderate with the exception of an area south of Murrays Beach where the Upper White Sandstone is missing and there is up to 50 feet of completely to highly weathered silty sandstone.

A much slower rate of drilling in the Lower Light Grey Sandstone indicated that this rock type is much harder than the other rock formations present in the area. Unconfined compressive testing of samples gave a range in strength from 5240 - 14,000 p.s.i. The Secant Modulus at a loading of 318 p.s.i. ranged from 0.9 - 3.6 x 10^6 p.s.i.

A sample of the Lower Light Grey Sandstone gave a loss of 6% after the sodium sulphate test and a loss of 33% in the Los Angeles abrasion test.

IX. EARTHQUAKE RISK

The seismicity of the Sydney Basin has been summarised by Doyle, Cleary & Gray (Ref. 9) and the possible seismic risk at Jervis Bay has been studied by Underwood (Ref. 10). With the exception of the shaking centred in the Robertson area some 40 miles to the north-west in 1961, no earthquake of significant size has been recorded from the area around Jervis Bay. Underwood concluded that the most likely source of shaking which might have damaging effects on a power station at Murrays Beach would be an earthquake resulting from movement along the major fault south-east of the station. However, the site investigation indicates that this major fault does not exist and that there is no evidence of any fault movement in recent geological time. The seismic risk in the Jervis Bay area is therefore considered to be low, but in order to evaluate any shaking which may occur, it is proposed to install a long period continuous recording seismograph close to the station site.

X. SELECTION OF THE MOST SUITABLE STATION LOCATION

From consideration of the maximum water levels, cooling water pumping costs and site geology, the

station site level (grade level) has been fixed at 15 feet above mean sea level (R.L. 115 ft.). The optimum position of the station, having regard for foundations, is the site where -

(i) rock capable of supporting the station structure is close to R.L. 115 ft.;

(ii) where there is a minimum of excavation to R.L. 115 ft.; and

(iii) where there is a maximum thicness of good quality rock below R.L. 115 ft.

Other factors which have to be taken into consideration are the length and position of the circulating water canals and the preservation of the countryside around the station area.

The level of the top of good quality rock is indicated by the drill holes sunk in the area and the seismic survey has been used to interpolate between drill holes. The usefulness of the seismic work has been limited by the presence of the relatively weaker band of Intermediate Grey Silty Sandstone below the Upper White Sandstone. Where the Upper White Sandstone is thick, the seismic survey located the top of bedrock but failed to indicate the weaker band. On the other hand, where the white sandstone is thin the seismic work sometimes picked up the upper level and at other times located the interface between the Intermediate Grey Silty Sandstone and the Lower Light Grey Sandstone. Thus the interface depths appear to vary greatly and in this situation the seismic work is difficult to interpret.

As the rocks in the Murrays Beach area dip to the north-west, the maximum depth of the Upper White Sandstone is found on the headland to the west of the beach. In this area it has been found that the seismic survey corresponds closely with the drill hole information. In order to preserve a nature strip along the coastline the station site should be at least 150 feet from the sea and with this provision, the station site has been located as shown in Figure 3. The drilling in this area indicates a thickness of Upper White Sandstone below grade level ranging from 26 feet at the south-east corner to 55 feet in the north-west corner. If the reactor and turbine house were located at the western end of the station area, there would be a minimum of 45 feet of good quality white sandstone below grade level.

XI. PERFORMANCE OF THE FOUNDATION ROCKS

The jointing at the selected station site is tight, the materials are reasonably uniform and it is considered that for a preliminary estimation of settlement the foundation can be treated as composed of several horizontal layers behaving in an elastic manner.

The settlement of a semi-infinite elastic medium with uniform strata can be calculated using the Steinbrenner approximation by which the settlement of a multi-layered mass is estimated by using the stress distribution for a homogeneous half-space, but using the relevant elastic parameters of each layer to calculate the settlement within each layer, the sum of such settlements being the surface settlement.

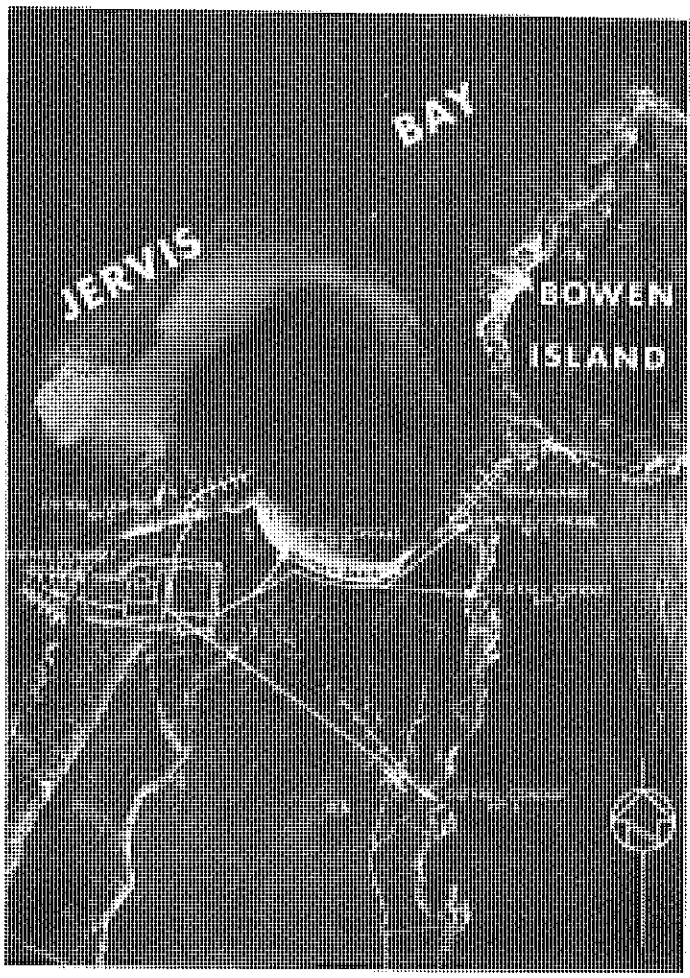

Fig. 3
Site Layout showing Five Alternative Circulating Water Conduit Locations

Based on the rock testing carried out on core samples from the station area, the following average Elastic Moduli values can be assumed:

Main part of Upper White Sandstone
0.2×10^6 p.s.i.

Base of Upper White Sandstone and Intermediate Grey Silty Sandstone
0.1×10^6 p.s.i.

Lower Light Grey Sandstone
1.3×10^6 p.s.i.

Using these values a typical column footing in the turbine house with dimensions 10 feet by 10 feet bearing a load of 2,500 tons would settle about 0.3 inches, if based on 20 feet of Upper White Sandstone and 50 feet of Intermediate Grey Silty Sandstone. If, however, the footing is located directly on the Intermediate Grey Silty Sandstone, the settlement would be about 0.5 inches and the load at the surface would be close to the ultimate unconfined compressive strength of the weathered rock.

A 150 foot diameter circular reactor building with an average loading of 5 tons per square foot would settle about 0.6 inches if sited on 20 feet

of Upper White Sandstone overlying 50 feet of Intermediate Grey Silty Sandstone and also about 0.6 inches if located directly on the Intermediate Grey Silty Sandstone. The loadings in this case are well below the ultimate unconfined compressive strength of the rock.

XII. CIRCULATING WATER SYSTEM

The alternative locations for intake and outfall canals which have been considered for this station are shown on Figure 3.

The intake canal will probably be situated to the west of the station site and will involve the excavation of a channel in the floor of Jervis Bay. The invert level of this channel will depend on the location of the outfall and examination of the possible recirculation between outfall and intake canals if a bay outfall is selected. Drilling on the shore at the intake has penetrated white sandstone to a depth of 50 feet below sea level and the marine sparker survey indicated a depth of 20 feet of sand above bedrock about 500 feet offshore. Depending on the invert level chosen, it would appear likely that about half the excavation required for the intake canal would be in sand and the remainder in white sandstone.

A total of five outfall routes has been examined (Fig. 3). Outfalls 1, 2 and 3 discharge into the ocean and Outfalls 4 and 5 into Jervis Bay. The geological investigation has shown that of the two channels into the Bay, Outfall 5 would be preferable as a maximum depth of excavation of 25 feet would be required and the invert of the canal would be on Upper White Sandstone. Outfall 4 would involve excavation to a maximum depth of 35 feet. The invert would be close to the top of the Intermediate Grey Silty Sandstone and the channel would pass through deep sand at Murrays Beach.

Of the ocean outfalls, Outfalls 1 and 2 would be constructed in deep sand and weathered silty sandstone south of Murrays Beach. At the eastern end of Murrays Beach, Outfall 1 would involve an open canal to Governor Head and Outfall 2 a short tunnel to the coast just south of Governor Head. In both cases, excavation would be carried out in the relatively weak rocks close to the contact between the Upper White Sandstone and the Intermediate Grey Silty Sandstone.

It has been considered that, if either Outfalls 1 or 2 were to be adopted and if cooling water must be prevented from entering the bay, it would be necessary to construct a breakwater between Governor Head and Bowen Island. Investigation of the breakwater site has shown that it would be located on a shelf of Lower Light Grey Sandstone averaging 20 feet below sea level. The rock from the excavation of Outfalls 1 or 2 would not be suitable for the construction of the breakwater and there is no available site for the establishment of a quarry in suitable rock close to the power station area.

Outfall 3 involves the construction of a tunnel between the station site and the ocean coast about half a mile south of Governor Head. The geological investigation has shown that the first 1,000 feet of this route would be excavated in deeply weathered silty sandstone and may be more economically constructed by cut and cover methods, the remainder of the tunnel - about 2,000 feet - would be through strong Lower Light Grey Sandstone.

The drilling and testing along this tunnel line has shown that the rock is sound and joints are widely spaced and tight. Minimal support should be required for the tunnel in the Lower Light Grey Sandstone and groundwater inflows should be small.

The ocean portal of Outfall 3 has been provisionally located in a cliff which drops sheer from 130 feet above sea level to about 20 feet below sea level. To minimise wave surge in the tunnel, a 'surge tank' would be required at the tunnel portal and this tank would discharge below sea level. The rock in this area is strong light grey sandstone which is cut by widely spaced minor faulting with the fault planes dipping to the west at about 40°. Both vertical and angled drilling close to the cliff face indicates that these fault planes are narrow and tight and should not present a great problem in the design of the portal structure.

XII. CONCLUSIONS

The geology of the area south-west of Governor Head has been examined using a combination of several field investigation methods supported by appropriate laboratory testing. This has shown that the area is composed of surface sand underlain by a series of sandstone and silty sandstones which dip gently to the north-west.

The rocks can be divided into three layers with the relatively strong Upper White Sandstone underlain by a somewhat weaker Intermediate Grey Silty Sandstone and the very strong Lower Light Grey Sandstone. The presence of the middle weaker layer has complicated the interpretation of the seismic survey especially when the Upper White Sandstone is thin.

Examination of the geological structures in the area has failed to locate the presence of any active major faulting. This supports the general conclusion that the seismic risk in the Jervis Bay area is low.

A station site has been selected in which the top of the Upper White Sandstone stratum is close to station grade level and there is a depth of at least 45 feet of this rock below grade level near the main station structures. In this way, the station loads are widely distributed on the weaker and more deformable Intermediate Grey Silty Sandstone.

The properties of the materials found along the alternative outfall routes has been examined. Of the bay outfalls, No. 5 is geologically preferable, while of the ocean outfalls, No. 3 appears to have fewer construction difficulties even although it requires some 3,000 feet of tunnel.

XIII. ACKNOWLEDGEMENTS

The author acknowledges with thanks the permission of the Chairman of the Electricity Commission of New South Wales and the Chairman of the Australian Atomic Energy Commission to present this paper which is based on work reported on in Reference 11. The assistance of the many people who contributed to this work is acknowledged and in particular to

Mr. C.K. McKinnon who carried out the settlement analysis.

REFERENCES

1. PACKHAM, G.H. - The Geology of New South Wales. Journal of Geological Society, Australia, Vol. 16, No. 1, 1969, pp. 357-366.

2. PERRY, W.J. and DICKINS, J.M. - Report on a Geological Survey of Commonwealth Territory, Jervis Bay. Bureau of Mineral Resources Record No. 1952/88, 1952.

3. TWIST, R.F. - Report on Geological Reconnaissance of the Nowra-Jervis Bay Area of P.E.L. 59, N.S.W. Geosurveys of Australia Ltd. (Unpublished Report) 1962.

4. JACKSON, M.J. - Engineering Geology and Economic Resources of Commonwealth Territory, Jervis Bay. Bureau of Mineral Resources Record No. 1969/88, 1969.

5. MacGREGOR, J.P.; LAMB, A.M. and McKINNON, C.K. - Investigations at Site J.S1 - Scottish Rocks. E.C.N.S.W. Power and Trans. Development Report No. C.I. 43, 1970.

6. MacGREGOR, J.P. - Investigation of the Structural Geology of Eastern Bherwerre Peninsula. E.C.N.S.W. Power and Trans. Development Report No. C.I. 44, 1970.

7. POLAK, E.J. and HILL, P. - Jervis Bay Power Station Site Seismic Refraction Survey, A.C.T. Bureau of Mineral Resources Record No. 1970/32, 1970.

8. JOHNSTON, D.A. - Report on the Availability of Aggregate Material for the Proposed Jervis Bay Power Station. Geological Survey of New South Wales, 1969.

9. DOYLE, H.A., CLEARY, J.R. and GRAY, N.M. - The Seismicity of the Sydney Basin. Journal of Geological Society Australia, Vol. 15, No. 2, 1968, pp. 175-181.

10. UNDERWOOD, R. - Modelling of Seismic Risk at Jervis Bay. Australian National University, Dept. of Geophysics, 1970.

11. McKINNON, C.K.; MacGREGOR, J.P. and HAWKINS, R. - Jervis Bay Nuclear Power Station, Investigations for Civil Works. E.C.N.S.W. Power and Trans. Development Report No. C.I. 49, 1970.

Some Properties of Weathered Greywacke

By

M. J. Pender, B.E. (Hons.)

(Soils Engineer, Ministry of Works, Central Laboratory, Lower Hutt, New Zealand)

SUMMARY.- The behaviour of weathered greywacke from a particular site in Wellington is discussed. The degree of weathering varied considerably and so the material was classed visually into four categories using a scheme for classifying weathered rock similar to that of Fookes and Horswill. The results of the usual soil mechanics classification tests confirmed the grading system as did the results of tests for the mechanical properties. Characteristic ranges of values for the various properties were found for each grade. Furthermore reasonable correlations were found between the void ratio of the material and the values of the mechanical properties.

I.- INTRODUCTION

Much of Wellington is built on an extensive deposit of greywacke which is found in various stages of decomposition ranging from unweathered rock to highly plastic clay. The material whose properties are discussed in this paper was obtained from one particular site in Wellington during the course of an investigation for a multistorey building. Although all the material present is weathered greywacke the degree of weathering varies considerably and in addition the stratigraphy is not simple. The overall assessment of the site and prediction of the likely performance of any foundation constructed there would be greatly facilitated if some means of sorting the material into characteristic types could be developed.

On the basis of visual logging it was possible to class the material into four grades. Similar approaches have been used elsewhere. Knill and Jones (Ref.1) have used a visual grading scheme for classifying weathered and/or fractured rock at dam sites whilst Ward, Burland and Gallois (Ref.2) have classed chalk into five grades to assess its deformation properties and Chandler (Ref.3) has used a fourfold grading scheme in discussing the properties of weathered marl. These have demonstrated that it is possible to classify weathered materials visually into grades which are confirmed by the values for the various properties. Each grade is associated with a characteristic range of values for properties such as density and modulus values. Saunders and Fookes (Ref.4) have compared these and other systems in a paper on the significance of rock weathering to foundation engineering. In Ref.4 information about the properties of a range of weathered rocks is summarised and it is apparent that there is little information available about the properties of weathered sandstone of which greywacke is a type. In New Zealand the term greywacke is applied to poorly sorted well indurated sandstone (Ref.5).

In this paper it is shown how a similar grading system is applicable to a particular site in Wellington. This visual grading is confirmed for the more weathered material by the standard classification tests used in soil mechanics and also by the range of values for the mechanical properties. In addition reasonable relations exist between the void ratio of the weathered material and the values for the mechanical properties.

II.- SAMPLING, DESCRIPTION AND GRADING OF THE MATERIAL

Continuous 4" diameter undisturbed samples were taken with a triple tube rotary core barrel. In this barrel, designed by Northey (Ref.6), the sample was not retained in the usual split liner but in a series of copper rings 4" I.D. and 2" or 4" long held in a split liner. Up to 32" of core could be recovered per run. With this barrel it was possible to obtain good quality undisturbed samples of the wide variety of material at the site. After sampling the core was wrapped in thick plastic sheeting and stored in a humid room in an attempt to maintain the in-situ moisture content. Presumably the material is saturated in-situ, but it is likely that there is a decrease in the degree of saturation associated with the stress relief on sampling. At present these cores provide the only means available of examining the material at the site.

The material was logged visually and could be divided into four groups ranging from completely weathered greywacke in the form of a red highly plastic clay to a moderately weathered material. In all the classification schemes discussed in references 1 to 4 the unweathered material has been termed grade I and the same idea of assigning the lower grade numbers to the least weathered material is followed here. An attempt is made to follow the classification system of Fookes and Horswill (Ref.4) for the weathering of hard rocks explained in reference 4 and the details of which are given in Table I. Following this system it seems that the least weathered material found at the site corresponds to Fookes's and Horswill's grade III and the most weathered to their grade

VI. The details of the four grades of weathered greywacke are set out below:

Grade VI. Dark red, stiff to very stiff homogeneous highly plastic clay; structure of parent rock no longer apparent although there are areas of grey, less weathered material; on drying slightly mottled texture evident.

Grade V. Very similar colour and texture to Grade IV but weathering more advanced; joints in parent material clearly marked; in some cases sandy texture of original rock not so evident as in Grade IV material; Grade V material easily crumbled to sandy silt under light finger pressure.

Grade IV. Light yellow-brown material; broken down to silty sand with moderate to firm finger pressure; occasional much harder lumps; original rock fabric still evident in the undisturbed material by virtue of the black manganese dioxide along joint planes during weathering; spacing of joints variable, ranging upward from $\frac{1}{2}$" and orientation random.

Grade III. Dense, brown, moderately weathered, very closely jointed material. Typical size of pieces ranges from $\frac{1}{2}$" upwards; separate pieces break under moderate hammer blow, brown colour extends through the broken pieces but diminishes towards centre.

The material in all four of these grades is weathered greywacke. Because the original rock fabric is still clearly discernable in grades III to V they are residual weathered materials. The exact origin of the grade VI material is not clear. At present it does seem that although it is derived from greywacke it was probably transposed to the site. The degree of weathering before this transposition is uncertain. As explained by Te Punga (Ref.7) greywacke weathered to a red colour is not uncommon around the Wellington area and it has been suggested that a different weathering mechanism might be responsible for this colour.

It was possible to perform the usual soil mechanics classification tests on grades IV, V and VI but grade III was more in the gravel range and so the bulk of the discussion from here is confined to the more weathered material. These tests showed that a characteristic range of values for the index properties is associated with each grade.

Particle size distribution curves provided the first confirmation of the grading scheme. Some typical curves for grades IV, V and VI are plotted in Fig.1. This shows that the weathering process increases the proportion of fine grained material present. On the basis of these particle size distribution curves the diagram has been divided into regions characteristic of each grade. One difficulty encountered in determining the particle size distribution curves for residual soils is the tendency for the coarser fraction to keep breaking down during the sieving process. In this case the sieving time was kept to a standard 15 minutes thus at least ensuring that any such effect was uniform throughout the results discussed here. An effort was also made to ensure that the pretreatment of the material was always the same. Before sieving and washing it was

TABLE I

CHARACTERISTICS OF THE CLASSIFICATION SCHEME FOR THE WEATHERING OF HARD ROCK BY FOOKES AND HORSWILL

Term	Grade	Rocks
True residual soil	VI	Rock is discoloured and completely changed to soil with original fabric completely destroyed.
Completely weathered	V	Rock discoloured and externally changed to a soil, but original fabric mainly preserved; properties of the soil depend partly on nature of parent rock.
Highly weathered	IV	Rock discoloured; discontinuities may be open and fabric of rock near to discontinuities altered; alteration penetrates deeply inwards, lithorelicts still present.
Moderately weathered	III	Rock discoloured; discontinuities may be open and surfaces have greater discolouration with alteration penetrating inwards; intact rock noticeably weaker, as determined in the field, than fresh rock.
Slightly weathered	II	Rock slightly discoloured; discontinuities may be open and have slightly discoloured surfaces; intact rock not, as determined in the field, weaker than fresh rock.
Fresh	I	Parent rock shows no discolouration, loss of strength or any other effects due to weathering.

crumbled under gentle finger pressure. Thus even if there may be some doubt about the "true" grading curve those discussed here are adequate for comparative purposes.

Plasticity tests gave a similar picture. As with the particle size analysis an attempt was made to keep the pretreatment of the material before the tests consistent. The material that passed the number 36 sieve was wetted up to well above the liquid limit and the separate points for the liquid limit and plastic limits were then reached by a continuous sequence of gradual drying, cycles of wetting and drying being carefully avoided. The values of the plasticity index (I_p) are plotted against the liquid limit (w_L) in Fig.2 and it can be seen that the points are spread along a narrow band, the regions of this diagram occupied by the various grades are shown. In Table II characteristic ranges of values for the classification test results are tabulated. This table includes values for the specific gravity (G) of the soil particles and the range of void ratios that seem to be associated with each grade.

Table II indicates that although there is some overlapping between the grades there is a range of values associated with each. A similar conclusion is reached when the values for the various mechanical properties are examined, these are tabulated in Table III.

Table III illustrates that there is a characteristic range of values for the various properties in each grade even though there is some overlapping at the transition from one grade to

TABLE II

INDEX PROPERTIES FOR GRADES IV TO VI WEATHERED GREYWACKE

Grade	Liquid Limit (%) (w_L)	Plasticity Index (%) (I_p)	% Passing 200 Sieve	% Finer than 2 microns	Specific Gravity (G)	Void Ratio (e)
IV	35	10	25-55	15	2.70-2.69	0.30-0.55
V	34-60	8-35	55-80	15-40	2.70-2.69	0.50-0.85
VI	60-100	>30	>80	40-60	2.74	0.75-1.40

TABLE III

MECHANICAL PROPERTIES FOR GRADES IV TO VI WEATHERED GREYWACKE

Grade	Coef.of Perm. (K) cm/sec.	Comp. Index (C_c)	Preconsol. Pressure (p_c) tons/ft^2	Angle of Int.Friction ϕ
IV	10^{-7}	0.1	>20	>35
V	4×10^{-6}-1×10^{-8}	0.1-0.35	24-10	35-15
VI	3×10^{-8}-5×10^{-9}	0.30-0.70	<10	<15

the next. The table also indicates the major limitation of the grading scheme. Each grade has a characteristic range of properties but the spread of values within a given grade can be fairly wide. For example, the compression index, C_c, may range between 0.70 and 0.30 for grade VI material. This suggests that for practical application some better means of estimating likely values would be useful. In the following sections of this paper the results of each of the individual types of test are discussed and it is shown that the void ratio of the material provides a more useful way of assessing the likely range of values for a given property.

III.- PERMEABILITY TESTS

Nineteen permeability tests were performed on samples of grades IV, V and VI material. Each sample was trimmed into a consolidation ring the inner surface of which had been smeared with silicone grease. The prepared sample was mounted with a porous stone at one end and connected to a supply of de-aired water at the other and placed in a constant temperature bath set at 20°C. The test set up was such that any tendency for the sample to swell on exposure to water was prevented. No attempt was made to ensure that the samples were fully saturated at testing but the calculated degree of saturation (S_r) indicated that all the material tested for permeability and also for consolidation and strength was either fully saturated or nearly so.

Falling head tests were done each of which was allowed to proceed for about two weeks. After several days the measured permeability settled down to a steady value and these are plotted against the void ratio in Fig.3. There is a fair amount of scatter in this diagram but it does show that as the void ratio increases there is a tendency for the permeability to decrease. This is probably a consequence of the increase in the proportion of clay sized particles during the weathering process.

IV.- CONSOLIDATION TESTS

A series of consolidation tests was performed and some typical results are plotted in Fig.4. The consolidometer used was capable of applying stresses up to 133 tons/ft^2 to a 3" diameter sample. The use of such high loads was necessary because of the high values of preconsolidation pressure exhibited by all grades of this material. Fig.4 shows that there is a considerable increase in the compressibility of the weathered greywacke from grades IV through to VI. This is shown more clearly in Fig.5 where the values of the compression index C_c, have been plotted against void ratio. This diagram shows that there is a surprisingly good correlation between the compression index and the void ratio.

The e, log p curves were determined with the usual load increment ratio of unity. The load increments were applied and the settlement plotted on a log time scale. This indicated that the primary consolidation phase for the tests on almost all of the material, the exception being some grade VI material, was complete in less than 10 minutes. The initial settlement on the application of the load occurred so quickly that it was not possible to plot the initial linear part of the settlement, log(time) curve for all the grade IV and most of the grade V material. Because of this there can be no comparison of c_v values for the various grades.

The preconsolidation pressure, p_c, for each of the consolidation tests was determined by the Casagrande construction and the results are plotted against void ratio in Fig.6. This shows that once again there is a fairly well defined relation between this parameter and the void ratio. In this case the amount of scatter is somewhat greater than that for the curve of C_c against void ratio but part of the problem here is probably related to the difficulty in determining the magnitude of the preconsolidation pressure. On the e, log p curves for this weathered greywacke it is not easy to decide on the point with the minimum radius of curvature. To get a more realistic estimate for this two values were determined - apparent upper and lower limits for p_c. The points plotted in Fig.6 are the average of these values, the range at each point was about 2 or 3 tons/ft^2. The preconsolidation pressures plotted in Fig.6 are about 2 to 8 times the present overburden pressure on the material.

The samples tested were of two sizes. The majority were trimmed into conventional 3" diameter by $\frac{3}{4}$" high consolidation rings, these results are drawn as round dots in Fig.6. Before trimming the inner surface of the rings was smeared with silicone grease. The remainder of the samples were tested without being removed from the 4" diameter, 2" high copper sampling rings and these results are plotted as squares. In both cases a floating ring type of consolidometer was used. Fig.5 and Fig.6 show that there is no significant difference between the results

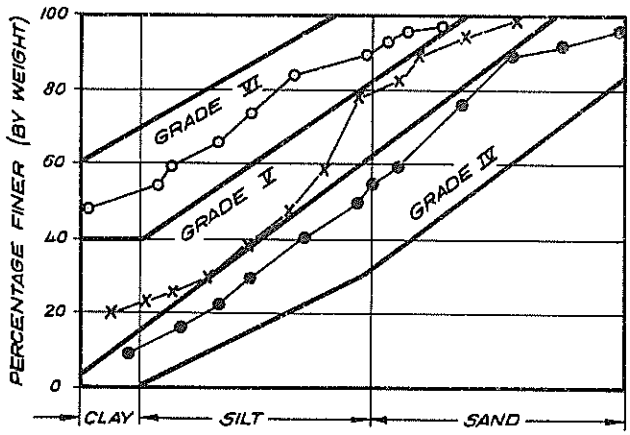

FIG.1 PARTICLE SIZE DISTRIBUTION CURVES

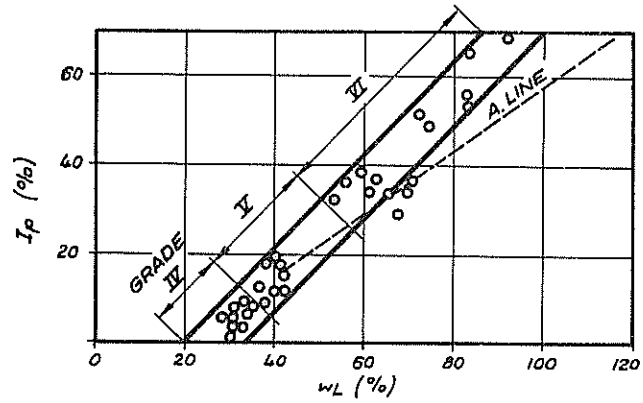

FIG.2 PLASTICITY CHART

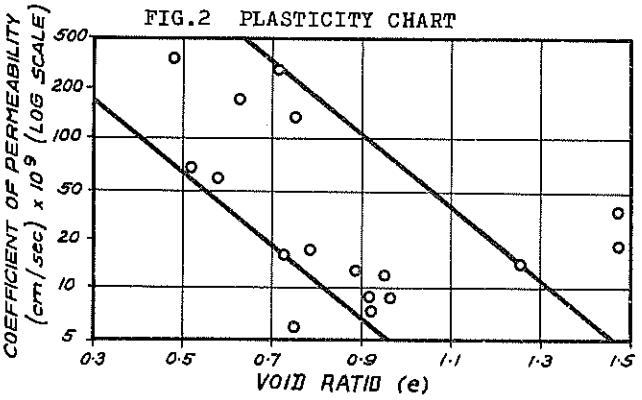

FIG.3 PERMEABILITY VALUES

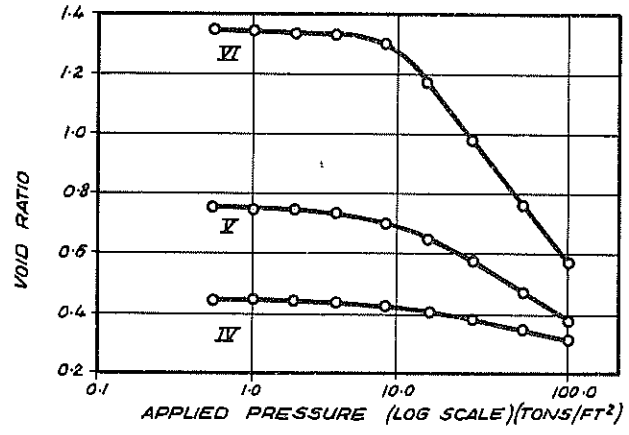

FIG.4 TYPICAL CONSOLIDATION CURVES

obtained from the two sizes of sample holders despite the difference in height to diameter ratios and the treatment of the inner surface.

Before moving onto the discussion of the triaxial test results the significance of large values obtained for the preconsolidation pressure requires comment. The usual explanation for preconsolidation is that at some time in the past history of the soil stresses of the order of the preconsolidation pressure have been applied to the material and subsequently removed. The material "remembers" this and it is reflected in the shape of the e, log p curve. However in the present case it seems to the writer that previous loading of the magnitude required is most unlikely.

It is known that when a material is loaded in a consolidometer at stresses less than the preconsolidation pressure the deformation is approximately recoverable whereas substantial irrecoverable deformation occurs, no doubt with interparticle movement and rearrangement, at higher stresses. When the applied stress approaches the preconsolidation pressure there is a definite change in curvature of the e log p curve. It is suggested here that this change in curvature as p_c is approached will be exhibited by any granular material that is found under stress conditions of magnitude such that only recoverable deformations are possible. In other words it seems to the writer that the so called "preconsolidation pressure" is merely a measure of the stresses that must be applied to the material before the onset of any substantial irrecoverable deformation on loading in a consolidometer.

The behaviour of weathered greywacke discussed in this paper is suggested as an example where the existence of an apparent preconsolidation pressure considerably greater than the existing overburden pressure may not be the result of the previous loading history. Rather it is thought to be a consequence of the weathering process. Initially the unweathered rock is very dense and as the weathering process proceeds the void ratio increases, each change of void ratio giving a material with slightly different consolidation properties. However at each stage of the weathering the resulting material is still comparatively dense and so large pressures have to be applied before there is any irrecoverable change of void ratio. As the void ratio increases the stress required to cause this irrecoverable deformation would be expected to decrease as suggested by Fig.6.

V.- TRIAXIAL TEST RESULTS

A number of consolidated undrained triaxial tests were performed and the resulting effective angle of internal friction is plotted against the initial void ratio of the material in Fig.7. The failure criterion used in determining ϕ' was the peak value of the principal effective stress ratio and a strain rate of 0.1%/minute was applied to all the samples. Once again it is seen that there is a reasonable relation between this parameter and the void ratio of the material. Three of the sixteen points plotted fall well outside the suggested band, at this point the reason for this is not clear. In Fig.8 the values of the effective cohesion intercepts obtained from these undrained

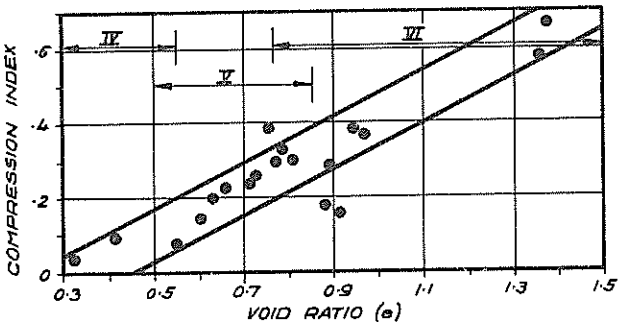

FIG.5 VALUES OF COMPRESSION INDEX

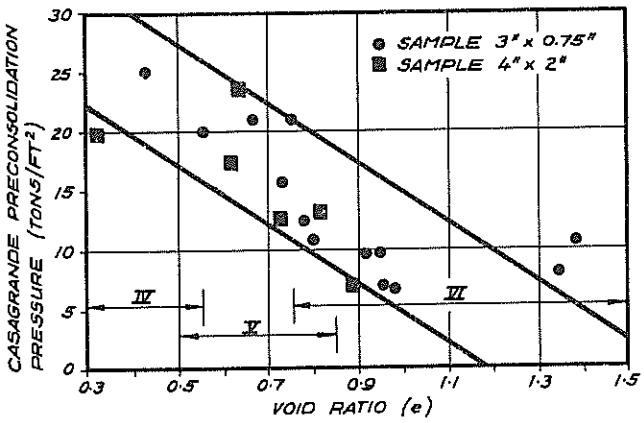

FIG.6 PRECONSOLIDATION PRESSURES

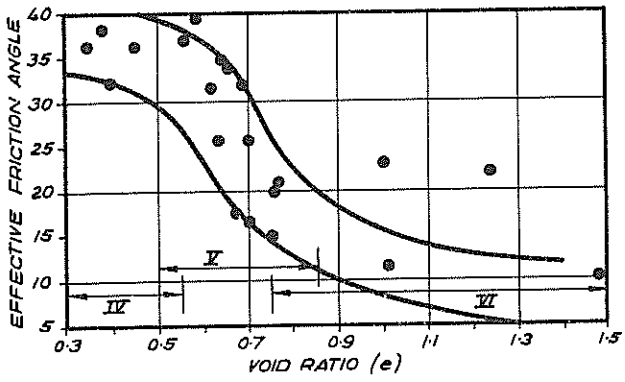

FIG.7 EFFECTIVE ANGLES OF INTERNAL FRICTION

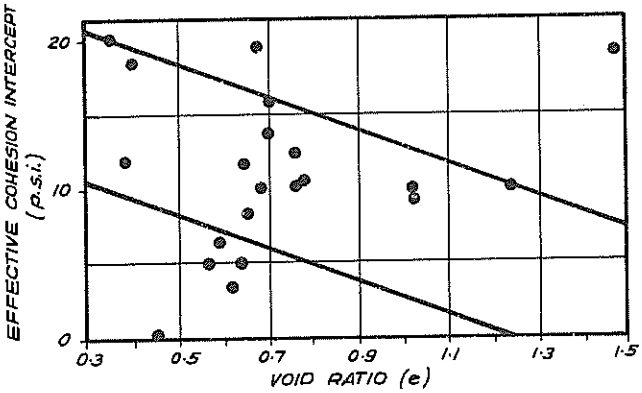

FIG.8 VALUES OF EFFECTIVE COHESION

triaxial series have been plotted against void ratio. The majority of the points fall into a fairly broad band which suggests that as the void ratio increases there is a general decrease in the effective cohesion intercept. Most of the pairs of values for c' and ϕ' were obtained from a triaxial series consisting of tests on 5 separate samples consolidated before testing at cell pressures ranging from 5 psi to 120 psi. Although the values of c' and ϕ' have been associated with one particular void ratio in Figs.7 and 8 there was in fact a range of values for the calculated void ratios of the samples tested in each triaxial series. Typically these variations ranged from 0.03 to 0.10 over the five samples for a given series. Variations of this order did not seem to have a significant effect on the graph for which the shear strength parameters were determined.

The majority of the triaxial samples failed by the formation of slip planes that became evident at about the same axial strain as the peak value of the principal effective stress ratio was reached. Despite the joint planes in the original greywacke still being evident in grades IV and V material only a very small number of the total number of samples tested actually failed along one of these planes.

Apart from the usual precautions of careful setting up and filling the cell base and pore pressure transducer with de-aired water no special effort was made to ensure full saturation of the sample and pore pressure measuring system for most of the triaxial tests. The calculated degrees of saturation suggested that the material was either fully saturated or within a few percent of saturation in most cases. Unfortunately the indirect procedure involved in calculating the degree of saturation is very prone to the cumulative effects of small errors and so it is only possible to specify the degree of saturation to within a few percent. Thus the exact degree of saturation of the samples tested remains uncertain but it seems probable that most of the samples were not quite fully saturated. The importance of this was investigated by a few series of tests conducted on samples saturated by the application of back pressure. Another effect was also investigated. Some of the triaxial results were obtained on samples 3" high by $1\frac{1}{2}$" in diameter with porous stones at each end while others were determined from tests on samples 4" high and 4" in diameter with the free ends developed by Rowe and Barden (Ref.8). In these there were two 0.012" thick rubber disks between the sample and each end platen. Silicone grease was smeared on the end platens and between the rubber disks before testing and the disks were also cut radially and circumferentially to reduce any restraint preventing free expansion of the sample. In Fig.9 the result of a triaxial series conducted on 12 samples of grade V material is plotted. The points were determined from tests on back pressure saturated and unsaturated samples some of which were 3" x $1\frac{1}{2}$" and the others 4" x 4". The back pressures used varied between 60 and 90 psi and saturation was checked by measuring the speed with which the pore pressure transducer responded to successive 5 psi increments in cell pressure. In all cases the reading from the pore pressure transducer reached a steady value in less than 10 seconds which is taken as evidence of

saturation. Fig.9 in which the twelve points are plotted suggests values of c' and ϕ' determined are not dependent on the sample size or the samples not being quite fully saturated. The initial void ratios for these twelve samples were in the range 0.64 ± 0.05. However it was noted that the form of the stress paths determined from samples with back pressure saturation was slightly different from those without the saturation. Thus any accurate consideration of stress paths or pore pressure parameters requires that measures must be taken to ensure that the sample and pore pressure measurement system are fully saturated.

It was also noted that the initial part of the stress-strain curve (principal effective stress difference v axial strain) was linear for these undrained tests. When the curves were corrected for initial bedding errors it was possible to determine the tangent modulus for the initial parts of these stress-strain curves. The corrected stress-strain curves were linear for the first one per cent or so of axial deformation. The tangent modulus values calculated from the slope of these curves are plotted against the effective consolidation pressure in Fig.10 for the same twelve samples that have already been discussed above. From this it is seen that there is an approximately linear relation between the tangent modulus value and the pressure under which the sample was consolidated. In addition Fig.10 suggests that the values measured for the tangent modulus are not particularly sensitive to the sample size or to the sample not being quite fully saturated. Similar linear relations were obtained for triaxial series on material with other initial void ratios. As the void ratio decreases the values for the tangent modulus increase. Similar behaviour was observed by Lumb (Ref.9) for the secant modulus measured from drained tests on residual soil from Hong Kong.

It must be noted that this initial linearity of the stress-strain curve does not mean that the material can be regarded as elastic. The fact that the modulus value is not independent of the applied stresses and that the deformation along the initial linear part of the stress-strain curve is not fully recoverable demonstrates this.

Examination of the stress conditions at the onset of the nonlinear part of the stress-strain curves reveals that the curves are linear until the stress path has almost reached the failure line. For samples consolidated at cell pressures up to about 30 psi the stress conditions at the onset of nonlinearity were very close to the failure line and at higher consolidation pressures a little below the line, the distance increasing with consolidation pressure. If this aspect of the behaviour is confirmed for drained tests a pseudo-elastic procedure would probably be suitable for predicting the settlement of the material under foundation loads.

VI.- CONCLUSIONS

This work on the properties of weathered greywacke found at a particular site in Wellington has shown that it is possible to relate the index and mechanical properties for the various materials to a scheme for classifying the weathering of hard rocks. For each grade there are characteristic ranges of values for the various

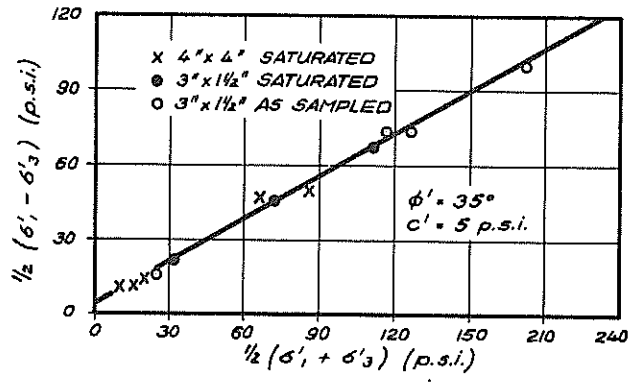

FIG.9 FAILURE POINTS FOR SPECIAL TRIAXIAL SERIES

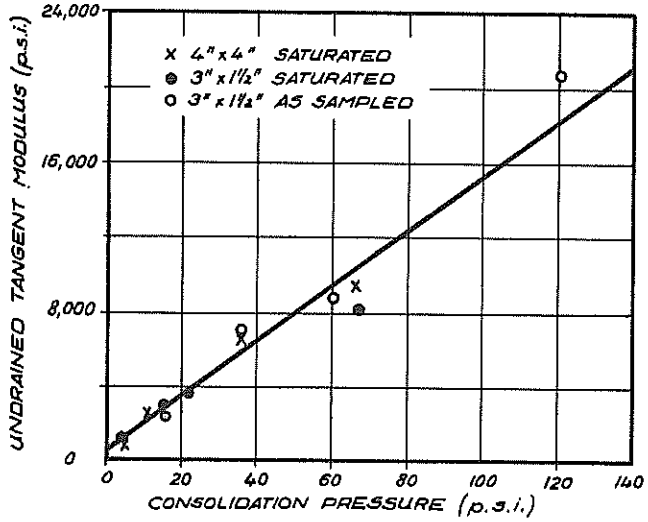

FIG.10 VALUES OF THE UNDRAINED TANGENT MODULUS

properties. It has also indicated the limitation of such a procedure in that for a particular grade the range of values for a property can be fairly wide.

Figures 3, 5, 6, 7 and 8 indicate that the magnitudes of the various mechanical properties for the weathered material are related to the void ratio of the material. Despite a certain amount of scatter among the points plotted, as is to be expected with a natural deposit, these diagrams do indicate a fairly uniform trend as the void ratio changes. This means that although in soil mechanics terms the weathering process results in a whole spectrum of materials with differing properties the current void ratio of the material gives a reasonable indication of the likely range for the values of the various properties for this particular weathered greywacke.

The majority of samples were tested at the degree of saturation after sampling and no specific procedure was used to ensure full saturation. A limited number of triaxial series with back pressure saturation indicated that the measurement of the effective angle of internal friction, the effective cohesion intercept and the tangent modulus is not particularly sensitive to the sample being a few per cent short of full saturation.

VII.- ACKNOWLEDGEMENTS

The laboratory work on which this paper is based was done at the Central Laboratory of the New Zealand Ministry of Works. The writer wishes to thank Mr J.H.H.Galloway, Laboratory Services Engineer, for his interest and the Commissioner of Works for permission to publish the paper and also the following members of the Technical Staff of the Laboratory who did the testing: J.Leca, N.P.Lemmon, T.A.Prieditis, S.H.Robson and F.A. Weston. The writer would also like to acknowledge the cooperation of Dr R.D.Northey, Head of the Soil Engineering Section, Department of Scientific and Industrial Research in making the use of the high capacity consolidometer possible.

VIII.- REFERENCES

1. KNILL,J.L. and JONES,K.S. - The Recording and Interpretation of Geological Conditions in the Foundations of the Roseires, Kariba and Latiyar Dams. Geotechnique, Vol.15 No.1, March, 1965, pp.94-124.

2. WARD,W.H., BURLAND,J.B. and GALLOIS,R.W. - Geotechnical Assessment of a Site at Mundford, Norfolk, for a large Proton Accelerator. Geotechnique, Vol.18, No.4, December 1968, pp.399-431.

3. CHANDLER,R.J. - The Effect of Weathering on the Shear Strength Properties of Keuper Marl. Geotechnique, Vol.19, No.3, Sept. 1969, pp.321-334.

4. SAUNDERS,M.K. and FOOKES,P.G. - A Review of the Relationship of Rock Weathering and Climate and its Significance to Foundation Engineering. Engineering Geology, Vol.4, No.4, Oct.1970, pp.289-235.

5. Report of Subcommittee on Greywacke Terminology. Newsletter Geological Society of New Zealand. No.26, November 1968.

6. NORTHEY,R.D. (in prep.) - Improvements in Soil Sampling: a Modified Triple-Tube Core Barrel.

7. TE PUNGA,M.T. - Relict Red-Weathered Regolith at Wellington. New Zealand Journal of Geology and Geophysics. Vol.7, No.2, May 1964, pp.314-339.

8. ROWE,P.W. and BARDEN,L. - Importance of Free Ends in Triaxial Testing. Journal of the Soil Mechanics and Foundations Division, ASCE, Vol.90, No.SM1, Jan. 1964.

9. LUMB,P. The Residual Soils of Hong Kong. Geotechnique, Vol.15, No.2, June 1965, pp.180-194.

Seismic Attenuation in Engineering Site Investigations

By

E. J. Polak, Dipl. Min. Eng., Ph.D., M.I.E.Aust.

(Geophysicist, Bureau of Mineral Resources, Geology and Geophysics)

SUMMARY. - During geophysical site investigations on sixteen engineering projects, the rate of attenuation of seismic energy travelling through the rock was measured with specially calibrated seismic refraction equipment. Attenuation factors were measured in bedrock and also, in cases where the bedrock/overburden interface was sloping, in the overburden. The results indicate that attenuation factor is related not only to the kind of rock but also to its porosity, jointing, and moisture content. Attenuation factor measurements may indicate discontinuities like faults and dykes, and may support and extend the evidence given by seismic velocity measurements in engineering site investigations.

I.- INTRODUCTION

During seismic refraction surveys, measurements of the pulse amplitude and frequency are not generally made (Ref. 1). These measurements are not difficult but require additional time, especially as the quality of recording must be much higher. The normal refraction technique therefore depends almost entirely on the velocities of longitudinal and (sometimes) transverse waves as the criteria for determination of properties of concealed rocks.

Laboratory and field experiments on the propagation of seismic waves in rocks show that the transmission of elastic energy is not perfect, and that several factors influence the loss of energy. Not all the losses can be explained by the radiation and the geometrical effects; some losses are due to departure from perfect elasticity, friction between particles, composition of rock, water content, etc. As the attenuation of stress in a solid body expresses the mechanical response of the body to applied stress, measurements of attenuation may reveal some of the physical properties. These properties, as well as those obtained from the transmission times of seismic pulses, can assist in planning engineering projects.

II.- NOTATION

A_o; A_1; A_2 = relative amplitudes

V_o; V_1; V_2 = seismic velocity in km/sec

d = distance

K = attenuation factor

θ = angle of dip

i = critical angle of refraction

III.- SEISMIC PULSE AMPLITUDE

When an explosive charge is detonated in the ground the expanding gases press on the rock radially near the shot. In the "fracture zone" the rock is shattered and a large amount of energy is converted to heat which increases the temperature of the gases in the cavity.

A short distance from the fracture zone, where the applied stress still produces permanent deformation by shearing and "plastic flow", the attenuation of seismic pulses is affected by the inelastic behaviour of the material.

Outside the plastic flow zone, the general theory of elastic wave propagation is applicable. This assumes a proportional relation between stress and strain.

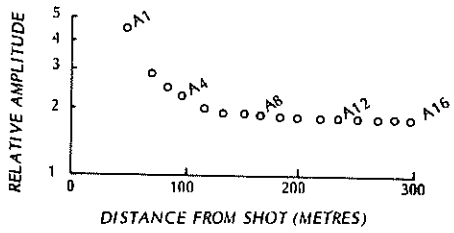

Fig. 1.

Fig. 1 shows the amplitude/distance curve obtained on a geophysical survey in Tasmania. The relative amplitudes are plotted on a logarithmic scale while the distance is linear.

A general formula giving the decrease of the amplitude of the seismic pulse is:

$$A_1 = A_o \exp(-kd) \qquad \ldots\ldots\ldots(1)$$

The formula does not include the factors of geometrical spreading and frequency. The geometrical effect of spreading can be omitted as the distances on which attenuation is measured are similar in engineering refraction surveys at different locations and for different purposes. This also applies to the frequencies, and the question whether the attenuation is due to "viscous damping" (Ref. 2 & 3) and therefore is proportional to the square of

its frequency, or is due to the "internal friction" (Ref. 4 & 5) and is directly proportional to frequency, does not arise. Fourier analyses were carried out on several records, and indicated that the maximum energy is transmitted at frequencies of 40 to 50 Hz. Born (Ref. 5) has shown that with frequencies below 150 Hz viscous damping is not important.

To avoid any confusion with the results of other investigators it is proposed to call the numerical value obtained from formula 1 the "attenuation factor". It means that corrections for the effect of frequency and geometrical spreading are not made.

IV.- INSTRUMENTATION AND FIELD PROCEDURE

Two standard seismic refraction units with 12 or 24 channels were used in the attenuation tests. Both units were calibrated for uniform response in frequency, phase, and amplitude.

After extensive tests with geophones of sizes ranging from 110 g to 1.5 kg and frequencies ranging from 2 to 40 Hz a set of 30 geophones weighing 110 g with natural frequency 20 Hz was chosen. These geophones produced best coupling with the ground, there was no differential movement of geophones relative to the ground, and no resonance of the geophone; good reproducibility was obtained with repeated shots, and identical results were obtained with "bundle tests", where all the geophones were placed together.

A pulse of 50 Hz frequency from an oscillator was fed parallel into all the channels after each record to obtain the relative gain of the amplifiers. The amplitude of the signals received through the ground by different geophones were calculated by dividing the amplitude of the deflection of a trace of the field record by the amplitude of the corresponding calibrating record.

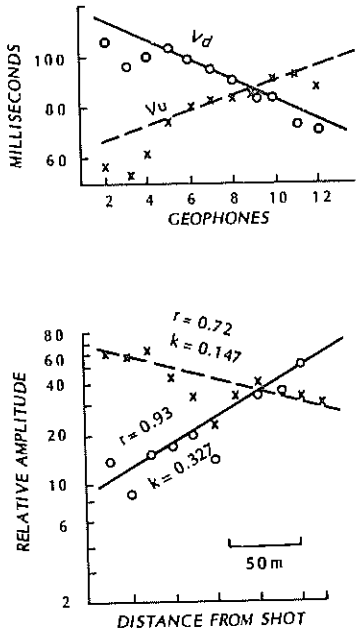

Fig. 2.

V.- CALCULATION OF RESULTS

Fig. 2 shows a complete set of the results of a field test at Koombooloomba, Queensland. The top graph in the figure shows the time-distance curves obtained from shots fired from both ends of the geophone spread. It is a standard plot as used in seismic refraction surveys. From this plot we obtain four values.

(i) The downslope velocity V_d = 3.3 km/sec

(ii) The upslope velocity V_u = 6.3 km/sec

(iii) The true velocity V = 5.4 km/sec

(iv) The angle of dip = $3^o45'$

At the bottom of Fig. 2 the relative values of the amplitude of the deflection on the field record are plotted against distance from shot to geophone. The best-fitting straight line is calculated using the least-squares method.

On geophones 2, 3, and 4 the times of first arrivals plot below the lines. These early arrivals are due to thinner overburden. The attenuation curve shows similar distortion. Geophone 6 indicates a smaller pulse amplitude without any corresponding anomaly in the time-distance curve. This anomalous attenuation may be the result of poor coupling between geophone and ground.

In the example in Fig. 2 the interface is sloping at $3^o45'$; therefore two values of attenuation factor are obtained:

The upslope attenuation factor k_u = 0.147

The downslope attenuation factor k_d = 0.327

Two formulae were developed for the case in Fig. 2:

(i) The true attenuation factor in a refractor with velocity V_1 is

$$k_1 = (k_d + k_u) / 2 \cos \theta \qquad \text{.....(2)}$$

(ii) The average attenuation factor k_o in the overburden with an average velocity V_o is

$$k_o = \left[k_d \cos(i-\theta) - k_u \cos(i+\theta)\right] / \sin 2\theta \qquad \text{.....(3)}$$

Critical angle of refraction, i, is calculated from Snell's Law (Ref. 1).

It is clear from the above example that in the case where an interface is parallel with the ground surface, only one value for the attenuation factor is obtained and the calculation of the attenuation factor in the overburden is impossible.

In the case of a sloping interface it is also possible to calculate the attenuation factor graphically.

Fig. 3 shows the results obtained at a damsite in Tasmania. The angle of dip of the interface (as obtained from the seismic velocities) is plotted against the attenuation factor k. A straight line is drawn through each pair of points. The intersection of this line with the zero dip line gives the value of the attenuation factor in the refractor (the bedrock).

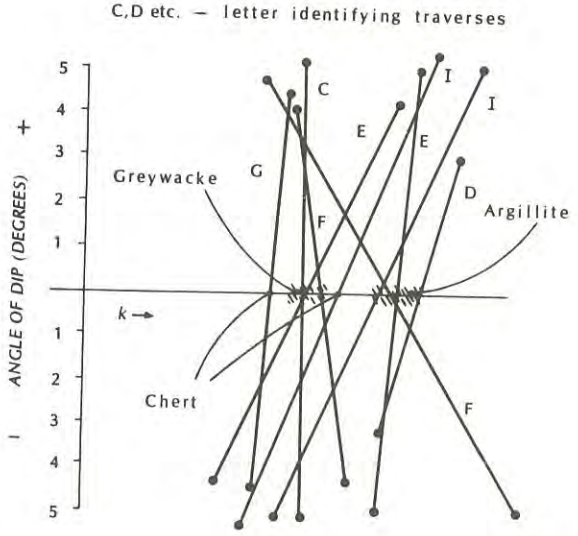

Fig. 3.

The site from which the attenuation factors are plotted in Fig. 3 was extensively drilled and the results of drilling were available to help in interpretation of geophysical data. The following conclusions were reached:

(a) An attenuation factor between 0.414 and 0.46 was found in an area in which boreholes proved that the bedrock is argillite.

An attenuation factor between 0.331 and 0.361 was found in an area of proved greywacke.

An attenuation factor of 0.382 was found in an area of chert; however on Traverse G where the presence of chert is suspected an attenuation factor of 0.304 was measured. It is possible that the attenuation factor of chert has a very wide range.

(b) Traverses E and D measured at right angles to each other indicate a small difference in attenuation factor. This difference is only 5 percent, which is equal to the possible error in attenuation measurement.

(c) The slopes of straight lines in Fig. 3 indicate that the attenuation factor in overburden can be higher or lower than those found in bedrock. A slope downwards to the left indicates that the overburden is characterised by a lower attenuation factor than that in the bedrock, as on Traverses E and I, which are both oriented at right angles to the slope. On Traverses C, D, and G the attenuation factor in the overburden nearly equals that in the bedrock; these traverses are oriented along the slope. On all these traverses the overburden consists of weathered argillite. The difference in the attenuation factor in the overburden - lower along the strike and higher along the slope - may be explained by the fact that the overburden slumps downwards towards the river and therefore decreases the compaction in the direction of the slope.

(d) The attenuation factor in wet, weathered argillite is lower than that in fresh argillite.

(e) The attenuation factor in the overburden on Traverse F is higher than that in the bedrock. Two drill-holes on this traverse indicate river gravels 12 metres thick above the water-table.

VI.- ATTENUATION VERSUS OTHER PROPERTIES OF ROCKS

The attenuation factor was measured on sixteen surveys by the Engineering Geophysics Group of the Bureau of Mineral Resources. The surveys were done in several States and in the Territory of Papua & New Guinea; the geological conditions differed greatly and the purpose of the surveys alternated between pure engineering and hydrology. It is therefore not surprising that when all the values of attenuation factor measured on those surveys are plotted on one graph against some other property (say specific gravity as in Fig. 4a) no simple relation is demonstrated. It is evident from the dispersion of points on the graph that attenuation is also influenced by some other property of the rocks, especially at lower specific gravities. In Fig. 4b the attenuation factor is plotted against the values of modulus of elasticity measured by the dynamic method in situ. In this case all the rocks with seismic velocities less than 2.0 km/sec were omitted. The correlation is much better.

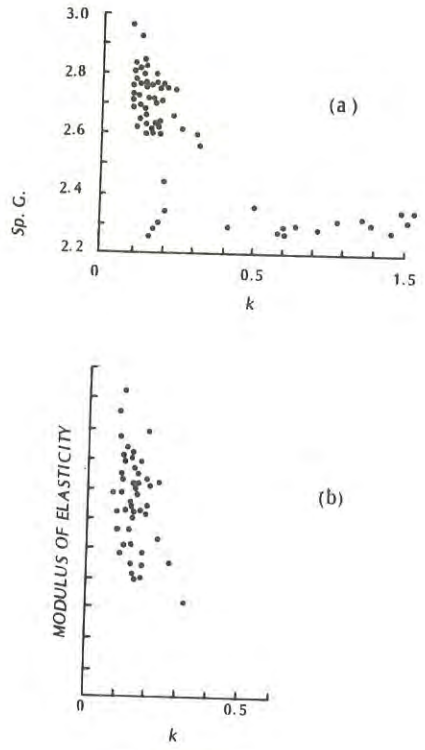

Fig. 4.

VII.- FACTORS THAT AFFECT ATTENUATION IN ROCKS

(a) Rock Type

O'Brien (Ref. 6) stated that attenuation is less in igneous rocks than in sedimentary rocks. The author's investigations generally confirm this statement, as illustrated by the following measured values.

(i) Igneous rocks

dolerite	0.230 to 0.345
granite	0.230 to 0.345
trachyte	0.2185 to 0.230

(ii) Sedimentary rocks

argillite	0.414 to 0.460
chert	0.299 to 0.280
greywacke	0.299 to 0.368
limestone	0.357
pyroclastics	0.368
quartzite	0.299 to 0.345
sandstone	0.357 to 0.575
(iii) Overburden	0.373 to 2.415

(b) Porosity, Jointing and Moisture Content

The influences of these three factors must be investigated together as they are very closely related.

The attenuation factor of dry consolidated rock is directly proportional to the porosity (and therefore to the seismic velocity). At low porosities there is no difference between attenuation in dry and wet rock. With increasing porosity in saturated solid rock the attenuation increases, especially if the pores are interconnected so that some energy is used in overcoming friction when liquid is forced through passages (Ref. 5 & 7). This relation does not apply to cavernous chert.

The attenuation is greatly reduced when an unconsolidated layer becomes water-saturated. In this case there is a bodily movement of liquid with material suspended in it. As an example wet sand has an attenuation factor of 0.207 to 0.598, moist sand 1.035 to 1.725, and dry sand 2.300 to 3.220. The presence of clay, expecially of the expansive type, lowers the attenuation factor greatly when wet.

(c) Pressure

All the engineering geophysical surveys deal with near-surface layers of rocks, so that the increase of pressure with depth is not significant. However, it is reasonable to infer that the attenuation factor will decrease with an increase in pressure. Indeed, during crustal studies (Ref. 8) the measured attenuation factors at a depth of about 30 km were 0.0014 and 0.0168.

(d) Faults and Dykes

The attenuation factor increases greatly across a fault or a shear zone, the increase depending on the characteristics of the material in the zone and the thickness of the zone.

On one survey the attenuation factor across a fault zone 0.6 m wide in quartzite was measured at 1.15 compared with 0.299 for the undisturbed state. Similarly in chert the attenuation factor increased from 0.345 to 0.552 when crossing a fault.

The presence of weathered dykes in granite increased the attenuation factor from 0.23 to 0.403.

(e) Attenuation Anisotropy

On one site in pyroclastics, attenuation factors were measured parallel and at right angles to the bedding. The attenuation parallel to the bedding was one-half of that measured at right angles. This case was complicated by the fact that the steeply dipping bedding planes were parallel to the sides of the gorge; the release of the pressure could have opened joints parallel to the bedding planes and so increase attenuation. Similar facts have been noted in another location, where the exfoliation of trachyte in a gorge influenced the attenuation at right angles to the faces of the gorge. On two other sites the results suggested that attenuation anisotropy was caused by slumping of overburden down the slope.

(f) Increased Attenuation in Thin Beds

This effect is quite common in seismic refraction work and was noted on four surveys. Quantitative investigation is impossible without drilling evidence.

VIII.- CONCLUSIONS

There are three characteristics of a seismic pulse travelling through a rock: the velocity, the shape of the pulse, and the amplitude.

Initially only the velocity was used to determine the depth and the character of the buried rock. With the advent of magnetic recording, the frequency of the pulse started to play a part in interpreting the characteristics of the rock. The data in this paper indicate that the attenuation of seismic waves in the rock can not only support the evidence provided by velocity but can give additional information to be used for the efficient engineering design of foundations.

IX.- ACKNOWLEDGEMENTS

The author wishes to thank Dr N.H. Fisher, Director of the Bureau of Mineral Resources, Geology & Geophysics for permission to publish these data. He also wishes to acknowledge the help given by several colleagues from the Bureau and the University of Melbourne. The data in this paper are drawn from the author's thesis (Ph.D) submitted to the University of Melbourne.

REFERENCES

1. HEILAND, C.A. - Geophysical Exploration. Prentice Hall, New York. 1946.

2. HOSALI, N.M. - On Seismic Waves in a Visco-Elastic Earth. Proc. Roy. Soc. (A) 104, 271, 1923.

3. SEZAWA, K. - On the Decay of Waves in Visco-Elastic Solid Bodies. Earth Res. Inst. Bull. 3, 19-27, 1927.

4. KIMBALL, A.L. - Vibration Prevention Engineering. John Wiley & Sons, London, 1927.

5. BORN, W.T. - The Attenuation Constants of Earth Materials. Geophysics, 6, 132-148, 1941.

6. O'BRIEN, P.N.S. - The Use of Amplitude and Frequency in Exploration Seismology. 5th World Petrol. Congress Sect. 1. paper 34, 627-644, 1959.

7. KOLTONSKI, W. and MALECKI, J. - Ultrasonic Detection of Mineral Layers. Acoustica 8, 307-314, 1958.

8. DOYLE, H.A., UNDERWOOD, R. and POLAK E.J. - Seismic Velocities from Explosions off the Central Coast N.S.W. Geol. Soc. Aust. 13 (2), 335-372, 1966.

Classification of Rock for Engineering Purposes

By
LEONARD OBERT, PH.D.
(Science Adviser—Mining Research, U.S. Bureau of Mines)
AND
CHARLES RICH
(Mining Engineer, U.S. Bureau of Mines)

SUMMARY -- Although a number of classifications for both intact rock and rock masses have been proposed, these classifications, in general, do not relate to specific engineering applications. This report outlines research in progress by the U.S. Bureau of Mines to develop rock mass classifications related to two ground support problems, namely, caveability of ground (as in a block caving mine), and attainable unsupported spans, (as in an open-stope mine). The mechanical and geological property data used in these classifications are obtained from cores taken from operating mines. Techniques for quantizing geological features in the cores are briefly described.

Many investigators have considered ways of classifying rock on the basis of some mechanical or quantifiable geological property of the rock, or some combination of these factors. These classifications can be divided into two categories; (1) classification of intact rock, and (2) classification of rock masses. The intact properties used in these classifications include the laboratory-determined unconfined compressive and tensile strengths, triaxial (confined) strengths and friction, deformation moduli, seismic velocities, and indentation (or hardness). Rock mass classifications have used, in addition to the intact mechanical properties, in-hole and cross-hole seismic velocities, and geological factors such as the percentage core recovery and joint (or fracture) spacing. These mechanical and geological properties can be obtained from measurements in exploration holes or cores taken from these holes.

However, a review of the literature disclosed that there is only very limited information on how these classifications relate to specific mining problems or applications. For example, it is logical to suppose that because processes such as pneumatic drilling, diamond drilling, or large-diameter boring (as with a tunneling machine) create mostly fresh rock surfaces, a classification based on the properties of intact rock should relate to drilling and boring capabilities or rates. There is very little information in the literature showing such a relationship and, in fact, a questionnaire sent to tunneling machine manufacturers revealed that they do not use any such classification. Some manufacturers do rate their machines in terms of an upper limit on the unconfined compressive strength of the rock that the machine will bore, but properties other than compressive strength affect boring rates. These manufacturers are more likely to estimate bore rates on the basis of an index established by boring in an equivalent rock type with a model drill.

The use of classifications for rock masses is almost as indefinite. For example, it might be expected that ground support requirements would relate to some rock mass classification based on measured rock properties. One report (1)[3] does classify "rock quality" in terms of RQD (rock quality designation)[4] and presents a chart, Table I, giving "Guidelines for Selection of Primary Support for 20-ft to 40-ft Tunnels in Rock." However, the literature does not contain any equivalent tables for support requirements for chambers or mine openings classified in terms of RQD or any other measured rock property. Moreover, as will be indicated later in this report, RQD may not be satisfactory for such purposes.

If geomechanics is to serve the excavation industry, it should answer such questions, because the most critical decision-making period is when the exploration cores from a project become available for observation and test. For example, consider a tunneling project: At the conclusion of exploration the following decisions must be made; can the tunnel be machine bored and, if so, will machine boring be economically favorable in comparison to conventional mining? What will be the expected rate of progress? Will the ground stand unsupported, or will support ranging from rock bolts, to heavy sets and concrete lining be required? Errors in judgment at this point can result in substantial delays that can be costly to either the contractor or owner, or both.

---

[1] Science Adviser-Mining Research, Office of Science Adviser-Mining Research, U.S. Bureau of Mines, Denver, Colo.

[2] Mining Engineer, Office of Science Adviser-Mining Research, U.S. Bureau of Mines, Denver, Colo.

[3] Underlined numbers in parentheses refer to items in the list of references at the end of this report.

[4] Rock quality designation (RQD) is the ratio of length of core recovered, counting only those pieces of intact rock 4 inches in length or longer, to the total length or core run.

Table I--Guidelines for selection of primary support for 20-ft. to 40-ft. Tunnels in Rock [Deere, et al (1)]

Rock Quality	Construction Methods	Steel Sets			ALTERNATIVE SUPPORT SYSTEMS(5)				
					Rock Bolts(3) (Conditional use in poor & very poor rock)		Shotcrete Conditional use in poor & very poor rock(4)		
							Total Thickness		
		Rock Load (B-Tunnel Width)	Weight of Sets	Spacing(2)	Spacing of Pattern Bolts	Additional Requirements and Anchorage Limitations(a)	Crown	Sides	Additional Support(4)
Excellent(1) RQD > 90	Boring Machine	(0.0 to 0.2)B	Light	None to Occasional	None to Occasional	Rare	None to occ. Local Application	None	None
	Drilling & Blasting	(0.0 to 0.3)B	Light	None to Occasional	None to Occasional	Rare	None to Occ. Local App. 2 to 3 in.	None	None
Good RQD = 75 to 90	Boring Machine	(0.0 to 0.4)B	Light	Occasional to 5 to 6 ft.	Occasional to 5 to 6 ft.	Occasional mesh & straps	Local App. 2 to 3 in.	None	None
	Drilling & Blasting	(0.3 to 0.6)B	Light	5 to 6 ft.	5 to 6 ft.	Occasional mesh & straps	Local App. 2 to 3 in.	None	None
Fair RQD = 50 to 75	Boring Machine	(0.4 to 1.0)B	Light to Medium	5 to 6 ft.	4 to 6 ft.	Mesh & straps as required	2 to 4 in.	None	Provide for rock bolts
	Drilling & Blasting	(0.6 to 1.3)B	Light to Medium	4 to 5 ft	3 to 5 ft.	Mesh & straps as required	4 in. or more	4 in. or more	Provide for rock bolts
Poor RQD = 25 to 50	Boring Machine	(1.0 to 1.6)B	Medium Circular	3 to 4 ft.	3 to 5 ft.	Anchorage may be hard to obtain. Considerable mesh and straps required.	4 to 6 in.	4 to 6 in.	Rock bolts as required (~4-6 ft. oc.)
	Drilling & Blasting	(1.3 to 2.0)B	Medium to Heavy Circular	2 to 4 ft.	2 to 4 ft.	Anchorage may be hard to obtain. Considerable mesh and straps required	6 in. or more	6 in. or more	Rock bolts as required (~4-6 ft. oc.)
Very Poor RQD < 25 (Excluding Squeezing & Swelling ground)	Boring Machine	(1.6 to 2.2)B	Medium to Heavy Circular	2 ft.	2 to 4 ft.	Anchorage may be impossible. 100% mesh and straps required.	6 inches or more on whole section		Medium sets as required
	Drilling & Blasting	(2.0 to 2.8)B	Heavy Circular	2 ft.	3 ft.	Anchorage may be impossible. 100% mesh and straps required.	6 inches or more on whole section		Medium to heavy sets as required
Very poor, Squeezing or Swelling gr.	Both Methods	Up to 250 ft.	Very Heavy Circular	2 ft.	2 to 3 ft.	Anchorage may be impossible. 100% mesh and straps required	6 inches or more on whole section		Heavy sets as required

NOTES: (1) In good and excellent quality rock, the support requirement will in general be minimal but will be dependent upon joint geometry, tunnel diameter and relative orientations of joints and tunnels.

(2) Lagging requirements for steel sets will usually be minimal in excellent rock and will range from up to 25% in good rock to 100% in very poor rock.

(3) Bolt diameter = 1 in. Length = 1/3 to 1/4 tunnel width. It may be difficult or impossible to obtain anchorage with mechanically anchored rock bolts in poor and very poor rock. Grouted anchors may also be unsatisfactory in very wet tunnels.

(4) Because shotcrete experience is limited, only general guidelines are given for support in the poorer quality rock.

(5) Table reflects 1963 technology in U. S. A. Groundwater conditions and the details of jointing and weathering should be considered in conjunction with these guidelines, particularly in the poorer quality rock. See Deere et al. (1) for discussion of use and limitations of the guidelines for specific situations.

In an exploratory investigation for an underground chamber such as that for a power station, the principal problem is to determine the span that will stand either unsupported, or with minimum support such as rock bolts and a wire-mesh-shotcrete surface treatment. Considering that spans ranging from 50 to 80 ft or more are generally required for such chambers, a critical evaluation of the rock that will form the roof of the chamber must be made.

In mining the problem is even more complex. Presuming that an ore body has been delineated by exploration, a mining method must be selected that will provide for a satisfactory recovery and rate of production from the deposit, and be otherwise economic. The selection of this method will be determined primarily by the properties of the rock that comprise the ore body, the immediate rock surrounding the deposit, and the rock forming the overlying cover. Assuming that a rational selection of the mining method can be made, it is generally necessary at this time to decide on production capabilities and hence the size of the shaft, the mill capacity, and other surface facility requirements. Also, a substantial part of the mining machinery must be ordered considerably in advance of the start of production. These decisions must be made almost immediately following exploration because of the large capital investment that is involved in bringing a modern mine into production. This capital investment may be in excess of $10 million, and in some instances over $100 million. Thus, the judgments that must be made on the basis of observations and tests on core or boreholes must be reliable or costly delays, and losses incurred in the purchase of improper equipment will result.

Because previous classifications based on observations and tests on exploration cores or in exploration cores or in exploration holes have been only indefinitely related to specific excavation problems, an investigation was initiated in which the problem was approached from a different direction. Two geomechanical problems were selected; namely, the caveability of rock (as experienced in block caving mines), and the attainable unsupported span (as experienced in open stope mines). Operational data related to ground support were collected (and are continuing to be collected) from a number of operating mines. Also, exploration cores were obtained from these mines (either from past explorations or from present borings). The cores included the rock types that comprise the ore body, the immediate rock surrounding the ore body and, whenever possible, from the overlying cover. A routine set of geological observations and mechanical property tests are performed on these cores. These data are than analyzed to ascertain which or what combination of these measured properties are significant in relation to the specified excavation problem. These selected data will form the basis for classification.

In so far as possible the mines selected for study have been chosen to include operations in a variety of rock types. Also, preferential consideration has been given to mines in which uncontrolled failures have been experienced, that is, failures due to misjudgments, because these failures are in effect a limiting test of the rock structure.

The combination of operational and geomechanical data that have been collected to date are much too extensive to present in detail. However, Table II includes the more significant operation data obtained from a number of block caving mines, together with a part of the geomechanical data. Table III presents the same information obtained from open stope mines.

Several interesting inferences already have been made from the analysis of these data. First, the unconfined compressive strength of the rock comprising or surrounding the ore body is only secondarily related to the unsupported span that can be mined. For example, borax ore (see Row 1, Table II), which is a combination of borax, kernite, and shale, is one of the weakest rock tested to date, having an unconfined compressive strength ranging from 1100 to 6000 psi. However, an unsupported area approximately 140 x 270 ft. has been mined in this rock type (2). Rooms 150 ft. wide are routinely mined in dome salt (halite), a rock that has an unconfined compressive strength of about 5000 psi and, hence, would be rated as one of the weaker rocks. On the other hand, a monzonite porphyry with a compressive strength of about 20,000 psi taken from a block caving mine (see Row 9, Table II), will cave freely if the span exceeds 10 ft. A comparison of these results leads to the rather obvious conclusion that some factor other than compressive strength dominates the length of span that can stand unsupported. As might be expected, in the cases cited this factor is the absence or occurrence of joints and fractures. Both borax ore and salt are virtually massive and unfractured rock types, whereas the monzonite porphyry has a joint and fracture spacing of about 3 to 24 inches. However, in an open-stope mine (see line 11, Table III) rooms with a span of 75 ft. have been mined and remained stable for many years in a jaspilite (roof rock) that has a joint spacing of 4 to 6 inches. Thus, there is some other factor than joint spacing that must be considered in relation to unsupported spans. This factor is not attributed to the type and extent of fill materials in joints and fractures, and the degree to which these fill materials indurate and recement.

The strengthening ability of even a weak bond across a joint plane is not too surprising if one considers that an average bond strength of, say, 5 psi across a horizontal joint plane will support 5 feet of underlying rock against the force of gravity. It is improbable that a diamond drill core can be taken across a joint plane that only has a bond strength of 5 psi.

Unfortunately, there has been no means of numerically evaluating the bond strength across joints except when the bond is strong enough so that a core can be taken across the joint plane. A research project, under the direction of Pincus[5] and Wipf[6], has been started to identify the alteration and decomposition products that form on joint planes and to determine which of these materials tend to indurate and recement. The rock materials used in these studies

---

[5] Howard J. Pincus, Dean and Professor, College of Letters and Science, The University of Wisconsin, Milwaukee; and U.S. BuMines Consultant.

[6] Robert A. Wipf, Graduate Student, University of Wisconsin, Milwaukee; and Intermittent employee, U.S. BuMines.

TABLE II - Characteristics of Caving Stopes

Mine and Location	Mining Method	Minimum Span or Area to Cave (ft)	Maximum Unsupported Span or Area (ft)	Stope Depth (ft)	Ore Deposit			Surrounding Rock			Overburden		
					Rock Type (Gangue)	Partings or Joints	Cohesion	Rock Type	Partings or Joints	Cohesion	Rock Type	Partings or Joints	Cohesion
Jennifer Boron, Calif.	Experimental block cave	?	113 - 149 x 272 Arching	300+	Borax C_o 1,100-6,600 CR 100	Clay fractures, borax-filled	Weak	Shale C_o 900-1,200	Partings, thin-bedded	Weak	Playa C_o 745-3,353 (CR ~ 5)	None	----
Grace Morgantown, Pa.	Continuous block cave	Undercut 15 x 25	4 x 6 Drift	1500+	Limestone, chlorite	4 Joint systems	Weak-medium	Limestone	4 Joint systems	Weak-medium	Sandstone, shale, quartzite		Weak
Climax Climax, Colo. Area A	Block cave assisted by longholing	> 200 x 200	200 x 200 No cave	1460+	Unmineralized quartz, granite, schist gneiss	Quartz-pyrite-filled JS 6-24	Strong	Granite, schist	Pyrite-, gouge-filled or open JS 1-24	Weak	Granite, schist	Weathered, gouge-filled or open JS 1-24	Weak
Area B	Block cave assisted by longholing	200 x 200	12 - 14 Drifts	1460+	Quartz, porphyry granite CR 84 - 98 RQD 68	Quartz-molybdenum-pyrite-filled JS 6 - 24	Strong	do.	do.	do.	do.	do.	do.
Area C	Block cave	100 x 200	< 12 ? Drifts	1460+	Quartz, porphyry, granite (C_o 17,680) CR 84, RQD 16	Sericite-molybdenum-pyrite-filled JS 1-24	Medium	do.	do.	do.	do.	do.	do.
Area D	Block cave	> 25	0	1460+	Quartz, porphyry, granite CR 86 - 84 RQD 8	Sericite-molybdenum-pyrite-filled or open JS > 1	Weak	do.	do.	do.	do.	do.	do.
Crestmore Riverside, Calif.	Block cave assisted by shrinkage stopes	80 x 200	60 x 200	730-915	Limestone (marble) C_o 4,430-19,900 RQD 55-70	Sporadic, tight, well-healed	Strong	Limestone (marble) C_o 4,430-19,900 RQD 55-70	Sporadic, tight, well-healed	Strong	Grano-diorite 0 - 200 ft	Solution channels, weathered or tight (JS 1-24)	Strong
White Pine White Pine, Mich.	Experimental longwall	125 x 320	> 80	400+	Shale C_o 12,750-26,050	Calcite-quartz-filled (JS > 12)	Weak-medium	Shale, laminar C_o 11,680-30,920	Calcite-quartz-filled (JS > 12)	Weak-medium	Sandstone C_o 16,940-23,720 CR 95+	Calcite-quartz-filled (JS > 12)	Weak-medium
San Manuel San Manuel, Ariz.	Block cave	> 10	0	1100+	Monzonite porphyry C_o 17,240-21,360 quartz monzonite C_o 10,909-27,625 rhyolite dikes C_o 20,000-39,960	Sericite-chlorite-clay-filled with hypothermal alteration 8 systems JS < 3-24	Weak	Monzonite porphyry C_o 17,240-21,360 quartz monzonite C_o 10,909-27,625 rhyolite dikes C_o 20,000-39,960	Sericite-chlorite-clay-filled with hypothermal 8 systems JS < 3-24	Weak	Conglomerate silt and marl C_o 541	Occasional fault	Medium-strong
Mather A and B Negaunee, Mich.	Block cave	< 6	0	2000+	Hematite, soft and plastic	Diorite dikes	----	Iron formation	3 Systems of joints diorite dikes (JS < 24)	Weak	Iron formation, greenstone C_o 26,200-39,800	3 Systems of joints (JS < 24)	Strong

( ) Estimated
JS Average joint spacing (in.).
RQD Rock Quality Designation (pct).
C_o Compressive strength (psi).
CR Core recovery (pct).

TABLE III - Characteristics of Self-Supported Stopes

Mine and Location	Mining Method	Extraction (%)	Maximum Unsupported Span or Area (ft)	Stope Height (ft)	Stope Depth (ft)	Ore Deposit			Surrounding Rock			Overburden		
						Rock Type	Partings or Joints	Cohesion	Rock Type	Partings or Joints	Cohesion	Rock Type	Partings or Joints	Cohesion
Hockley Hockley, Tex.	Room and random or regular pillar	60	70 x 130	40+ Flat roof	1400+	Dome salt CR 100	None	----	Dome salt	None	----	Massive anhydrite	?	----
Friedensville Friedensville, Pa.	Room and regular pillar	60	38	25 Arched roof	225+	Dolomite and quartz breccia	Sphalerite-pyrite-calcite-filled (JS > 12)	Weak-medium	Dolomite, limestone	Calcite-pyrite-mud-filled	Weak-medium	Sandstone, limestone	Calcite-clay-filled	Weak
Jennifer Boron, Calif.	Room and regular pillar	30-40	17	8 - 32 Flat roof	300+	Borax C_o 1,100-6,600 CR 100	Clay fractures, borax-filled	Weak	4-5 ft. Borax, then shale C_o 900-1200	Partings, thin-bedded	Weak	Playa C_o 745-3,353 (CR ~ 5)	None	----
Lead Hill #10 Federal Flat River, Mo.	Room and random pillar	90+	180 x 430	11-28 Flat arched roof	348+	Dolomite CR 90+	Partings, calcite-filled PS 6-24	Weak-medium	Dolomite CR 90+	Partings, calcite-filled PS 6-24	Weak-medium	Dolomite CR 90+	Partings, calcite-filled PS 6-24	Weak-medium
Tri-State District Mo., Kans., Okla.	Room and random pillar	60+	50	17+ Flat arched roof	400-700	Dolomite, chert	Occasional joints	----	Dolomite, chert	Occasional joints	----	Dolomite chert	Occasional joints	----
Clonan Mineville. N. Y.	Room and random pillar	67-80	125 - 200	150-200 Arched roof	400+	Massive magnitite C_o 20,500	Occasional joints	Strong	Massive gneiss C_o 27,100-34,300	JS > 24	Strong	Gneiss gabbro C_o 27,100-34,300	Occasional joints	Strong
Plasterco Saltville, Va.	Room and random pillar	80+	60 x 110	30-100 Arched roof	200+	Shale, gypsum	Calcite-filled (JS > 12)	Medium	Shale	Calcite-filled (JS > 12)	Weak-medium	Sandstone, limestone	Blocky	Weak-medium
Rifle Rifle, Colo.	Room and regular pillar	75	80 - 200	73 Flat roof	700-900	Marlstone C_o 16,600	Partings and occasional joints (PS > 18)	Weak-strong	Marlstone (shale) C_o 16,600	Partings and occasional joints (PS > 24)	Weak-strong	Marlstone C_o > 16,000	Partings PS > 24	Weak-strong
Crestmore Riverside, Calif.	Room and regular pillar	75+	60 - 200	25 Arched roof	730+ 915	Limestone (marble) C_o 4,430-19,900 RQD 55-70	Sporadic, tight, well-healed	Strong	Limestone (marble) C_o 4,430-19,900 RQD 55-70	Sporadic, tight, well-healed	Strong	Grano-diorite 0-200 ft.	Solution channels. weathered. tight (JS 1-24)	Weak-medium
White Pine White Pine, Mich.	Room and regular pillar	70-75	> 80	15-20 Flat roof	400+	Shale C_o 12,750-26,050	Calcite-quartz-filled (JS > 12)	Weak	Shale laminar C_o 11,680-30,920	Calcite-quartz-filled (JS > 12)	Weak-strong	Sandstone C_o 16,940-23,720 CR 95+	Calcite-quartz-filled (JS > 12)	Weak-medium
Cliffs Shaft Ishpeming, Mich.	Room and random pillar	75	65 x 75 90 x 230 rock bolted	90-100 Arched roof	850+	Specular hematite C_o 47,800	Tight (JS > 12)	Weak-medium	Argellaceous, slate C_o 47,800 / Jaspilite C_o 49,600	Tight (JS > 12) / Silica-filled (JS 4-6)	Weak-medium / Medium	Massive quartzite C_o 43,200	Tight JS > 24	Medium

( ) Estimated
PS Average parting separation (in.)
JS Average joint spacing (in.)

RQD Rock Quality Designation (pct)
C_o Compressive strength (psi)
CR Core recovery (pct)

Fig. 1 -- Photograph made from acetate peel (2X), Granite No. 1.

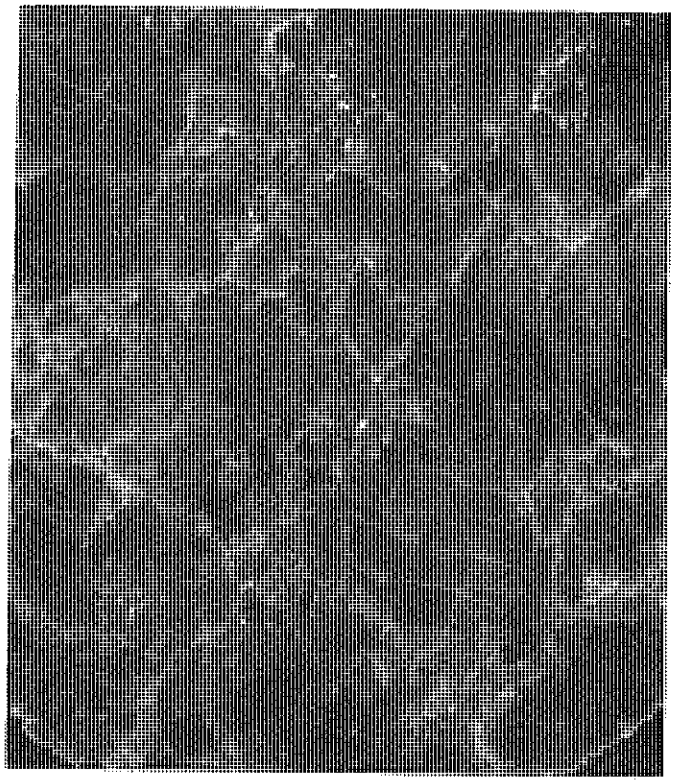

Fig. 2 -- Photograph made from acetate peel (2X), Granite No. 2.

are from the various mines in which other operational and geomechanical data are obtained. If this study can lead to even a rough quantitative classification of joint filling materials it would assist in assessing the ground supportability of the rock materials in exploration cores.

In block caving mines it is frequently reported that some areas are easy to cave, whereas others are more difficult to cave. This difference is due in part to the degree in spacing of joints and fractures. However, it is also due in part to the degree of alteration in the host rocks which, in turn, is probably related to the rock strength. An investigation, also under the direction of Pincus and Wipf, is in progress to determine if an alteration index for rock can be developed, that is, some quantitative measure of the degree of alteration. It is hypothesized that alteration is accompanied by the development of microfractures, and that the degree of microfracturing is related to the degree of alteration. Also, alteration may produce preferred spatial orientations of microfractures. The degree of microfracturing is being investigated by two techniques. The first involves applying a fluorescent dye penetrant to a sawed rock surface and observing the microcrack in this surface under ultraviolet light. In the second technique an acetate sheet softened in acetone is pressed against a sawed rock surface. When the sheet hardens it is peeled from the rock and the fractured detail observed on the peel.

The dye penetrant-ultraviolet light technique produces some visual enhancement of the microfractures, and even better detail is shown in the photograph of the peel. Photographs of peels taken from two granite specimens are shown in Figs. 1 and 2. The peel has a further advantage in that it can be subjected to an optical processing technique developed by Pincus (3,4), a technique that is helpful in determining if the microcracks lie in preferred directions. Using these methods, both the extent and orientation of microfractures can be quantized.

An up-hole or cross-hole seismic method is also being developed for evaluating in situ "rock quality." In this method a small charge is detonated in an exploration hole and the generated seismic signal picked up either at distant points within the same hole (up-hole) or in other exploration holes (cross-hole). From an analysis of the amplitude-frequency spectrum of the received signals, a seismic absorption coefficient for some specified frequency can be determined. This coefficient is sensitive to both rock type (5) and the degree of jointing and fracturing within a given body of rock (6). A "rock quality" index is being developed by comparing the absorption coefficient for a rock mass to the coefficient for an intact specimen taken from the same mass.

Collectively, the results from these studies indicate that at least three factors affect the caving properties of rock, or the ability of rock to sustain a specified unsupported span; namely, and in order of

importance, the joint and fracture spacing, the degree of bonding across joints and fractures, and the rock strength or the degree of alteration.

In relation to problems other than ground support, this investigation suggests that there will probably be as many rock classifications as there are engineering problems. Thus, there may be a classification for pit slope angles, drillability, boreability and blastability of rock, as well as other factors that enter into the excavation process. Also, it would appear that performing mechanical property or geological tests on rock is an unprofitable exercise unless the test results are related to some specific engineering problem.

REFERENCES

1. DEERE, D. U.; PECK, R.B.; MONSEES, J.E.; PARKER, H. W.; and SCHMIDT, B. - "Design of Tunnel Support Systems," Proc. 49th Annual Meeting, Highway Research Board, Jan. 1970.

2. OBERT, LEONARD and LONG, ALBERT E. - "Underground Borate Mining, Kern County, Calif.," BuMines Rept. of Investigation 6110, 1962, 67 pp.

3. PINCUS, HOWARD J. and DOBRIN, MILTON B. - "Geological Applications of Optical Data Processing," J. Geophys. Res., Vol. 71, No. 20, October 1966, pp. 4861-4869.

4. PINCUS, HOWARD J. - "Sensitivity of Optical Data Processing to Changes in Rock Fabric," Int'l. J. Rock Mech. & Min. Sci."; Vol. 6, 1969; Part I--Geometric Patterns, pp. 259-268. Part II--Standardized Grain Patterns, pp. 269-272. Part III--Rock Fabrics, pp. 273-276.

5. OBERT, LEONARD. - "Seismic Tests at the Pre-Gondola II and Buggy Sites, Final Report," BuMines, Denver Mining Res. Center, Rept. No. OSA-E-59-2, May 1969, 50 pp.

6. NICHOLLS, HARRY R.; SCHMECHEL, FRANK W.; and MUNSON, ROBERT D. - "Strength Properties of the Phillipson, Storke, and Ceresco Ridge Levels as Determined by Seismic Absorption Techniques," BuMines, Denver Mining Res. Center, November 1970, 11 pp.

Abstracts

INFORMATION RETRIEVAL

The following abstracts and keywords for each paper in these Proceedings are provided in the interests of improved information retrieval. Each reference 'card' is designed so that it can be cut out, placed on a 3 in. by 5 in. card and given an accession number in the reader's file. The accession number is then entered on the appropriate keyword cards. By matching selected keyword cards, all articles containing relevant information can be retrieved from the file. Information on this type of storage and retrieval system is given in "Information Retrieval for Soil Engineers", Committee on Information Retrieval, J.W. Hilf, Chmn, Journal of the Soil Mechanics and Foundations Division, ASCE, Vol. 93, No. SM5, Proc. Paper 5471, September, 1967, Part 2, pp. 1-180.

RESIDUAL STRENGTH IN DIRECT SHEAR

KEY WORDS: clays, direct shear tests, drained shear tests, residual strength, shear strength, slope stability, test procedures

ABSTRACT: Procedures for residual strength testing have not previously been satisfactorily defined. Several variables have therefore been investigated to determine their effects on the laboratory strength estimate. Selected results are used for illustration. An automatic reversing 6 cm square shear box was modified to allow half an inch displacement of the upper box before and after the central position. The main conclusions reach were: (1) area corrections are not applicable even when box displacements are very large (0.5 in. displacement of 2.36 in. box); (2) some soils require substantially more than quarter of an inch travel between reversals to mobilize the full residual strength - a shear box which can be displaced in both directions is then desirable; (3) speeds which are too great for drained conditions to be adequately established frequently give rise to load-displacement curves which do not level out between reversals; (4) commercial Kaolin gave a tan phi residual value of 0.18 for normal stresses of both 30 and 60 p.s.i.; (5) brittleness indices as high as 0.75 at 30 p.s.i. normal stress have been measured on some Australian soils.

REFERENCE: Cullen, R.M. and Donald, I.B., "Residual Strength Determination in Direct Shear", Proc. 1st Aust.-N.Z. Conf. on Geomechanics, Melbourne, 1971, pp. 1-10.

UNDRAINED SHEAR STRENGTHS IN CLAYS

KEY WORDS: clay, compression, extension, plane strain, triaxial, saturated, strength, undrained

ABSTRACT: A theoretical relationship is developed between undrained shear strengths in saturated clays for triaxial compression, triaxial extension and plane strain. The basic assumptions made are that at critical state the clay obeys a strength criterion in effective stress space of the Mohr-Coulomb type and also that a unique relationship exists at critical state between voids ratio and mean effective stress. Using these assumptions, which are based on experimental observations, it is predicted that undrained shear strengths in extension will be less than in compression by up to 30 per cent and plane strain values will be less than compression values by about 8 per cent on the average. A comparison of these theoretical differences with published experimental values shows promising agreement.

REFERENCE: Parry, R.H.G., "Undrained Shear Strengths in Clays", Proc. 1st Aust.-N.Z. Conf. on Geomechanics, Melbourne, 1971, pp. 11-15.

EFFECTS OF SALT CONTENT ON THIXOTROPIC BEHAVIOUR OF A COMPACTED CLAY

KEY WORDS: thixotropy, soil structure, electrical double layer, (particle orientation), compaction, shear strength, electrolyte (concentration)

ABSTRACT: Various amounts of salt (sodium chloride) were added to the clay to study the effects of salt on compaction, strength and thixotropic characteristics of the clay. An increase in salt content in the compacted Bangkok Clay resulted in an increase in dry unit weight on the dry side of optimum, an insignificant change in dry unit weight on the wet side of optimum, and a reduction in the compressive strength when compacted on the wet side of optimum. The effect of salt content on the thixotropic characteristics provided additional experimental evidence in support of Mitchell's hypothesis. The results indicated that the maximum thixotropic strength increase occurred at the maximum excess internal energy which resulted from the shear strains induced by the compaction process. The magnitudes of the shear strains were, in turn, dependent upon the soil structure.

From the test results it is postulated that the main factors influencing the soil structure are applied external stresses, interparticle contacts and physical interference between the particles. The short range interparticle forces are necessarily to be considered along with the long range interparticle forces.

REFERENCE: Sambhandharaksa, S. and Moh, Z.C., "Effects of Salt Content on Thixotropic Behaviour of a Compacted Clay", Proc. 1st Aust.-N.Z. Conf. on Geomechanics, Melbourne, 1971, pp. 16-23.

THE DEFORMATION AND YIELD OF CLAYS IN DIRECT SIMPLE SHEAR

KEY WORDS: elastic deformation, kaolin, plastic deformation, shear strains, shear tests, stress paths, stress-strain curves, yield surface

ABSTRACT: The validity of an idealized elasto-plastic model governing the yielding of clays has been studied by means of stress-controlled direct simple shear tests on saturated kaolin, using a number of different stress paths. The data confirm the existence of a unique state boundary surface which, together with the co-ordinate axes enclose all possible states of the clay studied. Plastic volumetric strains result from movement of the state path on this surface (yielding), while volumetric strains associated with stress paths beneath the surface are essentially elastic. Shear strains associated with volumetric yielding are shown to be small in magnitude for the particular test device used. Those shear strains associated with stress paths beneath the state boundary surface can be suitably represented by a strain contour pattern. Both the strain contour pattern and the state boundary surface itself appear to be independent of the stress path chosen, thus supporting previously published conclusions based on test data from the triaxial apparatus.

REFERENCE: Walker, L.K., "The Deformation and Yield of Clays in Direct Simple Shear", Proc. 1st Aust.-N.Z. Conf. on Geomechanics, Melbourne, 1971, pp. 24-30.

BRITTLE FRACTURE OF ROCK AT LOW CONFINING PRESSURES

KEY WORDS: brittle failures, compression tests, failure criteria, fracture mechanics, rock mechanics, stress-strain curves, underground structures

ABSTRACT: Recent advances in the study of the mechanics of brittle fracture in rock have been made possible by the ability to control the fracture process on the laboratory scale using stiff and servo-controlled testing machines. On the basis of fracture morphology and the shape of the associated complete stress-strain curves obtained in compression tests at low confining pressures, rocks may be classified in three broad behavioural classes. (a) Highly porous granular rocks in which a major feature in the structural break-down process is a collapse of the pore structure. (b) The majority of crystalline rocks in which the failure process involves the progressive development of large numbers of small inter- and intra- granular sub-axial cracks. Macro-shear surfaces appear only after the load-bearing capability of the specimen has been reduced considerably from its maximum. (c) Dense, ultra-fine grained rocks in which failure is almost impossible to control so that little is known about the fracture process. Experimental observations show the Mohr-Coulomb and Griffith crack criteria to be inapplicable to the majority of rocks. In the light of the experimental results discussed it is apparent that in some situations the fracture of rock around underground openings will be a controlled process while in others it will be violent and uncontrolled.

REFERENCE: Brown, E. T., "Brittle Fracture of Rock at Low Confining Pressures", Proc. 1st Aust.-N.Z. Conf. on Geomechanics, Melbourne, 1971, pp. 31-36.

LONG-TERM ROCK STRENGTH PREDICTION AND MEASUREMENT

KEY WORDS: cracking, creep, compressive strength, deformation, dolomites, gneisses, limestones, marbles, time factors

ABSTRACT: The strength and deformation behaviour of rocks are time-dependent; the design of permanent rock structures should be based on the long-term strengths. The direct method of determining the long-term strength of a rock involves applying a constant load to a specimen and recording the elapsed time until failure ensues. Methods of indirectly predicting the long-term strength, based on observing the deformation behaviour of a specimen in a short-term compression test, have been investigated. Following Bieniawski's postulated mechanism of brittle fracture, the stress level at which axial strains cease to be linearly elastic, or at which volumetric strain reverses its sign, should indicate the rock's long-term strength. By adjusting a compression machine to increase the load at a constant rate, and then observing the stress level at which the specimen becomes unable to accept this rate of loading, another simple predictor of long-term strength becomes available. For the most uniform rock studied, the predicted long-term strengths, as percentages of the short-term compressive strengths were: axial strain method, 89; volumetric strain method, 94; loading rate method, 88; directly measured long-term strength, less than 83 per cent of short-term strength.

REFERENCE: Singh, D.P. and Bamford, W.E., "The Prediction and Measurement of the Long-Term Strength of Rock", Proc. 1st Aust.-N.Z. Conf. on Geomechanics, Melbourne, 1971, pp. 37-44.

LIQUEFACTION OF SATURATED GRANULAR SOILS

KEY WORDS: liquefaction, granular materials, failure mechanics, design methods, earthquakes, blasts

ABSTRACT: This paper reviews the current status of published knowledge on the process of liquefaction in saturated granular soils. Methods of determining material properties and initial conditions defining liquefaction response are investigated and their relevance to predictive methods examined. The importance of documenting observed cases of liquefaction under earthquake or other dynamic loading is stressed as being the only means of testing the validity of the investigation and prediction techniques.

REFERENCE: Kurzeme, M., "Liquefaction of Saturated Granular Soils", Proc. 1st Aust.-N.Z. Conf. on Geomechanics, Melbourne. 1971, pp. 45-53.

THE COLLAPSE OF SANDS UPON SATURATION

KEY WORDS: sands, deformation, saturation, capillary pressures, settlement, shear stress, pore pressures

ABSTRACT: The following possible mechanisms of collapse of sandy soils following saturation have been examined experimentally and theoretically: (a) dissipation of initial capillary stresses, (b) reduction in normal force at particle contact by increase in pore pressure, and (c) contact instability due to decrease in shearing resistance on saturation.

The magnitudes of the initial capillary stresses were estimated to be quite low and the influence of their dissipation upon collapse behaviour did not appear to be as marked as the decrease in shearing resistance following saturation. This decrease in resistance was quite significant particularly at void ratios which were large in comparison with the critical void ratio. It was at these high void ratios that the largest collapses were observed. The increase in pore pressure during saturation was found to be negligible.

REFERENCE: Moore, P.J., and Millar, D.V., "The Collapse of Sands upon Saturation", Proc. 1st Aust.-N.Z. Conf. on Geomechanics, Melbourne, 1971, pp. 54-60.

STRESSES INDUCED BY MINING AT MOUNT CHARLOTTE

KEY WORDS: cracking, elastic theory, failure criteria, mining, Mohr failure theory, residual stress, rock excavation, rock mechanics, stress concentration, stress distribution, tunnel failures, underground structures

ABSTRACT: Mount Charlotte is a mechanized underground mine, extracting low-grade gold ore, at Kalgoorlie, Western Australia. Following a 'bump', or partial brittle failure of a rib pillar, a quick series of rough calculations of the stress concentrations around the stopes, generalized as rectangular holes, was carried out. The previously-measured high horizontal stress field was assumed to have an increasing trend with depth, similar to Hast's measurements. Calculations indicated that the maximum stress in the crown pillar after opening of the stopes was approximately 14,300 lb/sq. in. The next stage of the mining sequence involved blasting part of the crown pillar into the open stope beneath it. The maximum stress in the rib pillar then increased to 18,000 lb/sq. in. Failure of this pillar occurred 5 months later. The rock's mean compressive strength, measured in the laboratory, was 26,900 lb/sq. in. Estimates of the compressive strength of the rock mass range downwards from 20,800 lb/sq. in., so the deduced stresses were in good agreement with the rock's probable strength. The maximum stress in another rib pillar was calculated to be approximately 13,800 lb/sq. in., so it was predicted that this pillar would not prematurely fail, and the prediction proved to be correct.

REFERENCE: Bamford, W.E., "Stresses Induced by Mining Operations at Mount Charlotte", Proc. 1st Aust.-N.Z. Conf. on Geomechanics, Melbourne, 1971, pp. 61-66.

ROCK MECHANICS SURVEY AND MINE DESIGN AT KAMBALDA

KEY WORDS: design, digital computers, geological investigations, joints, mechanical properties, mining engineering, residual stress, rock mechanics, stress analysis, stress distribution, underground structures

ABSTRACT: A basic rock mechanics survey at the Kambalda Nickel Mines in Western Australia was carried out and the resulting data used in a mine design example. The survey consisted of a structural geological investigation; determination of the virgin stress field at the Durkin Mine; and measurement of the physical engineering parameters of representative rocks. These results were combined into a 'finite element' computer model, and a study was made of the variation in ground movement occurring near the Durkin shafts, caused by different mining methods and mining sequences. A rock stress field with high horizontal stresses of 3600 lb/sq. in. E-W and 1200 lb/sq. in. N-S, and a vertical stress of 1080 lb/sq. in. was measured at a depth of only 300 ft in the Durkin Mine. Rock mass physical properties were determined by combining geological structural statistics with laboratory test results using Protodyakonov's technique. The high stress field when simulated with the rock mass material properties in the finite element model, gave several significant results. The roof or back of most underground openings was naturally prestressed, indicating probable stable roof conditions. Very little stress change occurred in stope pillars and the rock surrounding the Durkin shafts when different mining methods were simulated.

REFERENCE: Dyson, L.A., "A Rock Mechanics Survey and its Use in an Underground Stability Analysis at Kambalda", Proc. 1st Aust.-N.Z. Conf. on Geomechanics, Melbourne, 1971, pp. 67-72.

HORIZONTAL PILLAR EXTRACTION AT MOUNT ISA MINES LIMITED - SOME ROCK MECHANICS ASPECTS

KEY WORDS: ground movements, pillar extraction, rock mechanics, rock stresses, underground mining

ABSTRACT: Two methods of stressed pillar extraction beneath fine fill are discussed. In part A, the removal of a high grade copper bearing pillar using cemented fill with an 'umbrella' of highly stressed and broken rock between the extracted area and fine dry running fill is described. Some results of movement monitoring in the highly stressed and broken rock are given. In part B the successful extraction of a large lead bearing horizontal pillar between stopes containing hydraulic fill is described and ground movements measured as a result of pillar extraction are compared with estimates by a finite element analysis.

REFERENCE: Edwards, D.B., "Horizontal Pillar Extraction at Mount Isa Mines Limited - Some Rock Mechanics Aspects", Proc. 1st Aust.-N.Z. Conf. on Geomechanics, Melbourne, 1971, pp. 73-79.

A COMPARATIVE THEORETICAL STUDY OF THE EFFECTS OF INCLINATION AND PROGRESSIVE MINING ON STOPE BEHAVIOUR

KEYWORDS: elastic theory, co-linear stopes, crack-tip analysis, finite element, stresses, displacements, progressive mining, ore pillars, Cobar N.S.W., Griffith crack

ABSTRACT: Using elastic theory and assuming plane strain conditions, both crack-tip and finite element analyses are applied to predict the stress and displacement field produced by the excavation of two co-linear stopes. The conditions are based on the simplified geometry and provisional stress modulus data of the C.S.A. Mine Cobar, N.S.W. The study takes into account the effects of the initial stress field, stope inclination, and progressive mining. The two methods of analyses give similar and complementary results; the crack-tip results are more general in nature while the finite element method allows a more realistic representation of the geometry. The components of the initial stress field, resolved parallel and perpendicular to the stope orientation, are the important factors relating to variations in the initial stress field and stope inclination. For two co-linear stopes the regions of stress concentration are above the upper stope, below the lower stope and in the pillar. The rate of stress increase in the pillar rises rapidly when the length of the ore pillar is reduced below one quarter of the final stope height.

REFERENCE: Gerrard, C.M., and Harrison, W. Jill, "A Comparative Theoretical Study of the Effects of Inclination and Progressive Mining on Stope Behaviour", Proc. 1st Aust.-N.Z. Conf. on Geomechanics, Melbourne, 1971, pp. 80-87.

THE GRAVITY FLOW OF MATERIAL IN THE SUB-LEVEL CAVING MINING SYSTEM

KEY WORDS: computer programming, flow, granular materials, graphical analysis, gravity, mathematical analysis, mining engineering, model tests

ABSTRACT: The exploitation of lower grade ore deposits has required a reduction in unit extraction costs. This is being achieved by mechanization and an increased scale of operations. The design of such large mining systems by the trial and error methods used in the past is not economically justified. Unfortunately the use of more sophisticated design techniques is restricted by the lack of data concerning the relationships between the design variables. This paper describes part of a research project which involves the investigation of design parameters for the sub-level caving mining method. The gravity flow of material, which is one of the most important factors in sub-level caving design, is discussed in some detail. Two-dimensional model tests are described and a statistical analysis of results it presented. These results have shown that the flow shape can be uniquely described by an eccentricity value.

REFERENCE: Just, G.D., and Free, G.D., "The Gravity Flow of Material in the Sub-level Caving Mining System", Proc. 1st Aust.-N.Z. Conf. on Geomechanics, Melbourne, 1971, pp. 88-97.

THE ESTABLISHMENT OF OPTIMIZED DESIGN PARAMETERS FOR A NEW GYPSUM MINE

KEY WORDS: rock mechanics, mine pillar design, gypsum, stratified deposit, homogeneous material, mechanical property determinations

ABSTRACT: The laboratory, theoretical, and 'in-situ' experimental work undertaken prior to the commencement of mining in a high grade gypsum deposit in Northern England is described. The deposit was horizontal and overlain by approximately 125 ft of Permo-Triassic and post-glacial sediments containing layers of unstable sand. An examination of cores indicated that the gypsum was extremely homogeneous and that no major discontinuities existed within an area of several square miles. The conclusions concerning the homogeneity of the deposit appeared to justify an attempt being made to establish mining dimensions by means of a programme of laboratory and theoretical studies. Large quantities of experimental data were processed statistically and the values obtained were used as the basis for designing an optimized mine layout. Once production had commenced, the deformation of the actual mine structure was monitored by 'in situ' instrumentation.

REFERENCE: Weir-Jones, I., "The Establishment of Optimized Design Parameters for a New Gypsum Mine", Proc. 1st Aust.-N.Z. Conf. on Geomechanics, Melbourne, 1971, pp. 98-104.

NON-LINEAR CONSOLIDATION - EFFECT OF LAYER DEPTH

KEY WORDS: consolidation, consolidation rate (one-dimensional, non-linear), time settlement relationship, pore pressure

ABSTRACT: This paper generalizes the previous theory published by Davis and Raymond which only dealt with a relatively thin layer and showed that, although the rate of pore pressure dissipation is slower than that of the classical Terzaghi linear theory, the degree of settlement is the same. This theory and its generalization are based on the assumption that the coefficient of consolidation is constant but that the coefficients of volume decrease and of permeability are not.

The generalization of the original theory takes into account the effects of non-linear behaviour on the rate of consolidation of deep layers. For such situations it is shown that the rate of pore pressure dissipation may be faster or slower than that of the classical Terzaghi linear theory depending on the ratio of the initial to the final effective stress at the top of the layer and on the ratio of the initial effective stress at the top to that at the bottom of the layer. The rate of settlement on the other hand is virtually always faster than that given by the classical theory and in the case of very deep layers subject to small consolidation pressures the increase in rate may have practical significance.

REFERENCE: Davis, E.H., "Non-Linear Consolidation and the Effect of Layer Depth", Proc. 1st Aust.-N.Z. Conf. on Geomechanics, Melbourne, 1971, pp. 105-111.

RECOMPRESSION CHARACTERISTICS OF PERTH OVERCONSOLIDATED CLAYS

KEY WORDS: correlations, foundations, overconsolidation, recompression, soil mechanics

ABSTRACT: The recompression properties of Perth overconsolidated clays are discussed in detail, with reference being made to laboratory tests on samples from a number of sites in the City area. Recommendations are made which should enable the accuracy of future settlement estimates to be improved. An analysis of the limited field records available offers some support for the approach presented.

REFERENCE: Frost, R.J., Walker, L.K., and Nixon, I.K., "Recompression Characteristics of Perth Overconsolidated Clays", Proc. 1st Aust.-N.Z. Conf. on Geomechanics, Melbourne, 1971, pp. 112-118.

CONSOLIDATION OF MORWELL BROWN COAL

KEY WORDS: coal, compressibility, consolidation tests, field tests, laboratory equipment, laboratory tests, pre-consolidation, temperature effects, time settlement relationship

ABSTRACT: In connection with investigations of the stability of a deep open cut brown coal (lignite) mine in Victoria, Australia, a series of one-dimensional laboratory consolidation tests has been carried out on brown coal. Samples were obtained from boreholes up to 700 ft (213 m) deep, and details are given of sampling and sample preparation. For reasons given, a major purpose of the tests was the estimation of the preconsolidation pressure. The use of different time intervals between loads, different load increment ratios, and temperatures up to 60°C were found to have an insignificant effect for engineering purposes on the value of preconsolidation pressure estimated by Casagrande's method. These variations, including the use of constant high temperature, were found to have relatively little effect on compressibility, but increases in temperature after the conclusion of consolidation at constant pressure led to further very significant volume decreases. A large field load test on coal showed behaviour in compression qualitatively and quantitatively similar to that observed in the laboratory tests.

REFERENCE: Green, D.C., "Aspects of the Consolidation of Morwell Brown Coal", Proc. 1st Aust.-N.Z. Conf. on Geomechanics, Melbourne, 1971, pp. 119-126.

PRIMARY/SECONDARY TRANSITION DURING THE CONSOLIDATION OF CLAY

KEY WORDS: consolidation, consolidation rate, degree of consolidation, primary consolidation, (scaling laws), secondary compression, settlement, settlement analysis, soil mechanics, time factors

ABSTRACT: Primary theory and in particular the t/H^2 similarity rule are shown to be unlikely to be relevant for thick strata of real soils. The conventional assumption that the transition from the primary to the secondary stages of consolidation occurs simultaneously at all depths within a clay stratum is shown to be an approximation. Whatever criterion is used to distinguish between primary and secondary processes the transition must take place at the drainage surface(s) immediately upon application of increments of load and progress through the stratum towards the mid-plane as consolidation proceeds. Although presented in the context of the one-dimensional consolidation of saturated clays the ideas presented are not restricted to that case. Depth-time loci of transition from the primary to the secondary stages are derived for an 'ideal' soil and for a 'real' soil. The need for a theory which unites the primary and secondary stages under the control of a single set of equations is emphasized. Only with the aid of such a unified theory may the results of tests on thin laboratory samples be used to predict the behaviour of thick field strata.

REFERENCE: Hawley, J.G., "The Primary/Secondary Transition during the Consolidation of Clay", Proc. 1st Aust.-N.Z. Conf. on Geomechanics, Melbourne, 1971, pp. 127-131.

AN INVESTIGATION OF THE THREE-DIMENSIONAL CREEP PROPERTIES OF A CLAY

KEY WORDS: clay, creep, pore pressure, rheological model, stress-strain-time, triaxial compression, viscosity

ABSTRACT: The strain-log time curve for an increment in deviator stress under undrained triaxial compression conditions is shown to be essentially a straight line over most of the range, the slope of which increases rapidly as the effective stress ratio q/p increases from the k_o condition to failure. If the increment is preceded by either secondary consolidation or a prolonged strain under a lower deviator stress, the strains and pore pressures in the early stages are considerably reduced and a 'delay' is introduced before the linear relationship is established. This behaviour is shown to be a function of previous strain rather than of time.

The effective stress ratio-strain curve is shown to be independent of loading procedure to a first approximation. Finally, a model is presented which attempts to take the observed properties into account.

REFERENCE: Newland, P.L., "An Investigation of the Three-dimensional Creep Properties of Clay", Proc. 1st Aust.-N.Z. Conf. on Geomechanics, Melbourne, 1971, pp. 132-137.

SETTLEMENT PROBLEMS INVOLVING CREEP

KEY WORDS: compression curves, creep, deformation, foundations, rock mechanics, settlement analysis

ABSTRACT: Although creep is not usually a critical factor in settlement analysis, it can, for some more sophisticated structures, present considerable difficulty. Long term predictions are by no means as easy or certain as for consolidation, and are greatly complicated by minor variations of environment.

From a review of literature, it is shown that empirical creep equations have no physical validity comparable with that of creep rate expressions. It is also shown that the continuity of creep curves is destroyed by any transient elastic or consolidation effects, whereas the continuity of creep rate is not. For these two reasons, any valid assessment of creep behaviour should be made through an analysis of creep rate. The effect of various environmental changes on creep rate behaviour is illustrated diagramatically.

REFERENCE: Parkin, A.K., "Application of Rate Analysis to Settlement Problems Involving Creep", Proc. 1st Aust.-N.Z. Conf. on Geomechanics, Melbourne, 1971, pp. 138-143.

DEFORMATION OF WALLS RETAINING SOFT CLAY BACKFILLS

KEY WORDS: retaining walls, clays, creep, shear stress, deformation, strain rate

ABSTRACT: The inter-relationship between the deformation and the lateral restraint of a retaining wall has been investigated both experimentally and theoretically. A rigid model wall retaining a soft clay backfill was allowed to yield by reducing the lateral support on the wall. Observations were made of the amount and rate of lateral wall deformation. These observations indicated that the rate of wall movement was inversely proportional to the lateral restraining force and, for the very soft clays, the rate of wall movement finally became constant. Predictions of the wall deformation as a function of time were made by means of the rate process theory supported by data from a series of torsion shear tests. These theoretical predictions were in reasonable agreement with the observations.

REFERENCE: Spencer, G.K., and Moore, P.J., "Deformation of Walls Retaining Soft Clay Backfills", Proc. 1st Aust.-N.Z. Conf. on Geomechanics, Melbourne, 1971, pp. 144-149.

ROCK STRUCTURES AND ASSOCIATED ROCK ALTERATION

KEY WORDS: dam foundations, (rock defects), strata, basalt, siltstones, faults, joints, engineering geology, (fracture porosity), chemical stability, (pyrite mineralization)

ABSTRACT: A case history illustrating the relationship of rock structure and hydrothermal alteration in basalt. Fracture zones associated with faults formed permeability paths for hypogene solutions which have altered basaltic rocks at depth. Subsequent supergene groundwater circulation has weathered the bedrock and the weathered mantle masks the zones of hypogene alteration. The rock foundations are intercalations of basalt and meta-sediments, predominantly indurated mudstones. At the dam site the 'axial plane' of an anticline dips at 70°W. The resultant discontinuity pattern is asymmetric to the valley profile and the rock cuts in the right abutment are less stable than those in the left abutment. Secondary fracture porosity within the bedrock is greatest in zones of brecciation associated with faults and most extensive where the latter are intersected by cross fractures. Decomposition of basalt was initiated by hypogene solutions associated with sulphide mineralization. Geological investigation during preliminary excavation work was utilized to redesign the concrete foundations.

REFERENCE: Bell, A.D.M., "Rock Structures and Associated Rock Alteration, Danjera Creek Dam, N.S.W.", Proc. 1st Aust.-N.Z. Conf. on Geomechanics, Melbourne, 1971, pp. 150-153.

EFFECTS OF STRUCTURE ON THE BEHAVIOUR OF ARGILLACEOUS SEDIMENTS

KEY WORDS: structure, directional effects, tectonic effects, mineralogical effects, argillaceous sediments, residual strength, montmorillonite

ABSTRACT: Structure of clays and clay shales is discussed from three points of view.

Directional effects, along or across the bedding, which appear to control the path or strain requirements in moving from peak to residual conditions. Examples are given to indicate that much smaller strains will be required to produce the residual strength along the bedding although its ultimate value may be independent of direction.

Tectonic effects are briefly reviewed. Faulting, folding of sedimentary series, and also the general consolidation and erosion cycle stress changes are all found to produce similar shear zones within argillaceous sediments. Examples of flexural slip are given.

Mineralogical effects are taken to include the presence of slightly variable seams or layers in otherwise 'homogeneous' clay formations. Examples from sites both in Australia and overseas are given to demonstrate how such layers will often control stability. In many cases the untypical behaviour can be put down to the localization of montmorillonite during deposition of the formation.

REFERENCE: James, P.M., "Some Effects of Structure on the Behaviour of Argillaceous Sediments", Proc. 1st Aust.-N.Z. Conf. on Geomechanics, Melbourne, 1971, pp. 154-159.

MOISTURE CHANGES AND SOIL STRUCTURE IN EARTH DAMS

KEY WORDS: optimum moisture content, soil moisture, soil compaction, pore pressure, adsorbed water, clay structure, earth dams, moisture control

ABSTRACT: During construction of several earth dams anomalous pore pressures were observed, and these were traced to changes in optimum moisture content. A relationship between the initial soil moisture content and optimum moisture content was established from over 1000 compaction tests. Furthermore, it was found that optimum moisture content varied with curing time. Accompanying changes of the actual soil moisture were also observed. The causes of moisture movement were briefly investigated and appeared unrelated to: interchange between free and adsorbed moisture; changes in electrolyte concentration and exchangeable sodium percentage; and changes in specific surface of soil crumbs. Microscopic examination indicated no change in soil structure. Base exchange capacity could be related to moisture change and the possibility of moisture movement towards equilibrium merits further investigation.

REFERENCE: Kotowicz, M.S. and Kiek, S.N., "An Investigation of Moisture Changes and Soil Structure in Earth Dams", Proc. 1st Aust.-N.Z. Conf. on Geomechanics, Melbourne, 1971, pp. 160-164.

FABRIC SYMMETRY AND MECHANICAL ANISOTROPY IN NATURAL SOILS

KEY WORDS: soil mechanics, anisotropy, compaction, deposition, structure, sand, clay, mechanical properties

ABSTRACT: Fabric analyses and triaxial tests have been performed on oriented, undisturbed specimens of two commonly occurring soils; a recent beach sand and a residual silty clay of uniform composition. The results indicate that both soils lack a vertical n-fold axis of symmetry ($n = \infty$) in their original, pre-testing geometrical fabric. They exhibit only a single vertical plane of symmetry, i.e. monoclinic symmetry. A vertical n-fold axis of symmetry ($n = \infty$) is also absent in the two soils as far as such mechanical properties as the secant modulus are concerned. The presently hypothetical symmetry elements of the secant modulus distribution pattern can be related to those of the original, pre-testing geometrical fabric, and these in turn to the major terrain features (direction of the coastline, or the orientation of the terrain slope). It is suggested therefore that current ideas on the frequency of occurrence of cross-anisotropy arising from gravitational compaction and consolidation in natural soils need to be reviewed.

REFERENCE: Lafeber, D. and Willoughby, D.R., "Fabric Symmetry and Mechanical Anisotropy in Natural Soils", Proc. 1st Aust.-N.Z. Conf. on Geomechanics, Melbourne, 1971, pp. 165-174.

ESTIMATING THE STRENGTH OF JOINTED SOILS

KEY WORDS: joints, residual soils, sampling, shear strength, statistical analysis

ABSTRACT: A theoretical study of the factors influencing the shear strength of a jointed mass of soil is made from a statistical point of view. The distribution of dip and bearing angles, as measured by a joint survey, is smoothed by using three simple theoretical distributions in combination. The effect of joint spacing is crudely accounted for by assuming the spacings to follow a Poisson distribution. The probability distribution of shear strength in the field is calculated for two residual soils from Hong Kong, making reasonable assumptions as to the variability of the parameters. The distributions are inevitably bimodal, and consequently the choice of a single-valued design strength to characterize the actual behaviour is difficult.

REFERENCE: Lumb, P., "Estimating the Strength of Jointed Soils", Proc. 1st Aust.-N.Z. Conf. on Geomechanics, Melbourne, 1971, pp. 175-179.

EFFECTS OF FISSURES ON THE PROPERTIES OF STIFF CLAYS

KEY WORDS: laboratory tests, field tests, plate load tests, shear tests, stiff clays, fissures, triaxial tests, effective stress, shear strength, deformation modulus, pore pressures, loading rate

ABSTRACT: The large variations in the shear strengths and moduli of stiff fissured clay measured in standard triaxial tests have led to the use of large in situ tests to measure these properties. The moduli have been measured by loading tests on plates at various depths in boreholes and effective strength parameters have been determined by in situ shear box tests. For plate tests the effects of the following factors are examined : plate diameter, fissure spacing, degree of confinement of the borehole, method of preparing the rest surface and the time between excavation and loading. In the shear box tests effective normal stresses between 17.5 and 100 kN/m^2 were used and in some cases pore pressure measurements were made on the plane of shear to check that the rate of shear was sufficiently slow. Large in situ tests have provided a better measure of the relevant strength and deformation parameters of two highly fissured clays and comparison of the results with laboratory tests has led to a better understanding of the influence of fissures.

The paper describes these tests, gives typical results to illustrate the influence of fissures and compares the results with laboratory tests. The use and limitations of in situ tests for determining the full-scale strength applicable to a particular problem are discussed.

REFERENCE: Marsland, A., "The Use of In-situ Tests in a Study of the Effects of Fissures on the Properties of Stiff Clays", Proc. 1st Aust.-N.Z. Conf. on Geomechanics, Melbourne, 1971, pp. 180-189.

ROLE OF POROSIMETRY IN GEOMECHANICS

KEY WORDS: compaction, fabric, dry density, porosity, porosimeter, void ratio

ABSTRACT: The most fundamental parameters used to characterize soils and rocks are those that are functions of the porosity. To date engineers have, of necessity, used gross porosity as the only practical measure. However, the application of the techniques of porosimetry enable the complete distributions of pore sizes and pore volumes to be determined. The theory and techniques of mercury intrusion porosimetry are described and the errors and limitations of the method are discussed. It is then shown that, by using porosimetry, information can be obtained on soil properties which has not hitherto been available. Moreover, it is possible to define several new parameters which can usefully supplement conventional measurements based on gross porosity. Finally, the role of porosimetry in investigating a well known engineering system is discussed and typical experimental data are presented.

REFERENCE: Shackel, B. and Nettleton, A.F.S., "The Role of Porosimetry in Geomechanics", Proc. 1st Aust.-N.Z. Conf. on Geomechanics, Melbourne, 1971, pp. 190-196.

INFLUENCE OF STRUCTURE ON THE DILATATION OF CLAY

KEY WORDS: clay, dilatation, diagenetic bond, recoverable strain energy, soil structure, overconsolidated clay

ABSTRACT: Soils having different soil structures were formed by sedimentation in sodium chloride and sodium hexametaphosphate solutions followed by leaching, to achieve various final salt concentrations. The dilatation characteristics were observed by the measurement of excess pore pressure in CIU triaxial tests.

It was observed that the tendency of the clay to dilate during shear was dependent on the stress history, the amount of recoverable strain energy in the soil, and the strength of the diagenetic bonds. The soil with the strongest diagenetic bonds stored the most recoverable strain energy during overconsolidation. Thus, it exhibited the greatest tendency to dilate because of the release of this energy during failure of the diagenetic bonds.

In normally consolidated soil strain energy was not stored in the diagenetic bonds, and therefore, dilatation did not occur.

REFERENCE: Nelson, J.D. and Siu, K.L., "The Influence of Structure on the Dilatation of Clay", Proc. 1st Aust.-N.Z. Conf. on Geomechanics, Melbourne, 1971, pp. 197-203.

THE COLLAPSE OF CLASTIC AGGREGATES

KEY WORDS: (clastic aggregates), failure mechanics, granular materials, internal friction, plane strain, sands, shear failure, shear strength, triaxial compression

ABSTRACT: Traditional analyses of the behaviour of natural materials are based on a cartesian element whose behaviour is assumed to represent that of a continuum. A preferred approach for materials in general and for natural aggregates of particles (such as sands) in particular, is to consider the material to be built up of random arrays of systematically packed zones (systones) of usually spherical particles. From an analysis of the failure of a typical clastic element or systone it is shown that the strength of a granular medium (and therefore its angle of internal friction) depends on the distribution angle which defines the rotundity of the particles, the orientation of the systone, and the angle of contact friction between particles. The orientation of systones is particularly important, since shear strength is dependent on the strength of the strongest systone which in the case of the simple disc unit is infinite. Analysis of a three-dimensional model built up from unit spheres shows that granular materials are stronger in plane strain than in triaxial compression, the magnitude of this difference depending upon systone orientation, and inter-particle friction. Experimental results obtained by a number of investigators are shown to be well represented by the predictions of this analysis.

REFERENCE: TROLLOPE, D.H., "The Collapse of Clastic Aggregates", Proc. 1st Aust.-N.Z. Conf. on Geomechanics, Melbourne, 1971, pp. 204-210.

ORIENTED DRILL CORE IN STRUCTURAL GEOLOGY

KEY WORDS: Mount Isa, Australia, rock, geological investigations, structural geology, core drilling, cores, analysis, fractures, bedding planes

ABSTRACT: All core from rock mechanics diamond drilling at Mount Isa is oriented to permit orientation and properties of bedding, foliation and fractures in rock to be studied. Three core orienting procedures are used (a) CRAELIUS device with NMLC triple tube drilling for other than vertical holes, (b) paint dribble on down hole stub of core for 4 in. diameter horizontal holes, using a single tube core barrel, and (c) a uniform marker of known orientation such as bedding.

For planar and linear features on core, the dip direction, dip and depth are recorded, together with a description of surfaces of breaks. Orientation data are rotated to their true position, corrected for biased sampling, then analysed to delineate orientation groups. Analysis within each orientation group is for spacing, sliding friction properties, continuity of natural planes, relative strength across fractures or bedding breaks, relationship of structure with rock types or areas, and other statistical treatment of data.

Without a true orientation for planar and linear features on core, where core can be fitted together, orientation groups can only be delineated relative to each other with only little subsequent analysis. Where core cannot be fitted together, even less, though still valuable, information can be obtained. The principal advantages of oriented drill core are that a true orientation can be found for core features, and where core is not intact, it can provide a link between adjacent sections of core.

REFERENCE: Bridges, M. C. and Best, E. J., "Application of Oriented Drill Core in Structural Geology at Mount Isa", Proc. 1st Aust.-N.Z. Conf. on Geomechanics, Melbourne, 1971, pp. 211-216.

DAMAGE IN A SMOOTH WORK PIECE BY A SLIDING DIAMOND

KEY WORDS: abrasion, cracking, damage, diamond, drilling, rock, sliding, surface

ABSTRACT: Optical methods were used to evaluate the early stages of damage caused by a loaded spherical diamond moving over a smooth surface, as a function of speed, radius, load and lubrication, for several homogeneous materials. New types of cracking patterns and abraded tracks have been observed. The statistical variation from track to track, and even within one track, is so great that quantitative conclusions are not possible at this stage, although some general effects of the variables are noted. Application to hard rock drilling is not straightforward and will probably have to await an evaluation of material removed.

REFERENCE: Graham, J., "Damage Induced in a Smooth Work Pie ce by a Sliding Diamond - an Approach to Hard Rock Drilling", Proc. 1st Aust.-N.Z. Conf. on Geomechanics, Melbourne, 1971, pp. 217-221.

SOME BASIC ASPECTS OF DIAMOND DRILLING

KEY WORDS: core drilling, diamonds, theory, bit design, operating variables, instrumentation, laboratory tests

ABSTRACT: A theoretical model of the cutting action of a diamond bit is introduced. Diamond bit design is discussed under the headings, bit type, diamond orientation, diamond exposure, diamond spacing, matrix properties and waterways. The theoretical relationships between the six operating variables, thrust, rotary speed, drilling torque, penetration rate, drilling fluid flow and fluid pressure, are developed. A laboratory test rig was developed to continuously record all six operating variables. Results show that drilling torque is proportional to thrust, and that penetration rate is proportional to rotary speed. Penetration rate increases with thrust, but the relationship is not linear. Specific energy of drilling reduces with thrust but is independent of rotary speed. All results are corrected back to new bit conditions by an exponential 'wear' curve.

REFERENCE: Rowlands, D., "Some Basic Aspects of Diamond Drilling", Proc. 1st Aust.-N.Z. Conf. on Geomechanics, Melbourne, 1971, pp. 222-231.

REDUCED SOIL STRENGTH AND STIFFNESS AT THE TOP OF TUBE SAMPLES

KEYWORDS: soil, decomposed mudstone, sampler, sampling, undisturbed sampling, intact sampling, research, shear strength, modulus of elasticity, disturbance, soil sampling, granite

ABSTRACT: An investigation is described designed to assess which part of a tube sample gives the more reliable estimate of the original soil properties in the ground. A decomposed granite and a decomposed mudstone were sampled with a 3 in. Auger Core Soil Sampler. In one set of tests at each site, each sample was long enough to permit an upper and lower test specimen to be cut, while in the other set the advance of the sampler was shorter, permitting only one test specimen per tube sample. Subsequently an immediate undrained triaxial compression test was made on the specimens in the laboratory. Secant modulus values for the single specimens were found to match closely those for the lower specimens, even though the sampling forces required to obtain the latter were much higher. The influence of these forces, and of soil disturbance arising from the sampling procedures, on variations in tube sample properties is discussed. It is concluded that the lower part of a sample should give a more reliable indication of actual soil ground conditions than the upper part.

REFERENCE: Lang, J. G., "Reduced Soil Strength and Stiffness at the Top of Tube Samples", Proc. 1st Aust.-N.Z. Conf. on Geomechanics, Melbourne. 1971, pp. 232-237.

MODEL STUDIES OF FRAGMENTATION BY EXPLOSIVES

KEY WORDS: blasts, craters, explosions, fragmented materials, graphical analysis, mining engineering, model tests, rock excavation, sieve analysis

ABSTRACT: Measurement of the size distribution of rock particles produced by explosive charges should indicate the relative effectiveness of any blasting design. Such data, although commonly used to optimize rock breakage in mineral processing, have not apparently been used to optimize the explosive rock breakage process. The paper describes the results of investigations into the size distribution of particles produced by blasting in small scale models. Crater testing techniques were used with the charge located at varying distances from the surface. A method of analysis has been developed to describe the particle size distribution in terms of the geometry and size of the explosive charge. The significance of these results to full-scale blasting operations is discussed in relation to the modelling parameters used in the experiments.

REFERENCE: Just, G.D. and Henderson, D.S., "Model Studies of Fragmentation by Explosives", Proc. 1st Aust.-N.Z. Conf. on Geomechanics, Melbourne, 1971, pp. 238-245.

ANALYSIS OF PILE LOADING TESTS IN A STIFF CLAY

KEY WORDS: driven piles, friction penetrometer, load increment duration, pile loading tests, pile settlement, soil parameter

ABSTRACT: Results are presented for loading tests performed on two steel shell piles driven into a stiff clay. The observed behaviour is compared with predictions based on soil parameters obtained from extensive sampling and laboratory testing, and from the results of in situ testing including S.P.T. soundings, and friction penetrometer soundings which provide a direct measurement of both end bearing and side friction for each type of soil.

The effect of load duration on the settlement characteristics of a single pile was examined by using three distinct loading periods. The data obtained indicate that the stress-strain relationship is not unique and is dependent on loading duration.

REFERENCE: Bromham, S.B. and Styles, J.R., "An Analysis of Pile Loading Tests in a Stiff Clay", Proc. 1st Aust.-N.Z. Conf. on Geomechanics, Melbourne, 1971, pp. 246-253.

MODEL TESTS ON PILES IN CLAY

KEY WORDS: foundations, laboratory tests, model tests, piles, settlement, soil mechanics

ABSTRACT: A series of tests on model piles in Kaolin is described. Single floating piles and end-bearing piles, and floating pile groups have been tested. Using control piles to obtain the soil moduli, theoretical predictions of pile settlements, based on elastic theory have been made. The good agreement found between predicted and observed settlements indicates that elastic theory can be successfully used to predict the effects of pile length and compressibility and group action on settlements.

REFERENCE: Mattes, N.S. and Poulos, H.G., "Model Tests on Piles in Clay", Proc. 1st Aust. - N.Z. Conf. on Geomechanics, Melbourne, 1971, pp. 254-260.

HIGH CAPACITY LOAD TEST FOR DEEP BORED PILES

KEY WORDS: anchors, boredpiles, concrete piles, pile bearing capacities, pile loading tests, sandstones, siltstones, time-settlement relationship

ABSTRACT: The purpose, scope, equipment and field procedures are described for an end bearing load test for high capacity bored piles founded at depths of from 30 to 50 ft in sandstones and siltstones. A jacking reaction of 400 tons was provided by three 80 ft deep, inclined grouted cable anchors. The loading was transferred from the ground surface by a prestressed pile to a 2 sq. ft circular bearing plate. The failure bearing pressure of 175 tons per sq. ft agreed closely with the pre-calculated ultimate capacity. The application of the load test results to the final design of the piles is also described. Two generalized conclusions are made.

REFERENCE: Moss, J.D., "A High Capacity Load Test for Deep Bored Piles", Proc. 1st Aust.-N.Z. Conf. on Geomechanics, Melbourne, 1971, pp. 261-267.

ANALYSIS OF MOVEMENTS OF BATTERED PILES

KEY WORDS: analysis, battered piles, foundations, pile groups, settlement, soil mechanics

ABSTRACT: Analyses are made of the axial displacement of a battered pile in an elastic soil mass subject to axial loading, and of the normal displacement due to normal loading and moment. It is found that these displacements are almost independent of the angle of batter of the pile over a practical range of batter angles, so that available solutions for a vertical pile may be used to analyse relatively simply the movements of a battered pile under a general loading system. The simplified method of analyzing a single pile is extended to the consideration of groups containing battered piles.

REFERENCE: Poulos, H.G. and Madhav, M.R., "Analysis of the Movements of Battered Piles", Proc. 1st Aust.-N.Z. Conf. on Geomechanics, Melbourne, 1971, pp. 268-275.

BEARING CAPACITY OF STRIP FOOTING

KEY WORDS: ultimate bearing capacity, strip footing, plastic theory, (roughness effects, non-associated flow rule)

ABSTRACT: Solutions, by the theory for a perfectly plastic material with a non-associated flow rule, are presented over the full range from the limiting case of no body forces (the Prandtl solution) to the limiting case for no surcharge. It is shown that in between these limiting cases the principle of superposition implied in the ordinary concept of bearing capacity coefficients N_q and N_γ is approximately true, the error being no more than a maximum of 30 per cent.

The results confirm previous solutions by Sokolovski and by Cox for smooth footings and also show that for such footings the nature of the flow rule of the material has no influence at all on the collapse load. On the other hand the results show that the ultimate bearing capacity of a rough footing may be as much as double that of a smooth footing when there is no surcharge although with increasing surcharge the effect of roughness decreases. Terzaghi's values of N_γ for a rough footing are shown to be significantly optimistic for high values of ϕ. The nature of the flow rule also has a theoretical influence when the footing is rough but, over the full range from a constant volume material to one which dilates at the extreme rate required by an associated flow rule, the influence is so small as to have negligible practical importance.

REFERENCE: Davis, E.H. and Booker, J.R., "The Bearing Capacity of Strip Footing from the Standpoint of Plasticity Theory", Proc. 1st Aust.-N.Z. Conf. on Geomechanics, Melbourne, 1971, pp. 276-282.

UPLIFT TESTING OF PROTOTYPE TRANSMISSION TOWER FOOTINGS

KEY WORDS: transmission tower, field tests, footings, prototype tests, uplift tests, bored piles, buried slab footings

ABSTRACT: A series of prototype field loading tests were carried out by the State Electricity Commission of Victoria to determine the uplift capacity of bored piles and buried slab footings for transmission towers. Tests were conducted on 17 bored piles in a stiff basaltic clay and uplift loads of 220,000 lb were applied. Their capacities at 0.5 in. displacement is compared with a 'tension limited shear' theory. A second series of uplift tests was conducted on 6 buried slab footings in a stiff basaltic clay and 5 buried slab footings in a granitic silty sand. Loadings of up to 500,000 lb were applied and the footing capacities at 0.5 in. displacement are compared with 'the cone of earth' resistance. Sub-surface displacements were observed and the effect of density of the backfill is discussed.

REFERENCE: McKenzie, R.J., "Uplift Testing of Prototype Transmission Tower Footings", Proc. 1st Aust.-N.Z. Conf. on Geomechanics, Melbourne, 1971, pp. 283-290.

STRESSES BENEATH GRANULAR EMBANKMENTS

KEY WORDS: soil mechanics, stresses, embankment, experimental, theoretical, model

ABSTRACT: Measurements were made of the normal and shear stresses along the base of a model embankment formed from a dry granular soil. The stresses were determined from the total loads applied to independently suspended rectangular rigid strips. These strips were assembled to form a base for the embankment 52.1 in. wide by 85.75 in. long. Studies were made of the stress distributions developed as the embankment was progressively formed with the base (foundation) held rigid, and with vertical displacement profiles applied to the base of the embankment after construction of the embankment. A comparison of the measured stresses with the values predicted by use of the linear elastic model showed that the normal stresses were closely predicted, and although the trends in shear stress distribution were correctly predicted the values were underestimated. Deformation of the base reduced normal stresses in the central regions and on the evidence obtained in these and earlier tests it became evident that the active and passive plasticity solutions were in qualitative agreement with measured values. However horizontal base movements are required to develop these states so that further experimental studies will be required to establish the applicability of the plasticity solutions to a real embankment supported on a compressible foundation.

REFERENCE: Lee, I.K. and Herington, J.R., "Stresses Beneath Granular Embankments", Proc. 1st Aust.-N.Z. Conf. on Geomechanics, Melbourne, 1971, pp. 291-297.

ABUTMENT STABILITY STUDIES FOR THE GORDON ARCH DAM

KEY WORDS: foundations, rock mechanics, abutment stability, arch dams, shear strength, uplift

ABSTRACT: Site investigation for the Gordon Arch Dam required extensive diamond drilling and driving of exploratory adits. Foundation weaknesses on the left abutment formed a large block of rock which could slide when loaded by the dam. Shear tests were carried out on samples taken from the potential sliding surfaces. Interpretation of the results and the subsequent stability analysis took into account the irregularities of these surfaces. The method of analysis is described. An outline is given of the underground drainage system required to control the percolation pressures within the abutment.

REFERENCE: Allen, D.T., "Abutment Stability Studies for the Gordon Arch Dam", Proc. 1st Aust.-N.Z. Conf. on Geomechanics, Melbourne, 1971, pp. 298-306.

ROCK SLOPE STABILITY

KEY WORDS: rock mechanics, slopes, stability analysis, field investigations, laboratory tests, review

ABSTRACT: Methods of slope stability analysis are briefly reviewed and it is concluded that the limit equilibrium technique is the only method currently available which offers the possibility of wide application in rock slope design. Discontinuum theories and model studies are seen as areas in which further development is likely to be productive. The problems of obtaining adequate input information on structural geology, rock properties and groundwater conditions are examined and methods of overcoming these problems are discussed. The influence of excavation techniques on the stability of rock slopes is briefly examined.

REFERENCE: Hoek, E., "Rock Slope Stability - How far away are reliable design methods?", Proc. 1st Aust.-N.Z. Conf. on Geomechanics, Melbourne, 1971, pp. 307-313.

A STATISTICAL METHOD FOR THE DESIGN OF ROCK SLOPES

KEY WORDS: joints (geology), statistical analysis, rock slopes, slope stability, probability of failure

ABSTRACT: The principal sources of uncertainty in the design of a rock slope are usually the location and orientations of the joints and other defects in the rock mass behind the slope. Steep rock slopes have a higher risk of failure than flatter ones mainly because of the greater probability of undercutting joints, or combinations of joints, in unstable orientations. Graphic procedures are introduced to determine the probability of failure of a rock slope by statistical analysis of joint orientations in conjunction with graphic kinematic and kinematic analyses of stability over a range of possible slope angles. The rock slope angle with the least total cost, being the sum of the cost of initial excavation plus the cost of partial slope failure, can then be determined. An example is given of the use of the two-dimensional normal distribution to represent the probability distribution of a joint set.

REFERENCE: McMahon, B.K., "A Statistical Method for the Design of Rock Slopes", Proc. 1st Aust.-N.Z. Conf. on Geomechanics, Melbourne, 1971, pp. 314-321.

ROCK MECHANICS INVESTIGATIONS FOR OPEN CUT

KEY WORDS: core drilling, core orientation, friction, geological investigations, joints, open cut, rock mechanics, shear strength, sliding, slope stability, stability analysis

ABSTRACT: Detailed structural measurements on oriented drill core were used to investigate the rock structure in the likely most critical batter of a proposed 550 ft deep open cut at Mount Isa, Australia. Three families of prominent weakness planes were determined: bedding planes, dipping steeply west; microfaults dipping steeply east; joints normal to bedding with two major subsets, dipping gently east and steeply north, respectively. Sliding friction tests on typical joints in the triaxial apparatus yielded values of $c = 50\text{-}200$ lb/in.^{2} and $\phi = 25^\circ\text{-}35^\circ$. Slope stability analyses were based on limit equilibrium of blocks sliding on the weakness planes; the east dipping joints are the only likely primary failure planes. Calculations show that, in the most critical case, stability can be maintained with only small values of cohesion on the joint plane provided the slope is fully drained. Wedge failure is a less critical mode of failure than plane failure. It is concluded that an overall slope angle of 50° should be used in initial design of the batter.

REFERENCE: Rosengren, K.J., "Rock Mechanics Investigations for a Large Open Cut at Mount Isa", Proc. 1st Aust.-N.Z. Conf. on Geomechanics, Melbourne, 1971, pp. 322-328.

GEOTECHNICAL INVESTIGATIONS IN BROWN COAL OPEN CUTS

KEY WORDS: coal, coal mining, extensometers, field investigations, geology, 'inclinometers', instrumentation, piezometers, slope stability

ABSTRACT: Major thermal power stations in the Latrobe Valley, Victoria, are fired with brown coal excavated from the large Yallourn and Morwell Open Cut . Batter stability problems arise because of the shape and depth of the open cuts, the geological structure of the coal seams, the presence of clay layers immediately beneath the coal seams, and from the piezometric pressures in the coal and underlying sand aquifers.

Field investigations include the mapping of geological structures, the measurement of surface and sub-surface movements, piezometric pressure observations in coal seams and interseam sediments. The physical properties of these materials are determined in the laboratory.

The paper describes the installation of piezometers and extensometers in boreholes to depths up to 720 ft, the development of extensometer anchors for brown coal, the sealing of piezometer and other installations by special chemical muds and the use of precise borehole inclinometers in difficult sub-surface conditions involving high water temperatures and pressures. Important data obtained from some of the installations are discussed.

REFERENCE: Gloe, C.S., James, J.P. and Barton, C.M., "Geotechnical Investigations for Slope Stability Studies in Brown Coal Open Cuts", Proc. 1st Aust.-N.Z. Conf. on Geomechanics, Melbourne, 1971, pp. 329-336.

THERMAL AND FREEZING METHODS TO SOIL STABILIZATION

KEY WORDS: soil stabilization, thermal, freezing, field data, deep cuts, grouting, cost

ABSTRACT: For the temporary stabilization of cuts the 'alluvial grouting' technique has been used in many countries for the last 10 years. However, this conventional grouting technique is often unreliable for the complicated and non-uniform Japanese alluvial soils. For this reason, thermal freezing and other methods are considered to be more reliable methods. In this paper, principal methods are outlined for thermal soil stabilization to strengthen the soil below the surface of a slope or under a foundation and, for temporary stabilization of deep cuts, the 'quick freezing' method using liquefied gas is described. Reference is made to a newly developed injection technique using pressures higher than those of conventional grouting.

REFERENCE: Fujii, T., "The Practical Application of Thermal and Freezing Methods to Soil Stabilization", Proc. 1st Aust.-N.Z. Conf. on Geomechanics, Melbourne, 1971, pp. 337-343.

INFORMATION RETRIEVAL FOR SOIL ENGINEERS

KEY WORDS: progressive failure, clay slopes, time dependent weakening, non-homogeneous swelling, deformation requirements, residual strength

ABSTRACT: Modes of time-dependent weakening in clay slopes are discussed and evidence is quoted to show that the dominant pre-slip mechanism of time-dependent weakening is a decay in cohesion, c', alone, while ϕ' remains at, or near to, the peak. That is, progressive failure (which may be defined as a simultaneous decay in both the c' and the ϕ' parameters) will be an untypical occurrence for the majority of clay slopes. Mention is then made of existing hypotheses of progressive failure which are suggested to provide an inadequate explanation of the process when it does occur. It is shown how large deformations, possibly of the order of feet, are necessary in the field to produce residual conditions along a potential slip plane. Neglecting landslides, such as deformations can generally be satisfied only under a certain set of conditions. The common conditions which meet the requirements are non-homogeneous or localized straining associated with the non-homogeneous swelling of swelling soils present in a cutting or valley slope. Examples are given in support of this hypothesis.

REFERENCE: James, P.M., "The Role of Progressive Failure in Clay Slopes", Proc. 1st Aust.-N.Z. Conf. on Geomechanics, Melbourne, 1971, pp. 344-348.

ANISOTROPY AND SAMPLE DISTURBANCE ON THE '$\phi_u = 0$' STABILITY ANALYSIS

KEY WORDS: anisotropy, clays, sample disturbance, shear strength, slopes, stability analysis, soil mechanics

ABSTRACT: Studies have shown that undrained strengths of many saturated clays vary with the direction of the failure plane. As such strength anisotropy is not taken into account in the conventional '$\phi_u = 0$' stability analysis for slopes in saturated clays, it has been suggested that the success of the '$\phi_u = 0$' method is in some measure due to the compensating effects of strength anisotropy and sample disturbance. The effects of strength anisotropy and sample disturbance on the '$\phi_u = 0$' stability analysis are examined analytically, with a view to assessing their combined effects. Using an idealized theoretical relationship to describe variations of undrained strength with direction, non-dimensional stability curves are presented for a range of slopes with varying degrees of strength anisotropy. The combined effects of strength anisotropy and sample disturbance are presented in chart form in terms of an 'error factor', which gives a direct indication of the discrepancy between factors of safety as found in the conventional '$\phi_u = 0$' analysis, and the in situ factor of safety taking into account strength anisotropy and sample disturbance. It is shown that the effects of strength anisotropy and sample disturbance tend to be compensating for flat slopes of normally consolidated clays in particular, although in some cases where a marked degree of anisotropy exists, the conventional '$\phi_u = 0$' method may overestimate the factor of safety. For heavily over-consolidated clays, the effects are additive, the conventional method being somewhat conservative.

REFERENCE: Martin, G.R. and Kayes, T.J., "Effects of Anisotropy and Sample Disturbance on the '$\phi_u = 0$' Stability Analysis", Proc. 1st Aust.-N.Z. Conf. on Geomechanics, Melbourne, 1971, pp. 349-354.

EARTH PRESSURE PROBLEM USING A ROD MODEL ANALOGUE

KEY WORDS: retaining walls, earth pressures, model tests, plane strain, displacements, strains, granular materials, sands, rotation, analogues

ABSTRACT: The paper presents results obtained from a small rigid retaining wall rotating about its top into brass-rod fill material used to model a granular medium deforming in plane strain. Detailed measurements were made of the variation of the wall pressure distribution with wall rotation and the complete displacement and strain fields produced in the model. These are discussed and compared with published data obtained from similar walls rotating into sand backfill. Whereas similarity between both measured and predicted results suggests that in these circumstances the rod material is a viable analogue for a loosely packed granular medium their kinematic behaviour is dissimilar. In contrast to a loose granular medium distinct velocity discontinuities develop in the rod material around which volumetric expansion occurs and changes of mean stress produce negligible volumetric strains.

REFERENCE: Butterfield, R. and Andrawes, K.Z., "An Investigation of an Earth Pressure Problem using a Rod Model Analogue", Proc. 1st Aust.-N.Z. Conf. on Geomechanics, Melbourne, 1971, pp. 355-360.

INSTRUMENTATION OF RAFT FOUNDATIONS IN PERTH

KEY WORDS: instrumentation, field investigations, raft foundations, field tests, settlements, differential settlements, earth pressures, pore pressures, laboratory tests, loads, displacements, stress, strain, design methods

ABSTRACT: The foundations of three multi-storey office buildings in Perth, Western Australia, have been instrumented by the CSIRO to investigate the performance of rafts over deep deposits of sands interbedded with clays and silts. The field observation program is one of the three interacting components of an Integrated Geomechanics Project, the others being the determination of initial conditions and material properties, and the prediction of raft performance. The reinforced concrete rafts range in size from 100 ft x 100 ft x 4 ft thick to 200 ft x 100 ft and 7 ft thick. The variables observed are contact stresses on the underside of the rafts by means of earth pressure cells; pore water pressures on the underside of the rafts and at depth by piezometers; total settlement and deflected shape of the raft by precise levelling; settlement at depth by vertical settlement gauges; lateral movement at depth by lateral displacement gauges; stresses and strains within the rafts by concrete stress and strain gauges; and column loads imposed on the rafts by concrete stress gauges and bonded strain gauges. The installation and calibration of the instrumentation is described and observations made during the construction phase of the projects are presented.

REFERENCE: Gerrard, C.M., Kurzeme, M., Andrews, D.C. and Topp, R.H., "Instrumentation of Raft Foundations in Perth", "Proc. 1st Aust.-N.Z. Conf. on Geomechanics, Melbourne, 1971, pp. 361-368.

AN INFINITELY PROGRAMMABLE STIFF LOADING FRAME

KEY WORDS: loading frame, computer control, stress, strain measurements, materials testing, stabilized, soils, rocks, hybrid modes, stiffness

ABSTRACT: The modification of a 30-ton loading frame is described which, by instrumenting specimens in a simple manner with electrical output gauges, i.e. load cells, pressure transducers, linear transducers, etc., has been coupled to a small computer, controlling movements in the frame and the environmental conditions of the specimen, according to any pre-selected program.

This procedure increases the effective stiffness of the system for stabilized soils and soft rocks, and permits the testing of such materials in the brittle fracture range in such a way that transient changes of structure corresponding to new internal total stress states can be held and examined in situ under stress.

The procedure also permits not merely the usual dynamic or kinematic testing modes, but an infinite range of hybrid and other test modes, for instance, constant rate of volumetric strain, constant principal stress ratio.

REFERENCE: Ingles, O.G. and Neil, R.C., "An Infinitely Programmable Stiff Loading Frame", Proc. 1st Aust.-N.Z. Conf. on Geomechanics, Melbourne, 1971, pp. 369-376.

PATTERNS OF STRAIN IN STRENGTH TEST SAMPLES

KEY WORDS: strain, platen lubrication, strength tests, triaxial tests, cylindrical tests, strength, compression, X-rays

ABSTRACT: The paper describes experiments in which the distribution of internal strain within strength test samples of various forms are measured using X-rays. The forms examined are the triaxial cylinder and cube under axial extension, the cube under axial compression and the rectangular plane strain compression sample. The influence of end restraint on the strain patterns is investigated. The results give proof of the benefits of using lubricated platens in the cylindrical triaxial extension test and in the plane strain compression test in providing homogeneous strain states within the samples. Strain homogeneity is in general not present in the samples tested with rough platens. Rigid zones develop at the rough platens in these tests and the conventional assumption of equality between the radial and tangential strains in the cylindrical extension test is proved invalid. With reference to cube samples, which were tested with lubricated platens, strain patterns giving a high degree of homogeneity were obtained in both triaxial extension and compression. These cube tests gave stress ratio - axial strain - lateral strain relationships comparable to those obtained from lubricated cylindrical tests reported here and previously. There is nothing in the results to suggest reasons for differences in extension strengths measured in the cylindrical and cube samples reported by some investigators.

REFERENCE: Kirkpatrick, W.M. and Younger, J.S., "Patterns of Strain in Strength Test Samples", Proc. 1st Aust.-N.Z. Conf. on Geomechanics, Melbourne, 1971, pp. 377-382.

CANTILEVER BEAM INSTRUMENTATION FOR CREEP BEHAVIOUR IN ROCKS

KEY WORDS: time-dependent deformation, creep in rocks, apparatus, cantilever bending tests, load-deflection curves, unloading curves, creep curves, examples

ABSTRACT: Time-dependent deformation or creep in rocks is of significance in mining engineering. The design and construction of apparatus for cantilever bending creep tests is described. Using this simple, inexpensive, reliable and accurate system, multiple tests can be conducted for up to sixteen rock samples. Rectangular beams as small as 4 cm x 1 cm x 0.2 cm are used for the tests. The end displacement of each cantilever beam is measured with a micrometer screw gauge. An electrical circuit detects the contact between the gauge and a stainless steel ball cemented to the beam. This system allows quick and precise measurements to be made. Reproducibility of readings for different operators is within 0.003 mm. The overall accuracy of the micrometer measuring system is approximately 0.5 per cent. Characteristic load-deflection curves, unloading and creep curves for sandy dolomite and diapiric breccia are included as examples.

REFERENCE: Klingmueller, L.M.L. and Wallace, M.J., "Simple Cantilever Beam Instrumentation for the Determination of Creep Behaviour in Rocks", Proc. 1st Aust.-N.Z. Conf. on Geomechanics, Melbourne, 1971, pp. 383-386.

PSYCHROMETRIC TECHNIQUES FOR FIELD MEASUREMENT OF NEGATIVE PORE PRESSURE IN SOILS

KEY WORDS: soil suction, negative pore pressure, field measurement, instrumentation, psychrometric technique, unsaturated soils

ABSTRACT: Results from field trials show that the psychrometric techniques described in this paper permit the measurement of negative pore pressure over the range normally encountered in engineering practice in Australia, viz. 0 to -1500 p.s.i. suction (pF 0 to 5.0), with an accuracy in routine use of ± 10 per cent (lower limit ± 5 p.s.i.) in the laboratory, or ± 50 per cent (lower limit ± 25 p.s.i.) in the field. These figures are better than those achieved previously by any other method, and are sufficiently accurate for field use.

REFERENCE: Richards, B.G., "Psychrometric Techniques for Field Measurement of Negative Pore Pressure in Soils", Proc. 1st Aust.-N.Z. Conf. on Geomechanics, Melbourne, 1971, pp. 387-394.

LABORATORY SHEAR TESTING OF WEAKNESS PLANES IN DIAMOND DRILL CORE

KEY WORDS: laboratory testing, shear strength, shear failure, displacement measurements, shear planes, diamond drill core

ABSTRACT: A laboratory machine capable of testing the shear strength of weakness planes intersecting diamond drill core is being used in the Mining Department at the University of Melbourne. The joint surfaces can be aligned in any direction relative to slickensiding by simple rotations prior to the test. A maximum of 40,000 lb load can be applied to drill core of various diameters with a constant volume displacement pump for shear loading and a lever arm mechanism for the normal load. Both peak and residual shear strengths are observed by continuously measuring the shear and normal displacements on either side of the joint surface. Examples of tests conducted are given.

REFERENCE: Waghorne, E.P., "Laboratory Shear Testing of Weakness Planes in Diamond Drill Core", Proc. 1st Aust.-N.Z. Conf. on Geomechanics, Melbourne, 1971, pp. 395-400.

TERRAIN EVALUATION AS A BASIS FOR ENGINEERING GEOLOGY

KEY WORDS: engineering geology, terrain, information retrieval, classification, climate, geology

ABSTRACT: Engineering geology and terrain evaluation are complementary to each other. One collects information about natural materials whilst the other provides methods for processing the information. Geotechnical information can be processed and stored for subsequent retrieval and can be extrapolated from one area to another by relating it to the terrain from which it was gathered. For this purpose terrain must be capable of classification at various defined significant homogeneous levels. Such a system of terrain classification can be based upon the principle that terrain is the result of the interaction of geology and climate with time as the operator.

REFERENCE: Grant, K., "Terrain Evaluation as a Basis for Engineering Geology", Proc. 1st Aust.-N.Z. Conf. on Geomechanics, Melbourne, pp. 401-408.

UNDERGROUND INVESTIGATIONS FOR A LARGE EXCAVATION

KEY WORDS: Victorian Arts Centre, site investigation, underground structures, freezing, rock foundations, aquifers, silty clays, grouting, bentonite, field tests

ABSTRACT: The north end of the Victorian Arts Centre will be placed underground to an average depth of 90 ft on a site of 1-3/4 acres in area. A site investigation has revealed the following stratum in order of depth; (a) filling of clay rubble and gravel to 25 ft; (b) soft organic silty clay at depths of 40-100 ft below ground; (c) sand and gravel aquifer varying from 0-25 ft thick on the southern half of the site; silurian mudstone bedrock at depths varying from 75-100 ft below the surface.

Based on the nature of these materials and the architectural requirements the solution adopted consists of a massive perimeter retaining wall spanning between a strutting frame at the surface and the bedrock at the bottom. Several types of wall and construction methods have been assessed including excavation within sheeting and excavation by mining methods. These methods may be assisted by techniques such as ground freezing, bentonite displacement and pressure grouting. Field and laboratory investigations of the relevant water, soil, and rock parameters are described together with an analysis of the rock stability for the completed structure.

REFERENCE: Johnson, R.M., "Underground Investigations for a Large Excavation at Victorian Arts Centre", Proc. 1st Aust.-N.Z. Conf. on Geomechanics, Melbourne, 1971, pp. 409-415.

PRELIMINARY GEOLOGICAL AND FOUNDATION INVESTIGATIONS FOR A NUCLEAR POWER STATION

KEY WORDS: engineering geology, foundation investigations, nuclear power plants, rock testing, seismic investigations, seismicity, sandstones, settlements

ABSTRACT: The area chosen as a possible site for the power station has been investigated by several field methods supported by laboratory testing. The site is underlain by a series of sandstones overlain by sand; these rocks dip to the north-west and the situation is complicated by the presence of a band of weaker rock below the highest sandstone. The geological structure is simple; there is no evidence of faulting which would affect the station structures. A station location has been chosen with a minimum of 45 ft of strong sandstone above the weaker band and testing of the materials has indicated that major footings would settle about half an inch.

Examination of the intake and five possible outfall routes has indicated that, of these, one outfall to the Bay and one outfall to the ocean are to be preferred as they present fewer construction problems.

REFERENCE: McGregor, J.P., "Preliminary Geological and Foundation Investigations for a Nuclear Power Station at Jervis Bay, New South Wales", Proc. 1st Aust.-N.Z. Conf. on Geomechanics, Melbourne, 1971, pp. 416-422.

SOME PROPERTIES OF WEATHERED GREYWACKE

KEY WORDS: index tests, mechanical properties, preconsolidation pressure, residual soils, sandstone, soil mechanics, weathering

ABSTRACT: Variations in the properties of weathered greywacke from a site in Wellington are described. The material was classed visually into four grades using a scheme for classifying weathered rock. The results of the usual soil mechanics classification tests confirmed this grading scheme as did the results of tests determining the mechanical properties. Each grade had a characteristic range of values for the various properties. It was also found that there were reasonable relations between the void ratio of the weathered material and the values of the various mechanical properties. Thus it is concluded that although the grading scheme provides a means of assessing the likely values for the properties of this particular weathered greywacke, knowledge of the void ratio provides a better means of doing this.

REFERENCE: Pender, M.J., "Some Properties of Weathered Greywacke", Proc. 1st Aust.-N.Z. Conf. on Geomechanics, Melbourne, 1971, pp. 423-429.

SEISMIC ATTENUATION IN ENGINEERING SITE INVESTIGATIONS

KEY WORDS: foundation investigations, geophysics, seismic investigations, refraction, amplitude, attenuation, rock properties

ABSTRACT: During geophysical site investigations on sixteen engineering projects, the rate of attenuation of seismic energy travelling through the rock was measured with specially calibrated seismic refraction equipment. Attenuation factors were measured in bedrock and also, in cases where the bedrock/overburden interface was sloping, in the overburden. The results indicate that attenuation factor is related not only to the kind of rock but also to its porosity, jointing, and moisture content. Attenuation factor measurements may indicate discontinuities like faults and dykes, and may support and extend the evidence given by seismic velocity measurements in engineering site investigations.

REFERENCE: Polak, E.J., "Seismic Attenuation in Engineering Site Investigations", Proc. 1st Aust.-N.Z. Conf. on Geomechanics, Melbourne, 1971, pp. 430-434.

CLASSIFICATION OF ROCK FOR ENGINEERING PURPOSES

KEY WORDS: rock, rock mass, classification, engineering, mining, cores, ground support, caveability, spans, block caving, open-stope

ABSTRACT: Although a number of classifications for both intact rock and rock masses have been proposed, these classifications, in general, do not relate to specific engineering applications. This report outlines research in progress by the U.S. Bureau of Mines to develop rock mass classifications related to two ground support problems, namely, caveability of ground (as in a block caving mine), and attainable unsupported spans, (as in an open-stope mine). The mechanical and geological property data used in these classifications are obtained from cores taken from operating mines. Techniques for quantizing geological features in the cores are briefly described.

REFERENCE: Obert, L.A. and Rich, C., "Classification of Rock for Engineering Purposes", Proc. 1st Aust.-N.Z. Conf. on Geomechanics, Melbourne, 1971, pp. 435-441.

Author Index